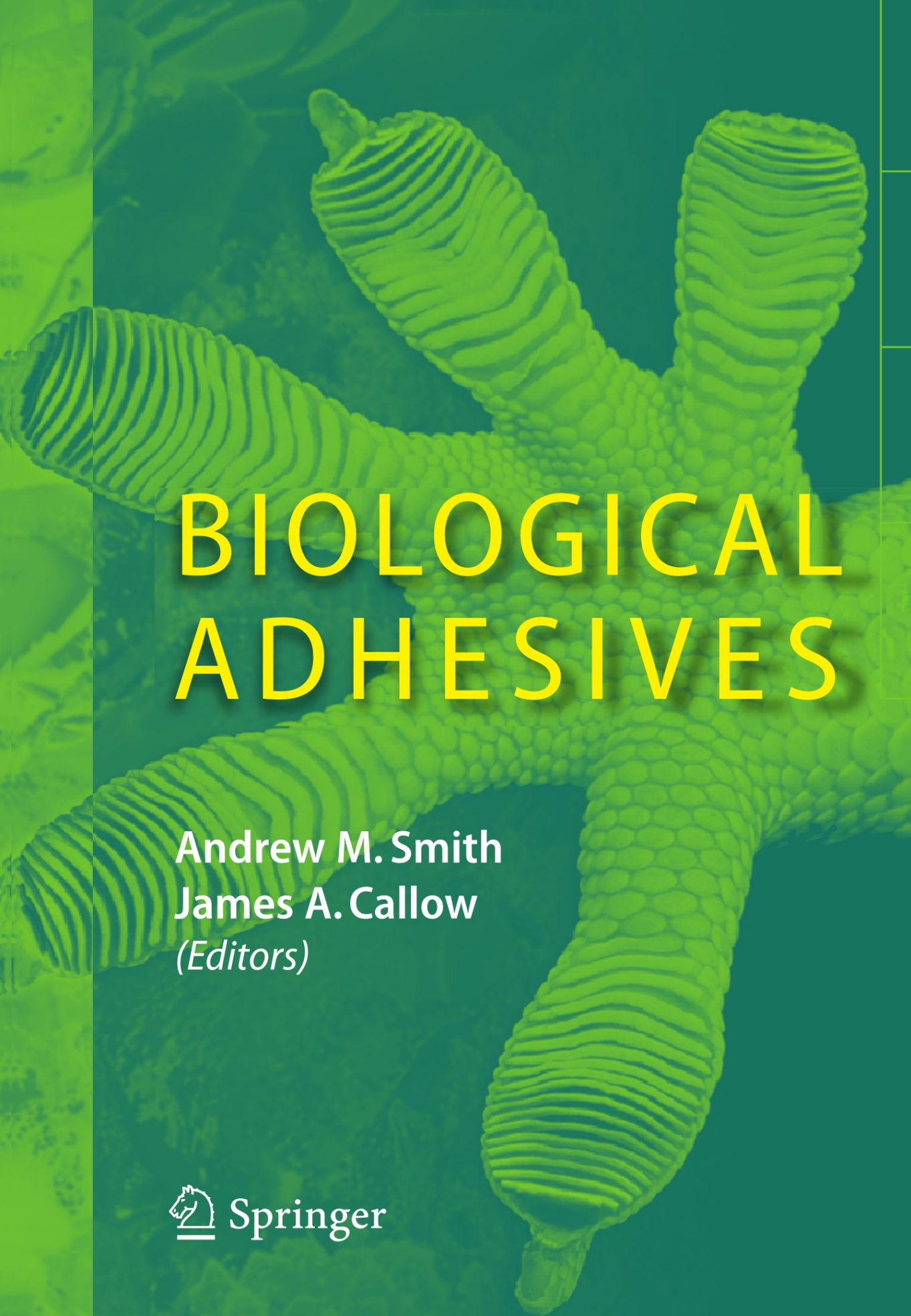
BIOLOGICAL
ADHESIVES
Andrew M. Smith
James A. Callow
(Editors)
Springer

Biological Adhesives

A.M. Smith J.A. Callow (Eds.)

Biological Adhesives

With 58 Figures, 3 in Color, and 15 Tables

Springer

Dr. Andrew M. Smith
Associate Professor
Department of Biology
Ithaca College
953 Danby Road
Ithaca, NY 14850
USA

Dr. James A. Callow
Mason Professor of Botany
School of Biosciences
The University of Birmingham
Birmingham B15 2TT
UK

Front cover illustration: Gecko foot, photo taken by Mark Moffett
Back cover illustration: Algal holdfast, photo taken by Luke Miller

Library of Congress Control Number: 2006921554

ISBN-10 3-540-31048-7 Springer Berlin Heidelberg New York
ISBN-13 978-3-540-31048-8 Springer Berlin Heidelberg New York

Springer is a part of Springer Science+Business Media

springer.com

Printed in Germany

Editor: Dr. Sabine Schreck, Heidelberg, Germany
Desk editor: Dr. Andrea Schlitzberger, Heidelberg, Germany
Cover design: Design & Production GmbH, Heidelberg, Germany
Production and typesetting: SPI Publisher Services

Printed on acid-free paper 39/3100 5 4 3 2 1 0

Preface

Many organisms, ranging from microscopic bacteria and fungi through much larger marine algae and terrestrial vertebrates, use adhesive polymers. The performance of these adhesives can be remarkable, and their diversity suggests the potential for developing glues that are markedly different from those currently available. Biological adhesives can vary widely in structure and capabilities, and often perform in ways that differ greatly from conventional man-made adhesives. Many of these adhesives form strong attachments under water–a feat that is greatly complicated by the difficulty in displacing water from the adhesive interface and the problems in dealing with water's ability to weaken many forms of chemical bonds. Another interesting characteristic is that many of these glues are highly deformable and likely to be biocompatible. Finally, unlike most artificial adhesives, they can be remarkably complex, involving a wide range of interactions and components with different functions. While this complexity can be daunting for researchers, it allows a great deal of flexibility in applications.

Another important characteristic that deserves further mention is the non-specific nature of these adhesives. They can often adhere to many different types of surfaces. This book focuses exclusively on such non-specific glues, rather than adhesive molecules more generally. There is a large and important literature on adhesion involving recognition of specific ligands. This information is best reviewed in other books, and will not be covered here. This will allow a more in-depth look at the properties of non-specific glues and their potential for practical applications.

Despite their great potential, many of these adhesives are only recently becoming better understood. There are a number of reasons for this. One of the most important may be the small size of many organisms that adhere strongly. A large number of microbes, fungal and algal spores, microscopic invertebrates, and invertebrate larvae use adhesive polymers to stick to whatever surface they encounter. It is difficult to isolate these glues and perform biochemical analyses, though, due to the miniscule amounts involved. Furthermore, adhesives in general must often be highly insoluble in order to function for extended periods. In many cases they can only be studied effectively during the time immediately after secretion and before they solidify. Another, more subtle issue has been the interdisciplinary nature of the field. To study biological adhesives, it is helpful to know sufficient organismal

diversity to identify potentially interesting glues and model organisms, sufficient biochemistry to analyze the glue, and sufficient engineering and mechanics to interpret the structure and properties of the glue. Because it is difficult to have expertise in these different areas, historically much published information on glues has tended towards untested speculation. A related issue is that published research on glues ranges from basic to applied, biochemical to mechanical, and organismal to molecular. As a result, it tends to be scattered in disparate literatures often housed in different libraries and even different schools. This book should bring these areas together and bridge them so that future scientists can more easily draw on the wealth of information that is now becoming available.

Despite the difficulties, the study of biological adhesives seems to have reached a critical mass. Work is advancing rapidly as modern methods open up new avenues for studying glues, and as we build upon a firmer understanding of the basic biochemical and mechanical principles involved in adhesion.

Recent work has made substantial progress in understanding the glues of microscopic organisms. Polysaccharides and glycoproteins seem to play a large role in the adhesion of bacteria, fungi, and larval and microscopic algae. Often, these organisms secrete a substantial quantity of extracellular polymeric substances to adhere. The size of these organisms, though, has posed unique challenges to the identification and characterization of specific glue polymers. These polymers also may share similarity with cell wall polymers and materials that have other functions. Those challenges are being overcome, and the potential now exists for detailed understanding of these glues. Callow and Callow (Chap. 4) and Epstein and Nicholson (Chap. 3) review work on the adhesives involved in algal and fungal settlement on substrates. This work demonstrates the utility of monoclonal antibodies and molecular genetic techniques in identifying potential adhesive polymers and providing evidence of their function. The use of atomic force microscopy, especially modified versions that do not lead to evaporation of wet adhesives, has also provided insight into the mechanics and curing of these glues (Callow and Callow, Chap. 4; Chiovitti et al. Chap. 5).

Landini et al. (Chap. 2) review work on bacterial adhesives demonstrating the power of molecular genetics to study not only the nature of the adhesive, but the factors controlling its production and secretion. It is worth remembering that these adhesives are complex secretions where the manner, timing and circumstances under which they are laid down can markedly affect the nature of the end product. Furthermore, as Chiovitti et al. (Chap. 5) note in their review of diatom adhesion, there will be considerable variation in structure and properties of the adhesive according to function.

The glues of barnacles and mussels are better understood than most. Collecting sufficient material for biochemistry is not as problematic, and researchers have made great strides in dealing with the natural insolubility of the glues and the difficulty in using standard biochemical techniques

with polymers that are often designed to stick to other polymers and exposed surfaces. Kamino (Chap. 8) reviews what is known of barnacle adhesion. This work highlights the multifunctionality of the glues; there are a number of components, each with an apparently unique function. The structural information available for these proteins is becoming sufficient to begin unraveling structure/function questions. Sagert et al. (Chap. 7) review mussel adhesion, where work has probably advanced furthest. Perhaps it also demonstrates best the complexity and unusual biochemistry of biological glues. There is a variety of interesting mechanisms that may contribute to the cohesive and adhesive interactions of the glue. This diversity contributes to the glue's ability to work so effectively on many different surfaces under a variety of conditions. It is also worth noting that many of these mechanisms depend on post-translational modification of proteins; this is just one more complicating factor in the analysis of biological glues.

There are many other glues that are just recently becoming better understood. Potin and Leblanc (Chap. 6), describe progress in understanding the adhesion of brown algae. The apparent importance of halogen chemistry is an interesting variant of crosslinking chemistry. Echinoderm adhesion has been a subject of interest for many years, and recent work has begun the process of unraveling the physico-chemical characteristics of adhesion (Flammang, Chap. 10). Echinoderms are of particular interest because adhesives are used in different groups for such diverse functions as larval settlement, adult motility, stable attachment, and defense.

Many of these adhesives have high water content, with some being hydrogels. These gels can depend on tangling and crosslinking of large polysaccharides or heavily glycosylated proteins, or they can be primarily proteinaceous. Smith (Chap. 9) outlines the factors affecting the mechanics of such gels and reviews variation and similarity in the structure of adhesive gels from gastropods. With gastropod glues, the ability to identify key proteins and manipulate the components of the glue provides a powerful experimental tool. Graham et al. (Chap. 11) review recent work on the structure and practical potential of protein hydrogels used by certain frogs as defensive secretions. This is another intriguing glue with great potential for guiding biomimetic applications.

In contrast to the adhesive systems described in other chapters, geckos do not secrete a glue, they utilize adhesion between solid surfaces. The mechanics of the arrays of fine hair-like setae on their feet give rise to striking functional properties. Analysis of the mechanical principles has yielded a number of important insights, as reviewed by Autumn (Chap. 12).

The potential for development of practical adhesives using a biomimetic approach exists for all these adhesives. Haag (Chap. 1) reviews the effectiveness of various adhesives extracted or derived from bacterial secretions while Lee et al. (Chap. 13) review work on adhesives derived from research on mussel glues. These chapters highlight the power of a biomimetic approach, with

Lee et al. in particular showing the potential for making synthetic glues when the physico-chemical properties of the natural adhesive are established well enough to provide guidance.

As research in this area progresses, similarities that suggest common underlying principles may emerge, while simultaneously more and more variation in the details becomes clear. It is our hope that bringing together all this information will stimulate further research by providing ideas for experimental approaches and by providing insight into both the common features of glues and the myriad ways that adhesion can be achieved. Ultimately, detailed characterization of the structure of the adhesive polymers and their properties may provide the raw material to inspire a new generation of adhesives for use in medicine, biotechnology and a range of other applications.

February 2006 *Andrew M. Smith and James A. Callow*

List of Contributors

K. Autumn
Department of Biology, Lewis & Clark College, Portland, OR 97219-7899, USA

J.A. Callow
School of Biosciences, The University of Birmingham, Birmingham B15 2TT, UK

M.E. Callow
School of Biosciences, The University of Birmingham, Birmingham B15 2TT, UK

A. Chiovitti
School of Botany, University of Melbourne, Victoria 3010, Australia

J.L. Dalsin
Department of Biomedical Engineering, Northwestern University, 2145 N Sheridan Road, Evanston, IL 60208, USA

C. Dorel-Flamant
Unité de Microbiologie et Génétique UMR CNRS 5122 composante INSA, 10, rue Dubois, 69 622 Villeurbanne Cedex, France

T.M. Dugdale
School of Botany, University of Melbourne, Victoria 3010, Australia

L. Epstein
Department of Plant Pathology, University of California, Davis, CA 95616-8680, USA

P. Flammang
Universite de Mons-Hainaut, Laboratoire de Biologie marine, Academie Universitaire Wallonie-Bruxelles, Mons, Belgium

V. Glattauer
CSIRO Molecular & Health Technologies, Ian Wark Laboratory, Bag 10, Clayton South, Victoria 3169, Australia

L.D. Graham
CSIRO Molecular & Health Technologies, Sydney Laboratory, P.O. Box 184, North Ryde, NSW 1670, Australia

A.P. Haag
Specialty Biopolymers Corporation, 524 Professional Drive, Ste. E, Bozeman, MT 59718, USA

G. Jubelin
Unité de Microbiologie et Génétique UMR CNRS 5122 composante INSA, 10, rue Dubois, 69 622 Villeurbanne Cedex, France

K. Kamino
Marine Biotechnology Institute, 3-75-1 Heita, Kamaishi, Iwate 026-0001, Japan

P. Landini
Dipartimento di Scienze Biomolecolari e Biotecnologie, Università di Milano, Via Celoria 22, 20133 Milano, Italy

C. Leblanc
UMR 7139 CNRS/UPMC, Marine Plants and Biomolecules & LIA-DIAMS, Station Biologique, BP 74, F-29682 Roscoff Cedex, France

B.P. Lee
Department of Biomedical Engineering, Northwestern University, 2145 N Sheridan Road, Evanston, IL 60208, USA

P.B. Messersmith
Department of Biomedical Engineering, Northwestern University, 2145 N Sheridan Road, Evanston, IL 60208, USA

R.L. Nicholson
Department of Botany and Plant Pathology, Purdue University, W. Lafayette, IN 47907, USA

Y.Y. Peng
CSIRO Molecular & Health Technologies, Ian Wark Laboratory, Bag 10, Clayton South, Victoria 3169, Australia

P. Potin
UMR 7139 CNRS/UPMC, Marine Plants and Biomolecules & LIA-DIAMS, Station Biologique, BP 74, F-29682 Roscoff Cedex, France

J.A.M. Ramshaw
CSIRO Molecular & Health Technologies, Ian Wark Laboratory, Bag 10, Clayton South, Victoria 3169, Australia

J. Sagert
Department of Molecular, Cell & Developmental Biology, University of California, Santa Barbara, CA 93106, USA

A.M. Smith
Department of Biology, Ithaca College, Ithaca, NY 14850, USA

C. Sun
Department of Molecular, Cell & Developmental Biology, University of California, Santa Barbara, CA 93106, USA

M.J. Tyler
School of Earth & Environmental Sciences, University of Adelaide, South Australia 5005, Australia

P.R. Vaughan
CSIRO Molecular & Health Technologies, Ian Wark Laboratory, Bag 10, Clayton South, Victoria 3169, Australia

J.H. Waite
Department of Molecular, Cell & Developmental Biology, University of California, Santa Barbara, CA 93106, USA

J.A. Werkmeister
CSIRO Molecular & Health Technologies, Ian Wark Laboratory, Bag 10, Clayton South, Victoria 3169, Australia

R. Wetherbee
School of Botany, University of Melbourne, Victoria 3010, Australia

Contents

1 Mechanical Properties of Bacterial Exopolymeric Adhesives and their Commercial Development

ANTHONY P. HAAG

1.1 Introduction

In industry and society today, there is a need for products which provide environmentally friendly features, such as 1) reduced usage of toxic components and VOCs (volatile organic compounds), 2) reduced dependence on depleting petrochemical resources, 3) safer production processes, and 4) less environmental impact of products after their use (Gross and Kalra 2002). The motivation for exploring biopolymers for use in adhesive applications is to exploit their unique properties to address these needs. Additional incentive for development of biological materials is economics. As the world economy grows and more demand is placed on depleting petrochemical feedstocks, products derived from renewable, biological resources are becoming more cost competitive.

Biopolymers are utilized by all organisms for numerous functions in varied environments and thus have evolved into a diversity of chemical compositions. Biopolymers offer the material scientist a source of unique compositions which are unavailable by synthetic means with which to search for novel properties, such as adhesive strength. The discovery of new compositions and optimization of their production is also becoming easier with new, sophisticated biological methods. In the future, biologically derived materials will increasingly fill needs in commercially important applications.

In biofilms, a widespread form of bacterial existence, cells form highly hydrated cohesive masses that adhere to surfaces. Extracellular polymeric substances are largely responsible for the structure and properties of biofilms, including the adhesion of cells to surfaces and to each other. In addition to facilitating the growth of the bacterial colony, biofilms can be problematic and result in, for example, corrosion and fouling in industrial systems, and resistance to antibiotics on medical devices (Costerton and Stewart 2001; Flemming and Wingender 2001). The mechanical properties of biofilms have been described as those of a viscoelastic fluid in which the biofilm behaves elastically at low shear stress and viscously at higher shear stress (Klapper et al. 2002). Thus, extracellular polymeric substances impart substantial mechanical properties to biofilms in their natural environment.

Specialty Biopolymers Corporation,
524 Professional Drive, Ste. E, Bozeman, MT, USA 59718

Biological Adhesives
(ed. by A.M. Smith and J.A. Callow)

Extracellular polymeric substances in biofilms are composed of polysaccharides, proteins, and nucleic acids (Flemming and Wingender 2001). Protein components are generally attributed to the initial adhesion processes (formation of a conditioning layer) and polysaccharides, in addition to various other biological functions, are largely responsible for the subsequent adhesive interactions and provide cohesive strength. This review will focus primarily on exopolysaccharides which are often the predominant extracellular component in bacterial biofilms and most readily developed for commercialization.

Bacterial exopolysaccharides have found use in other applications such as thickening and gelling agents for aqueous mixtures and have undergone a significant amount of commercial development. Examples are xanthan gum (from *Xanthomonas campestris*), gellan (*Sphingomonas paucimobilis*), curdlan (*Agrobacterium radiobacter*), dextran (*Leuconostoc mesenteroides*), and levan (*Bacillus polymyxa*). Scleroglucan and pullulan, although of fungal origin, show similar behavior. Sodium alginate is produced commercially from algae but structurally similar materials are also produced by the bacteria *Azotobacter vinelandii* and *Pseudomonas aeruginosa*. Structures of some of the polysaccharides described in this chapter are shown in Fig. 1.1. General structural features of polysaccharides which are useful in adhesives include high molecular weight and polar functional groups. Mechanical properties generally improve with molecular weight (Lazaridou et al. 2003) and native bacterial polysaccharides often possess molecular weights greater than 10^6 Da. Lower molecular weights can be produced, if desired, by control of culture conditions or depolymerization of the native product followed by fractionation. The polar and hydrogen-bonding functional groups of polysaccharides, such as ethers, hydroxyls, and carboxylates, impart good adhesion to high energy surfaces such as wood and metal and also strong interchain interaction for cohesive strength. The hydroxyl and carboxylate groups of polysaccharides also offer potential sites for synthetic derivatization and crosslinking which can be utilized to modify the adhesive properties. Tertiary structures, such as helices, are formed by some bacterial polysaccharides and account for their notable mechanical properties. Other distinguishing properties of bacterial exopolysaccharides are hydrophilicity, ability to form hydrogels (structure dependent), biodegradability, production from renewable resources, and generally low toxicity.

Xanthan gum, gellan, and dextran are produced commercially at volumes greater than 1 million lb/year. Production of most bacterial exopolysaccharides is accomplished by batch-wise fermentation in stirred tanks equipped with efficient agitation for the resulting highly viscous mixtures. Glucose and sucrose are commonly used as the carbon and energy sources. Raw materials account for a significant fraction of the product cost so substitution of cheaper carbon sources, such as agricultural waste products is advantageous. In the production of xanthan gum, which is the most successful industrial biopolymer produced by fermentation, yields of 30 g/L and productivities of 0.7 g/l-h are reported (Born et al. 2002). After the fermentation operation, the mixture is sterilized, and the biopolymer is isolated by precipitation into

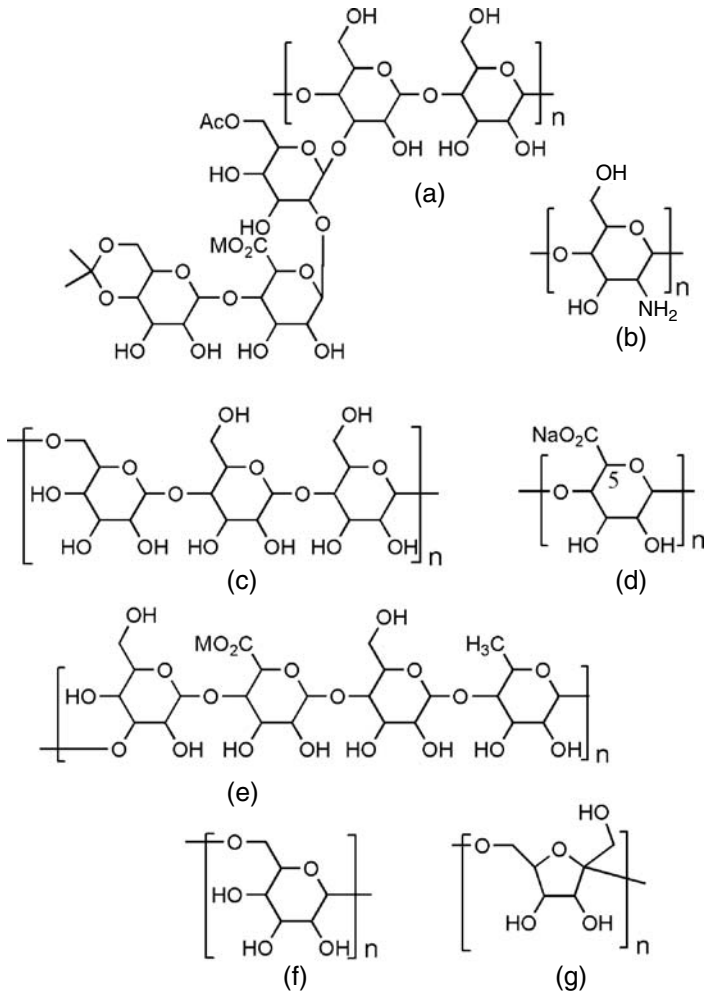

Fig. 1.1. Structures of some of the polysaccharides referred to in this chapter. (a) Xanthan gum (M=metal), (b) chitosan, (c) pullulan, (d) sodium alginate (note mixture of epimers at C-5), (e) gellan, (f) dextran, and (g) levan

isopropanol and then dried. Cell biomass is not separated for industrial grades of xanthan; higher purity grades are obtained by removal of the biomass by filtration or absorption. Xanthan gum is currently produced globally at a volume of 40 million lb/year (Sutherland 2002) and sells for $4.5/lb (Chemical Market Reporter 2005).

Their performance in nature, unique chemical compositions, economics of production from renewable resources, and biodegradability make bacterial exopolysaccharides attractive candidates for development as adhesive materials. This review summarizes recent efforts to identify adhesive materials

derived from bacterial exopolysaccharides and evaluates their mechanical properties for adhesive applications. Comparisons include descriptions of adhesive composition and preparation, testing procedures, and testing results. In addition to the bacterial products, selected structurally related polysaccharides from plant and animal sources are briefly compared.

1.2 Adhesive Development

1.2.1 Mechanical Testing of Adhesive Bonds

The search for practical adhesives relies on evaluation of mechanical properties. Fundamental studies of the physical and mechanical properties of bacterial exopolysaccharides on the nanoscopic, molecular level in their native, aqueous environments have been accomplished with atomic force microscopy (AFM) (Dufrene 2002; Kawakami et al. 2004). In addition to the fact that mechanical properties measured on the molecular level are not directly relatable to adhesive strengths observed on the macroscopic level, the test conditions are also different than those in most industrial adhesive applications in which the adhesive is in a dry state and subject to varying levels of humidity and temperature. Thus, evaluation of new adhesives should employ conditions simulating expected uses. Standard methods have been developed by professional testing organizations such as the American Society for Testing and Materials (ASTM) for specific applications. The three forces to which adhesives are subjected are shear, peel, and cleavage (Fig. 1.2) (Pocius 1991). Shear strengths can be measured under tension or compression. Peel and cleavage tests measure similar forces, but the former is used with deformable substrates. Preliminary testing of adhesives for metal bonding applications generally employ single-lap shear test specimens with 3.2 cm^2 bond area (ASTM D 1002) or butt-joined bar specimens (ASTM D 2095). Preliminary testing of wood adhesives generally employ two methods: three-ply plywood specimens assembled from 1.6 mm-thick veneers with a 6.4 cm^2 bond area are sheared under tension (ASTM D 906); and two 19 mm-thick wood blocks with 19.4 cm^2 bond area are sheared under compression (ASTM D 905). Results are expressed in terms of stress or pressure, that is, the force required to break the bond divided by the bond area. Analysis of the bond failure mode is also commonly reported and indicates whether the bond failed at the adhesive-substrate interface (adhesive failure), within the adhesive itself (cohesive failure), or in the substrate (substrate failure).

Testing methods for bonding biological materials, such as tissue and skin, have been designed for these unique substrates, for example, ASTM F 2255-03 (“Test Method for Strength Properties of Tissue Adhesives in Lap-Shear by Tension Loading”) (McDermott et al. 2004). In vivo testing of adhesive films on human skin has also been developed (Repka and McGinity 2001).

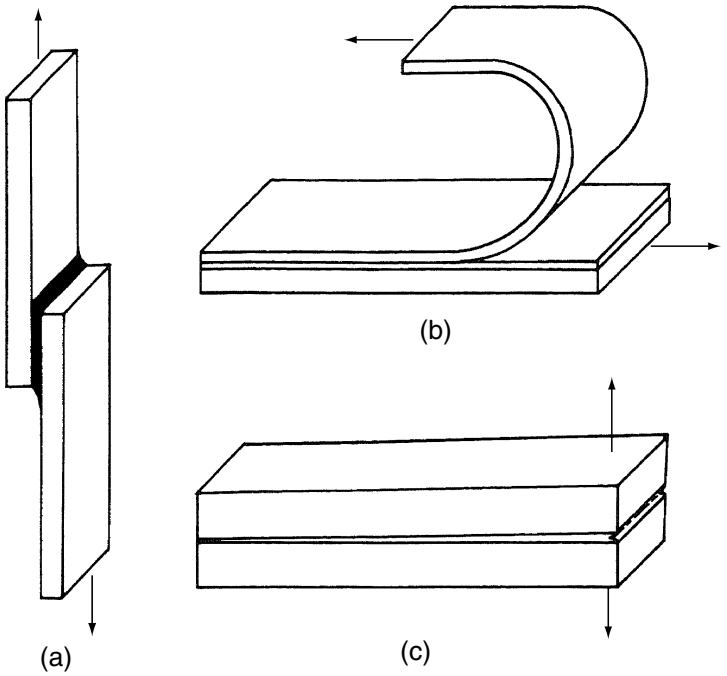

Fig. 1.2. Illustrations of forces to which adhesive bonds are subjected: (a) a standard lap shear specimen where the black area shows the adhesive. The adherends are usually 25 mm wide and the lap area is 312.5 mm2. The *arrows* show the direction of the normal application of load; (b) a peel test where the loading configuration, shown by the *arrows*, is for a 180 ° peel test; (c) a double cantilever beam test specimen used in the evaluation of the resistance to crack propagation of an adhesive. The normal application of load is shown by the *arrows*. This load is applied by a tensile testing machine or other mechanical means of holding open the end of the specimen (Pocius 1991). Reprinted with permission of John Wiley & Sons, Inc., copyright ©1991

1.2.2 Bacterial Exopolymer Adhesives

1.2.2.1 Polysaccharide Adhesive Viscous Exopolymer

The marine bacterium *Alteromonas colwelliana* LST produces an exopolysaccharide which it uses to adhere strongly to surfaces under severe conditions in its natural environment. It also synthesizes tyrosinase, dihydroxyphenylalanine (DOPA), and related quinones which participate in water-resistant adhesive production in higher organisms (Yamada et al. 2000). Therefore, the mechanical properties of "polysaccharide adhesive viscous exopolysaccharide" (PAVE) isolated from several strains of this bacterium were evaluated on commercially relevant substrates (Labare et al. 1989). An efficient process for production of PAVE from one strain of bacteria was demonstrated (5–11 g/l). Depending on culture conditions, the carbohydrate/protein ratio in PAVE as

determined by classical colorimetric methods ranged from 1 to 14. The adhesives used for screening of shear strengths were prepared from mucoid exopolymers of nine bacterial strains scraped from agar surfaces prepared with various media. No further chemical characterization was described. The PAVE material was formulated for use in adhesive testing in three ways: as isolated in concentrated form, or diluted with acetone 10 or 100 times.

Adhesive testing utilized lap-shear specimens. Substrates composed of glass, aluminum, brass, stainless, hot-rolled steel, wood (unspecified species or conditioning), and acrylic plastic were bonded with 2.5 cm^2 overlap area using adhesives from nine bacterial strains. Two shearing test configurations were used–the first employed application of a torque force (applied 5 cm from midjoint) and the second method applied a tensile force. The authors state that the two methods reflect strengths of adhesion and cohesion, respectively.

Testing results using the torque method on glass substrates showed strengths of 1.0–4.4 kg/cm torque for the nine adhesives. Cure times of seven days gave higher strengths than one day. PAVE prepared from a tyrosinase and DOPA producing strain (TAC-1) gave higher results (100%) than the corresponding DOPA-negative variant strain (TAC-2). Adhesive strengths varied for some PAVE preparations when formulated in water or acetone. In the tensile shear tests, adhesive strengths of PAVE prepared from nine bacterial strains were evaluated on seven substrate materials. Each adhesive showed unique surface dependent shear strengths (up to 0.5 MPa, Tables 1.1 and 1.2). In this series, PAVE prepared from the DOPA producing strain again showed

Table 1.1. Relative shear strength of crude PAVE preparation from marine bacteria on metal surfaces[a]. Numbers in parentheses are standard deviations (Labare et al. 1989). Reprinted with permission of the authors and Brill NV

Strain[b]	Surfaces Aluminum		Brass		Stainless steel		Hot-rolled steel	
MPF-1	8.7	(5.4)	17.5	(7.3)	8.2	(6.8)	7.6	(5.1)
RAM-1	7.6	(0.8)	8.4	(3.9)	8.0	(4.8)	17.3	(5.7)
KAN-1	10.0	(0.9)	10.8	(6.8)	7.6	(3.8)	22.1	(0.6)
TAC-1	0.0	(0.0)	0.5	(0.2)	2.9	(2.5)	14.2	(6.7)
TAC-2	6.8	(1.4)	12.9	(6.6)	4.1	(0.9)	11.5	(3.1)
PAS-1	12.8	(3.1)	25.6	(17.0)	12.2	(6.7)	5.3	(4.2)
MPL-1	12.5	(3.4)	22.5	(0.2)	7.1	(3.1)	6.0	(1.0)
DLS-T	4.3	(2.1)	9.5	(3.6)	2.9	(0.2)	31.2	(9.5)
DPR-8	18.1	(16.7)	ND[c]	-	15.6	(9.8)	17.1	(6.8)

[a] Crude PAVE was extracted with acetone, stored for seven days at 25 °C, spread on a 2.5 × 2.5 cm area, clamped, cured for seven days, and tested for shear force (kg) using Instron

[b] Bacteria were grown in brain-heart infusion + 2.3% NaCl medium for 24 h except MPL-1, TAC-2, and DPR-8, which were grown in BHI, BHI + extra salts, and marine agar + casein hydrolysate, respectively

[c] ND=no data

Table 1.2. Relative shear strength of crude PAVE preparations from marine bacteria on non-metal surfaces[a]

Strain[b]	Surfaces Acrylic		Glass		Wood	
MPF-1	3.7	(1.7)	6.7	(0.3)	25.2	(1.5)
RAM-1	6.5	(0.5)	6.5	(0.5)	13.8	(6.7)
KAN-1	9.6	(1.3)	6.1	(2.7)	17.5	(2.6)
TAC-1	3.0	(0.7)	6.1	(2.5)	9.8	(1.9)
TAC-2	2.9	(1.5)	3.1	(1.9)	3.7	(0.6)
PAS-1	10.8	(7.9)	9.9	(2.8)	36.4	(8.3)
MPL-1	4.8	(0.6)	4.0	(0.6)	13.0	(1.4)
DLS-T	3.2	(1.8)	11.5	(1.0)	16.8	(0.8)
DPR-8	10.0	(8.6)	11.6	(0.9)	19.4	(2.3)

[a] Crude PAVE was extracted with acetone, stored for seven days at 25 °C, spread on a 2.5 × 2.5 cm area, clamped, cured for seven days, and tested for shear force (kg) using Instron
[b] Bacteria were grown in brain-heart infusion + 2.3% NaCl medium for 24 h except MPL-1, TAC-2, and DPR-8, which were grown in BHI, BHI + extra salts, and marine agar + casein hydrolysate, respectively

a 100% higher shear strength on glass compared to the DOPA-negative strain, but the effect was not consistent for other substrate materials. Overall, the PAVE products showed encouraging but relatively low adhesive strengths. The highest shear strengths were on wood, hot-rolled steel, and glass. Although no commercial adhesive benchmarks were tested for comparison during this study, adhesive shear strengths of 1–50 MPa (3.2 cm^2 bond area) are common (Pocius 1991) in similar tests. Further analysis of the value of these adhesives should include testing of the effects of moisture and application rate, and determination of adhesive composition and polymer structure.

The DOPA-based crosslinking concept continues to be a productive approach to improve mechanical properties, in particular moisture resistance of adhesives derived from the amine-functionalized polysaccharide, chitosan (see Sect. 1.2.3.3).

1.2.2.2 Biomass Fermentation Residue

Economical viability of a bioconversion process for ethanol production from cellulosic biomass requires the development of other valuable coproducts. The fermentation residues have been found to be potentially useful as wood adhesives. Ruminal cellulolytic bacteria ferment cellulose, hemicelluloses, and pectin to ethanol. During the degradation process, adherence to the cellulose substrate is mediated by adhesins. The fermentation residue (FR) consists of incompletely fermented biomass, adherent bacterial cells, and associated exopolymer adhesins.

Initial studies focused on fermentation of purified cellulose with the anaerobic bacteria *Ruminococcus albus* and *Ruminococcus flavefaciens* (Weimer et al. 2003). After incubation, the fermentation residue was separated from the liquid phase and lyophilized. Characterization of the FR showed 14–23% alkali-soluble carbohydrate and 0.4–5% protein. Monosaccharide composition was similar in the exopolysaccharide from three bacterial strains (approximately 0.7 glucose/0.02 galactose/0.08 mannose/0.18 xylose [mol fraction]). Adhesives were formulated by mixing lyophilized FR with water (33 wt%) and commercial phenol-formaldehyde (PF) adhesive. The method used to test adhesive strength employed aspen veneers which were conditioned at 30% relative humidity (RH) and 27 °C, bonded with adhesive, assembled into three-ply panels, pressed at 1.1 MPa/180 °C/10 min, and later cut to testing size. Half of the plywood specimens were tested for shear strength at 30% RH and half were tested after a vacuum-pressure water soak treatment. Percentage of wood failure was also measured.

Shear strengths of plywood panels bonded with FR alone were half that of PF (1.8 and 3.4 MPa, respectively) under dry conditions and one-fifth that of PF under wet conditions. However, substitution of up to 73% of PF with FR produced shear strengths and % wood failure nearly equal to that of PF alone under dry conditions. The FR/PF blends were also nearly as strong as PF alone under the wet conditions. The FR from *R. albus* gave superior shear strengths to two strains of *R. flavefaciens* although the fermentations with the latter were less complete (greater residue dry weight).

Subsequent work explored residues derived from fermentation of a more practical biomass substrate, lucerne (*Medicago sativa* L., alfalfa) fiber, with *Ruminococcus flavefaciens* and *Clostridium thermocellum* (Weimer et al. 2005). The preparation of FRs and adhesives, and the adhesive testing method were the same as in the earlier work. The composition of the FR from both bacteria (alkaline extract) was 4.2–2.8% protein, 7.7–7.8% carbohydrate, 0.8–1.2% uronic acid, with the remainder being fiber, lignin, and ash.

FR was blended with PF and used to bond plywood panels. Shear strengths of specimens bonded with 30% FR/PF were 2.5–2.8 MPa under dry conditions, equivalent to specimens bonded with PF containing 30% of a common extender additive (30% RH) (Fig. 1.3). The shear strength of 30% FR/PF was significantly higher than that of a 30% blend of unfermented fiber and PF, and also twofold higher than a 45% blend of FR/PF. Wood failure of specimens bonded with the 30% FR/PF blend was nearly 100% under dry conditions. Under wet conditions, shear strengths of specimens bonded with 30% FR/PF were 1.7–2.0 MPa, significantly higher than specimens bonded with either 30% commercial extender/PF or 30% unfermented fiber/PF. Wood failure of specimens bonded with the 30% FR/PF blend was nearly 100% under wet conditions. Note that the adhesives prepared from the two bacterial sources gave similar results. The composition of the FRs showed considerable differences but the alkali-extractable carbohydrate content was the same. The monosaccharide compositions were also very similar suggesting that observed shear strengths correlate with the carbohydrate content and structure.

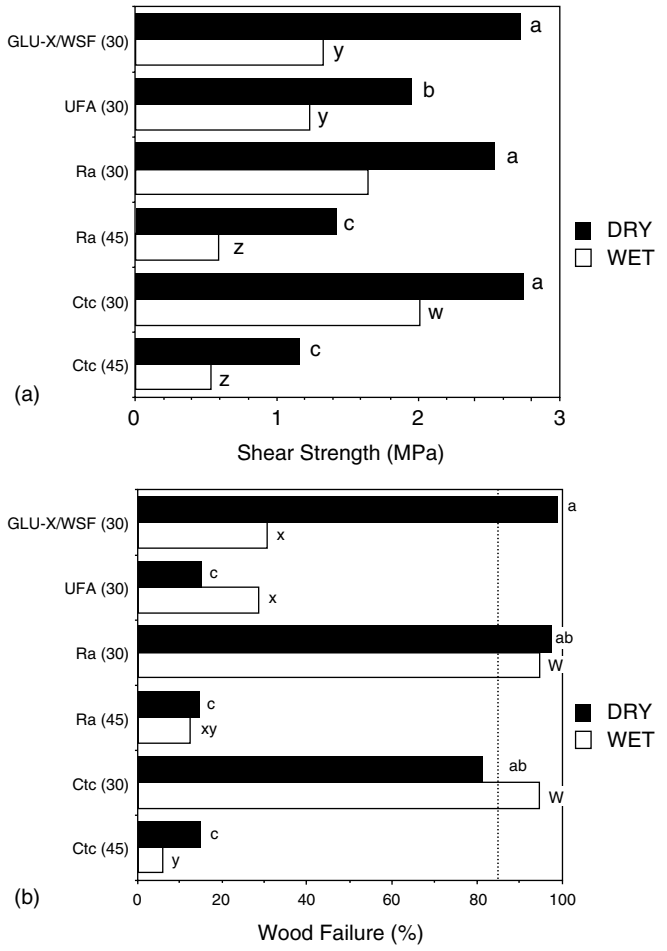

Fig. 1.3. (a) Shear strength. (b) Wood failure data, both for plywood adhesives formulated with PF resin and the indicated co-adhesive. GLU-X/WSF=GLU-X and walnut shell flour extenders, UFA=unfermented lucerne fiber, Ra=residue from *R. albus* 7 lucerne fiber fermentation, Ctc=residue from C. *thermocellum* ATCC 27405 lucerne fiber fermentation. Values in *parentheses on the vertical axis labels* indicate percentages (dry weight basis) of additive, with the remainder being PF (see reference for formulations). In the case of GLU-X/WSF, each was added at 15% by dry weight for a total of 30%. Different a, b, c letters indicate significant differences ($P<0.01$) in shear strength or wood failure among the panels under dry conditions. Different w, x, y, z letters indicate significant differences ($P<0.01$) in shear strength or wood failure among the panels under wet (VPS) conditions. The vertical line in B indicates the industry standard for wood failure (85%). Reprinted with permission of the authors (Weimer et al. 2005)

The sources of adherence during degradation by ruminal cellulolytic bacteria are cellulose-binding domains of cellulosome components, pilin-like proteins in fimbrae, and exopolymer materials synthesized following irreversible adsorption to cellulose fibers. That is, the intrinsic affinity of

adhesins for cellulose is likely to contribute, in part, to adhesive strength compared to other bio-based adhesives for bonding wood. Overall, the proposed use of FR as an adhesive alters the bioconversion strategy: production of FR with an estimated value similar to ethanol obviates the need for high substrate conversion and requisite costly pretreatments.

1.2.2.3 Montana Biotech Adhesive

A water-based bacterial exopolymer adhesive was developed as an alternative to VOC-containing adhesives (Combie et al. 2004). Testing of adhesive strength was performed on aluminum and coated aluminum substrates. Bacterial isolates from the culture collection of Montana Biotech SE, Inc. (Rock Hill, SC, USA) were screened for production of adhesive exopolymers. The adhesive material which gave the best adhesive testing results in the initial screening was then selected for the following studies.

MB (Montana Biotech) adhesive was produced by an unidentified organism and isolated from the liquid medium, after separation of cells, by precipitation with alcohol. Its molecular weight was 10^6 Da and it was composed of >95% carbohydrate (dry weight basis). Other structural information was not disclosed. More hydrophobic derivatives were also prepared in order to increase moisture resistance. Partially methylated or acetylated derivatives of dried MB adhesive were prepared by reaction with methyl iodide or acetic anhydride, respectively. Water solubility decreased as degree of substitution increased.

Flatwise tensile strengths were determined using two butt-joined cylindrical aluminum specimens (alloy 2024, 1.56 cm^2 cross-sectional area). After pressing for 1 h at ambient temperature and RH, the specimens were set at 35 °C and 23% RH for seven days. Tensile strength was measured at ambient temperature with a manually operated Mark 10 BGI force measuring instrument. Shear strengths were determined using aluminum 2024 coupons which were either anodized with sulfuric acid and hot water sealed; anodized and epoxy coated; or anodized, epoxy undercoated and topcoated with "chemical agent resistant coating", CARC. The coupons were bonded in a single lap shear configuration with 3.2 cm^2 bond area, pressed for 1 h, and after setting, tested on an Instron universal testing machine.

Tensile strengths of approximately 7 MPa were reported for MB adhesive-bonded Al 2024. The adhesive was resistant to organic solvents (48 h soak) and showed superior strength over other, commercially available polysaccharides. The MB adhesive showed a low moisture resistance. After initially setting for seven days at 35 °C, the bonded specimens were soaked in water for 2 h at ambient temperature and retained only 5% of their initial shear strength. A partially acetylated derivative when set under the same conditions showed the same shear strength as the nonderivatized MB adhesive, but after a 2 h water soak retained 37% of its initial strength. Another test for

moisture resistance employed exposure to 75% RH conditions for seven days after an initial set at 35 °C for seven days at low RH. Under these conditions, MB adhesive retained 10% of its initial tensile strength while the partially acetylated derivative retained 66%. The shear strength of MB adhesive-bonded aluminum and aluminum coated with epoxy and CARC ranged from 4.5–5.6 MPa.

In addition to the initial studies with aluminum substrates and organic coatings, MB adhesive was also evaluated as a wood adhesive (Haag et al. 2004). Many wood adhesives have VOC and/or toxic components such as formaldehyde which is now classified as a carcinogen. In addition most adhesives are based on depleting petrochemical resources. The water-based MB adhesive was well suited to applications with porous substrates such as wood which allow for facile absorption and evaporation of the water solvent.

The exopolysaccharide used in these studies was prepared as described above but a lower molecular weight product was obtained, approximately 40 KDa as measured by size exclusion chromatography. A partially acetylated derivative, MB-OAc, was also prepared from this material by reaction with acetic anhydride. The adhesive strengths were determined using a standard method for initial evaluations of wood adhesives, ASTM D 905, "Standard Test Method for Strength Properties of Adhesive Bonds in Shear by Compression Loading". In this method, two wood boards (1.9 cm thick × 6.4 cm wide × 30.5 cm long) are bonded, pressed overnight, allowed to set for one week at 53% RH and 22 °C, cut to size for testing (19.4 cm^2 bond area), and then shear strength was measured. Experiments to determine moisture resistance utilized setting conditions of 53% (moderate) RH for one week followed by an additional week at either 53% RH or 94% (high) RH.

The shear strength of MB adhesive was initially evaluated on substrates of two wood species (sugar maple, a hardwood, and Douglas fir, a softwood) and two wood composites (particleboard and medium density fiberboard). It was also compared to a commercial polyvinylacetate (PVA)-based wood adhesive. MB adhesive showed a shear strength of 12.5 MPa on maple, 73% of that observed with PVA adhesive. Substrates bonded with MB adhesive showed cohesive bond failure in contrast to the PVA adhesive which failed largely in the adhesive mode. Shear strengths observed with the other, softer substrates were 12.2, 2.1, and 2.5 MPa for Douglas fir, medium density fiberboard, and particleboard, respectively, which were not significantly different than that of the PVA adhesive. These all showed high percentages of substrate failure, that is, the wood or composite failed before the adhesive bond.

The setting rate (shear strength vs time) of maple substrates bonded with MB adhesive was measured at 53% RH at 22 °C. Half of the maximum shear strength was obtained within an 8-h period while full strength was reached in 48 h.

To determine the uniqueness of the MB adhesive polysaccharide composition, the shear strengths of maple substrates bonded with aqueous mixtures of some commercially available polysaccharides were measured at 53% RH. Sodium carboxymethylcellulose, a synthetic cellulose derivative, and pullulan

showed shear strengths that were not significantly different than MB adhesive. Dextrin, a starch derivative, and sodium alginate were both significantly lower.

Long term performance, or durability, of adhesive joints is affected by environmental conditions such as humidity and temperature. Adhesives that resist these effects have more applications and are of greater value. Evaluation of the moisture resistance of MB adhesive-bonded maple substrates was performed after setting for one week at 53% RH and then an additional week at either 53% RH or 94% RH. Specimens subjected to the high humidity conditions gave shear strengths that were only 1% (0.2 MPa) of specimens subjected to the moderate humidity conditions (Table 1.3). In contrast, when subjected to the high humidity conditions, the PVA-based benchmark adhesive retained 72% of its moderate humidity strength. However, the partially acetylated MB-OAc adhesive showed a substantial improvement in moisture resistance under the high RH conditions and retained 35% of its shear strength (5 MPa) obtained at moderate humidity. The shear strength of MB-OAc at moderate RH was not significantly different than that of the native, nonderivatized MB adhesive. These results demonstrated that moisture resistance can be significantly improved through manipulation of polysaccharide structure.

1.2.2.4 Specialty Biopolymers Adhesive

Another bacterial exopolymer-based adhesive has been developed by Specialty Biopolymers Corporation (Bozeman, MT, USA) and has shown improved properties over the previously described MB adhesive for bonding wood substrates. The Specialty Biopolymers (SB) adhesive is composed of a polysaccharide of undisclosed structure with a molecular weight of 500 KDa

Table 1.3. Influence of relative humidity on shear strength of MB adhesive and its partially acetylated derivative. Reprinted from Int. J. Adhesion and Adhesives (Haag et al. 2004) with permission from Elsevier

Adhesive	Relative humidity (%)	Mean strength (MPa)	Percentage of strength achieved at 53% RH	Number of replicates	CV (%)	p-Value at 95% confidence level[a]
PVA	53	24.0		8	19	0.0004
PVA	53→94	17.2	72	10	6	
MB	53	16.3		8	23	
MB	53→94	0.2	1	3	12	
MB-OAc	53	14.4		8	24	0.29
MB-OAc	53→94	5.1	35	9	34	

[a] Probability based on two-tail student t-test that shear strength of candidate adhesive is significantly different from that of MB adhesive

and formulated as a 33% solution in water. A partially acetylated derivative of SB adhesive (SB-OAc) was also prepared by reaction with acetic anhydride and formulated in aqueous ethanol. Testing of shear strength of bonded wood blocks under compression was performed as described above in Sect. 1.2.2.3 using ASTM method D 905.

The shear strength of SB adhesive was first evaluated in a survey with two wood species and two composites at 53% RH and 22 °C. Maple substrates bonded with SB adhesive had a shear strength of 14.6 MPa which was 79% of that of a benchmark, interior grade PVA-based adhesive. The SB adhesive bond failed in the cohesive mode and also showed 18% wood failure. The corresponding PVA bond failed in the adhesive mode with 17% wood failure. Douglas fir bonded with SB adhesive showed a shear strength of 12.5 MPa which was 93% of the shear strength of the PVA benchmark adhesive. The SB adhesive-bonded specimens showed 79% wood failure. SB adhesive-bonded particleboard and medium density fiberboard showed 88 and 55% of the shear strength of the PVA adhesive, respectively. Shear strengths of the bonded composites were improved by initially performing a light surface sanding and resulted in no significant difference from that obtained with the PVA adhesive.

The set rate (shear strength vs time) was determined at two humidities, 53 and 23% RH, and at 22 °C. Shear strength reached a maximum in 48 h and half of maximum in 8 h at both RHs. However, the maximum shear strength at 23% RH was 50% higher than at 53% RH (20 and 14 MPa, respectively).

Moisture resistance of SB adhesive was studied in comparison to the PVA adhesive. After a one-week set at 53% (moderate) RH, bonded maple specimens were exposed to 94% (high) RH for increased times. The PVA adhesive retained 69% of its shear strength after four weeks exposure to high RH as compared to its initial shear strength at moderate RH (Fig. 1.4). SB adhesive retained only 9% of its shear strength after three weeks exposure to high RH as compared to its initial shear strength measured at moderate RH. The loss in bond strength of SB adhesive-bonded specimens upon exposure to high RH could not be avoided by performing the initial set at a lower RH (23%). These results are consistent with a reversible setting mechanism in which the shear strength is dependent on the water concentration in the adhesive bond. During the setting process, removal of water and increase in strength is driven by evaporation and absorption into the wood until equilibrium is established. Subsequently, moisture content in the bond and shear strength changes with relative humidity. The rate of that change depends on the mass and dimensions of the wood substrates which also absorb moisture and affect its mass transfer to the bond.

Based on the evidence that the bond strength of SB adhesive is limited by its interaction with water at high RH, the SB adhesive was chemically modified to impart a more hydrophobic character. Partial acetylation afforded a water-insoluble product, SB-OAc, which could be dissolved in aqueous ethanol for application. SB-OAc-bonded maple specimens which were set

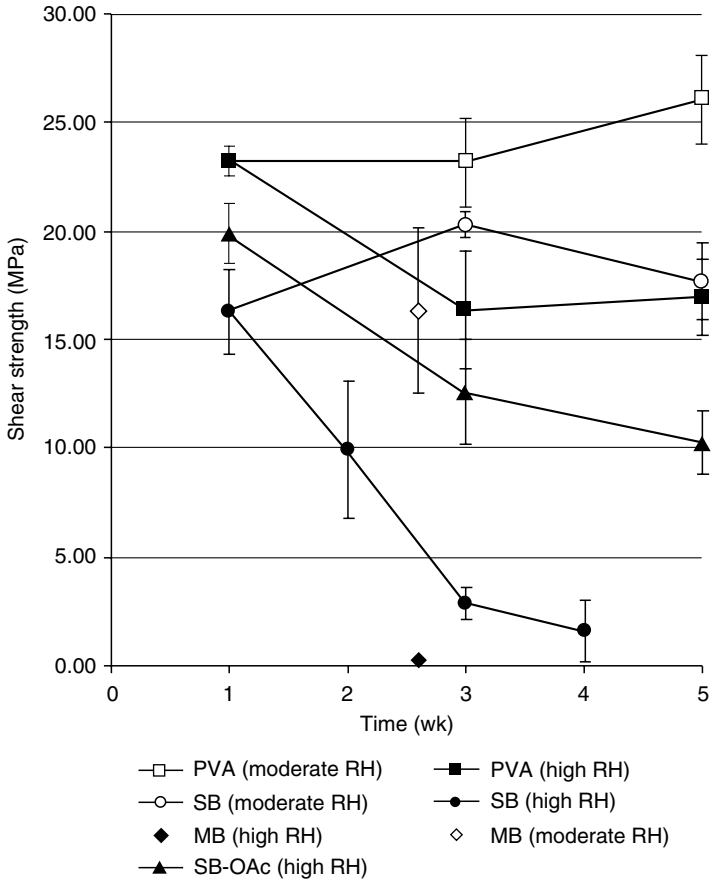

Fig. 1.4. The effect on shear strength of prolonged exposure of bonded maple substrates to high or moderate RH after an initial one-week set period at moderate RH. *Error bars* represent ±1 standard deviation. To facilitate comparison, MB data from Haag et al. (2004) is included. Reprinted from Int J Adhesion Adhesives (Haag et al. 2006), with permission from Elsevier

for one week at 53% RH showed a slightly higher shear strength than SB adhesive and 86% of that obtained with the PVA adhesive. At high RH, the SB-OAc bonded specimens retained 51% (10 MPa) of their initial strength at 53% RH (Fig. 1.4). Thus, these results support earlier observations in which partial acetylation effectively improved moisture resistance. Both of the acetylated derivatives of SB and MB adhesives, with the same degrees of acetylation (58–57%, respectively), showed substantial improvement in moisture resistance. However SB-OAc showed a significantly higher shear strength than MB-OAc at both moderate and high RH. This indicates that the extent to which acetylation affects moisture resistance is dependent on polysaccharide structure.

Overall, the performance of SB adhesive demonstrates that bacterially derived adhesives can possess shear strengths and setting rates at low to moderate humidities which may be suitable for construction of indoor wooden furniture and cabinetry.

1.2.3 Related Polysaccharide-based Adhesives

Starch is a polysaccharide that is widely used in paper-bonding applications. Cellulose derivatives (e.g., nitro- and ethylcellulose) have also been used for many years in organic solvent-based adhesives. It is useful to compare the mechanical properties of bacterial adhesives with those of polysaccharides from other sources in order to discern relationships between structure and performance.

1.2.3.1 Pullulan and Chitosan

Pullulan is a commercially available, high molecular weight, water soluble exopolysaccharide produced by the fungus *Aureobasidium pullulans*. It has been developed for various applications which exploit its mechanical and rheological properties, for example, films, fibers, coatings, and aqueous thickeners (Leathers 2003). Chitosan is an amine-functional polysaccharide soluble in dilute acid which is produced by deacetylation of chitin, a major component in crustacean exoskeletons, and is also found in the cell walls of the fungus *Mucor rouxii*. It is available commercially in large quantities from the former source.

Pullulan and chitosan were very briefly examined as wood adhesives by Mayer et al. (1990). Pullulan was prepared as a 50 wt% solution in water and chitosan was prepared as a 20 wt% solution in 2% aqueous acetic acid. Pine wood blocks were bonded with each adhesive, pressed, and allowed to dry. Shear strengths were 5 and 3 MPa for pullulan and chitosan, respectively, although setting conditions (time, temperature and relative humidity) were unspecified. The shear strength of a commercial PVA-based adhesive measured 5 MPa under the same conditions. These preliminary results indicate that pullulan, chitosan, and possibly other polysaccharides possess mechanical properties that may allow them to be effective adhesives although additional information such as moisture resistance is needed. These results are consistent with observations with other polysaccharides described in Sect. 1.2.2.3.

1.2.3.2 Konjac Glucomannan

Konjac glucomannan (KGM) is a polysaccharide extracted from the tuber of *Amorphohallus Konjac*, K Koch. It is a copolymer of glucose and mannose with β-1,4-linkages. An acetyl group is attached to 1 per 19 sugar units. KGM forms a gel in the presence of alkaline coagulant which causes deacetylation.

KGM has been used in many applications, including food and chemical engineering, and is commercially available. Chitosan, described above, was also investigated with KGM as a wood adhesive (Umemura et al. 2003).

Due to the high viscosity of its aqueous solutions, KGM (molecular weight 1200 KDa) adhesive was applied by first wetting the wood panels with water and then sprinkling on a measured amount of KGM powder. Chitosan (molecular weight 35 KDa, 80–90% degree of deacetylation) adhesive was prepared by dissolution in 1% aqueous acetic acid.

Shear strengths of three-ply plywood specimens were tested under tension. The veneers were composed of rotary-peeled lauan of 1.6 mm thickness and 9% moisture content. The bonded plywood assemblies were cold pressed at 1 MPa for 10 min followed by 15 min at 130 °C. The assemblies were cut into tensile shear specimens according to Japanese Industrial Standard K6851. Testing followed conditioning of the specimens at room temperature (relative humidity was not specified). For determination of moisture resistance, specimens were immersed in water at 30 °C for 3 h, cooled in water, and tested wet.

KGM-bonded plywood showed a maximum shear strength of 1.6 MPa with 30% wood failure under dry conditions. Under these conditions, a commercial urea-formaldehyde adhesive showed a shear strength of 1.8 MPa and 20% wood failure. It was also observed that higher shear strengths were obtained at lower KGM mixture concentrations. At the higher concentrations (10–20 wt%), a highly stable structure is known to form and as a result, the wettability of KGM to the veneer may be reduced. During the water-soak test for moisture resistance, the KGM-bonded plywood specimens delaminated. In contrast, the urea-formaldehyde adhesive showed a shear strength of 2.0 MPa and 30% wood failure. No difference in shear strength was observed between KGM formulated in alkaline solution or neutral water.

Chitosan-bonded plywood showed a maximum shear strength of 2.1 MPa with 20% wood failure under dry conditions. Best results were obtained at spread rates of 20–40% of that used for urea-formaldehyde. A shear strength of 1.7 MPa was obtained in the water soak test. Although the moisture resistance of chitosan was inferior to that of urea-formaldehyde (2.0 MPa), it was very good compared to other biopolymer-based adhesives, such as casein and soybean glues (0.9 and 0.6 MPa, respectively). Chitosan could be blended with KGM to increase its moisture resistance. In addition, a blend of the two was superior to either component alone at the same application rate under dry conditions.

1.2.3.3 Dopamine-crosslinked Chitosan

Enzyme catalyzed reactions of DOPA-containing proteins are responsible for the water resistant properties of adhesives produced by marine animals. There is evidence that the water resistance results from crosslinking of intermediate DOPA-derived quinones and primary amines of protein. Yamada et al. (2000) investigated the possibility that the enzyme catalyzed reaction of

dopamine (3,4-dihydroxyphenethylamine) could confer water resistance to an adhesive prepared from the commercially available, amine-containing polysaccharide, chitosan.

Adhesive solutions were prepared by mixing aqueous chitosan (0.5 % (w/v), 30 mmol/l in amine groups), adjusted to pH 6, with dopamine (10 mmol/l) and tyrosinase (60 U/ml). After mixing the adhesive components and standing for 24 h, the mixture was applied to cleaned glass slides with 6.25 cm^2 overlap area, pressed together with binder clips, immersed in water, and allowed to set at room temperature. After 24 h, the bonded assemblies were removed from the water, unclipped, and tested for shear strength using a mechanical testing machine under tension.

Initially, the viscosity of a mixture of chitosan, tyrosinase, and dopamine was monitored. The mixture developed 140,000 cP in 24 h (a 1000-fold increase) indicative of a crosslinking reaction. Testing of specimens bonded with the enzymatically treated chitosan/dopamine adhesive showed a shear strength of 0.45 MPa, whereas chitosan alone had no measurable shear strength under these conditions. In this study, a mixture of chitosan and glutaraldehyde, a known crosslinker for chitosan, was also tested and showed 0.3 MPa shear strength. These results indicate that tyrosinase and dopamine, and also other chemical crosslinkers, can confer water-resistant properties to chitosan. Although the shear strengths reported are relatively low, this may be due to the dilute concentrations of the adhesive solutions (0.5% chitosan) and underwater curing conditions.

1.3 Outlook

The observation of strong adhesion of bacterial biofilms to surfaces has led to exploration and development of bacterial exopolymers as potential commercial adhesives. Useful mechanical properties, in terms of adhesive strengths, have been observed on commercially relevant substrate materials. Most of the adhesives which have been studied are water-based and appear to be best suited for bonding porous surfaces such as wood which readily allow for water evaporation or absorption, required for setting in some cases. These adhesives are predominantly composed of polysaccharides which are high molecular weight polymers with polar functionalities, features which impart strong adhesion to high energy surfaces and high cohesive strength. There may be additional structural components contributing to adhesive strength which have not been characterized.

The polar functional groups of polysaccharides also impart a hydrophilic character and result in adhesive strengths that are sensitive to moisture. Approaches that have led to improved moisture resistance are 1) crosslinking (e.g., DOPA containing derivatives), 2) derivatization with more hydrophobic groups, such as acetate esters, and 3) blending with a moisture resistant

adhesive (e.g., phenol-formaldehyde). Although these approaches could be accomplished with synthetic additives (crosslinkers such as aldehydes, isocyanates, or epoxies), numerous synthetic modifications, or blending with synthetic adhesives, the benefits of using 100% bio-based adhesives are not fully realized. Ideally, natural biopolymers with latent crosslinking ability or increased hydrophobic character will be developed using modern biological and biochemical research methods.

Finally, biopolymers from various sources are being developed for other applications with unique requirements in addition to adhesion. For example, biocompatibility is essential for materials used in medical applications. Hydrogels derived from alginate have been very useful in wound care and tissue engineering where they provide desirable mechanical properties in a hydrophilic environment (Drury et al. 2004). Chitosan has been employed effectively as a tissue adhesive in which it was enzymatically crosslinked in situ (Chen et al. 2003). Thermoplastic polysaccharide derivatives have been employed as adhesive films to deliver drugs via the skin (Repka and McGinity 2001). In addition, chitosan has been used to produce films for pattern transfer in microelectronics applications (Wu et al. 2005). The pattern transfer operation employed a biomimetic electrochemical oxidation reaction using phenolic components similar to that observed in mussel adhesive. The use of biomaterials to produce micro- or nanostructured assemblies has been termed "biofabrication" (Wu and Payne 2004). These new applications demonstrate that valuable performance can be achieved via the polysaccharide structure. Bacterial exopolysaccharides possess structures and properties, including adhesion, that make them a potential source of materials for these applications. A task for scientists in the future is to produce these valuable materials in an economical way. The use of industrial bacterial fermentation processes in combination with biological engineering offers many advantages.

Acknowledgments. The author would like to thank Gill Geesey (Montana State University and Specialty Biopolymers Corporation) for reviewing the manuscript, Marc Mittelman and Harry Ridgway (Specialty Biopolymers Corporation), Peter Suci (Montana State University), and Joan Combie (Montana Biotech SE, Inc.) for their ideas and support in the development of bacterial exopolymer adhesives.

References

Born K, Langendorff V, Boulenguer P (2002) Xanthan. In: Steinbuchel A (ed) Biopolymers, vol 5. Polysaccharides I, polysaccharides from prokaryotes. Wiley-VCH, Weinheim, pp 259–297

Chemical Market Reporter (2005) 267:26

Chen T, Embree HD, Brown EM, Taylor MM, Payne GF (2003) Enzyme-catalyzed gel formation of gelatin and chitosan: potential for in situ applications. Biomaterials 24:2831–2841

Combie J, Haag A, Suci P, Geesey G (2004) Adhesive produced by microorganisms. In: Nelson W (ed) Agricultural applications of green Chemistry. ACS symposium series, vol 887. ACS, Washington, DC, pp 53–62

Costerton JW, Stewart PS (2001) Battling biofilms. Sci Am 285:3–9
Drury JL, Dennis RG, Mooney DJ (2004) The tensile properties of alginate hydrogels. Biomaterials 25:3187–3199
Dufrene YF (2002) Atomic force microscopy, a powerful tool in microbiology. J Bacteriol 184:5205–5213
Flemming HC, Wingender J (2001) Relevance of microbial extracellular polymeric substances, part I. Structural and ecological aspects. Water Sci Technol 43:1–8
Gross RA, Kalra B (2002) Biodegradable polymers for the environment. Science 297:803–807
Haag AP, Maier RM, Combie J, Geesey GG (2004) Bacterially derived biopolymers as wood adhesives. Int J Adhesion Adhesives 24:495–502
Haag AP, Geesey GG, Mittelman MW (2006) Bacterially derived wood adhesive. Int J Adhesion Adhesives 26:177–183
Kawakami M, Byrne K, Khatri B, Mcleish TCB, Radford SE, Smith DA (2004) Viscoelastic properties of single polysaccharide molecules determined by thermally driven oscillations of an atomic force microscope cantilever. Langmuir 20:9299–9303
Klapper I, Rupp CJ, Cargo R, Purvedorj B, Stoodley P (2002) Viscoelastic fluid description of bacterial biofilm material properties. Biotech Bioeng 80:289–296
Labare MP, Guthrie K, Weiner RM (1989) Polysaccharide exopolymer adhesives from periphytic marine bacteria. J Adhesion Sci Technol 3:213–223
Lazaridou A, Biliaderis CG, Kontogiorgos V (2003) Molecular weight effects on solution rheology of pullulan and mechanical properties of films. Carboh. Polymers 52:151–166
Leathers TD (2003) Biotechnological production and applications of pullulan. Appl Microbiol Biotechnol 62:468–473
Mayer JM, Greenberger M, Ball DH, Kaplan DL (1990) Polysaccharides, modified polysaccharides and polysaccharide blends for biodegradable materials. Polymeric materials: science and engineering. Proceedings of ACS Division of Polymer Science and Engineering, vol 63. ACS, Washington, DC, pp 732–735
McDermott MK, Chen T, Williams CM, Markley KM, Payne GF (2004) Mechanical properties of biomimetic tissue adhesive based on the microbial transglutaminase-catalyzed crosslinking of gelatin. Biomacromols 5:1270–1279
Pocius AV (1991) Adhesives. In: Kroschwitz JI (ed) Encyclopedia of chemical technology, 4th edn, vol 1. Wiley, New York, pp 445–466
Repka MA, McGinity JW (2001) Bioadhesive properties of hydroxypropylcellulose topical films produced by hot-melt extrusion. J Controlled Release 70:341–351
Sutherland I (2002) A sticky business. Microbial polysaccharides: current products and future trends. Microbiol Today 29:70–71
Umemura K, Inoue A, Kawai S (2003) Development of new natural polymer-based wood adhesives I: dry bond strength and water resistance of konjac glucomannan, chitosan, and their composites. J Wood Sci 49:221–226
Weimer PJ, Conner AH, Lorenz LF (2003) Solid residues from *Ruminococcus* cellulose fermentations as components of wood adhesive formulations. Appl Microbiol Biotechnol 63:29–34
Weimer PJ, Koegel RG, Lorenz LF, Frihart CR, Kenealy WR (2005) Wood adhesives prepared from lucerne fiber fermentation residues of *Ruminococcus albus* and *Clostridium thermocellum*. Appl Microbiol Biotechnol 66:635–640
Wu LQ, Payne GF (2004) Biofabrication: using biological materials and biocatalysts to construct nanostructured assemblies. Trends Biotechnol. 22:593–599.
Wu LQ, Ghodssi R, Elabd YA, Payne GF (2005) Biomimetic pattern transfer. Adv. Funct. Mater. 15:189–195
Yamada K, Chen T, Kumar G, Vesnovsky O, Topoleski LDT, Payne GF (2000) Chitosan based water-resistant adhesive. Analogy to mussel glue. Biomacromols 1:252–258

2 The Molecular Genetics of Bioadhesion and Biofilm Formation

Paolo Landini[1], Gregory Jubelin[2], and Corinne Dorel-Flamant[2]

2.1 Biofilm Formation and its Regulation

In natural habitats, microorganisms are often found attached to solid surfaces and organized in structured communities known as biofilms. Such communities are characterized by the presence of a large number of different bacterial species, usually associated with eukaryotic microorganisms, typically in close contact with a surface, either organic or abiotic. A striking feature of many biofilms is the extensive production of an extracellular matrix (extracellular polymeric substance, EPS), which is mainly composed by complex polysaccharides and proteins, although high content of extracellular DNA has also been reported, for instance for biofilms formed by *Pseudomonas aeruginosa* (Whitchurch et al. 2002). This form and organization differ significantly from the planktonic state of bacteria, i.e. free-living cells, which is the condition mostly studied in the laboratory (Costerton et al. 1995). The tightly associated cells constituting a bacterial biofilm are able to coordinate their physiological and metabolic state, thus almost resembling the subdivision of functions of a multicellular organism (Costerton et al. 1995; Shapiro 1998; Caldwell 2002).

Transition from the single-cell (planktonic) mode of growth to a complex structure such as the biofilm occurs in a sequential, developmental process (Stoodley et al. 2002; Reisner et al. 2003). The process of adhesion to a surface, i.e. the first step of biofilm formation, is strongly affected by physico-chemical properties of both bacterial cells and surfaces, such as electric charge and hydrophobicity; often bacteria have to overcome electric charge repulsion in order to attach to a surface (Jucker et al. 1996). Upon adhesion, bacteria might sense contact with the surface and induce specific gene expression, leading to further development of the biofilm (Davies et al. 1993; Sauer and Camper 2001; Otto and Silhavy 2002; Wang et al. 2004). In the presence of environmental conditions allowing bacterial growth, attached cells can divide and form a microcolony. Establishment of stronger cell-cell contacts allows the

[1] Dipartimento di Scienze Biomolecolari e Biotecnologie, Università di Milano, Via Celoria 22, 20133 Milano, Italy
[2] Unité de Microbiologie et Génétique UMR CNRS 5122 composante INSA, 10, rue Dubois, 69 622 Villeurbanne CEDEX, France

Biological Adhesives
(ed. by A.M. Smith and J.A. Callow)

microcolony to differentiate finally into a mature biofilm whose three-dimensional structure is in part determined by the amount and nature of the produced EPS (Ghigo 2003). Formation, maturation and maintenance of the biofilm are achieved through expression of specific genes in response to a variety of environmental and physiological signals. It seems obvious that extracellular structures are essential for adhesion to a surface; indeed, most of identified factors are linked to the cell's outer membrane (Davies and Geesey 1995; Prigent-Combaret et al. 1999; Otto and Silhavy 2002). For almost all the adhesins so far identified as important in biofilm formation, corresponding regulatory cues and environmental signals leading to their expression have been characterized. Indeed, gene expression regulation of biofilm determinants often requires a combination of different environmental signals, which can modulate the activity of complex regulatory networks of both specific and global regulators. In this chapter, after an overview of some general regulatory pathways controlling biofilm-related gene expression, we will focus our attention on one model systems: the curli, adhesion fibers of Enterobacteria regulated through a complex interplay of environmental signals and regulatory proteins. Finally, we will introduce a second model system, i.e. regulation of exopolysaccharides via the accumulation of the di-c-GMP signal molecule, a form of gene expression regulation at the enzyme activity level.

2.1.1 Environmental Factors Leading to Biofilm Formation

Bacterial genes are mainly regulated at the level of transcription; external stimuli or stresses can induce regulatory responses and alter the pattern of gene expression. Many transcription factors can modify gene expression according to environmental conditions, and several of these regulatory factors are known to influence biofilm formation. For instance, temperature regulation plays a role in the expression of several biofilm determinants, and in pathogenic bacteria this regulation is linked to sensing the host (up-regulation at host temperature) or to the detachment from the host (up-regulation at lower temperatures; see also in the "Global regulators" and "Curli" sections) such as in the case of the *Yersinia pestis hms* (haemin storage) genes (Perry et al. 2004), which are expressed at a temperature lower than 33 °C. Temperature, in combination with other stimuli, controls the expression of fimbrial adhesion determinants: *Vibrio cholerae* expresses TCP (toxin-co-regulated pilus, belonging to the Type IV pili group) in the host intestinal surface, whereas attachment to borosilicate at lower temperatures is mediated by the mannose-sensitive hemagglutin (MSHA) pilus (Watnick et al. 1999). Nutrient availability can also influence biofilm formation, and opposite effects have been reported in different bacterial species. For instance, *E. coli* biofilm formation was found to be repressed by the presence of nutrients, such as glucose (Jackson et al. 2002), which on the contrary promotes biofilm formation of enteroaggregative *E. coli* (Sheikh et al. 2001) and of

Salmonella enteritidis (Bonafonte et al. 2000). Glucose-mediated modulation of biofilm formation appears to take place through two molecular mechanisms: transcription regulation by the cAMP/CRP regulon or by its Vfr protein counterpart in *Pseudomonas aeruginosa* (Vasil and Ochsner 1999; Whitchurch et al. 2005), and by translational regulation mediated by the *csrA* protein, which represses the expression of exopolysaccharide biosynthetic genes such as the *pga* operon by binding to its mRNA (Wang et al. 2005).

Availability of iron and presence or absence of oxygen are also crucial factors for biofilm formation; indeed, anoxia negatively affects initial adhesion in *E. coli* K12 (Landini and Zehnder 2002) and surface colonization in *Pseudomonas* species via inhibition of cellulose biosynthesis (Spiers et al. 2003). In *P. aeruginosa*, iron acts as the signal for induction of adhesion genes at high intracellular concentrations, while low iron concentration results in increased twitching motility, which in turn inhibits surface attachment (Bollinger et al. 2001).

Expression of exopolysaccharides such as alginate and colanic acid, and of the OmpX protein are triggered by surface adhesion (Davies and Geesey 1995), in agreement with the observations that these factors are mainly involved in later stages of biofilm formation (Davies and Geesey 1995; Danese et al. 2000; Prigent-Combaret et al. 2000; Otto and Silhavy 2002). However, the signal transduction pathway triggered by interaction with a surface has yet to be identified.

2.1.2 Quorum Sensing

Quorum sensing allows bacterial cells to activate the expression of a large number of genes in response to cell density, and one of its functions is the cell's adaptation to a biofilm lifestyle. While gene regulation by quorum sensing is common to both Gram-positive and Gram-negative bacteria, the molecular mechanisms for gene regulation differ substantially. In Gram-negative bacteria, gene activation is mediated by the production of low molecular weight pheromones, so-called autoinducers, freely diffusible through the membrane due to the presence of a fatty acid moiety. Arguably, the most important autoinducers belong to the chemical class of the acyl-homoserine lacton family (acyl-HSLs) (Fuqua et al. 1994). In contrast, short peptides, synthesized by the ribosomes and often subjected to extensive post-translational modification, act as quorum sensing signal molecules in Gram-positive bacteria, where they trigger signal transduction via a two-component regulatory system (Miller and Bassler 2001; Li et al. 2002). For both Gram-positive and Gram-negative bacteria pheromone accumulation enables the cell to sense that a sufficient local concentration of bacteria (quorum) has been reached to initiate a concerted population response. Quorum sensing plays a direct role in biofilm formation and maintenance via regulation of exopolysaccharide biosynthesis (e.g. rhamnolipids in *Pseudomonas aeruginosa*) and is involved

in several important biological processes, such as competence (in Gram-positives), plasmid conjugative transfer, iron uptake, production of virulence factors and secondary metabolites, as well as adaptation and survival in stationary phase. Acyl-homoserine lactone signal molecules are produced during infection by *P. aeruginosa* isolates from lungs of cystic fibrosis patients (Singh et al. 2000), as well as by biofilms growing on urethral catheters (Stickler et al. 1998). *Pseudomonas* strains lacking the autoinducer produce thinner, less structured biofilms which are more susceptible to biocides (Davies et al. 1998). These observations suggest that quorum sensing might be a possible target for prevention of biofilm formation, possibly in association with more classical antimicrobial agents (Hentzer et al. 2003). Within the biofilm, quorum sensing-dependent genes are expressed at higher levels in cells near the surface, and expression decrease with the height of the biofilm (de Kievit et al. 2001). Thus, quorum sensing appears to be required for the differentiation of individual cells to a complex multicellular structure and differentiation of the mature biofilm. Although quorum sensing clearly plays a pivotal role in global gene expression regulation, cell density signals are integrated by additional signals depending on physiological and environmental conditions, allowing to finely tune gene expression in response to the different needs; for instance, iron limitation and the nutritional status of the cells can affect, and even override, quorum sensing regulation (Bollinger et al. 2001). Interestingly, despite such a wide conservation among bacteria, the main quorum sensing systems appear to be missing in *E. coli*, although there is evidence for the existence of the autoinducer-2 signal, a cleavage product of *S*-ribosyl-homocysteine found in a large number of bacterial species (Schauder et al. 2001).

2.1.3 Global Regulators

The integration of environmental, cellular and physiological signals necessary for finely tuned modulation of biofilm gene expression corresponds to complex regulation at the molecular level. In addition to specific regulators, expression of genes encoding for microbial adhesion and biofilm formation factors is under the control of global regulatory proteins, which link gene expression to the general physiological status of the cell. For instance, Type I pili are regulated by a specific protein, PapI, whose transcription is in turn under the control of the Lrp (Leucine Responsive Protein) global regulator (van der Woude et al. 1992), a sensor of amino acid intracellular concentration. This feature of "tandem regulation" including specific regulatory proteins and global effectors tends to be extremely common; curli fibers are also regulated by the specific activator CsgD and by the histone-like protein H-NS (see the "Curli" section of this chapter). Most global regulators display a loose degree of specificity in DNA binding and regulate transcription of many genes by modifying the architecture of their regulatory regions, often in

concerted fashion with more specific regulators. In addition to the already cited proteins H-NS and Lrp proteins, global regulators include the integration host factor IHF, the general nucleoid-associated protein Fis, the HU proteins and several others (Vicente et al. 1999).

The H-NS protein, a global regulator and chromosome organizer able to bind to DNA regions with an intrinsic curvature (bent DNA), appears to have a direct relationship with biofilm formation. H-NS is able to inhibit formation of complexes between promoters and $E\sigma^{70}$-RNA polymerase (the main form of RNA polymerase during the exponential phase of growth). Binding of H-NS to several bacterial promoters depends on the bending of the promoter regions, more than to specific sequences (Spurio et al. 1997). However, RNA polymerase associated with σ^S, an alternative σ factor mainly active in stationary phase of growth, can by-pass H-NS inhibition. This effect by the H-NS protein is called exponential silencing and also takes place at the *csgBA* promoter, thus preventing transcription of the structural units of curli subunits during exponential phase of growth (Arnqvist et al. 1994). In *E. coli* strains unable to produce curli, *hns* mutants display better adhesion properties when grown in anaerobic conditions. H-NS inhibition of adhesion is mediated by lower LPS and FliC (flagellin) production, which can act as negative determinants for initial attachment to hydrophilic surfaces (Landini and Zehnder 2002). Negative regulation by H-NS can be temperature-dependent, i.e. H-NS can act as a temperature sensor for the bacterial cell. This was clearly shown at the *virF* promoter by DNA binding experiments with H-NS (Falconi et al. 1998): DNA bending depends on the temperature, which thus modulates H-NS binding affinity to the *virF* promoter region of *Shigella flexneri*, a pathogenic enterobacterium; the VirF protein activates an expression cascade leading to production of virulence factors. At temperatures up to 32 °C, strong bending of DNA allows H-NS binding and formation of a rigid loop structure not accessible to RNA polymerase. At higher temperatures (i.e. around the host temperature of 37 °C), the loop structure becomes unstable and the repression effect by H-NS cannot any longer take place, leading to *virF* transcription. Although the *virF*-dependent virulence factors so far identified are not involved in adhesion, it is likely that host colonization factors in pathogenic bacteria might be regulated in a similar fashion.

The alternative σ^S subunit of RNA polymerase (encoded by the *rpoS* gene and therefore also called RpoS protein) also appears to affect biofilm formation directly, although its precise role is still controversial. RpoS controls the expression of many genes during the stationary phase of growth and is considered to be the master regulator of the general stress response in *E. coli* (Hengge-Aronis 1999). Thus, its role in biofilm formation would be consistent with the observations that biofilms take place more readily in stationary phase of growth or in non-optimal growth conditions (Prigent-Combaret et al. 2001; Landini and Zehnder 2002). In *Pseudomonas aeruginosa*, the quorum sensing system is related to RpoS expression through mutual control (Latifi et al. 1996; Whiteley et al. 2000). Indeed, *rpoS* mutants of *E. coli* build

thinner biofilms when grown in continuous cultures (Adams and McLean 1999). Schembri et al. found 46% of RpoS-dependent genes to be differently expressed in biofilms and deletion of *rpoS* rendered *E. coli* incapable of establishing sessile communities (Schembri et al. 2003). Additional information on regulation of biofilm genes by *rpoS* comes from different studies performed on *rpoS* mutants of *E. coli* in various growth conditions and genetic backgrounds (Lacour and Landini 2004; Patten et al. 2004; Weber et al. 2005). Several adhesin-encoding genes, such as the curli-encoding *csg* genes, as well as genes of unknown function known to be differently expressed in biofilms, such as *yddX*, were found to be *rpoS*-regulated. In contrast, other investigators reported that expression of RpoS in *P. aeruginosa* is repressed in biofilms, and *rpoS*-deficient mutants not only formed better biofilms than wild type cells but were more resistant to antimicrobial treatment (Whiteley et al. 2001). Consistent with a possible negative role of RpoS in biofilm formation are the observations that *rpoS* negatively affects expression of Type 1 fimbriae in *E. coli*, also factors for biofilm formation (Dove et al. 1997). Thus, it is possible that RpoS can play both a negative and a positive role in biofilm formation depending on biofilm determinant and growth or environmental conditions. Different and even opposite effects might take place in different bacteria, or even in bacterial strains with different genetic background. Indeed, it is interesting that the *tnaA* gene is negatively regulated by *rpoS* in MC4100 (Patten et al. 2004) and positively regulated in MG1655 (Lacour and Landini 2004). The *tnaA* gene encodes tryptophanase, which turns tryptophan into indole, which has been shown to be a biofilm-promoting signal molecule in enteropathogenic *E. coli* (Martino et al. 2003). Thus, a functional *rpoS* gene might both stimulate and prevent indole-dependent biofilm formation.

2.2 A Case of Complex Regulatory Control: The Curli Factors (Thin Aggregative Fimbriae) of Enterobacteria

2.2.1 Curli Fibers: A Major Determinant for Biofilm Formation in Enterobacteria

Curli (Fig. 2.1) were first described by Olsen and his colleagues in 1989 using *E. coli* isolates taken either from cows suffering from mastitis or from bovine faecal material (Olsen et al. 1989). All the isolates able to form a complex with the serum protein fibronectin in vitro also produced an extracellular structure made up of fine amyloid fibres, named curli (Chapman et al. 2002). These observations were soon followed by a description of fimbriae with a similar appearance in *Salmonella enterica* serotype Enteridis (Collinson et al. 1991). A comparison of the genetic and morphological characteristics of these surface structures confirmed that there was close homology between them (Collinson et al. 1996; Romling et al. 1998). Since then the term “curli” has

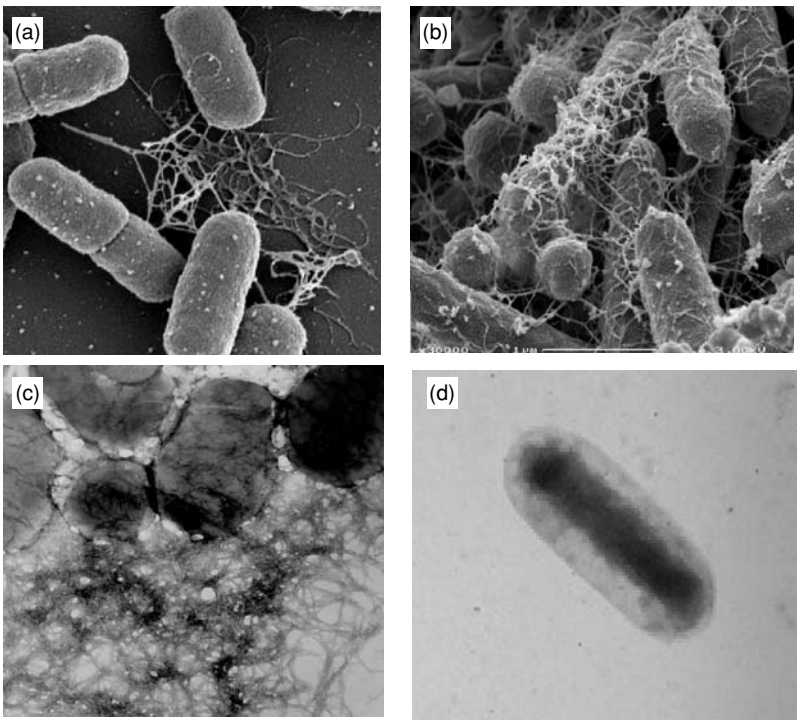

Fig. 2.1. Morphological structure of curli in *E. coli*. Scanning electron microscopy (SEM): (a) cell-to-surface interaction; (b) cell-to-cell interactions; (c) negative staining of MG1655 *ompR234*; (d) *csgA*- derivative (strains described in Prigent-Combaret et al. 2000)

been used for the structure previously described as "thin aggregative fimbriae" (=SEF17 or "Tafi") in *Salmonella*.

Curli production occurs in several enterobacteria, including *E. coli*, *Salmonella enterica*, *S. typhimurium* and *Citrobacter* spp. *enterica* (Collinson et al. 1991; Zogaj et al. 2003). The presence of curli has been observed in different groups of *E. coli* (Hammar et al. 1995; Cookson et al. 2002) and, in particular, in enteropathogenic isolates from different geographical locations (Collinson et al. 1991). Curli production by *E. coli* 0157:H7 is uncommon but it can occur in association with *csgD* promoter point mutations (Uhlich et al. 2001). Many of sepsis-inducing *E. coli* strains both in humans (Bian et al. 2000) and in birds also produce curli (Maurer et al. 1998). The ability of 71 strains of *Salmonella enterica* originating from produce, meat or clinical sources to form biofilms was investigated by Solomon et al. They found that all clinical isolates and meat-related isolates, and a total of 80% of the produce-related isolates produced curli (Solomon et al. 2005). Likewise, several *E. coli* K12 strains do not produce curli, even though they have the genetic material needed (Olsen et al. 1993b). So, the genes required for curli synthesis

seem to be widely distributed in enterobacteria. However, the expression of these genes, and thus the production of curli fibers, seems to be determined by the environmental micro-niche normally occupied by the bacteria. Production of curli can be visualized directly through electron microscopy (Fig. 2.1).

The genes involved in curli synthesis are grouped in the same genetic locus in two distinct and divergently transcribed operons (Hammar et al. 1995). The first operon contains the *csgB*, *csgA* and *csgC* genes. The function of the *csgC* gene (or *orfC*) is still unknown (Hammar et al. 1995). Whilst CsgA is secreted into the extracellular medium in a soluble form, CsgB, which is located on the surface of the bacterial envelope, induces a conformational change in CsgA which triggers off its polymerisation into curli (Hammar et al. 1996). The second operon includes the genes *csgD*, *csgE*, csgF and *csgG* which code, respectively, for a transcriptional regulator of the LuxR family and for three proteins required for the secretion and assembly of curli. The *csg* locus organization and the role of some of the curli structural and transport subunits are shown in Fig. 2.2. The CsgD protein is an essential activator for the transcription of the *csgBA* operon. CsgG is a lipoprotein attached to the external membrane which assures the stability of the monomers CsgA and CsgB and their passage across the external membrane (Loferer et al. 1997). The CsgF protein seems to have a particular effect on nucleation and, similarly, the CsgE protein facilitates the nucleation of the CsgA protein and also renders it more stable (Chapman et al. 2002). Upon in vitro incubation of the monomers CsgA-His at 4 °C, Chapman and his colleagues were able to observe the spontaneous formation of fibres adopting a structure rich in β folded layers typical of amyloid fibres which fix Congo red in the same way as curli do (Chapman et al. 2002). Hence the main function of the secretion system and the assembly of the curli fibres may be to block the polymerisation of CsgA inside the cell and to speed it up at the cell surface.

2.2.2 Conditions for the Expression of Curli

Enterobacteria normally colonise the gastro-intestinal system of mammals but they can also live for a considerable length of time in the environment. Favourable conditions for curli production are more often present outside the digestive tract. In fact these attachment structures are synthesised by bacteria grown to the stationary phase in a medium with low osmolarity and at a temperature below 32 °C (Olsen et al. 1989, 1993a). The transcription of the curli operons also varies according to the oxygen concentration of the medium, certain nutrient deficiencies (phosphate and nitrogen), low levels of iron, pH and the presence of ethanol (Gerstel and Romling 2001). These are the conditions established for the strains of *E. coli* and Salmonella spp. that have been most extensively studied but there are also numerous examples of isolates producing curli in different conditions from these. For example, curli

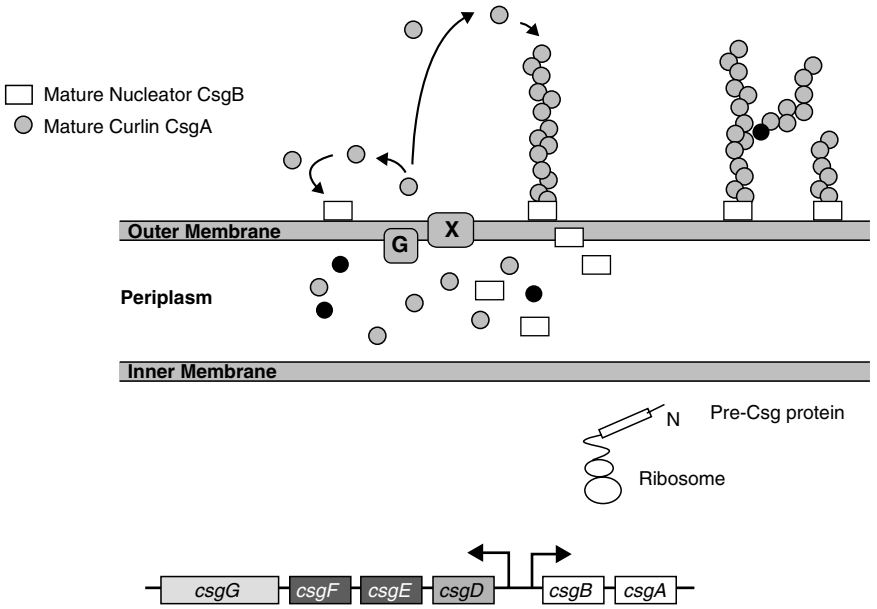

Fig. 2.2. Organization of the *csg* genes and curli biosynthesis. The genes necessary to curli biosynthesis are grouped in two divergent operons (*arrows* show direction of transcription). The CsgB and CsgA monomers cross the cytoplasmic membrane due to the presence of a signal peptide of 20 amino acids. CsgG is a lipoprotein which allows translocation of curli monomers across the outer membrane with a still unknown mechanism. The CsgB protein, localized at the cell surface, can induce a conformation change in CsgA leading to its polymerisation. Modified from Soto and Hultgren (1999)

produced by strains in the EcoR collection were analysed at 26 and at 37 °C. This collection brings together a group of natural *E. coli* isolates from various hosts and from very different geographical locations. Out of 72 isolates, 42 formed curli at 26 °C, 13 both at 26 and at 37 °C, one isolate produced curli at 37 °C only and 16 isolates did not produce curli in any of the conditions tested (Olsen et al. 1993b). In certain K-12 strains lack of curli expression can be explained by the presence of an amber mutation in the *rpoS* gene, the gene which codes for the sigma S factor necessary for the transcription of *csg* genes. Other examples of changes in expression patterns have been described, particularly in pathogenic strains, where curli gene transcription can be independent of temperature and osmolarity but is affected by phase variation (Uhlich et al. 2002; Kim and Kim 2004).

As for the majority of virulence factors, the regulation of curli synthesis is extremely complex and depends on several environmental parameters. This section details all the mechanisms currently known to participate in the regulatory control network of curli production in *E. coli* and *S. typhimurium*. Figure 2.3 summarizes the role of the main players in curli regulation.

2.2.3 Regulation by Osmolarity

At low osmolarity, the small proportion of phosphorylated OmpR protein (OmpR-P) is sufficient to ensure transcription of the *csgDEFG* operon (Romling et al. 1998; Vidal et al. 1998). OmpR-P binds just upstream of the –35 and –10 boxes of the operon promoter *csgDEFG*, allowing its transcription (Prigent-Combaret et al. 2001; Gerstel et al. 2003). The transcriptional regulator CsgD in turn stimulates transcription of the *csgBA* operon and, thus, curli production, possibly by binding to an 11-bp sequence immediately upstream of the –35 element of the *csgB* promoter (Brombacher et al. 2003). If the osmolarity of the medium increases, the transcription of the two operons is suppressed. The two-component system of CpxA/CpxR and the global regulator H-NS form the basis of the *csg* gene regulation by osmolarity in *E. coli* (Dorel et al. 1999; Jubelin et al. 2005). It appears that the repression of curli at high osmolarity is not governed by the same mechanisms if the increased osmolarity is due to increased salt (NaCl) or sugar (sucrose) concentration. Thus, *E. coli* is able to distinguish the nature of the osmolyte. In a strong salt concentration the Cpx pathway is activated and the phosphorylated form of the CpxR regulator (CpxR-P) accumulates in the cell. By means of multiple binding sites in the regulatory region of the two curli operons, CpxR-P establishes a gradual repression dependent on the osmolarity level in the cell. However, when the high osmolarity is caused by an accumulation of sucrose, the repression of the curli genes is independent of CpxR and it is the global regulator H-NS which ensures the suppression of transcription.

It might be interesting to note that curli regulation by osmolarity is different in *S. typhimurium*. The repressor function of the CpxR and H-NS proteins

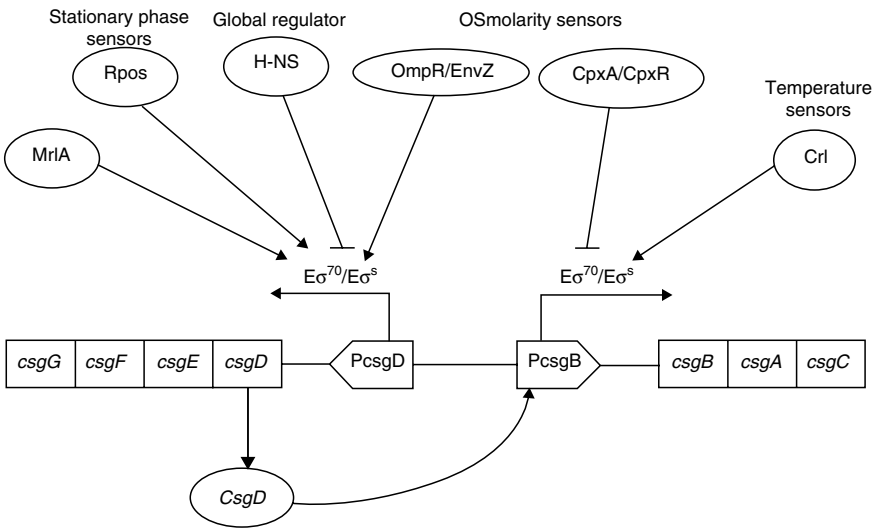

Fig. 2.3. Model of complex regulation of the curli operons. See text for details

has not yet been studied in high osmolarity conditions in *S. typhimurium*. Furthermore, as well as having an activator effect on the transcription of the *csgDEFG* operon, OmpR also seems to be able to play a repressor role in certain conditions. Gerstel et al. have shown that over-production of the constitutively active protein OmpR D55E leads to repression of curli synthesis in *S. typhimurium*. Indeed, the promoter region of the *csgDEFG* operon contains several OmpR binding sites identical to the region of the *ompF* gene where both activation and repression are ensured by OmpR (Lan and Igo 1998; Gerstel et al. 2003).

2.2.4 Regulation According to the Bacterial Growth Phase

Quantification of the CsgA transcripts in the *E. coli* strain HB101 (pCRL20) has shown that messenger RNA accumulates during the period when the metabolic rate has slowed down, usually referred to as the "stationary growth phase" (Arnqvist et al. 1992). Thus, transcription of the *csgBA* operon occurs mainly at the beginning of the stationary growth phase. Indeed, adaptation to slow metabolism modifies the expression of a large number of genes in order to respond to nutrient deficiency conditions (Pratt and Silhavy 1998; Lacour and Landini 2004). A lot of these genes have a promoter that is specifically recognised by the sigma S factor (σ^S or RpoS). When the bacterial culture enters into the stationary phase, RpoS accumulates in the bacteria and can assemble with the $\alpha_2 \beta\beta$ 'subunits, which form the core RNA polymerase (also called E), to initiate transcription of σ^S-dependent genes. Olsen et al. have shown that the transcription of curli genes depends on the σ^S factor since it does not take place in an *rpoS* mutant strain, consistent with production of curli exclusively during the stationary growth phase (Olsen et al. 1993b). However, regulation does not seem to be this simple. In fact, mutations inactivating the *hns* gene restore curli production in an *rpoS* mutant; however, curli expression retains dependence on stationary phase of growth (Arnqvist et al. 1994). These results demonstrate that the promoters of the curli operons can be recognized by a sigma factor other than RpoS (probably σ^{70}). In the *rpoS* mutant strains, absence of σ^{70}-dependent transcription would be caused by specific repression by H-NS. However, the observation that curli gene regulation by the growth phase is retained in the *rpoS* mutant shows that induction of transcription in the stationary growth phase is not simply due to σ^S. Other, as yet unknown, mechanisms are undoubtedly involved in this regulatory process.

2.2.5 Thermoregulation

In an environment characterized by weak osmolarity, curli production in K-12 strains of *E. coli* occurs at 26–30 °C whereas it is suppressed at 37 °C. This temperature control is absent in several strains of *E. coli,* and notably in the bacteria that are pathogenic to humans which can produce curli at 37 °C. Bypass

of temperature regulation can be obtained in *S. typhimurium* by substituting a single nucleotide in the promoter region of the *csgDEFG* operon (Romling et al. 1998). A model of the mechanism responsible for thermoregulation in *E. coli* K-12 has recently been proposed and it involves both the Crl and RpoS proteins. The Crl protein, whose production is thermoregulated, interacts with σ^S and strengthens the binding of the $E\sigma^S$ complex to the promoter of the *csgBA* operon (Bougdour et al. 2004). At 30 °C there is up to 30 times more Crl in the cell, compared with the amount present at 37 °C. This regulation must take place post-transcriptionally, since the level of *crl* mRNA is not affected by temperature (Arnqvist et al. 1992). Through its interaction with RpoS, the accumulation of Crl at 30 °C leads to an increase in the affinity of the RNA polymerase to the promoter sequences of the curli operon. This mechanism results in a fourfold increase in the transcription of the *csgBA* operon at 30 °C, compared with 37 °C. The Crl effect is not specific to curli operons and it is present in numerous other genes regulated by RpoS (Pratt and Silhavy 1998). Moreover, this activation of RpoS by Crl is co-ordinated with a second thermoregulation mechanism which results in an increase in RpoS synthesis at low temperatures. The regulatory RNA *dsrA,* whose amount is higher at lower growth temperatures due to increased production and stability, stimulates the translation of *rpoS* messenger RNA (Repoila and Gottesman 2001). Thus, two mechanisms which control the thermoregulation of curli genes have been found and they are both dependent on RpoS. Nevertheless, curli production in the double *rpoS hns* mutant is still regulated by temperature, as seen in the wild-type (Arnqvist et al. 1994). This form of regulation is independent of Crl, since this protein does not affect $E\sigma^{70}$ binding to the *csgBA* promoter (Bougdour et al. 2004). These results suggest that other thermoregulatory mechanisms must be involved in curli regulation.

2.2.6 Regulation as a Result of Oxygen Concentration

The expression of the *csgDEFG* operon in *S. typhimurium* can vary by a factor of 3.5 in relation to the concentration of oxygen (Gerstel and Romling 2001). In a rich culture medium, the highest expression level of *csgD* has been found to be in a micro-aerobic atmosphere (approximately 5% oxygen). Surprisingly, maximum expression of *csgD* is obtained in aerobic conditions in a minimum medium. Hence, oxygen availability influences curli expression via a mechanism that is still poorly understood but which depends on the level of nutrients in the culture medium. However, experiments have shown that the expression level of csg*D* is reduced by 70% in micro-aerobic conditions in an *ihf* mutant (Gerstel et al. 2003). In addition, IHF interacts directly with two sites in the promoter region of the *csgDEFG* operon. As a result of extensive work on in vitro binding by IHF, H-NS and OmpR regulators to the *csgD* promoter, Gerstel et al. proposed a model explaining the increase in *csgD* expression observed in micro-aerobic conditions during culture in a rich medium. In aerobic condi-

tions OmpR binds to the *csgD* promoter at several sites and, notably, at many which are responsible for a suppression of *csgD* transcription. The DNA region where the OmpR "repressor sites" are located also includes several binding sites for the IHF protein. In micro-aerobic conditions IHF can outcompete OmpR and bind to the *csgD* promoter. The repression induced by OmpR is lifted and IHF facilitates the start of transcription (Gerstel et al. 2003).

2.2.7 Other Regulatory Systems

Regulatory mechanisms affecting curli synthesis in response to environmental signals such as iron deficiency still need to be identified. By the same token, it has been shown that inactivation of different genes coding for regulatory proteins results in a modification of *csg* gene expression. Even if a direct interaction has not always been demonstrated, the genetic results suggest that these regulators are an integral part of the network controlling curli production. This is the case, for example, for the RcsC/RcsB two-component system (Ferrieres and Clarke 2003; C. Dorel, unpubl. data). The Rcs system plays a role in curli regulation in response to a disruption of the cell envelope. This system is also known to respond to variations in osmolarity, to the extracellular concentration of divalent ions, such as magnesium, and to attachment to solid surfaces (Ferrieres and Clarke 2003; Hagiwara et al. 2003).

Finally, the deletion of a gene whose function is unknown (*yehV*) abolishes curli production in *E. coli* and *S. typhimurium* (Brown et al. 2001). This gene has been re-named *mlrA* (*merR*-like regulator) by the authors because of the similarity between the reduced protein and the MerR regulator involved in mercury resistance.

2.3 GGDEF and EAL Regulatory Proteins: Regulation of Exopolysaccharide Biosynthesis at the Enzyme Level

So far, we have focused on regulation at the transcription level; however, expression of biofilms-related genes is often subjected to regulation at different levels, in order to achieve very precise control of biofilm determinant production. In this last section, we describe regulation of exopolysaccharide production by accumulation of a signal molecule, bis-(3′,5′)-cyclic diguanylic acid (c-di-GMP).

2.3.1 The GGDEF-EAL Protein Family

Several bacterial proteins containing the GGDEF-EAL domains are directly involved in the expression of virulence and/or biofilm factors and, more specifically, in the biosynthesis of extracellular polysaccharides (EPS). The

GGDEF domain, named after the conserved central sequence motif gly-gly-asp-glu-phe, catalyzes condensation of two GTP molecules to a bis-(3′,5′)-cyclic diguanylic acid (c-di-GMP) (Ross et al. 1991; Ausmees et al. 2001), a role consistent with the similarity of the GGDEF motif to eukaryotic adenylate cyclases (Pei and Grishin 2001). Intracellular levels of free c-di-GMP are probably regulated by the guanlylate cyclase activity of GGDEF and by the opposite action of a phosphdiesterase A, which catalyzes the breakdown of c-di-GMP to two GMP molecules (Tal et al. 1998). This function is putatively linked to a domain, termed EAL by the conserved residues glu-ala-leu, which could participate in metal binding and might form the phosphodiesterase active site. Interestingly, EAL domains are often found at the C-terminal domains of GGDEF proteins, thus coupling the two activities in a single enzyme (Galperin et al. 2001).

Cyclic di-GMP was originally identified as the trigger molecule for cellulose (1,4-β-D-glucan) biosynthesis of *Gluconacetobacter xylinus* (formerly called *Acetobacter xylinus*) (Ross et al. 1990). The cellulose-synthesizing complex is a transmembrane complex constituted by cellulose synthase (BscA) and by the c-di-GMP binding protein (BcsB) (Ross et al. 1991; Kimura et al. 2001). c-di-GMP bound by BcsB is released to the BcsA synthase, possibly through protein-protein interactions (Weinhouse et al. 1997). Intracellular levels of c-di-GMP are regulated by several isoenzymes, the diguanylate cyclase (DGC) and phosphodiesterase A (PDEA) proteins, all containing both GGDEF and EAL domains (Tal et al. 1998). Both the DGC and the PDEA isoenzymes contain N-terminal oxygen sensing regions, and the PDEA1 protein was indeed shown to be activated by O_2, suggesting an influence of oxygen tension on cellulose production (Chang et al. 2001). Cellulose can act as a factor for microbial adhesion and biofilm formation, which in turn are oxygen-dependent in cellulose-producing bacteria (Spiers et al. 2003). The work by the group of Romling has shown that *Escherichia coli* and *Salmonella typhimurium* are also able to produce cellulose, whose production also depends on production of c-di-GMP by a GGDEF protein, AdrA. AdrA activates cellulose production at the posttranslational level (Zogaj et al. 2001), thus similar to the role of GGDEF proteins in cellulose production by *G. xylinus*. Interestingly, the *adrA* gene is positively controlled by the CsgD protein (AgfD in Salmonella), i.e. the activator of curli-encodin genes (Romling et al. 2000; Brombacher et al. 2003). Co-regulation of curli and cellulose biosynthesis by the CsgD protein results in the production of an extracellular matrix, composed of both proteinaceous and polysaccharide factors, leading to cell aggregation, surface colonization and to the so-called 'rdar' (rough, dry and red) morphotype (Romling et al. 2000).

There is increasing evidence that the central role of GGDEF-EAL proteins in biofilm formation is widely conserved among bacteria. In *Yersinia pestis* the expression of the haemin storage system (*hms*) and biofilm formation is dependent on the GGDEF containing HmsT protein (Hare and McDonough 1999; Jones et al. 1999). A *hms*-homolog system has recently been identified

in *E. coli* and termed *pga*; the *pga* locus is responsible for production of an *N*-acetyl-glucosamine polymer, and includes a GGDEF protein-encoding gene (*ycdT*), which, however, does not appear to be directly involved in regulation of polysaccharide production (Wang et al. 2005). In *Vibrio parahaemolyticus* biofilm formation and polysaccharide production are regulated by a signaling pathway involving the GGDEF-EAL motif-containing ScrC sensor (Guvener and McCarter 2003). Finally, in *Pseudomonas aeruginosa* the GGDEF proteins WspR and FimX are respectively involved in autoaggregation of cells (D'Argenio et al. 2002), and in regulation of twitching motility in response to environmental cues (Huang et al. 2003). The importance of GGDEF proteins goes well beyond biofilm formation, as they appear to be master regulators of several biological processes, such as cell differentiation in the bacterium *Caulobacter crescentus*. Interestingly, however, a main step in cell differentiation in *C. crescentus* is the transition of flagellated swarmer to adhesive stalked cells, regulated by the GGDEF PleD protein (Hecht and Newton 1995; Aldridge et al. 2003). Thus, control of cell cycle and cell differentiation in *C. crescentus* might have evolved from a genetic program for cell adhesion.

References

Adams JL, McLean RJC (1999) Impact of *rpoS* deletion on *Escherichia coli* biofilms. Appl Environ Microbiol 65:4285–4287

Aldridge P, Paul R, Goymer P, Rainey P, Jenal U (2003) Role of the GGDEF regulator PleD in polar development of *Caulobacter crescentus*. Mol Microbiol 47:1695–1708

Arnqvist A, Olsen A, Pfeifer J, Russell DG, Normark S (1992) The Crl protein activates cryptic genes for curli formation and fibronectin binding in *Escherichia coli* HB101. Mol Microbiol 6:2443–2452

Arnqvist A, Olsén A, Normark S (1994) σ^S-dependent growth-phase induction of the *csgBA* promoter in *Escherichia coli* can be achieved in vivo by σ^{70} in the absence of the nucleoid-associated protein H-NS. Mol Microbiol 13:1021–1032

Ausmees N, Mayer R, Weinhouse H, Volman G, Amikam D, Benziman M, Lindberg M. (2001) Genetic data indicate that proteins containing the GGDEF domain possess diguanylate cyclase activity. FEMS Microbiol Lett 204:163–167

Bian Z, Brauner A, Li Y, Normark S (2000) Expression of and cytokine activation by *Escherichia coli* curli fibers in human sepsis. J Infect Dis 181:602–612

Bollinger N, Hassett DJ, Iglewski BH, Costerton JW, McDermott TR (2001) Gene expression in *Pseudomonas aeruginosa*: evidence of iron override effects on quorum sensing and biofilm-specific gene regulation. J Bacteriol 183:1990–1996

Bonafonte MA, Solano C, Sesma B, Alvarez M, Montuenga L, Garcia-Ros D, Gamazo C (2000) The relationship between glycogen synthesis, biofilm formation and virulence in *Salmonella enteritidis*. FEMS Microbiol Lett 191:31–36

Bougdour A, Lelong C, Geiselmann J (2004) Crl, a low temperature induced protein in *Escherichia coli* that binds directly to the stationary phase sigma subunit of RNA polymerase. J Biol Chem 279:19540–19550

Brombacher E, Dorel C, Zehnder AJ, Landini P (2003) The curli biosynthesis regulator CsgD coordinates the expression of both positive and negative determinants for biofilm formation in *Escherichia coli*. Microbiology 149:2847–2857

Brown PK, Dozois CM, Nickerson CA, Zuppardo A, Terlonge J, Curtiss R III (2001) MlrA, a novel regulator of curli (AgF) and extracellular matrix synthesis by *Escherichia coli* and *Salmonella enterica* serovar Typhimurium. Mol Microbiol 41:349–363

Caldwell DE (2002) The calculative nature of microbial biofilms and bioaggregates. Int Microbiol 5:107–116

Chang AL, Tuckerman JR, Gonzalez G, Mayer R, Weinhouse H, Volman G, Amikam D, Benziman M, Gilles-Gonzalez MA (2001) Phosphodiesterase A1, a regulator of cellulose synthesis in *Acetobacter xylinum*, is a heme-based sensor. Biochemistry 40:3420–3426

Chapman MR, Robinson LS, Pinkner JS, Roth R, Heuser J, Hammar M, Normark S, Hultgren SJ (2002) Role of *Escherichia coli* curli operons in directing amyloid fiber formation. Science 295:851–855

Collinson SK, Emody L, Muller KH, Trust TJ, Kay WW (1991) Purification and characterization of thin, aggregative fimbriae from *Salmonella enteritidis*. J Bacteriol 173:4773–4781

Collinson SK, Clouthier SC, Doran JL, Banser PA, Kay WW (1996) *Salmonella enteritidis agfBAC* operon encoding thin, aggregative fimbriae. J Bacteriol 178:662–667

Cookson AL, Cooley WA, Woodward MJ (2002) The role of type 1 and curli fimbriae of Shiga toxin-producing *Escherichia coli* in adherence to abiotic surfaces. Int J Med Microbiol 292:195–205

Costerton JW, Lewandowski Z, Caldwell DE, Korber DR, Lappin-Scott HM (1995) Microbial biofilms. Annu Rev Microbiol 49:711–745

D'Argenio DA, Calfee MW, Rainey PB, Pesci EC (2002) Autolysis and autoaggregation in Pseudomonas aeruginosa colony morphology mutants. J Bacteriol 184:6481–6489

Danese PN, Pratt LA, Kolter R (2000) Exopolysaccharide production is required for development of *Escherichia coli* K-12 biofilm architecture. J Bacteriol 182:3593–3596

Davies DG, Geesey GG (1995) Regulation of the alginate biosynthesis gene *algC* in *Pseudomonas aeruginosa* during biofilm development in continuous culture. Appl Environ Microbiol 61:860–867

Davies DG, Chakrabarty AM, Geesey GG (1993) Exopolysaccharide production in biofilms: substratum activation of alginate gene expression by *Pseudomonas aeruginosa*. Appl Environ Microbiol 59:1181–1186

Davies DG, Parsek MR, Pearson JP, Iglewski BH, Costerton JW, Greenberg EP (1998) The involvement of cell-to-cell signals in the development of a bacterial biofilm. Science 280:295–298

De Kievit TR, Gillis R, Marx S, Brown C, Iglewski BH (2001) Quorum-sensing genes in *Pseudomonas aeruginosa* biofilms: their role and expression patterns. Appl Environ Microbiol 67:1865–1873

Dorel C, Vidal O, Prigent-Combaret C, Vallet I, Lejeune P (1999) Involvement of the Cpx signal transduction pathway of *E. coli* in biofilm formation. FEMS Microbiol Lett 178:169–175

Dove SL, Smith SGJ, Dorman CJ (1997) Control of *Escherichia coli* type 1 fimbrial gene expression in stationary phase: a negative role for RpoS. Mol Gen Genet 254:13–20

Falconi M, Colonna B, Prosseda G, Micheli G, Gualerzi CO (1998) Thermoregulation of *Shigella* and *Escherichia coli* EIEC pathogenicity. A temperature-dependent structural transition of DNA modulates accessibility of *virF* promoter to transcriptional repressor H-NS. EMBO J 17:7033–7043

Ferrieres L, Clarke DJ (2003) The RcsC sensor kinase is required for normal biofilm formation in *Escherichia coli* K-12 and controls the expression of a regulon in response to growth on a solid surface. Mol Microbiol 50:1665–1682

Fuqua WC, Winans SC, Greenberg EP (1994) Quorum sensing in bacteria: the LuxR-LuxI family of cell density -responsive transcriptional regulators. J Bacteriol 176:269–275

Galperin MY, Nikolskaya AN, Koonin EV (2001) Novel domains of the prokaryotic two-component signal transduction systems. FEMS Microbiol Lett 203:11–21

Gerstel U, Romling U (2001) Oxygen tension and nutrient starvation are major signals that regulate *agfD* promoter activity and expression of the multicellular morphotype in *Salmonella typhimurium*. Environ Microbiol 3:638–648

Gerstel U, Park C, Romling U (2003) Complex regulation of *csgD* promoter activity by global regulatory proteins. Mol Microbiol 49:639–654

Ghigo JM (2003) Are there biofilm-specific physiological pathways beyond a reasonable doubt? Res Microbiol 154:1–8

Guvener ZT, McCarter LL (2003) Multiple regulators control capsular polysaccharide production in *Vibrio parahaemolyticus*. J Bacteriol 185:5431–5441

Hagiwara D, Sugiura M, Oshima T, Mori H, Aiba H, Yamashino T, Mizuno T (2003) Genome-wide analyses revealing a signaling network of the RcsC-YojN-RcsB phosphorelay system in *Escherichia coli*. J Bacteriol 185:5735–5746

Hammar M, Arnqvist A, Bian Z, Olsen A, Normark S (1995) Expression of two *csg* operons is required for production of fibronectin- and congo red-binding curli polymers in *Escherichia coli* K-12. Mol Microbiol 18:661–670

Hammar M, Bian Z, Normark S (1996) Nucleator-dependent intercellular assembly of adhesive curli organelles in *Escherichia coli*. Proc Natl Acad Sci USA 93:6562–6566

Hare JM, McDonough KA (1999) High-frequency RecA-dependent and -independent mechanisms of Congo red binding mutations in *Yersinia pestis*. J Bacteriol 181:4896–4904

Hecht GB, Newton A (1995) Identification of a novel response regulator required for the swarmer-to-stalked-cell transition in *Caulobacter crescentus*. J Bacteriol 177:6223–6229

Hengge-Aronis R (1999) Interplay of global regulators and cell physiology in the general stress response of *Escherichia coli*. Curr Opin Microbiol 2:148–152

Hentzer M, Wu H, Andersen JB, Riedel K, Rasmussen TB, Bagge N, Kumar N, Schembri MA, Song Z, Kristoffersen P, Manefield M, Costerton JW, Molin S, Eberl L, Steinberg P, Kjelleberg S, Hoiby N, Givskov M (2003) Attenuation of *Pseudomonas aeruginosa* virulence by quorum sensing inhibitors. EMBO J 22:3803–3815

Huang B, Whitchurch CB, Mattick JS (2003) FimX, a multidomain protein connecting environmental signals to twitching motility in *Pseudomonas aeruginosa*. J Bacteriol 185:7068–7076

Jackson DW, Simecka JW, Romeo T (2002) Catabolite repression of *Escherichia coli* biofilm formation. J Bacteriol 184:3406–3410

Jones HA, Lillard JW Jr, Perry RD (1999) HmsT, a protein essential for expression of the haemin storage (Hms+) phenotype of *Yersinia pestis*. Microbiology 145:2117–2128

Jubelin G, Vianney A, Beloin C, Ghigo JM, Lazzaroni JC, Lejeune P, Dorel C (2005) CpxR/OmpR interplay regulates curli gene expression in response to osmolarity in *Escherichia coli*. J Bacteriol 187:2038–2049

Jucker BA, Harms H, Zehnder AJB (1996) Adhesion of the positively charged bacterium *Stenotrophomonas (Xanthomonas)* maltophilia to glass and teflon. J Bacteriol 178: 5472–5479

Kim SH, Kim YH (2004) *Escherichia coli* O157:H7 adherence to HEp-2 cells is implicated with curli expression and outer membrane integrity. J Vet Sci 5:119–124

Kimura S, Chen HP, Saxena IM, Brown RM Jr, Itoh T (2001) Localization of c-di-GMP-binding protein with the linear terminal complexes of *Acetobacter xylinum*. J Bacteriol 183:5668–5674

Lacour S, Landini P (2004) σ^S-dependent gene expression at the onset of stationary phase in *Escherichia coli*: function of σ^S-dependent genes and identification of their promoter sequences. J Bacteriol 186:7186–7195

Lan CY, Igo MM (1998) Differential expression of the OmpF and OmpC porin proteins in *Escherichia coli* K-12 depends upon the level of active OmpR. J Bacteriol 180:171–174

Landini P, Zehnder AJ (2002) The global regulatory *hns* gene negatively affects adhesion to solid surfaces by anaerobically grown *Escherichia coli* by modulating expression of flagellar genes and lipopolysaccharide production. J Bacteriol 184:1522–1529

Latifi A, Foglino M, Tanaka K, Williams P, Lazdunski A (1996) A hierarchical quorum-sensing cascade in *Pseudomonas aeruginosa* links the transcriptional activators LasR and RhIR (VsmR) to expression of the stationary-phase sigma factor RpoS. Mol Microbiol 21:1137–1146

Li YH, Tang N, Aspiras MB, Lau PC, Lee JH, Ellen RP, Cvitkovitch DG (2002) A quorum-sensing signaling system essential for genetic competence in *Streptococcus mutans* is involved in biofilm formation. J Bacteriol 184 2699–2708

Loferer H, Hammar M, Normark S (1997) Availability of the fibre subunit CsgA and the nucleator protein CsgB during assembly of fibronectin-binding curli is limited by the intracellular concentration of the novel lipoprotein CsgG. Mol Microbiol 26:11–23

Martino PD, Fursy R, Bret L, Sundararaju B, Phillips RS (2003) Indole can act as an extracellular signal to regulate biofilm formation of *Escherichia coli* and other indole-producing bacteria. Can J Microbiol 49:443–449

Maurer JJ, Brown TP, Steffens WL, Thayer SG (1998) The occurrence of ambient temperature-regulated adhesins, curli, and the temperature-sensitive hemagglutinin tsh among avian *Escherichia coli*. Avian Dis 42:106–118

Miller MB, Bassler BL (2001) Quorum sensing in bacteria. Annu Rev Microbiol 55:165–199

Olsen A, Jonsson A, Normark S (1989) Fibronectin binding mediated by a novel class of surface organelles on *Escherichia coli*. Nature 338:652–655

Olsen A, Arnqvist A, Hammar M, Normark S (1993a) Environmental regulation of curli production in *Escherichia coli*. Infect Agents Dis 2:272–274

Olsen A, Arnqvist A, Hammar M, Sukupolvi S, Normark S (1993b) The RpoS sigma factor relieves H-NS-mediated transcriptional repression of *csgA*, the subunit gene of fibronectin-binding curli in *Escherichia coli*. Mol Microbiol 7:523–536

Otto K, Silhavy TJ (2002) Surface sensing and adhesion of *Escherichia coli* controlled by the Cpx-signaling pathway. Proc Natl Acad Sci USA 99:2287–2292

Patten CL, Kirchhof MG, Schertzberg MR, Morton RA, Schellhorn HE (2004) Microarray analysis of RpoS-mediated gene expression in *Escherichia coli* K-12. Mol Genet Genom 272: 580–591

Pei J, Grishin NV (2001) GGDEF domain is homologous to adenylyl cyclase. Proteins 42:210–216

Perry RD, Bobrov AG, Kirillina O, Jones HA, Pedersen L, Abney J, Fetherston JD (2004) Temperature regulation of the hemin storage (Hms(+)) phenotype of *Yersinia pestis* is post-transcriptional. J Bacteriol 186:1638–1647

Pratt LA, Silhavy TJ (1998) Crl stimulates RpoS activity during stationary phase. Mol Microbiol 29:1225–1236

Prigent-Combaret C, Vidal O, Dorel C, Lejeune P (1999) Abiotic surface sensing and biofilm-dependent regulation of gene expression in *Escherichia coli*. J Bacteriol 181:5993–6002

Prigent-Combaret C, Prensier G, Le Thi TT, Vidal O, Lejeune P, Dorel C (2000) Developmental pathway for biofilm formation in curli-producing *Escherichia coli* strains: role of flagella, curli and colanic acid. Environ Microbiol 2:450–464

Prigent-Combaret C, Brombacher E, Vidal O, Ambert A, Lejeune P, Landini P, Dorel C (2001) Complex regulatory network controls initial adhesion and biofilm formation in *Escherichia coli* via regulation of the *csgD* gene. J Bacteriol 183:7213–7223

Reisner A, Haagensen JA, Schembri MA, Zechner EL, Molin S (2003) Development and maturation of *Escherichia coli* K-12 biofilms. Mol Microbiol 48:933–946

Repoila F, Gottesman S (2001) Signal transduction cascade for regulation of RpoS: temperature regulation of DsrA. J Bacteriol 183:4012–4023

Romling U, Sierralta WD, Eriksson K, Normark S (1998) Multicellular and aggregative behaviour of *Salmonella typhimurium* strains is controlled by mutations in the *agfD* promoter. Mol Microbiol 28:249–264

Romling U, Rohde M, Olsen A, Normark S, Reinkoster J (2000) AgfD, the checkpoint of multicellular and aggregative behaviour in *Salmonella typhimurium* regulates at least two independent pathways. Mol Microbiol 36:10–23

Romling U, Bokranz W, Rabsch W, Zogaj X, Nimtz M, Tschape H (2003) Occurrence and regulation of the multicellular morphotype in *Salmonella serovars* important in human disease. Int J Med Microbiol 293:273–285

Ross P, Mayer R, Weinhouse H, Amikam D, Huggirat Y, Benziman M, de Vroom E, Fidder A, de Paus P, Sliedregt LA, van der Mare GA, van Boom JH (1990) The cyclic diguanylic acid regulatory system of cellulose synthesis in *Acetobacter xylinum*. Chemical synthesis and biological activity of cyclic nucleotide dimer, trimer, and phosphothioate derivatives. J Biol Chem 265:18933–18943

Ross P, Mayer R, Benziman M (1991) Cellulose biosynthesis and function in bacteria. Microbiol Rev 55:35–58
Sakellaris H, Hannink NK, Rajakumar K, Bulach D, Hunt M, Sasakawa C, Adler B. (2000) Curli loci of *Shigella* spp. Infect Immun 68:3780–3783
Sauer K, Camper AK (2001) Characterization of phenotypic changes in *Pseudomonas putida* in response to surface-associated growth. J Bacteriol 183:6579–6589
Schauder S, Shokat K, Surette MG, Bassler BL (2001) The LuxS family of bacterial autoinducers: biosynthesis of a novel quorum-sensing signal molecule. Mol Microbiol 41:463–476
Schembri MA, Kjaergaard K, Klemm P (2003) Global gene expression in *Escherichia coli* biofilms. Mol Microbiol 48:253–267
Shapiro JA (1998) Thinking about bacterial populations as multicellular organisms. Annu Rev Microbiol 52:81–104
Sheikh J, Hicks S, Dall'Agnol M, Phillips AD, Nataro JP (2001) Roles for Fis and YafK in biofilm formation by enteroaggregative *Escherichia coli*. Mol Microbiol 41:983–997
Singh PK, Schaefer AL, Parsek MR, Moninger TO, Welsh MJ, Greenberg EP (2000) Quorum-sensing signals indicate that cystic fibrosis lungs are infected with bacterial biofilms. Nature 407:762–764
Solomon EB, Niemira BA, Sapers GM, Annous BA (2005) Biofilm formation, cellulose production, and curli biosynthesis by Salmonella originating from produce, animal, and clinical sources. J Food Prot 68:906–912
Soto GE, Hultgren SJ (1999) Bacterial adhesins: common themes and variations in architecture and assembly. J Bacteriol 181:1059–1071
Spiers AJ, Bohannon J, Gehrig SM, Rainey PB (2003) Biofilm formation at the air-liquid interface by the *Pseudomonas fluorescens* SBW25 wrinkly spreader requires an acetylated form of cellulose. *Mol Microbiol* 50:15–27
Spurio R, Falconi M, Brandi A, Pon CL, Gualerzi CO (1997) The oligomeric structure of nucleoid protein H-NS is necessary for recognition of intrinsically curved DNA and for DNA bending. EMBO J 16:1795–1805
Stickler DJ, Morris NS, McLean RJ, Fuqua C (1998) Biofilms on indwelling urethral catheters produce quorum-sensing signal molecules in situ and in vitro. Appl Environ Microbiol 64:3486–3490
Stoodley P, Sauer K, Davies DG, Costerton JW (2002) Biofilms as complex differentiated communities. Annu Rev Microbiol 56:187–209
Tal R, Wong HC, Calhoon R, Gelfand D, Fear AL, Volman G, Mayer R, Ross P, Amikam D, Weinhouse H, Cohen A, Sapir S, Ohana P, Benziman M (1998) Three *cdg* operons control cellular turnover of cyclic di-GMP in *Acetobacter xylinum*: genetic organization and occurrence of conserved domains in isoenzymes. J Bacteriol 180:4416–4425
Uhlich GA, Keen JE, Elder RO (2001) Mutations in the csgD promoter associated with variations in curli expression in certain strains of *Escherichia coli* O157:H7. Appl Environ Microbiol 67:2367–2370
Uhlich GA, Keen JE, Elder RO (2002) Variations in the csgD promoter of *Escherichia coli* O157:H7 associated with increased virulence in mice and increased invasion of HEp-2 cells. Infect Immun 70:395–399
Van der Woude MW, Braaten BA, Low DA (1992) Evidence for global regulatory control of pilus expression in Escherichia coli by Lrp and DNA methylation: model building based on analysis of pap. Mol Microbiol 6:2429–2435
Vasil ML, Ochsner AO (1999) The response of *Pseudomonas aeruginosa* to iron: genetics, biochemistry and virulence. Mol Microbiol 34:399–413
Vicente M, Chater KF, de Lorenzo V (1999) Bacterial transcription factors involved in global regulation. Mol Microbiol 33:8–17
Vidal O, Longin R, Prigent-Combaret C, Dorel C, Hooreman M, Lejeune P (1998) Isolation of an *Escherichia coli* K-12 mutant strain able to form biofilms on inert surfaces: involvement of a new *ompR* allele that increases curli expression. J Bacteriol 180: 2442–2449

Wang Q, Frye JG, McClelland M, Harshey RM (2004) Gene expression patterns during swarming in *Salmonella typhimurium*: genes specific to surface growth and putative new motility and pathogenicity genes. Mol Microbiol 52:169–187

Wang X, Dubey AK, Suzuki K, Baker CS, Babitzke P, Romeo T. (2005) CsrA post-transcriptionally represses *pgaABCD*, responsible for synthesis of a biofilm polysaccharide adhesin of *Escherichia coli*. Mol Microbiol 56:1648–1663

Watnick PI, Fullner KJ, Kolter R (1999) A role for the mannose-sensitive hemagglutinin in biofilm formation by *Vibrio cholerae* El Tor. J Bacteriol 181:3606–3609

Weber H, Polen T, Heuveling J, Wendisch VF, Hengge R (2005) Genome-wide analysis of the general stress response network in Escherichia coli: sigmaS-dependent genes, promoters, and sigma factor selectivity. J Bacteriol 187:1591–1603

Weinhouse H, Sapir S, Amikam D, Shilo Y, Volman G, Ohana P, Benziman M (1997) c-di-GMP-binding protein, a new factor regulating cellulose synthesis in *Acetobacter xylinum*. FEBS Lett 416:207–211

Whitchurch CB, Tolker-Nielsen T, Ragas PC, Mattick JS (2002) Extracellular DNA required for bacterial biofilm formation. Science 295:1487

Whitchurch CB, Beatson SA, Comolli JC, Jakobsen T, Sargent JL, Bertrand JJ, West J, Klausen M, Waite LL, Kang PJ, Tolker-Nielsen T, Mattick JS, Engel JN (2005) *Pseudomonas aeruginosa fimL* regulates multiple virulence functions by intersecting with Vfr-modulated pathways. Mol Micro 55:1357–1378

Whiteley M, Parsek MR, Greenberg EP (2000) Regulation of quorum sensing by RpoS in *Pseudomonas aeruginosa*. J Bacteriol 182:4356–4360

Whiteley M, Bangera MG, Bumgarner RE, Parsek MR, Teitzel GM, Lory S, Greenberg EP (2001) Gene expression in *Pseudomonas aeruginosa* biofilms. Nature 413:860–864

Zogaj X, Nimtz M, Rohde M, Bokranz W, Romling U (2001) The multicellular morphotypes of *Salmonella typhimurium* and *Escherichia coli* produce cellulose as the second component of the extracellular matrix. Mol Microbiol 39:1452–1463

Zogaj X, Bokranz W, Nimtz M, Romling U (2003) Production of cellulose and curli fimbriae by members of the family *Enterobacteriaceae* isolated from the human gastrointestinal tract. Infect Immun 71:4151–4158

3 Adhesion and Adhesives of Fungi and Oomycetes

Lynn Epstein[1] and Ralph L. Nicholson[2]

3.1 Introduction

During the past decade there has been an increased recognition of the importance of adhesion of fungi to host surfaces–both plant and animal–before penetration (Mendgen et al. 1996; Epstein and Nicholson 1997; Hardham 2001; Osherov and May 2001; Tucker and Talbot 2001). Observational studies with microscopy indicate that many fungi adhere tenaciously onto inert surfaces such as polystyrene in addition to host substrata. This is perhaps not surprising since, for example, the aerial surfaces of plants are hydrophobic and relatively inert, and aquatic fungi can adhere to rocks. Microscopy of fungi that are in the process of adhering also indicates that fungal-substratum adhesion is mediated by a glue, i.e., a secreted macromolecule that extends from the fungus onto the adjacent surface and binds to it in a relatively non-specific manner. Here, we will primarily focus on fungal cell-substratum adhesion that is mediated by a glue.

We will use the term 'adhesin' to indicate a molecule that mediates a comparatively specific attachment between a ligand on a fungus and a receptor on its host's substratum. However, whether an adhesin is somewhat non-specifically "sticky" or has a conformational "good fit" for a particular substratum is not always clear, particularly with the literature on adhesion of animal pathogenic fungi to the extracellular matrices of mammalian cells. The cells of the human commensal and pathogen *Candida albicans*, for example, adhere to inert substrata such as polystyrene (Masuoka et al. 1999). Consequently, while we will focus on examples of glue-mediated adhesion of fungi to substrata, we will also mention some of the best-characterized examples of cell-cell adhesion in which at least one of the cells is a fungus, and the adhesin may have glue-like properties.

3.2 Prevalence and Importance of Adhesion in Fungi and Oomycetes

Cell-substratum adhesion is common in all taxonomic classes of microscopic fungi (Nicholson and Epstein 1991; Jones 1994). Cell-substratum adhesion

[1] Department of Plant Pathology, University of California, Davis, CA 95616-8680, USA
[2] Department of Botany and Plant Pathology, Purdue University, W. Lafayette, IN 47907, USA

Biological Adhesives
(ed. by A.M. Smith and J.A. Callow)

also is common in the oomycetes, which include such economically important plant pathogens such as *Phytophthora* spp., *Pythium* spp., and *Plasmopara spp*. (Hardham 2001). Although oomycetes are stramenopiles, i.e., are phylogenetically distinct from fungi, and are most closely allied to diatoms, brown algae, and some parasitic protozoans (Gunderson et al. 1987), we will include them here because they traditionally have been classified as fungi. More importantly, oomycetes and fungi share environments in which glues are secreted and function.

3.2.1 Adhesion as Part of Many Stages of Morphogenesis in Many Fungi

In a single organism, multiple stages of development can be adherent and can involve differing mechanisms of adhesion. With wind-disseminated plant pathogens such as *Botrytis cinerea* (Doss et al. 1993) and *Erysiphe graminis* (see Sect. 3.2.3.2), hydrophobic interactions between a hydrophobic spore and the leaf cuticle can secure the initial contact. With water-disseminated pathogens such as *Colletotrichum graminicola*, initial adhesion of spores requires the release of a glue (Nicholson and Epstein 1991; Epstein and Nicholson 1997). Since most fungal spores require free water for germination, later stages of adhesion for both air- and water-disseminated spores occur in an aqueous environment. Regardless, less perturbable adhesion is temporally and spatially associated with de novo material on the cell surface (Hamer et al. 1988; Kwon and Epstein 1993; Braun and Howard 1994a). It is important to note that the fungal interface with its environment is biochemically complex and multifunctional, i.e., glues are only one component of surface-associated compounds and adhesion is only one function of the extracellular matrix (Nicholson and Epstein 1991). In addition, non-glue components in the extracellular matrix can alter the surface and increase the strength of attachment; *Uromyces viciae-fabae* urediospores release cutinases and esterases that degrade the plant cuticle and enhance spore adhesion (Deising et al. 1992).

The strength of attachment varies with the fungus and the cell type. For example, *Nectria haematococca* mating population I conidia and germlings adhere to polystyrene and to plant surfaces, but they do not adhere as tenaciously as spores or germlings of *Colletotrichum graminicola* or germlings of the rust fungus *Uromyces appendiculatus*. Unfortunately, relatively few papers quantify the strength of adhesion. Comparisons between studies would be facilitated by utilization of flow cells in which shear force can be determined (Li and Palecek 2003). Mechanical penetration from appressoria requires firm adhesion. Using a microscopic method, Bechinger et al. (1999) estimated that *Colletotrichum graminicola* appressoria had a turgor pressure of 5.4 MPa and exerted an approximate force of 17 μN. Consequently, the glue that affixes the appressorium to the plant surface must be able to withstand this force.

3.2.2 Functions of Adhesion

Even if we limit our discussion to fungal-substratum adhesion that occurs on the plant host surface before penetration, adhesion serves multiple functions (Table 3.1). Most obviously, adhesion keeps a fungus from being blown or rinsed from a potentially suitable environment. Whether contact is required can depend upon the environmental conditions; many species of fungal spores germinate readily regardless of contact in a nutritive liquid medium, but in an oligotrophic environment, efficient germination requires contact with a substratum (Chaky et al. 2001). In *Phyllosticta ampelicida,* adhesion of pycnidiospores is required for germination (Kuo and Hoch 1996). In fungi such as *Erysiphe graminis*, spore adhesion may facilitate "preparation of the infection court", i.e., alteration of the host surface so that it favors fungal development (see Sect. 3.2.3.1). That is, a tightly adherent spore or germling may be able to effectively maintain a higher concentration of its lytic enzymes at the interface between its wall and the substratum surface. *Nectria haematococca* mutants with conidia and germlings

Table 3.1. Functions of fungal glues on the surface of the plant host

Benefits of adhesion for the fungus	Cell types	Examples of organisms[a]	References with experimental evidence
Prevents displacement by water and/or wind	Conidia, germlings, hyphae, appressoria	All	Reviewed in Epstein and Nicholson (1997)
Limits germination to potential host tissue (Required for contact-stimulated germination)	Conidia	Pa	Kuo and Hoch (1996)
Increases the surface area of contact with its host	Germlings, hyphae	Cg	Apoga et al. (2004)
Facilitates chemical interaction between pathogen and host	Conidia, germlings	Nh	Jones and Epstein (1990)
Required for thigmotropism	Germlings	Ua	Epstein et al. (1987)
Required for thigmodifferentiation	Appressoria, Hyphopodia	Cg Eg Ua	Chaky et al. (2001) Yamaoka and Takeuchi (1999) Epstein et al. (1985)
Required for host penetration via mechanical pressure	Appressoria, hyphopodia, cysts	Cg Mg	Bechinger et al. (1999) Howard et al. (1991)

[a] This list provides examples and is a not comprehensive survey. All, applies to all fungi in this list; Cg, *Colletotrichum graminicola*; Eg, *Erysiphe graminis*; Mg, *Magnaporthe grisea*; Nh, *Nectria haematococca* mating population I (anamorph *Fusarium solani* f. sp. *cucurbitate* race I); Pa, *Phyllosticta ampelicida*; Ua, *Uromyces appendiculatus*

with reduced adhesiveness were less virulent than the wild type when deposited on the cucurbit fruit surface, but were equally virulent when deposited within the fruit tissue (Jones and Epstein 1990). Adhesion of germlings to a substratum maximizes fungal reception of surface signals and absorption of nutrients from the host substratum because adherent germlings and hyphae are flattened on the bottom; in contrast, germlings and hyphae that have not developed attached to a substratum are round in cross-section (Epstein et al. 1987).

Some fungi have contact-induced responses, and these generally require attachment. Rust fungi such as *Uromyces appendiculatus* display a type of thigmotropism, i.e., contact-dependent growth in which physical cues from leaf surface topography orient hyphal growth towards stomata (Hoch et al. 1987). Many fungi, including *U. appendiculatus* and *Colletotrichum* spp., display thigmodifferentiation, i.e., contact-dependent differentiation. Here, adhesion is required to induce formation of appressoria (Apoga et al. 2004); indeed the researchers demonstrated that to induce appressorial formation, *C. graminicola* germlings require 4 μm of continuous contact with a hydrophobic substratum. *U. appendiculatus* germlings that were rendered non-adherent with proteases continued to grow but were unable to establish pathogenicity because they were unable to grow thigmotropically or undergo thigmodifferentiation (Epstein et al. 1985, 1987). Finally, since fungi mechanically penetrate the plant surface from appressoria (Howard et al. 1991), we can deduce that firm adhesion is required for appressorial function. Indeed attachment is so integral to appressorial function that appressoria are often defined as adherent.

3.2.3 Selected Examples

Recent sequencing of whole fungal genomes makes comparisons of adherent and non-adherent fungi possible. The ascomycetous yeasts *Saccharomyces cerevisae* and *Candida albicans* are comparatively non-adherent and adherent, respectively. The ascomycetes *Magnaporthe grisea* and *Botrytis cinerea* have adherent conidia, germlings and appressoria (Hamer et al. 1988; Doss et al. 1993, 1995; Braun and Howard 1994b; Xiao et al. 1994; Spotts and Holz 1996) but *Neurospora crassa* is non-adherent. The basidiomycete *Ustilago madydis* has hyphae that grow attached to the leaf and then produces appressoria (Snetselaar and McCann 2001).

Fungi that are adherent and that seem likely to be sequenced include *Colletotrichum graminicola* and *Erysiphe graminis*. *C. graminicola* is amenable to a range of molecular strategies (Epstein et al. 1998).

3.2.3.1 Colletotrichum graminicola (Teleomorph, Glomerella graminicola), Causal Agent of Anthracnose on Corn

The maize anthracnose pathogen, *C. graminicola*, produces conidia in acervuli. A complex mixture of high molecular weight glycoproteins surrounds the conidia. The glycoproteins have several roles. They act as an anti

desiccant allowing the conidia to survive for an extended time during periods of drought and severe changes in temperature (Nicholson and Moraes 1980; Bergstrom and Nicholson 1999). In addition, the mucilaginous matrix contains mycosporine-alanine, a self-inhibitor of germination (Leite and Nicholson 1992). The mucilage also contains a cutinase and non-specific esterase that assist in the process of adhesion and recognition of the infection court (Pascholati et al. 1993). Ungerminated conidia of *C. graminicola* adhere to artificial hydrophobic surfaces, yet the same conidia are unable to bind to hydrophilic surfaces (Mercure et al. 1994). Materials released by the conidia, including the adhesive material, were easily observed by scanning electron microscopy (Mercure et al. 1995). The matrix complex was isolated, partially characterized and contains a mixture of high molecular weight glycoproteins (Sugui et al. 1998).

3.2.3.2 Erysiphe graminis (Teleomorph, Blumeria graminis) Causal Agent of Powdery Mildew of Barley

The powdery mildew pathogen of barley *E. graminis* produces conidia that release a liquid exudate upon contact with the hydrophobic surface of the barley leaf (Kunoh et al. 1988). To ensure that contact is successful, the conidial exudate contains a cutinase that degrades the host cuticle at the contact site (Nicholson et al. 1988; Pascholati et al. 1992). The substrata and the geometry of the interface between the conidium and the substratum affect the release of extracellular material by *E. graminis* conidia (Carver et al. 1999; Wright et al. 2002). On hydrophobic surfaces, a pad of extracellular material is released within 1 min after contact with the substratum. This phenomenon did not occur on a hydrophilic surface, suggesting that the hydrophobicity of the surface is critical to recognition of the host by the pathogen.

3.3 Challenges in Identifying Adhesives in Fungi

As indicated above, great progress has been made in documenting the spatial and temporal expression of cell-substratum attachment and in the development of adhesiveness. However, identification of the components of glues can present both biochemical and genetic challenges (Vreeland and Epstein 1996).

3.3.1 Genetic 'Knockout' and 'Knockin' Strategies

Adhesion-reduced and non-adhesive mutants provide a superb tool to investigate the role of adhesion. For example, adhesion-reduced mutants of the plant pathogenic fungus *Nectria haematococca* were less virulent than the wild-type when deposited on the intact surface of cucurbit fruits, but were equally virulent when deposited into wounded fruits; the results indicated

that adhesion is a virulence factor in the "natural" environment, and suggested that adhesion prevents displacement by water and assists in efficient localization of secreted enzymes on the host surface (Jones and Epstein 1990). Mutants can be used to formulate hypotheses about the adhesive compound; in the biocontrol yeast *Rhodosporidium toruloides,* the mannose-binding lectin Concanavalin A (Con A) eliminated adhesion in the wild-type and bound to the region of bud development in the wild-type where the yeast adhered, but did not bind to the same region in the mutant (Buck and Andrews 1999b).

Site-directed mutagenesis provides the most powerful technique to demonstrate that a specific gene is involved in the adhesive process. With the medically important fungi, there are multiple examples in which a putative adhesin gene has been knocked out, and there is a resultant loss of adhesiveness and virulence (Gale et al. 1998; Brandhorst et al. 1999; Loza et al. 2004; Zhao et al. 2004); adhesion and virulence was restored after the mutant strain had the disrupted gene restored. Amongst the plant pathogenic fungi, researchers have focused more on genes that reduce pathogenicity; in a few cases, these genes also affect fungal attachment. For example, disruption of the *Colletotrichum lagenarium* mitogen-activated protein (MAP) kinase *CMK1* does not affect mycelial growth, but interrupts production of conidia, conidial adhesion, conidial germination, and appressorial formation (Takano et al. 2000). Disruption of *Magnaporthe grisea acr1* (Lau and Hamer 1998) affects conidiogenesis so that an acr1-mutant has conidiophores that produce conidia in a head-to-tail chain rather than sympodially. That is, a new conidium is produced from the tip of an older conidium rather than from a conidiophore. In the wild type, conidial adhesion is mediated by mucilage released from the spore tip. The acr1-conidia fail to produce the spore tip mucilage, are non-adherent, and are inefficient in forming appressoria. While mutants in regulatory genes are extremely informative about pathways (e.g., Liu and Kolattukudy 1999), they are not as useful for adhesion studies as knockouts of genes directly involved in glue production. However, if multiple compounds serve as building blocks of a glue, single gene knockouts may only result in, at best, quantitatively discernible differences from the wild-type.

Researchers have used 'knockin' strategies to identify individual genes from *C. albicans* that transform the generally non-adhesive *Saccharomyces cerevisae* into an organism that adheres to polystyrene (Barki et al. 1993; Fu et al. 1998; Li and Palecek 2003). These researchers screened libraries rather than specific genes, which resulted in identification of potentially new adhesins. However, successful utilization of this strategy to identify a glue depends upon there being a single or perhaps tandem genes that are expressed in a sticky organism that are not expressed in the non-adherent organism. Using a strategy similar to that described in Barki et al. (1993), the Epstein laboratory was not successful in identifying *Colletotrichum graminicola* genes that rendered *S. cerevisae* transformants adhesive.

3.3.2 Biochemical Strategies

From a biochemical perspective, there are several reasons why identification of even a single fungal adhesive has remained a challenge. Particularly compared to *S. cerevisae* and *C. albicans*, the cell surfaces of filamentous fungi are complex and poorly characterized. As discussed in greater detail below (Sect. 3.4.2), fungi probably produce glycoprotein-(or proteoglycan-) based glues. Perhaps not surprisingly, the external layer of fungal cell walls is largely composed of heavily glycosylated proteins (de Nobel et al. 2001). Indeed, all proteins in the wall may be glycosylated because glycosylation is part of the pathway of secreted proteins. Cell surface labeling of proteins by iodination and biotinylation indicate that there are many (glyco)proteins on the cell surfaces of fungi (Epstein et al. 1987; Apoga et al. 2001; de Nobel et al. 2001; de Groot et al. 2004; Weig et al. 2004). Adding to the complexity of identifying one or few proteins out of many, the macromolecules on the surface are highly cross-linked. For example, in *S. cerevisae*, the glycosylphosphatidylinositol-dependent (GPI) cell wall proteins are bound to the plasma membrane and to β1,6-glucan; the β1,6-glucan is bound to chitin and to β1,3-glucan, which also is bound to chitin (de Nobel et al. 2001). Non-GPI cell wall proteins are also cross-linked to the wall. For example, in the animal pathogen *Blastomyces dermatitidis*, the proteinaceous adhesin is secreted through the wall, localizes on the cell surface and then reassociates with cell wall chitin (Brandhorst and Klein 2000).

Several properties of glues also make identification a challenge. Although assays, such as retention of microspheres, can be useful in identifying potential adhesives, there are limitations in that glues are transiently sticky (Vreeland and Epstein 1996). That is, a glue must be sufficiently non-sticky to be secreted to the wall surface, sticky during glue formation, and then typically, non-sticky after "curing" or "hardening." The ultimate loss of stickiness is accompanied by dramatic changes in solubility; fungal glues are extremely insoluble. Thus, there are always concerns that compounds that are not involved in adhesion are co-purified when the adhesive is sticky, and polymerized with the glue after hardening.

3.4 Fungal and Oomycete Glues

3.4.1 Features

Conidia of most fungal species must be alive in order for adhesion to occur (Slawecki et al. 2002). As indicated previously, although there may be some initial passive attachment of fungal spores to a surface, stronger adhesion seems mediated by secreted material on the cell surface (Epstein and Nicholson 1997; Apoga and Jansson 2000). Microscopic observations, including

transmission electron microscopy with freeze-substituted specimens (Caesar-TonThat and Epstein 1991) are consistent with the interpretation that adhesives are liquid upon release and spread over the surface. The spreading of the adhesive obviously occurs underwater in aquatic fungi (Jones 1994), but also occurs underwater for most terrestrial fungi, which require "free water" to germinate. Thus, the glue must either displace or completely mix with the water molecules that are already on the surface. Microscopic observations are also consistent with the interpretation that the cell surface changes over time as the adhesive material is polymerized into a stronger, crosslinked-compound (Caesar-TonThat and Epstein 1991; Apoga and Jansson 2000). Mature adhesives often appear to have a fibrous component (Watanabe et al. 2000).

As indicated above, many fungi adhere well to inert surfaces including teflon (Hamer et al. 1988). Overall, for the purpose of attachment, the predominant feature of a leaf surface appears to be its hydrophobicity. Many fungi adhere more tenaciously to hydrophobic than to hydrophilic surfaces (Epstein and Nicholson 1997). Terhune and Hoch (1993) found that the extent of adhesion of germlings of *Uromyces appendiculatus* to inert surfaces correlated closely with substratum hydrophobicity. However, other features on the leaf surface may also affect adhesion. The rust fungus *Uromyces viciae-fabae*, for example, secretes cutinases and esterases which change the potential binding sites on the surface, and enhance adhesion (Deising et al. 1992). Buck and Andrews (1999b) utilized attachment mutants to conclude that localized positive charges, and not hydrophobic interactions, mediate attachment of the yeast *Rhodosporidium toruloides*. Adhesion to roots is not as well characterized as to leaves (Recorbet and Alabouvette 1997), and roots have potential carbohydrate receptors to which an adhesin could bind.

3.4.2 Composition of Glues

During the last two decades we have learned much about why and when fungi adhere. We still know relatively little about how fungi adhere. Most researchers have deduced the composition of the glues by testing for the loss of adhesiveness with enzymes, lectins, antibodies, and inhibitors of specific metabolic pathways. Such indirect evidence indicates that fungal adhesives are glycoproteins (Chaubal et al. 1991; Jones 1994; Kuo and Hoch 1996; Pain et al. 1996; Bircher and Hohl 1997; Epstein and Nicholson 1997; Sugui et al. 1998; Hughes et al. 1999; Apoga et al. 2001). The carbohydrate moieties on glycoproteins seem particularly important in adhesion. In many fungi, including *Bipolaris sorokiniana, Colletotrichum graminicola*, *Magnaporthe grisea*, *Nectria haematococca*, and *Phyllosticta ampelicida*, substratum adhesion is at least partially blocked by the lectin Con A (Hamer et al. 1988; Shaw and Hoch 1999; Apoga et al. 2001). Experimental evidence, including block-

age of adhesion with the snowdrop lectin, indicates that mannose residues are involved in the adhesive mechanism (Kwon and Epstein 1997a).

There have been a few reports that fungal adhesives are carbohydrates (Pringle 1981), but whether the adhesives are actually glycoproteins or proteoglycans is unknown. The carbohydrate residues on the *Magnaporthe grisea* conidial spore tip mucilage may be modified carbohydrates. Buck and Andrews (1999a) reported that a mannose-containing compound, and possibly a mannoprotein, was involved in attaching the yeast *Rhodosporidium toruloidesto* to polystyrene and barley leaves. Determination of whether lipids, for example, are part of the appressorial adhesive (Ebata et al. 1998; Ohtake et al. 1999) requires additional experimental evidence.

3.4.3 Secretion and Crosslinking, with a Focus on Transglutaminases

The precursors of fungal glues must be secreted in a water-soluble form so that the material migrates through the wall to the cell surface. Either in the wall or on the cell surface, the glue must polymerize into a high molecular mass. Theoretically, a variety of oxidases could polymerize the glue; a catechol oxidase polymerizes the glue in mussels and a haloperoxidase may polymerize algal glues (Vreeland et al. 1998). Transglutaminases (EC 2.3.2-13) may be the polymerizing agents of fungal glues. Transglutaminases form a calcium-dependent interpeptidic cross-link between a glutamic acid and a lysine residue. Certainly transglutaminases serve functions in fungal cell walls that are distinct from adhesives; transglutaminases crosslink proteins in ascomycete walls (Ruiz-Herrera et al. 1995; Iranzo et al. 2002) which helps to reduce the pore size of the fungal wall. In addition, transglutaminases in the oomycete *Phytophthora sojae* serve as elicitors of plant host defense (Brunner et al. 2002), which perhaps is an indication that transglutaminases are present on the cell surface. Fabritius and Judelson (2003) identified a family of transglutaminases (M81 M81C, M81D and M81E) in the plant pathogen *P. infestans*. Thus, transglutaminases are present, apparently on the surface, of fungal and oomycete walls. Adhesion of oomycete zoospores and some fungal spores requires Ca^{++} (Shaw and Hoch 2000, 2001), as do transglutaminases. For example, adhesion of encysting zoospores of *P. cinnamomi* was enhanced with increasing Ca^{++} concentration from 2 to 20 mmol/l; chelation of Ca^{++} with EGTA eliminated adhesion (Gubler et al. 1989). Interestingly, with the *Candida albicans* adhesin Hwp1, the host transglutaminase covalently links the pathogen to the host epithelial cell (Staab et al. 1999).

3.4.4 Cell-surface Macromolecules with Apparent Adhesive Properties

Potential fungal glues are summarized in Table 3.2 and several are discussed below.

Table 3.2. Fungal macromolecules that potentially function as fungal-substratum glues

Organism	Glue component	Comments	Reference
Candida albicans	Eap1	GPI-CWP[a] that is involved in adhesion to polystyrene and to epithelial cells	Li and Palecek (2003)
Colletotrichum lindemuthianum	110-kDa glycoprotein on the conidial wall	Adhesion disrupted by monoclonal antibody UB20, which binds to several glycoproteins including the 110 kDa	Hughes et al. (1999)
Nectria haematococca mating population I	90-kDa mannoprotein	Spatially and temporally associated with adhesion of macroconidia; specifically associated with conditions in which adhesion is induced	Kwon and Epstein (1997a,b)
Rhodosporidium toruloides	Mannose-containing compound	Involved in adhesion to polystyrene and barley leaves	Buck and Andrews (1999a,b)
Phytophthora cinnamomi	220-kDa protein with thrombospondin type 1 repeats	Thrombospondin type 1 repeats are found in adherent cells in animals and in apicomplexan parasites	Robold and Hardham (2005)
Saccharomyces cerevisae	Flo11p	GPI-CWP that is involved in adhesion to substrata (including polystyrene), cell-cell adhesion, and filamentous growth	Reynolds and Fink (2001); Braus et al. (2003)

[a] GPI-CWP, glycosylphosphatidylinositol-dependent cell wall proteins

3.4.4.1 PcVsv1, a Protein on Encysting Zoospores of Phytophthora cinnamomi

The oomycete *Phytophthora cinnamomi* causes serious diseases on a wide range of host plants. As with many oomycetes, *P. cinnamomi* are disseminated by motile zoospores. The zoospores contain an adhesive in secretory vesicles (Hardham and Gubler 1990). About 2 min after contact with a solid surface, the material in the vesicles is secreted onto the ventral surface of the zoospores and the spores become sticky. The adhesive process is part of the process of transformation of zoospores into adherent cysts. Within 20–30 min, the encysted spores penetrate the underlying plant tissue. Adhesion is essential because a zoospore that is developing into a cyst must not be dislodged from a potential infection site, and because a mature cyst must be sufficiently glued to the host surface so that the fungus can penetrate the host tissue.

Hardham and Gubler (1990) identified a monoclonal antibody that specifically bound material in the secretory vesicles and on the developing adhesive

surface, i.e., the antigen was spatially and temporally consistent with being a component of the glue. Robold and Hardham (2005) screened a *P. cinnamomi* cDNA library with the antibody, and then selected and cloned a gene that encodes for PcVsv1 (*P. cinnamomi* ventral surface vesicle) protein with an approximate mass of 220 kDa. Not surprisingly for an adhesive material, PcVsv1 contains a repetitive motif–47 copies of a ca. 50 amino acid length segment that has homology to the thrombospondin type1 repeat. Thrombospondin motifs are found in proteins involved in attachment in animals and in apicomplexan parasites, including *Plasmodium*, *Cryptosporidium* and *Eimeria* (Tomley and Soldati 2001; Deng et al. 2002; Tucker 2004). In animals, the thrombospondin motifs occur in proteins in the extracellular matrix, i.e., potentially in the location in which adhesion occurs.

More experimental evidence is required before PcVsv1 can be declared the glue, or a component of the glue. Experimental strategies could include determination of the following: loss of adhesiveness with silencing of *Pcvsv1*; demonstration that PcVsv1 behaves as a glue *in vitro;* and interference with the development of adhesiveness with compounds that specifically bind PcVsv1, e.g., the antibody that binds to PcVsv1. To date, evidence that is consistent with PcVsv1 being involved in the adhesive process are 1) that the antibodies against PcVsv1 bind to multiple adherent oomycetes, i.e., *Phytophthora spp*., *Pythium spp*., *Plasmopara spp*., and *Albugo sp*. and 2) that Southern blotting and/or BLAST searches demonstrate the presence of PcVsv1 homologues in *Phytophthora spp*. (Robold and Hardham 2004, 2005). Even if thrombospondin is a glue component in oomycetes, it is probably not involved in adhesion of true fungi; based on a survey of sequences, Robold and Hardham (2005) found no evidence of thrombospondin motifs in either true fungi, or in plants or green algae.

Other proteins of *Phytophthora* spp. may be involved in some aspects of adhesion, although probably not as components of the glue *per se*. Göernhardt et al. (2000) identified the car90 (for cyst germination specific acidic repeat) protein on the surface of *Phytophthora infestans* germlings; the protein is transiently expressed during cyst germination and appressorium formation, i.e., during an adherent portion of the *P. infestans* lifecycle. The car90 protein contains 120 repeats of the consensus sequence TTYAPTEE. Because the repetitive sequence has homology with human mucins, the authors suggested that the car90 protein "may serve as a mucous cover protecting the germling from desiccation, physical damage, and adverse effects of the plant defense response." Because the protein is potentially viscous and sticky, the authors further speculated that car90 "may assist in adhesion to the leaf surface." Gaulin et al. (2002) identified the CBEL (for cellulose-binding elicitor lectin) glycoprotein on the surface of hyphae of *Phytophthora parasitica* var. *nicotianae*. However, while transgenic strains lacking CBEL did not adhere to and develop on cellulose *in vitro*, they appeared to have normal adhesion and development on the plant surface and *in planta*.

3.4.4.2 90-kDa Mannoprotein on Macroconidia of Nectria haematococca

We selected *N. haematocca* as a model biochemical system because, unlike *C. graminicola* and *U. appendiculatus*, the *N. haematocca* glue components seem somewhat detergent-soluble. When exposed to some but not all carbon sources, macroconidia of *Nectria haematococca* mating population I (anamorph, *Fusarium solani* f. sp. *curcurbitae* race I) become adhesive within 5 min and adhere at the spore apices to substrata and to other spores (Jones and Epstein 1989). At the same time, the macroconidia produce mucilage at the spore tips which binds Con A and the snowdrop lectin (SDL), and produce a 90-kDa glycoprotein which binds Con A and SDL; Con A and SDL inhibit macroconidial adhesion (Kwon and Epstein 1993, 1997a). When exposed to media that induce germination but not adhesiveness, neither the spore tip mucilage nor the 90-kDa glycoprotein are produced (Kwon and Epstein 1993). Adhesion of both ungerminated macroconidia and germlings was inhibited by a polyclonal IgG prepared against the 90-kDa glycoprotein (Kwon and Epstein 1997a). Anti-adhesive activity of the IgG was reduced by incubation of the antibodies with mannan; the mannan alone has no effect on adhesion. The anti-90-kDa IgG did not bind to the deglycosylated glycoprotein. Thus, we conclude that the 90-kDa glycoprotein and specifically its mannose residues are specifically involved in adhesion of *N. haematococca* macroconidia.

Visualization of the macroconidial tip mucilage and the detection of the 90-kDa glycoprotein is transient over time, consistent with compounds which become increasingly polymerized. Although *N. haematococca* macroconidia in zucchini extract are adherent for a 3-h incubation period, the macroconidial tip mucilage and the 90-kDa glycoprotein are primarily detectable only for the first hour. Macroconidia incubated in an adhesion-inducing medium with transglutaminase inhibitors (either 1 mm iodoactetamide or 10 mmol/l cystamine) adhere significantly less, have less of the macroconidial tip mucilage that is spatially associated with adhesion, and have less recoverable 90-kDa glycoprotein that is temporally associated with adhesion; the inhibitors do not affect the presence of other extractable compounds visualized on the protein blot. In addition, the fact that two reducing agents do not affect adhesion suggests that the iodoacetamide and cystamine are interfering with the adhesion process, and are not inhibiting adhesion by chemical reduction.

Thus the data are consistent with the following model. Within minutes of incubation in an adhesion-inducing medium, at the macroconidial apices, *N. haematococca* spores secrete a sticky lower-molecular-weight and more-water-soluble precursor of a 90-kDa glycoprotein (Kwon and Epstein 1993). At the spore apex, the glycoprotein is partially polymerized by a transglutaminase into a somewhat sticky 90-kDa form (Kwon and Epstein 1997a). After 1–2 h, the 90-kDa glycoprotein is extracellularly modified so that it is no longer sticky. After 2 h, adhesion is no longer localized at the spore apex; the macroconidia adhere along the entire lower spore surface, and later along the

germ tube-substratum interface. Mutant analysis suggests that compounds other than the 90-kDa glycoprotein are involved in this later stage of adhesion (Epstein et al. 1994). However, inhibition of both spore and germling adhesion by anti-90-kDa IgGs suggest that related compounds may be involved in spore and germling adhesion (Kwon and Epstein 1997a).

The 90-kDa compound is hydrophobic, contains mannose, has N-linked carbohydrates, has sites for O-linked carbohydrates (18% serine and threonine), and has an amino acid composition with ca. 38% hydrophobic and 62% hydrophilic residues (Kwon and Epstein 1997b). Genetic data and an *in vitro* system are required to demonstrate that the 90-kDa glycoprotein is a fungal glue *per se*.

3.4.4.3 The Mannoprotein SC3, a Schizophyllum commune Hydrophobin

Aerial plant surfaces are hydrophobic and many fungi and oomycetes adhere more tenaciously to hydrophobic surfaces such as polystyrene than to hydrophilic surfaces such as glass (Sela-Buurlage et al. 1991; Terhune and Hoch 1993; Kuo and Hoch 1996; Wright et al. 2002). Fungal hydrophobins are small (approximately 100 amino acids), secreted, moderately hydrophobic proteins with eight conserved cysteine residues and a common hydropathy profile, but highly variable amino acid sequences (Kershaw and Talbot 1998). Despite the variability in sequence, complementation experiments in *Magnaporthe grisea* with heterologous hydrophobin genes indicate that hydrophobins from different species encode for functionally related proteins (Kershaw et al. 1998).

Hydrophobins are interesting candidates as components of adhesives because they are structural proteins on the fungal surface that self-assemble into insoluble aggregates (Wösten et al. 1994). Moreover, the self-assembly occurs at the interface between a hydrophobic and a hydrophilic surface, which includes the environment in which most foliar plant pathogens have to adhere, i.e., a leaf surface covered with water. At least some hydrophobins, including Sc3 are glycosylated with mannose residues (de Vocht et al. 1998), as are many fungal glues. However, while the conidial rodlet hydrophobins, e.g., *Magnaporthe grisea* MPG1 (Kershaw et al. 1998) may allow for an initial hydrophobic interaction between a wind-blown spore and a leaf, it would be a comparatively weak attachment. Indeed, a hydrophobin mutant of *M. grisea Mpg1* adhered as well as the wild-type, indicating that the MPG1 hydrophobin is not involved in adhesion (Talbot et al. 1996).

Although currently there is no compelling evidence that a hydrophobin is a component of a strong glue, two *Schizophyllum commune* hydrophobins are involved in attachment. SC4 coats the surface of hyphae within the fruiting body (Schuren and Wessels 1990). As such, it serves in cell-cell adhesion. SC3 is involved in aerial hyphal formation. In comparison to the wild type, *sc3* mutants are reduced in adhesiveness to hydrophobic substrates (Wösten et al. 1994).

Hydrophobins have the interesting property of forming amphipathic membranes (Scholtmeijer et al. 2002). That is, hydrophobins form a membrane with a hydrophobic and a hydrophilic side; the hydrophobic side binds to hydrophobic surfaces and the hydrophilic side binds to hydrophilic surfaces. In so doing, a hydrophobin changes the polarity of its substratum. In the context of fungal-plant interactions, *Colletotrichum graminicola*, *Erysiphe graminis* and *Uromyces viciae-fabae* spores, for example, secrete material that increases the hydrophilicity of the surface (Nicholson et al. 1988; Deising et al. 1992; Pascholati et al. 1993). Here, we speculate that some of these changes could be mediated by hydrophobins.

3.4.4.4 Selected Glycosylphosphatidylinositol-dependent (GPI) Cell Wall Proteins

GPI cell wall proteins (GPI-CWP) are the most abundant proteins in fungal walls (de Groot et al. 2005). They have a GPI anchor to the plasma membrane at the C terminus and a signal peptide at the N terminus (de Nobel et al. 2001). GPI-CWP often have a repeated motif and a binding site that links the protein to the β1,6-glucan part of the wall. Here we will discuss GPI-CWP that are clearly adhesins, but that may have more non-specific glue-like properties.

The human pathogen *Candida albicans* adheres to polystyrene and to medical devices, in addition to human epithelial cells; *C. albicans* is more adherent than *Saccharomyces cerevisiae*. Li and Palecek (2003) expressed a library of *C. albicans* in a strain of *S. cerevisae flo8*Δ and screened for adhesive cells on polystyrene. They isolated a gene *EAP1* (enhanced adherence to polystyrene) which encodes for a GPI-CWP. Using expression in both *S. cerevisae* and in a *C. albicans* mutant, they demonstrated that Eap1 affects adhesion on both polystyrene and on epithelial cells. In the diploid *C. albicans* SC5314, in one allele, the predicted protein product has 70 PATEST repeats in one allele (comprising 37% of the protein) and 13 in the other (NCBI accession numbers EAK95619 and EAK95520). Following the PATEST repeat, there are nine or ten repeats of TPAAPGTPVESQP. Eap1 has homology to *C. albicans* Hwp1p and to *S. cerevisae* Flo11p, which are discussed below. The *C. albicans eap1* complements *flo 11* mutations in *S. cerevisae*.

In low-glucose, *Saccharomyces cerevisae* adheres to plastic and yeast cells agglutinate (Reynolds and Fink 2001). Genetic manipulation indicates that adhesion and agglutination requires the cell surface glycoprotein Flo11p. Flo11p increases cell surface hydrophobicity and is expressed when *S. cerevisae* grows as filaments, pseudohyphae, and invasively through agar but is not expressed in yeast cells (Braus et al. 2003). Based on the deduced amino acid sequence, Flo11p (also named MUC1 and YIR019C) contains 1367 amino acids of which 50% are either serine or threonine and 10% are proline. Starting at amino acid 333, there are 38 repeats of SSTTESS. This residue,

which comprises 19% of Flo11p is contained within 22 copies of S/T SSTTESS S/V (A)P V/A PTP and 16 copies of S/T SSTTESSSAPV.

3.5 Fungal Adhesins

Attachment of fungi to host cells is a critical part of fungal pathogenesis in animals (Sundstrom 2002). Examples of fungal adhesins that bind to animal cells are shown in Table 3.3. Similar to the fungal glues, most adhesins are glycoproteins, and at least several are mannoproteins (Fukazawa and Kagaya 1997), with mannan involvement in adhesion (Kanbe and Cutler 1998). Hazen and colleagues (Masuoka et al. 1999) have argued that cell surface hydrophobicity is an important factor in adhesion of *Candida albicans* to host epithelial cells and to plastic, that adhesion is a virulence factor, and that hydrophobic glycoproteins on the surface of the cells contribute, if not determine, cell surface hydrophobicity.

Table 3.3. Examples of animal pathogenic fungi that produce adhesins, and their receptors

Fungus	Fungal adhesin	Apparent host binding site	Reference
Blastomyces dermatitidis	BAD1 (=WI-1) protein	Binds yeast to CD11b/CD18 and CD14 receptors on human macrophages	Newman et al. (1995); Brandhorst et al. (1999); Brandhorst and Klein (2000)
Candida albicans	Members of the ALS (agglutinin-like sequence) gene family (GPI-CWP[a]): Als3, Als1, Als4, Als5 (=Ala1)	Different Als (in their N-terminal regions) may have different specificities, e.g., for laminin, collagen, fibronectin, endothelial and/or epithelial cells.	Fu et al. (1998); Hoyer (2001); de Groot et al. (2004); Loza et al. (2004); Zhao et al. (2004)
Candida albicans	Eap1, a GPI-CWP	Epithelial cells	Li and Palecek (2003)
Candida albicans	Int1, a RGD-protein	Epithelial cells	Gale et al. (1998)
Candida albicans	Mannan core and oligomannosyl side chains of the acid-stable portion of phosphomanno-protein	Marginal zone macrophages	Kanbe and Cutler (1998)
Candida glabrata	Epa1, a GPI-CWP	Epithelial cells	Cormack et al. (1999)

[a] GPI-CWP, glycosylphosphatidylinositol-dependent cell wall proteins

Several of the fungal adhesins, including Hwp1, Ala1p/Als5p, Als1p from *Candida albicans* and Epa1p from *Candida glabrata* are GPI-cell wall proteins. The arginine-glycine-aspartic (RGD) tripeptide sequence appears to be a critical site in both some fungal adhesins and plant and animal host receptors (Hostetter 2000; Senchou et al. 2004). Corrêa et al. (1996) concluded that thigmosensing of appressorium-inductive surfaces by the rust fungus *Uromyces appendiculatus* involved an RGD sequence, probably on a transmembrane, integrin-like glycoprotein.

3.6 Conclusions

Although many fungi produce glues, we have yet to characterize one definitively. Fungal glues are typically formed in an aqueous environment, and as such they may provide models for commercial glues, including for biomedical applications. The commercially available Tisseel® (Baxter Corporation) is used during surgery as a sealant. Just before use, the Tisseel® ingredients, fibrinogen and thrombin, are mixed; in mammals, thrombin activates fibrinogen which forms fibrin clots. The example is particularly relevant because many animal pathogenic fungi adhere to host fibrinogen and a putative adhesive from the oomycete *Phytophthora cinnamomi* is a protein with thrombospondin type 1 repeats (Robold and Hardham 2005).

Adhesion is a common feature of pathogenic fungi, regardless of whether they are pathogens in plants or animals. In addition, adhesion can be disrupted experimentally using enzymes that degrade the glue or compounds that block adhesion without directly killing the cell (Epstein et al. 1987). Consequently, anti-adhesives provide an appealing disease control strategy because they do not require uptake into the fungus and they do require disruption of a eukaryotic pathway. At least some of the antifungal activity of surfactants and detergents may be because they render plant surfaces less hydrophobic. Stanley et al. (2002) demonstrated that the phenolic zosteric acid (*p*-(sulfo-oxy) cinnamic acid) inhibits adhesion and infection by conidia of *Magnaporthe grisea* and *Colletotrichum lindemuthianum*; concentrations that are effective as an anti-adhesive are not toxic to either the plant hosts or fungi.

Genetic technologies should facilitate identification of fungal glues (Robold and Hardham 2005). The adherent *Magnaporthe grisea* (Hamer et al. 1988; Howard et al. 1991) has been sequenced and is amenable to targeted gene disruption. Within the next five years, the sequences of several other filamentous fungi that are and are not adherent should be available. Similarly, cDNA microarrays from an adherent fungus at adherent and non-adherent stages of development should allow the selection of putative adhesives for targeted gene disruption. In addition, "in silico" proteomics (Weig et al. 2004; de Groot et al. 2005) will facilitate identification of putative adhesives.

Because fungal glues are generally glycoproteins or conceivably proteoglycans, we predict that selection of secreted proteins with repetitive motifs should allow an initial selection for further demonstration of function by either targeted gene disruption or gene silencing.

References

Apoga D, Jansson H-B (2000) Visualization and characterization of the extracellular matrix of *Bipolaris sorokiniana*. Mycol Res 104:564–575

Apoga D, Jansson H-B, Tunlid A (2001) Adhesion of conidia and germlings of the plant pathogenic fungus *Bipolaris sorokiniana* to solid surfaces. Mycol Res 105:1251–1260

Apoga D, Barnard J, Craighead HG, Hoch HC (2004) Quantification of substratum contact required for initiation of *Colletotrichum graminicola* appressoria. Fung Genet Biol 41:1–12

Barki M, Koltin Y, Yanko M, Tamarkin A, Rosenberg M (1993) Isolation of a *Candida albicans* DNA sequence conferring adhesion and aggregation on *Saccharomyces cerevisiae*. J Bacteriol 175:5683–5689

Bechinger C, Giebel K-F, Schnell M, Leiderer P, Deising HB, Bastmeyer M (1999) Optical measurements of invasive forces exerted by appressoria of a plant pathogenic fungus. Science 285:1896–1899

Bergstrom GC, Nicholson RL (1999) The biology of corn anthracnose: knowledge to exploit for improved management. Plant Dis 83:596–608

Bircher U, Hohl HR (1997) Surface glycoproteins associated with appressorium formation and adhesion in *Phytophthora palmivora*. Mycol Res 101:769–775

Brandhorst T, Klein B (2000) Cell wall biogenesis of *Blastomyces dermatitidis*: evidence for a novel mechanism of cell surface localization of a virulence-associated adhesin via extracellular release and reassociation with cell wall chitin. J Biol Chem 275:7925–7934

Brandhorst T, Wüthrich M, Warner T, Klein B (1999) Targeted gene disruption reveals an adhesin indispensable for pathogenicity of *Blastomyces dermatitidis*. J Exp Med 189:1207–1216

Braun EJ, Howard RJ (1994a) Adhesion of *Cochliobolus heterostrophus* conidia and germlings to leaves and artificial surfaces. Exp Mycol 18:211–220

Braun EJ, Howard RJ (1994b) Adhesion of fungal spores and germlings to host surfaces. Protoplasma 181:202–212

Braus GH, Grundmann O, Brueckner S, Moesch H-U (2003) Amino acid starvation and Gcn4p regulate adhesive growth and *FLO11* gene expression in *Saccharomyces cerevisiae*. Mol Biol Cell 14:4272–4284

Brunner F, Rosahl S, Lee J, Rudd JJ, Geiler C, Kauppinen S, Rasmussen G, Scheel D, Nuernberger T (2002) Pep-13, a plant defense-inducing pathogen-associated pattern from *Phytophthora* transglutaminases. EMBO J 21:6681–6688

Buck JW, Andrews JH (1999a) Attachment of the yeast *Rhodosporidium toruloides* is mediated by adhesives localized at sites of bud cell development. Appl Environ Microbiol 65:465–471

Buck JW, Andrews JH (1999b) Localized, positive charge mediates adhesion of *Rhodosporidium toruloides* to barley leaves and polystyrene. Appl Environ Microbiol 65:2179–2183

Caesar-TonThat TC, Epstein L (1991) Adhesion-reduced mutants and the wild type *Nectria haematococca*: an ultrastructural comparison of the macroconidial walls. Exp Mycol 15: 193–205

Carver TLW, Kunoh H, Thomas BJ, Nicholson RL (1999) Release and visualization of the extracellular matrix of conidia of *Blumeria graminis*. Mycol Res 103:547–560

Chaky J, Anderson K, Moss M, Vaillancourt L (2001) Surface hydrophobicity and surface rigidity induce spore germination in *Colletotrichum graminicola*. Phytopathology 91: 558–564

Chaubal R, Wilmot VA, Wynn WK (1991) Visualization, adhesiveness, and cytochemistry of the extracellular matrix produced by urediniospore germ tubes of *Puccinia sorghi*. Can J Bot 69:2044–2054

Cormack BP, Ghori N, Falkow S (1999) An adhesin of the yeast pathogen *Candida glabrata* mediating adherence to human epithelial cells. Science 285:578–582

Corrêa A Jr, Staples RC, Hoch HC (1996) Inhibition of thigmostimulated cell differentiation with RGD-peptides in *Uromyces* germlings. Protoplasma 194:91–102

De Groot PWJ, de Boer AD, Cunningham J, Dekker HL, de Jong L, Hellingwerf KJ, de Koster C, Klis FM (2004) Proteomic analysis of *Candida albicans* cell walls reveals covalently bound carbohydrate-active enzymes and adhesins. Eukaryotic Cell 3:955–965

De Groot PW, Ram AF, Klis FM (2005) Features and functions of covalently linked proteins in fungal cell walls. Fungal Genet Biol 42:657–675

Deising H, Nicholson RL, Haug M, Howard RJ, Mengden K (1992) Adhesion pad formation and the involvement of cutinase and esterases in the attachment of uredospores to the host cuticle. Plant Cell 4:1101–1111

De Nobel H, Sietsma JH, van den Ende H, Klis FM (2001) Molecular organization and construction of the fungal cell wall. In: Howard RJ, Gow NAR (eds) The Mycota, vol VIII. Biology of the fungal cell. Springer, Berlin Heidelberg New York, pp 181–200

Deng MQ, Templeton TJ, London NR, Bauer C, Schroeder AA, Abrahamsen MS (2002) *Cryptosporidium parvum* genes containing thrombospondin type 1 domains. Infect Immun 70:6987–6995

De Vocht ML, Scholtmeijer K, van der Vegte EW, deVries OMH, Sonveaux N, Wösten HAB, Ruysschaert J-M, Hadziioannou G, Wessels JGH, Robillard GT (1998) Structural characterization of the hydrophobin SC3, as a monomer and after self-assembly at hydrophobic/hydrophilic interfaces. Biophys J 74:2059–2068

Doss RP, Potter SW, Chastagner GA, Christian JK (1993) Adhesion of non-germinated *Botrytis cineria* conidia to several substrata. Appl Environ Biol 59:1786–1791

Doss RP, Potter SW, Soeldner AH, Christian JK, Fukunaga LE (1995) Adhesion of germlings of *Botrytis cinerea*. Appl Environ Microbiol 61:260–265

Ebata Y, Yamamoto H, Uchiyama T (1998) Chemical composition of the glue from appressoria of *Magnaporthe grisea*. Biosci Biotech Biochem 62:672–674

Epstein L, Nicholson RL (1997) Adhesion of spores and hyphae to plant surfaces In: Carroll G, Tudzynski P (eds) The Mycota, vol V. Plant relationships, part A. Springer, Berlin Heidelberg New York, pp 11–25

Epstein L, Laccetti L, Staples RC, Hoch HC, Hoose WA (1985) Extracellular proteins associated with induction of differentiation in bean rust uredospore germlings. Phytopathology 75:1073–1076

Epstein L, Laccetti LB, Staples RC, Hoch HC (1987) Cell-substratum adhesive protein involved in surface contact responses of the bean rust fungus. Physiol Mol Plant Pathol 30:373–388

Epstein L, Kwon YH, Almond DE, Schached LM, Jones MJ (1994) Genetic and biochemical characterization of *Nectria haematococca* strains with adhesive and adhesion-reduced macroconidia. Appl Environ Microbiol 60:524–530

Epstein L, Lusnak K, Kaur S (1998) Transformation-mediated developmental mutants of *Glomerella graminicola*. Fung Genet Biol 23:189–203

Fabritius A-L, Judelson HS (2003) A mating-induced protein of *Phytophthora infestans* is a member of a family of elicitors with divergent structures and stage-specific patterns of expression. Mol Plant Microbe Interact 16:926–935

Fu Y, Rieg G, Fonzi WA, Belanger PH, Edwards JE Jr, Filler SG (1998) Expression of the *Candida albicans* gene *ALS1* in *Saccharomyces cerevisiae* induces adherence to endothelial and epithelial cells. Infect Immun 66:1783–1786

Fukazawa Y, Kagaya K (1997) Molecular bases of adhesion of *Candida albicans*. J Med Vet Mycol 35:87–99

Gale CA, Bendel CM, McClellan M, Hauser M, Becker JM, Berman J, Hostetter MK (1998) Linkage of adhesion, filamentous growth, and virulence in *Candida albicans* to a single gene, *INT1*. Science 279:1355–1358

Gaulin E, Jauneau A, Villalba F, Rickauer M, Esquerre-Tugaye MT, Bottin A (2002) The CBEL glycoprotein of *Phytophthora parasitica* var. *nicotianae* is involved in cell wall deposition and adhesion to cellulosic substrates. J Cell Sci 115:4565–4575

Göernhardt B, Rouhara I, Schmelzer E (2000) Cyst germination proteins of the potato pathogen *Phytophthora infestans* share homology with human mucins. Mol Plant Microbe Interact 13:32–42

Gubler F, Hardham AR, Duniec J (1989) Characterising adhesiveness of *Phytophthora cinnamomi* zoospores during encystment. Protoplasma 149:24–30

Gunderson JH, Elwood H, Ingold A, Kindle K, Sogin ML (1987) Phylogenetic relationships between chlorophytes, chrysophytes, and oomycetes. Proc Natl Acad Sci USA 84:5823–5827

Hamer JE, Howard RJ, Chumley FG, Valent B (1988) A mechanism for surface attachment in spores of a plant pathogenic fungus. Science 239:288–290

Hardham AR (2001) Cell biology of fungal infection of plants. In: Howard RJ, Gow NAR (eds) The Mycota: biology of the fungal cell, vol 7. Springer, Berlin Heidelberg New York, pp 91–123

Hardham A, Gubler F (1990) Polarity of attachment of zoospores of a root pathogen and prealignment of the emerging germ tube. Cell Biol Int Rep 14:947–956

Hoch HC, Staples RC, Whitehead B, Comeau J, Wolf ED (1987) Signaling for growth orientation and cell differentiation by surface topography in *Uromyces*. Science 235:1659–1662

Hostetter MK (2000) RGD-mediated adhesion in fungal pathogens of humans, plants and insects. Curr Opin Microbiol 3:344–348

Howard RJ, Ferrari MA, Roach DH, Money NP (1991) Penetration of hard substrates by a fungus employing enormous turgor pressures. Proc Natl Acad Sci USA 88:11281–11284

Hoyer LL (2001) The ALS gene family of *Candida albicans*. Trends Microbiol 9:176–180

Hughes HB, Carzaniga R, Rawlings SL, Green JR, O'Connell RJ (1999) Spore surface glycoproteins of *Colletotrichum lindemuthianum* are recognized by a monoclonal antibody which inhibits adhesion to polystyrene. Microbiology 145:1927–1936

Iranzo M, Aguado C, Pallotti C, Canizares JV, Mormeneo S (2002) Transglutaminase activity is involved in *Saccharomyces cerevisiae* wall construction. Microbiology 148:1329–1334

Jones EBG (1994) Fungal adhesion. Mycol Res 98:961–981

Jones MJ, Epstein L (1989) Adhesion of *Nectria haematococca* macroconidia. Physiol Mol Plant Pathol 35:453–461

Jones MJ, Epstein L (1990) Adhesion of macroconidia to the plant surface and virulence of *Nectria haematococca*. Appl Environ Microbiol 56:3772–3778

Kanbe T, Cutler JE (1998) Minimum chemical requirements for adhesin activity of the acid-stable part of *Candida albicans* cell wall phosphomannoprotein complex. Infect Immun 66:5812–5818

Kershaw MJ, Talbot NJ (1998) Hydrophobins and repellents: proteins with fundamental roles in fungal morphogenesis. Fung Genet Biol 23:18–33

Kershaw MJ, Wakley GE, Talbot NJ (1998) Complementation of the *Mpg1* mutant phenotype in *Magnaporthe grisea* reveals functional relationships between fungal hydrophobins. EMBO J 17:3838–3849

Kunoh H, Yamaoka N, Yoshioka H, Nicholson RL (1988) Preparation of the infection court by *Erysiphe graminis*: I. Contact mediated changes in morphology of the conidium surface. Exp Mycol 12:325–335

Kuo K-C, Hoch HC (1996) Germination of *Phyllosticta ampelicida* pycnidiospores: prerequisite of adhesion to the substratum and the relationship of substratum wettability. Fung Genet Biol 20:18–29

Kwon YH, Epstein L (1993) A 90-kDa glycoprotein associated with adhesion of *Nectria haematococca* macroconidia to substrata. Mol Plant Microbe Interact 6:481–487

Kwon YH, Epstein L (1997a) Involvement of the 90 kDa glycoprotein in adhesion of *Nectria haematococca* macroconidia. Physiol Mol Plant Pathol 51:287–303

Kwon YH, Epstein L (1997b) Isolation and composition of the 90 kDa glycoprotein associated with adhesion of *Nectria haematococca* macroconidia. Physiol Mol Plant Pathol 51:63–74

Lau GW, Hamer JE (1998) *Acropetal:* a genetic locus required for conidiophore architecture and pathogenicity in the rice blast fungus. Fungal Genet Biol 24:228–239
Leite B, Nicholson RL (1992) Mycosporine-alanine: a self-inhibitor of germination from the conidial mucilage of *Colletotrichum graminicola*. Exp Mycol 16:76–86
Li F, Palecek S (2003) *EAP1*, a *Candida albicans* gene involved in binding human epithelial cells. Eukaryotic Cell 2:1266–1273
Liu ZM, Kolattukudy PE (1999) Early expression of the calmodulin gene, which precedes appressorium formation in *Magnaporthe grisea*, is inhibited by self-inhibitors and requires surface attachment. J Bacteriol 181:3571–3577
Loza L, Fu Y, Ibrahim AS, Sheppard DC (2004) Functional analysis of the *Candida albicans ALSI* gene product. Yeast 21:473–482
Masuoka J, Wu G, Glee PM, Hazen KC (1999) Inhibition of *Candida albicans* attachment to extracellular matrix by antibodies which recognize hydrophobic cell wall proteins. FEMS Immunol Med Microbiol 24:421–429
Mendgen K, Hahn M, Deising H (1996) Morphogenesis and mechanisms of penetration by plant pathogenic fungi. Annu Rev Phytopathol 34:367–386
Mercure EW, Leite B, Nicholson RL (1994) Adhesion of ungerminated conidia of *Colletotricum graminicola* to artificial hydrophobic surfaces. Physiol Mol Plant Pathol 45:421–440
Mercure EW, Kunoh H, Nicholson RL (1995) Visualization of materials released from adhered, ungerminated conidia of *Colletotrichum graminicola*. Physiol Mol Plant Pathol 46:121–135
Newman SL, Chaturvedi S, Klein BS (1995) The WI-1 antigen on *Blastomyces dermatitidis* yeasts mediates binding to human macrophage CD18 and CD14 receptors. J Immunol 154:753–761
Nicholson RL, Epstein L (1991) Adhesion of fungi to the plant surface: prerequisite for pathogenesis. In: Cole GT, Hoch HC (eds) The Fungal spore and disease initiation in plants and animals. Plenum Press, New York, pp 3–23
Nicholson RL, Moraes WBC (1980) Survival of *Colletotrichum graminicola*: importance of the spore matrix. Phytopathology 70:255–261
Nicholson RL, Yoshioka H, Yamaoka N, Kunoh H (1988) Preparation of the infection court by *Erysiphe graminis*. II. Release of esterase enzyme from conidia in response to a contact stimulus. Exp Mycol 12:336–349
Ohtake M, Yamamoto H, Uchiyama T (1999) Influences of metabolic inhibitors and hydrolytic enzymes on the adhesion of appressoria of *Pyricularia oryzae* to wax-coated cover-glasses. Biosci Biotech Biochem 63:978–982
Osherov N, May GS (2001) The molecular mechanisms of conidial germination. FEMS Microbiol Lett 199:153–160
Pain NA, Green JR, Jones GL, O'Connell RJ (1996) Composition and organisation of extracellular matrices around germ tubes and appressoria of *Colletotrichum lindemuthianum*. Protoplasma 190:119–130
Pascholati S, Yoshioka H, Kunoh H, Nicholson RL (1992) Preparation of the infection court by *Erysiphe graminis* f. sp. *hordei*: cutinase is a component of the conidial exudate. Physiol Mol Plant Pathol 41:53–59
Pascholati SF, Deising H, Leite B, Anderson D, Nicholson RL (1993) Cutinase and non-specific esterase activities in the conidial mucilage of *Colletotrichum graminicola*. Physiol Mol Plant Pathol 42:37–51
Pringle RB (1981) Nonspecific adhesion of *Bipolaris sorokiniana* sporelings. Can J Plant Pathol 3:9–11
Recorbet G, Alabouvette C (1997) Adhesion of *Fusarium oxysporum* conidia to tomato roots. Lett Appl Microbiol 25:375–379
Reynolds TB, Fink GR (2001) Bakers' yeast, a model for fungal biofilm formation. Science 291:878–881
Robold AV, Hardham AR (2004) Production of monoclonal antibodies against peripheral vesicle proteins in zoospores of *Phytophthora nicotianae*. Protoplasma 223:121–132
Robold AV, Hardham AR (2005) During attachment *Phytophthora* spores secrete proteins containing thrombospondin type 1 repeats. Curr Genet 47:307–315

Ruiz-Herrera J, Iranzo M, Elorza MV, Sentandreu R, Mormeno S (1995) Involvement of transglutaminase in the formation of covalent cross-links in the cell wall of *Candida albicans*. Arch Microbiol 164:186–193

Scholtmeijer K, Janssen MI, Gerssen B, de Vocht ML, van Leeuwen BM, van Kooten TG, Wösten HAB, Wessels JGH (2002) Surface modifications created by using engineered hydrophobins. Appl Environ Microbiol 68:1367–1373

Schuren FHJ, Wessels JGH (1990) Two genes specifically expressed in fruiting dikaryons of *Schizophyllum commune*: homologies with a gene not regulated by mating type genes. Gene 90:199–205

Sela-Buurlage MB, Epstein L, Rodriguez RJ (1991) Adhesion of ungerminated *Colletotricum musae* conidia. Physiol Mol Plant Pathol 39:345–352

Senchou V, Weide R, Carrasco A, Bouyssou H, Pont-Lezica R, Govers F, Canut H (2004) High affinity recognition of a *Phytophthora* protein by *Arabidopsis* via an RGD motif. Cell Mol Life Sci 61:502–509

Shaw BD, Hoch HC (1999) The pycnidiospore of *Phyllosticta ampelicida*: surface properties involved in substratum attachment and germination. Mycol Res 103:915–924

Shaw BD, Hoch HC (2000) Ca^{2+} regulation of *Phyllosticta ampelicida* pycnidiospore germination and appressorium formation. Fung Genet Biol 31:43–53

Shaw BD, Hoch HC (2001) Ions as regulators of growth and development. In: Howard RJ, Gow NAR (eds) The Mycota, vol VIII. Biology of the fungal cell. Springer, Berlin Heidelberg New York, pp 73–89

Slawecki RA, Ryan EP, Young DH (2002) Novel fungitoxicity assays for inhibition of germination-associated adhesion of *Botrytis cinerea* and *Puccinia recondita* spores. Appl Environ Microbiol 68:597–601

Snetselaar KM, McCann MP (2001) From bud to appressorium: morphology of the *Ustilago maydis* transition from saprobic to parasitic growth. Phytopathology 91:S165 (abstract)

Spotts RA, Holz G (1996) Adhesion and removal of conidia of *Botrytis cinerea* and *Penicillium expansum* from grape and plum fruit surfaces. Plant Dis 80:691–699

Staab JF, Bradway SD, Fidel PL, Sundstrom P (1999) Adhesive and mammalian transglutaminase substrate properties of *Candida albicans* Hwp1. Science 283:1535–1538

Stanley MS, Callow ME, Perry R, Alberte RS, Smith R, Callow JA (2002) Inhibition of fungal spore adhesion by zosteric acid as the basis for a novel, nontoxic crop protection technology. Phytopathology 92:378–383

Sugui JA, Leite B, Nicholson RL (1998) Partial characterization of the extracellular matrix released onto hydrophobic surfaces by conidia and conidial germlings of *Colletotricum graminicola*. Physiol Mol Plant Pathol 52:411–425

Sundstrom P (2002) Adhesion in *Candida* spp. Cell Microbiol 4:461–469

Takano Y, Kikuchi T, Kubo Y, Hamer JE, Mise K, Furusawa I (2000) The *Colletotrichum lagenarium* MAP kinase gene *CMK1* regulates diverse aspects of fungal pathogenesis. Mol Plant Microbe Interact 13:374–383

Talbot NJ, Kershaw M, Wakley GE, De Vries OMH, Wessels JGH, Hamer JE (1996) *MPG1* encodes a fungal hydrophobin involved in surface interactions during infection-related development of the rice blast fungus *Magnaporthe grisea*. Plant Cell 8:985–999

Terhune BT, Hoch HC (1993) Substrate hydrophobicity and adhesion of *Uromyces* urediospores and germlings. Exp Mycol 17:241–252

Tomley FM, Soldati DS (2001) Mix and match modules: structure and function of microneme proteins in apicomplexan parasites. Trends Parasitol 17:81–88

Tucker RP (2004) Molecules in focus. The thrombospondin type 1 repeat superfamily. Int J Biochem Cell Biol 36:969–974

Tucker SL, Talbot NJ (2001) Surface attachment and pre-penetration stage development by plant pathogenic fungi. Annu Rev Phytopathol 39:385–417

Vreeland V, Epstein L (1996) Analysis of plant-substratum adhesives. In: Jackson JF, Linskens H-F (eds) Modern methods of plant analysis, vol 17. Plant cell wall analysis. Springer, Berlin Heidelberg New York, pp 95–116

Vreeland V, Waite JH, Epstein L (1998) Polyphenols and oxidases in substratum adhesion by marine algae and mussels. J Phycol 34:1–8

Watanabe K, Parbery DG, Kobayashi T, Doi Y (2000) Conidial adhesion and germination of *Pestalotiopsis neglecta*. Mycol Res 104:962–968

Weig M, Jansch L, Gross U, de Koster CG, Klis FM, de Groot, PWJ (2004) Systematic identification *in silico* of covalently bound cell wall proteins and analysis of protein-polysaccharide linkages of the human pathogen *Candida glabrata*. Microbiology 150:3129–3144

Wösten HAB, Schuren FHJ, Wessels JGH (1994) Interfacial self-assembly of a hydrophobin into an amphipathic membrane mediates fungal attachment to hydrophobic surfaces. EMBO J 13:5848–5854

Wright AJ, Thomas BJ, Kunoh H, Nicholson RL, Carver TLW (2002) Influences of substrata and interface geometry on the release of extracellular material by *Blumeria graminis* conidia. Physiol Mol Plant Pathol 61:163–178

Xiao J-Z, Ohshima A, Kamakura T, Ishiyama T, Yamaguchi I (1994) Extracellular glycoprotein(s) associated with cellular differentiation in *Magnaporthe grisea*. Mol Plant Microbe Interact 7:639–644

Yamaoka N, Takeuchi Y (1999) Morphogenesis of the powdery mildew fungus in water (4) The significance of conidium adhesion to the substratum for normal appressorium development in water. Physiol Mol Plant Pathol 54:145–154

Zhao X, Oh S-H, Cheng G, Green CB, Nuessen JA, Yeater K, Leng RP, Brown AJP, Hoyer LL (2004) ALS3 and ALS8 represent a single locus that encodes a *Candida albicans* adhesin; functional comparisons between Als3p and Als1p. Microbiology 150:2415–2428

4 The *Ulva* Spore Adhesive System

James A. Callow and Maureen E. Callow

4.1 Introduction

Ulva (formerly *Enteromorpha*, Hayden et al. 2003) is a cosmopolitan intertidal green alga. Dispersal and vegetative reproduction in this organism is achieved via the production of vast numbers of microscopic, 'naked' (i.e. lacking a cell wall), motile zoospores (Fig. 4.1a). Like other dispersal stages of sessile marine organisms (e.g. the larvae of invertebrates), the zoospores need to locate and bind to a surface quickly in order to complete their life history. Once the zoospore has detected a suitable surface it undergoes 'settlement', involving the loss of the flagella, the secretion of an adhesive which anchors the settled spore to the substratum and the production of a new cell wall (Fig. 4.1b,c). Spore germination occurs within a few hours, cell division and growth giving rise to sporelings–young plants that are also firmly attached to the substratum by adhesive secreted by the rhizoids.

A practical consequence of this natural dispersal and settlement process is that the spores also settle on man-made surfaces, creating the problem of biofouling–the unwanted growth of organisms on surfaces. *Ulva* spp. are major contributors to 'soft-fouling' in the marine environment. Controlling biofouling without the use of toxic biocides is essentially a matter of controlling interfacial adhesion, and an understanding of adhesion processes in the context of the applied problem of biofouling has been the driver of much of the fundamental and applied research on the adhesion and adhesives of marine organisms. Other chapters in this volume are concerned with the adhesives of other marine fouling organisms–viz. diatoms (Chap. 5), mussels (Chap. 7) and barnacles (Chap. 8). In this chapter we consider the case of the green alga *Ulva*-which has become a model organism for understanding adhesion in soft-fouling algae.

It is frequently remarked that in an environment characterised by a wide range of substrates, temperatures, salinities and conditions of turbulence, the adhesives used by marine organisms need to display some remarkable properties to facilitate rapid and permanent bonding (although temporary adhesives are also known such as those used by the cypris larvae of barnacles in initial surface bonding). To be effective underwater an adhesive must be discharged

School of Biosciences, The University of Birmingham, Birmingham B15 2TT, UK

Biological Adhesives
(ed. by A.M. Smith and J.A. Callow)

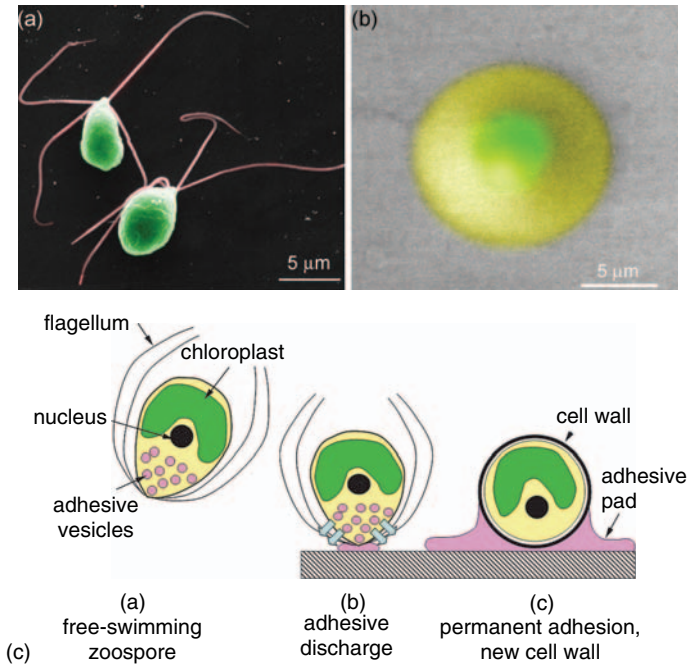

Fig. 4.1. (a) False colour SEM image of zoospores of *Ulva linza*. (b) False colour environmental-SEM image of a settled spore of *Ulva linza* showing the annular pad of adhesive surrounding the central spore body (copyright 2005, from Walker et al. 2005, reproduced by permission of Taylor and Francis Group, LLC, http://www.taylorandfrancis.com). (c) Cartoon depicting the course of events involved in the settlement and adhesion of *Ulva* spores

quickly from the attaching organism in order to secure the propagule. The adhesive must have initially fluid properties in order to spread or 'wet' the surface, but it must also have a surface tension that prevents it from simply dissolving in the water. Having wet the surface the adhesive must bond to that surface in a process that must involve the exclusion of water molecules. Finally the adhesive must 'cure' quickly to achieve a cohesive strength sufficient to bond the organisms under turbulent conditions. The main purpose of this chapter is to explore what we know, or may predict, of the properties of the *Ulva* zoospore adhesive system in the context of these requirements.

4.2 Cell Biological and Biochemical Aspects

4.2.1 The 'Adhesive Apparatus'

The pioneering work of Evans and Christie (1970) established the ultrastructural basis of the adhesion process. Swimming spores contain a single posterior chloroplast and central nucleus but the anterior region is characterised by

numerous membrane-bound vesicles with electron-dense contents, 150–300 nm diameter, which are abstricted from Golgi cisternae (Fig. 4.2). Since the vesicles are absent from settled spores it was inferred that, during adhesion, their contents must be secreted by exocytosis from the anterior region, to form the extracellular adhesive, which was visualized in TEMs as fibrillar material surrounding the settled spore. The electron dense contents of 'adhesive vesicles' (Evans and Christie 1970) and the secreted adhesive (Christie et al. 1970) were shown to be sensitive to proteolytic enzymes (see also Pettitt et al. 2005 for more recent evidence on the effect of proteases on adhesion). EM cytochemistry of the vesicles and the extracellular adhesive indicated the presence of glycoproteins (Callow and Evans 1974, 1977). Studies on the identity of the contents of the adhesive vesicles are described in Sect. 4.2.2.

The settlement of zoospores is an active process involving a pre-settlement behaviour which features the 'probing' of a candidate surface, during which the spore makes many rapid and periodic contacts with the surface, each contact usually involving rotation on an apical papilla (Callow et al. 1997). Settlement is selective, spores can respond to a range of chemical, physical, topographic and

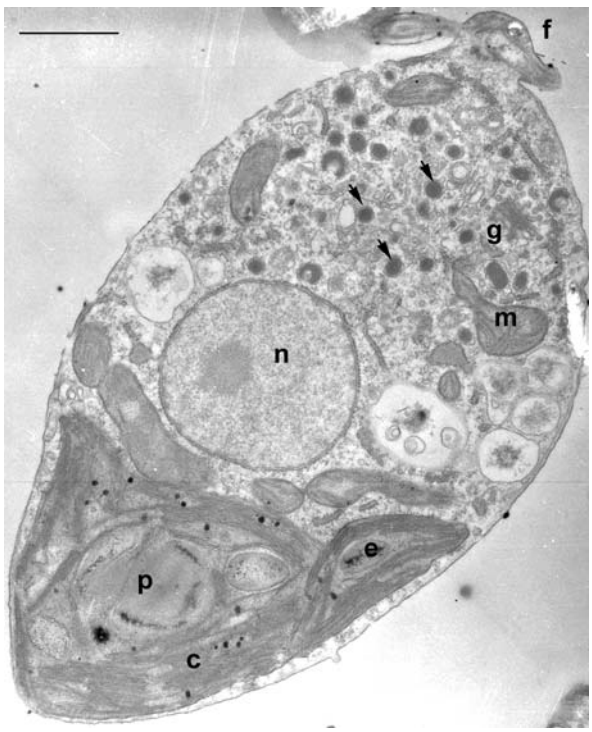

Fig. 4.2. Transmission electron micrograph of a longitudinal section through a zoospore of *Ulva* illustrating the general ultrastructure and adhesive vesicles (single posterior chloroplast, c; pyrenoid, p; nucleus, n; mitchondrion, m; flagella, f; eyespot, e; Golgi body, g). Adhesive vesicles (*arrowed*) are electron-dense bodies, surrounded by a single membrane, and located in the anterior region of the cell. Figure kindly provided by Prof. LV Evans

biological cues (see Sect. 4.3.2) and it seems likely that cue detection is part of this pre-settlement behaviour. The detection of an appropriate cue then triggers irreversible commitment to adhesion, involving a partial flattening of the anterior region of the spore against a surface, intense cytoplasmic activity, the discharge of the contents of the adhesive vesicles and the withdrawal of the flagellar axonemes into the cell (the lipoprotein sheaths are shed into the water column). This process may occupy as little as 30–60 s and is followed by the synthesis of a new cell wall.

The cellular mechanisms leading to adhesive vesicle exocytosis are not well understood although recent experiments have shed some insight into the membrane trafficking and internal signalling processes. When cells were treated with the membrane traffic inhibitor Brefeldin A, fewer zoospores settled on surfaces (Callow et al. 2001). In both plant and animal cells Ca^{2+} plays a major regulatory role in controlling exocytosis through its involvement in signalling cascades (e.g. Battey and Blackbourn 1993). In the brown alga *Fucus serratus*, free $[Ca^{2+}]_{cyt}$ is involved in the fertilisation-triggered events of exocytosis that lead to the formation of a new cell wall around the naked egg cell (Roberts et al. 1994)–an analogous process to the secretion of the *Ulva* adhesive. Thompson et al. (in prep.) used fluorescent Ca^{2+} indicator dyes to follow transient changes in cytosolic Ca^{2+} ($[Ca^{2+}]_{cyt}$) in settling zoospores. Although there are problems with this approach connected with internal compartmentalisation of these dyes, results indicated that settling zoospores undergo transient elevations in $[Ca^{2+}]_{cyt}$. One potential source of such elevated $[Ca^{2+}]_{cyt}$ is the external sea water, through the opening of Ca^{2+} channels in the plasma membrane in response to the recognition of a settlement-triggering external stimulus. Support for this is the reduced level of spore settlement obtained through the use of a range of external calcium channel inhibitors (Thompson et al., in prep.).

The process of exocytosis of adhesive vesicles is rapid–typically a spore that commits to adhesion completes the process within 1 min (Callow et al. 1997). Cells undergoing such an active exocytosis have 'membrane retrieval' processes by which the membranes of the emptied cytoplasmic vesicles are recycled to prevent major expansion of the cell plasma membrane (Samuels and Bisalputra 1990). Thompson et al. (in prep.) used the fluorescent dye FM 1-43 to examine membrane recycling processes. They showed that, in swimming spores, FM 1-43 labelled the external plasma membrane of the cell, with no internal labelling. As the spores settled an FM 1-43 labelled spot appeared within 30–60 s of the spore settling suggesting that as the surface membrane is augmented by fusion of adhesive vesicles, some of the plasma membrane is internalised into an endosomal compartment.

4.2.2 Use of Monoclonal Antibodies to Identify the Contents of Adhesive Vesicles

Biochemical characterisation of the contents of the adhesive vesicles has been an important but frustrating goal. As a step towards this, Stanley et al. (1999) used a monoclonal antibody strategy to produce probes that could be used to

identify the contents of adhesive vesicles. The approach involved the raising of monoclonal antibodies (mAbs) to settled cells displaying surface adhesive. Immunolocalisation methods were used to screen the resulting hybridomas for antibodies which recognise the contents of vesicles in unsettled spores and the secreted extracellular materials of adhered spores. Two mAbs (Ent1 and Ent 6) with these characteristics were described but detailed studies on the timing of the release of the recognized antigens, their relative abilities to inhibit adhesion in spore settlement assays, plus other lines of evidence, suggested slightly different roles for the antigens recognised by these mAbs in the settlement and adhesion process (for further details see Stanley et al. 1999). Most studies have focussed on the antigens detected by Ent 6. By indirect immunofluorescence (IIF), Ent 6 strongly labelled the internal contents of the anterior region of unsettled zoospores with no labelling of flagella or the posterior, chloroplast-containing region. The surface of settled spores was also labelled. Immunogold electron microscopy of chemically fixed zoospores showed that Ent 6 labelled the contents of the adhesive vesicles of swimming spores and materials secreted to the surface of spores within a few minutes of settlement. At later time points material extending from the cell surface was labelled and there was also extensive labelling of the new cell wall that develops at later time points. There was also extensive internal labelling in settled spores and higher resolution cryofixation methods applied to settled spores showed clearly that this internal labelling was associated with the intensely-developed Golgi system found in the former apical region of the spore (Callow JA et al. 2000b). This suggests that a continued synthesis of adhesive material is required even after the spore has settled. Ent 6 did not label any cytoplasmic components of vegetative cells of *Ulva* but strongly labelled the mature cell wall.

Taken together, the continued synthesis after settlement and the extensive labelling of cell walls by the antibodies suggests that the material found in spore adhesive vesicles is not a discrete polymer, synthesised and packaged into the vesicles purely for the purpose of spore adhesion. Rather, it seems likely that the spore adhesive is related to a constituent of the normal plant cell wall. When packaged into the spore adhesive vesicles, the polymer provides an almost instantaneous supply of adhesive to secure initial spore adhesion. There is subsequent consolidation of adhesion through continued secretion of the same, or similar glycoproteins into the new cell wall. Adhesion of the zoospore is thus viewed as an extension of cell wall synthesis, with cross-links between these glycoproteins and other cell wall matrix components providing a strong physical continuum between the cell and the adhesive at the substratum interface. Plant cell walls are well known to contain glycoproteins, notably members of the hydroxyproline-rich superfamily known as ‘extensins’, some of which have self-associating, adhesive-like properties (Kieslisewski and Lamport 1994).

To demonstrate further a role in adhesion for the antigens recognised by the two mAbs, functional inhibition assays of adhesion were performed with Ent 6 (Stanley et al. 1999). Both the purified Ent 6 immunoglobulin and its

$F(ab)_2$ fragment, blocked initial adhesion at low (nmol/l) concentrations. The simplest interpretation of this result is that the antibodies bound to the adhesive as it was secreted, thus reducing the ability of the adhesive to form interfacial bonds with the surface.

4.2.3 Biochemical Characteristics of the Adhesive Antigens

Immunoblots of extracts of swimming spores in SDS-sample buffer run on SDS-PAGE, showed strong labelling by both mAbs of a major band at 110 kDa but with some size-polydispersity and a number of minor bands of lower and higher M_r (Stanley et al. 1999). It appears that the adhesive antigen is not a discrete molecular entity but rather a family of related molecules in which there may be variable degrees of glycosylation and/or variable number of repetitive motifs. The basis of this heterogeneity is not known but parallels are found in the hydroxyproline-rich 'superfamily' of extensins found in plant cell walls in which variable numbers of tandem repeat motifs contribute to microheterogeneity (Kieliszewski and Lamport 1994).

The soluble 110-kDa antigen was present in extracts of sporulating thallus but was absent from vegetative tissue. A band shift to approx. 95 kDa was obtained following digestion of spore extracts with peptide *N*-glycosidase (PNGase), suggesting that the antigen is an *N*-linked glycoprotein; complete deglycosylation with anhydrous HF gave a similar band shift suggesting that there is little *O*-linked glycosylation. The antigen was sensitive to pronase digestion but not periodate oxidation suggesting that the epitope is proteinaceous.

Size exclusion chromatography of the native, undenatured adhesive antigen (Callow JA et al. 2000b) gave a single high molecular weight peak eluting in the void volume ($M_r > 1.3 \times 10^6$), which was separated into two major components (M_r 430 kDa (peak I) and 43 kDa (peak II)) in the presence of EDTA and a non-ionic detergent. Denaturing SDS-PAGE immunoblots showed that peak I corresponded to the major 110-kDa component detected in SDS-PAGE of whole extracts, with some polydispersity. Peak II gave a number of bands between 80 and 45 kDa.

4.2.4 Experiments on Cross-linking

Immunoblots of gels, on which extracts of spores harvested at different times after settlement were run, showed that with time progressively smaller amounts of the sample-buffer soluble Ent 6 antigen could be extracted, presumably due to extensive cross-linking during curing (Stanley et al. 1999). A similar experiment showed that the cross-linking could be inhibited by the SH-reducing agent dithiothreitol, and the SH-capping Ellman's Reagent (Humphrey et al. 2005). The same reagents also reduced the adhesion strength of spores, the

implication being that the firm bonding of spores to their substrates depends at least partially on the development of cohesive properties created by cross-linking of the adhesive, and that this involves S-S bond formation.

4.2.5 Molecular Aspects

While the antigens defined by the Ent 1 and 6 monoclonal antibodies provide realistic candidates for the *Ulva* spore adhesive for the reasons outlined above, a full understanding of the adhesive mechanism requires that these glycoproteins be fully characterised. We need to know the amino acid sequence(s) of the proteins and the nature of the glycan moieties. The encoding gene sequences need to be cloned to facilitate an understanding of the molecular genetics of adhesive synthesis and expression. To date none of these objectives has been unambiguously achieved. Major stumbling blocks to the purification and amino acid sequencing of the adhesive protein(s) have been: a) low levels of material for chemical analysis; b) the rapid cross-linking of the adhesive that occurs following release, or on extraction, which renders conventional biochemical purification difficult; c) difficulty in unequivocally identifying what is adhesive during extraction/purification procedures–currently the only criterion that can be used is reaction with the Ent 1/6 antibodies. Alternative, nucleic-acid (cDNA) based approaches, from which an amino acid sequence may be inferred, have also been attempted. Since mAb probes to the adhesive are available, immunoselection from a cDNA expression library is an obvious route. Unfortunately several attempts to do this in the authors' laboratory using Ent 1(an IgG) have given equivocal results, while a number of clones were isolated that had sequences that could be relevant to adhesive functions–there were also several clones emerging from primary and secondary immunoscreens that had no obvious connection with adhesion. While these are likely to be false positives, they mean that a candidate sequence cannot be unequivocally identified. However, newer genetic technologies–specifically cDNA microarrays–do offer a way forward. The *Ulva* EST library (Stanley et al. 2005) can be used to compare stages in the development of the organism where one may anticipate changes in the pattern of expression of adhesive genes. This theme is elaborated further in Sect. 4.4.

4.3 Physical and Mechanical Properties of the Adhesive

4.3.1 Imaging the Adhesive by ESEM

Callow et al. (2003) used environmental scanning electron microscopy (ESEM) to image the secreted adhesive in its natural, hydrated state, i.e. without fixation or dehydration. Results revealed that settled spores were surrounded by

a pad of adhesive material–often in a simple, symmetrical annular shapes (Fig. 4.1b), with occasionally more irregular profiles. Observations made on spores that had been settled between 1 and 5 h revealed no obvious time-dependent differences in the profiles of the adhesive pads. The 'featureless' appearance of these adhesive pads, without any evident structure, contrasts markedly with the fibrillar appearance of adhesive material surrounding settled spores when viewed by transmission electron microscopy (Evans and Christie 1970) or conventional SEM (Stanley et al. 1999); it is likely therefore that the fibrillar appearance in these reports was an artefact of dehydration during specimen preparation. The precise size and shape of adhesive pads in ESEM was sensitive to water vapour pressure (Callow et al. 2003), suggesting that the adhesive material is hygroscopic in character. Other lines of evidence (see Sect. 4.3.3) also suggest that the spore adhesive is hydrophilic in character and it may be that the ability of this polymer to adsorb or 'mix' with water molecules is an important part of the interfacial bonding mechanism underwater.

4.3.2 The Influence of Surface Properties on Adhesion and Adhesive Spreading

The range of marine surfaces available for colonisation by spores of *Ulva* is vast and most seem to be utilised by this opportunistic genus. A number of 'cues' are involved in attracting spores to a particular surface on which to settle and attach. Negative phototaxis guides zoospores and zygotes to areas of low light, although diffusible chemical cues released from surface-associated organisms such as bacteria, may also guide the swimming spores towards a suitable surface on which to settle (Joint et al. 2000, 2002; Tait et al. 2005; Wheeler et al. 2006). We have also shown that settlement is strongly influenced by a number of surface properties including wettability (Callow ME et al. 2000; Finlay et al. 2002a; Ista et al. 2004) and microtopography (Callow et al. 2002; Hoipkemeier-Wilson et al. 2004; Carman et al. 2006). Both of these surface properties are relevant to understanding how the *Ulva* adhesive system works.

4.3.2.1 Studies on the Influence of Surface Wettability Using SAMs

Traditionally, since the work of Baier (1973), settlement and adhesion of fouling organisms has been associated with low surface free energy of the substrate. The effect of surface energy on adhesion is often studied by employing widely different materials, ranging from urethanes and epoxies (high energy), to silicones and fluorinated materials (low energy). However, such diverse materials have substantially different chemistries and physical properties such as modulus, and more recently those interested in fundamental adsorption and adhesion phenomena have used surfaces formed from self-assembled monolayers (SAMs) on gold-coated glass or some other common substrate

(Sigal et al. 1998; Callow ME et al. 2000; Ostuni et al. 2001). SAM surfaces are more fully characterized and uniform with respect to properties such as surface topography, modulus, frictional coefficients, and can be made with a variety of functional groups (an outstanding example of how systematic variations in molecular properties of oligoether SAMs can be used to analyse protein adhesion to surfaces can be seen in Herrewerth et al. 2003). The use of mixed alkane thiolate SAMs of different wettability, and patterned on the same slide, is particularly revealing since a wide range of surface properties is simultaneously presented to attaching organisms, allowing 'choice' experiments to be conducted. Callow ME et al. (2000) examined the settlement of *Ulva* zoospores on mixed patterned SAMs. There was a positive correlation between the number of spores that attached to the SAMs and increasing contact angle (hydrophobicity). Video microscopy of a patterned arrangement of SAMs showed that a greater number of zoospores were engaged in swimming and 'searching' above the hydrophobic sectors, than the hydrophilic sectors, suggesting that the cells were able to 'sense' that the hydrophobic surfaces were more favourable for settlement. In a subsequent paper, Finlay et al. (2002b) showed that adhesion strength of the settled spores, as measured by resistance to detachment in a turbulent flow cell, was greatest on a hydrophilic SAM surface. Studies on SAMs of similar wettability but different frictional coefficients (through varying the alkanethiol chain length) have recently been used to show that surface frictional properties are also a factor in controlling the adhesion strength of attached *Ulva* spores (Bowen et al., in prep.).

4.3.2.2 Adhesive Wetting studies

For an adhesive to bind to other surfaces it has to "wet" that surface and whether it does so will depend on the competition between the adhesive and water interacting with the surface. The interaction is complex, involving the displacement of water from the adhesive and the surface, formation of contact between the adhesive and surface as well as the formation of the cohesive contacts of the water molecules that were displaced from the adhesive and the surface. Callow et al. (2005) examined whether the effect of substratum surface energy in controlling adhesion was correlated with differential wetting of the surface by the adhesive. A range of alkanethiol SAMs and grafted monolayers of PDMS and fluorocarbon (CF_3) were used; pad diameter was assessed by ESEM. It was shown that the size of the pad was strongly influenced by the wettability of the surface; with large pads being formed on the more hydrophilic surfaces and small pads on the more hydrophobic substrates. These results are not consistent with standard thermodynamic wetting theory based on the Young-Dupré equations for a three-phase system (surface, fluid adhesive, liquid water) since standard theory would predict that a fluid adhesive should more easily 'wet', i.e. spread more, on a less wettable surface. In a novel extension of thermodynamic wetting theory, it was shown that this

apparent contradiction can be explained if the adhesive was very polar in character-enabling it to compete effectively with water to 'wet' a hydrophilic surface (Callow et al. 2005). This is consistent with the ESEM studies (Sect. 3.3.1) showing that the spore adhesive pad is hygroscopic. Interestingly, a recent study on mussel byssus adhesion also reveals greater adhesive spreading on hydrophilic substrates (Aldred et al. 2006).

4.3.2.3 Influence of Surface Topography

Although zoospores respond to a variety of cues (Callow and Callow 2000), the response to surface topography appears to be particularly well developed. When provided with a choice of topographies, zoospores choose places that are energetically most favourable, e.g. in depressions and corners, which, in addition, provide maximum contact for secreted adhesive (Granhag et al. 2004). The most favoured topography appears to be those with features similar in size to that of the spore body i.e. ca. 5 μm (Callow et al. 2002; Hoipkemeier-Wilson et al. 2004; Carman et al. 2006). Out of a wide range of surface features evaluated, only one topographical pattern has consistently inhibited settlement. Carman et al. (2006) microfabricated in polydimethylsiloxane elastomer, a biomimetic topography (Sharklet AF™) inspired by the skin of fast moving sharks. The diamond-like biomimetic pattern inhibited settlement of *Ulva* spores by ~85% compared to a smooth surface in the same elastomer. However, those spores that did settle on the biomimetic surface are strongly attached, presumably as a consequence of the micron-size channels filling with adhesive.

4.3.3 Nanomechanical and Viscoelastic Properties of the Spore Adhesive

Atomic Force Microscopy (AFM) in its 'force mode' relies upon the sensitive detection, by laser, of deflections to a sharp cantilever-mounted tip (typically with a tip radius of the order 20–50 nm), as it interacts with a surface through successive approach-retract cycles in the z-direction. The resulting force curves allow the measurement of mechanical properties of materials at the nanoscale, including parameters such as adhesive strength, viscoelasticity and modulus. AFM in an 'environmental cell' has been used to examine some of the properties of the *Ulva* spore adhesive in its natural, hydrated state (Callow JA et al. 2000a; Walker et al. 2005).

The modulus of the adhesive pad was determined from analysis of force-indentation curves (Walker et al. 2005). Fresh adhesive (because of the time taken to align a cantilever tip with the optically transparent, small adhesive pad 'fresh' in practice means approximately 15 min after a spore has settled on a surface) showed two characteristic regions in the force-indentation curve. Sneddon mechanics were used to model the elastic deformation

revealing the modulus of an outer ~600 nm thick layer to be approximately 0.2±0.1 MPa, while the modulus of the inner layer was about 3±1 MPa. The obtained modulus, for the outer layer of fresh adhesive, was comparable to previous results (Callow JA et al. 2000a). Older adhesive pads (approx. 1 h after settlement) showed displacements in the approach curve which would be consistent with the formation of a harder 'crust' indicative of a more rapid 'curing' of the surface layer with time. Callow JA et al. (2000a) also showed that with time after settlement the elastic modulus increased, i.e. the adhesive became harder, less compressible.

The forces acting upon AFM tips were also measured from force curves obtained as the AFM tip retracts from the surface of the adhesive pad. The force required to separate the tip from the sample provides an estimate of adhesion strength. Callow JA et al. (2000a) showed that freshly released spore adhesive has a mean adhesion strength of 173 mN/m, with a maximum value for a single adhesion event of 458 mN/m. Taken at face value these measurements indicate a very sticky biological adhesive but caution must be exercised since neither the surface area of contact between the tip and the adhesive is accurately known, nor the number of adhesive strands adhering to the tip. Corrections for nominal tip radius give adhesive forces of the order 17 nN, which again indicate a 'strong' adhesive but this value is still likely to be compromised by the unknown number of adhesive strands that contribute to it, so comparisons with other systems are inappropriate.

Irrespective of the absolute values for adhesion strength or forces, within minutes of release the adhesive undergoes a progressive 'curing' process becoming less adhesive, and less extensible with a 65% reduction in adhesion strength values after 60 min of settlement (Callow JA et al. 2000a).

Walker et al. (2005) also observed a hysteresis between the loading and unloading force curves when the spore adhesive was being stretched. The hysteresis is typically shown by viscoelastic materials in which the relationship between stress and strain depends on time, or loading rate. Analysis of loading rate profiles revealed stress "thinning" or pseudoplastic behaviour, probably caused by changes in adhesive chain entanglement. Pseudoplastic behaviour is characteristic of long chain, highly folded molecules that exhibit classical variation of viscosity with shear rate. The results suggest that the spore adhesive molecules are highly folded/entangled at rest, such entanglements presumably contributing to the cohesive strength of the system. Under shear the molecules become less entangled, more liquid, and this reduction in cohesive properties may thus contribute to the detachment of settled spores under shear.

One approach towards reducing the fouling of ship hulls in the marine environment, through non-biocidal means, is to coat the hull with a low surface energy, elastomeric material such as PDMS (polydimethylsiloxane), the intention being to reduce the interfacial adhesion energy between the surface and the adhesive polymers secreted by the fouling organisms (e.g. Kavanagh et al. 2003; Sun et al. 2004). Walker et al. (2005) used AFM to determine

whether weak attachment of *Ulva* spores to PDMS is reflected in the intrinsic adhesive properties of the spore adhesive. For this purpose, the work of adhesion between AFM tips coated with a monolayer of grafted PDMS and the spore adhesive pad was examined. The work of adhesion between the fresh spore adhesive and the PDMS tip was determined to be less than 1.5 mJ/m^2.

4.3.4 Adhesive Strength of the Whole Spore System

Section 4.3.2 describes how Atomic Force Microscopy (AFM) has been used to study the viscoelastic properties of the secreted spore adhesive. However, AFM measurements of the viscoelastic properties of the adhesive per se do not give information of the interfacial adhesion properties of the whole system and various methodologies have been applied to the assessment of adhesion strength. For macrofouling organisms like barnacles, tubeworms and oysters, a common approach is to apply a mechanical shear force parallel to the base of the organism (Swain and Schultz 1996; Kavanagh et al. 2001). In the case of soft, microfouling species such as algae, such an approach is impossible and hydrodynamic methods are more appropriate. Finlay et al. (2002b) measured the strengths of attachment of *Ulva* spores to a standard glass surface using a water jet apparatus. Surface impact pressures of ~250 kPa (equivalent to a wall shear stress of 325 Pa) were required to quantitatively remove attached spores after 4 h contact with a surface. The development of adhesive and cohesive strength was shown to be highly time-dependent: after 8 h in contact with a surface, spores did not detach, even at surface pressures in excess of 250 kPa. Spores settled in groups are more resistant to detachment than single spores, which suggests that the adaptive value of gregarious settlement behaviour may lie in the greater resistance of groups to detachment forces in a naturally turbulent environment.

4.4 Conclusions and Further Perspectives

The main aim of this chapter has been to review the current state of knowledge on the nature and properties of the *Ulva* spore adhesive. We have also considered aspects of the cell biology and behaviour of spores that contribute to the discharge of the adhesive, and how properties of a surface contribute to the interfacial bonding process. An outstanding requirement remains a more detailed knowledge of the molecular structure of the adhesive molecule(s) itself, without which a comprehensive understanding of the functional properties of the adhesive cannot be obtained. Yet it seems that the very properties of the molecule that contribute to its adhesive functionality, its molecular size, surface bonding properties and propensity to self-aggregation and cross-linking, are those that continue to thwart unequivocal molecular characterisation.

Other strategies using molecular genetics are therefore being explored. Stanley et al. (2005) have recently sequenced ca. 2000 EST (Expressed Sequence Tag) clones from a cDNA library prepared to sporulating tissue of *Ulva linza*. Since the bioadhesive secreted by *Ulva* spores is formed in vesicles in the developing zoospores contained within the fruiting thallus (Stanley et al. 1999), this should mean that ESTs coding for the adhesive proteins should also be well-represented. A notable feature of the EST library is the abundance of sequences encoding proteins involved in some aspect of cell wall or extrametrical structure or assembly. In particular, significant similarities were obtained to hydroxyproline-rich cell wall proteins (extensins) from a range of flowering plants, the hydroxyproline-rich pherophorins found in the extracellular matrix of *Volvox,* and pherophorin-like proteins found in *Chlamydomonas* and some flowering plants.

Eukaryotic cells secrete polysaccharides and structural glycoproteins that self-assemble to form the extracellular matrices of animals and the cell walls of plants. There are some striking parallels despite obvious differences. Both types of matrix consist of interpenetrating polymeric networks whose properties underpin all aspects of growth and development. Both employ hydroxyproline-rich glycoproteins (HRGPs) as major scaffolding components, namely collagen in animals and the HRGP extensin superfamily in algae and higher plants. HRGPs form the predominant components of the cell wall or extracellular matrix of the Volvocales, a green algal group, which includes *Chlamydomonas* and the colonial *Volvox*. Molecular studies of these proteins have revealed many commonalities (Ferris et al. 2001). They generally form elongated, flexible, rod-like molecules with marked peptide periodicity (i.e. these proteins are 'modular', like mussel adhesives); the repeat motifs are dominated by hydroxyproline in a polyproline II helical conformation, and the hydroxyproline is extensively modified by arabinosyl/galactosyl side chains which stabilise the helical conformation. This has led to the proposal of a 'superfamily' derived from an ancient gene family. Some, such as the extensins and pherophorins, become crosslinked to form mechanically strong covalent cell wall networks and other supramolecular structures. The HRGP superfamily of proteins would be ideally suited to diverse roles in adhesion and cell wall assembly and the similarities between *Ulva* sequences and other hypro-rich proteins (Stanley et al. 2005) are therefore relevant to an understanding of the processes involved in adhesion. We have recently shown (Humphrey et al. 2005) that the cross-linking of *Ulva* spore adhesive after secretion is sensitive to the same thiol-capping reagents that prevent cross-linking of *Volvox* DZ1 (Ender et al. 2002). Without molecular characterisation of the *Ulva* adhesive protein it is not possible to say whether this similarity in properties is coincidental, or indicative of a more fundamental homology, but clearly further investigation of the potential role of the HRGP superfamily in *Ulva* adhesion is warranted.

One obvious approach would be to use newer genetic technologies–specifically expression microarrays based on sequences contained in the *Ulva*

EST library (Stanley et al. 2005)–to compare the expression of adhesion-related genes during different stages in the development of the organism or in situations where one may anticipate changes in the pattern of expression of adhesive genes. However, while this provides a different route to explore adhesives and adhesion processes in *Ulva*, the evidence will be, at best, correlative, and the full power of the molecular genetics approach cannot be realised without parallel studies on adhesion mutants, genomics, gene knock-outs, transformants etc. Unfortunately, *Ulva* does not readily lend itself to such approaches and it may be that those interested in the fundamentals of algal adhesives should focus on a more tractable system that displays a similar adhesion biology. This may be found in the brown alga *Ectocarpus*, zoospores of which contain vesicles that discharge their contents during settlement, as in *Ulva* (Baker and Evans 1973). *Ectocarpus* is a more tractable alga than *Ulva* for laboratory-based genetic studies, being readily cultured and with many strains and mutants. *Ectocarpus* is also rapidly becoming a model seaweed for molecular genetic studies (Peters et al. 2004), with a genome sequencing project currently underway (http://www.nies.go.jp/biology/mcc/people/kasai/abstract/cock-e.htm).

Acknowledgments. Financial support from the Natural Environmental Research Council (NER/T/S/2000/00623-5), EC Contract G5RD-CT-2001-005452 (Algal Bioadhesives) and the United States Office of Naval Research Awards N00014-96-0373 and N00014-02-1-0311 is acknowledged.

References

Aldred N, Ista LK, Callow ME, Callow JA, Lopez GP, Clare AS (2006) Mussel (*Mytilus edulis*) byssus deposition in response to variations in surface wettability. J R Soc Interface 3:37–43 doi:10.1098/rsif.2005.0074

Baier RE (1973) Influence of the initial surface condition of materials on bioadhesion. Proc 3rd Int Congr Marine Corrosion and Fouling. Northwestern University Press, Evanston, Illinois, pp 633–639

Baker JR, Evans LV (1973) The ship fouling alga *Ectocarpus* I. Ultrastructure and cytochemistry of plurilocular reproductive stages. Protoplasma 77:1–13

Battey NH, Blackbourn HD (1993) The control of exocytosis in plant cells. New Phytol 125:307–338

Callow JA, Crawford SA, Higgins MJ, Mulvaney P, Wetherbee R (2000a) The application of atomic force microscopy to topographical studies and force measurements on the secreted adhesive of the green alga *Enteromorpha*. Planta 211:641–647

Callow JA, Stanley MS, Wetherbee R, Callow ME (2000b) Cellular and molecular approaches to understanding primary adhesion in *Enteromorpha*: an overview. Biofouling 16:141–150

Callow JA, Osborne MP, Callow ME, Baker F, Donald AM (2003) Use of environmental scanning electron microscopy to image the spore adhesive of the marine alga *Enteromorpha* in its natural hydrated state. Coll Surf B Biointerfaces 27:315–321

Callow JA, Callow M, Ista L, Lopez G, Chaudhury M (2005) The influence of surface energy on the wetting behaviour of the spore adhesive of the marine alga *Ulva linza* (syn. *Enteromorpha linza*). J R Soc Interface 2:319–325

Callow ME, Callow JA (2000) Substratum location and zoospore behaviour in the fouling alga *Enteromorpha*. Biofouling 15:49–56

Callow ME, Evans LV (1974) Studies on the ship-fouling alga *Enteromorpha* III. Cytochemistry and autoradiography of adhesive production. Protoplasma 80:15–27
Callow ME, Evans LV (1977) Studies on the ship-fouling alga *Enteromorpha* IV. Polysaccharide and nucleoside diphosphatase localization. Phycologia 16:313–320
Callow ME, Callow JA, Pickett-Heaps JD, Wetherbee R (1997) Primary adhesion of *Enteromorpha* (Chlorophyta, Ulvales) propagules: quantitative settlement studies and video microscopy. J Phycol 33:938–947
Callow ME, Callow JA, Ista LK, Coleman SE, Nolasco AC, Lopez GP (2000) The use of self-assembled monolayers of different wettabilities to study surface selection and primary adhesion processes of green algal (*Enteromorpha*) zoospores. Appl Environ Microbiol 66:3249–3254
Callow ME, Crawford S, Wetherbee R, Taylor K, Finlay JA, Callow JA (2001) Brefeldin A affects adhesion of zoospores of the green alga *Enteromorpha*. J Exp Bot 52:1409–1415
Callow ME, Jennings AR, Brennan AB, Seegert CE, Gibson A, Wilson L, Feinberg A, Baney R, Callow JA (2002) Microtopographic cues for settlement of zoospores of the green fouling alga *Enteromorpha*. Biofouling 18:237–245
Carman ML, Estes TG, Feinberg AW, Schumacher JF, Wilkerson W, Wilson LH, Callow ME, Callow JA, Brennan AB (2006) Engineered antifouling microtopographies -correlating wettability with cell attachment. Biofouling doi:10.1.080/0892701050048454
Christie AO, Evans LVB, Shaw M (1970) Studies on ship-fouling alga *Enteromopha*. II. The effect of certain enzymes on the adhesion of zoospores. Ann Bot 34:467–482
Ender F, Godl K, Wenzl S, Sumper M (2002) Evidence for autocatalytic cross-linking of hydroxyproline-rich glycoproteins during extracellular matrix assembly in *Volvox*. Plant Cell 14:1147–1160
Evans LV, Christie AO (1970) Studies on the ship-fouling alga *Enteromorpha*. I. Aspects of the fine structure and biochemistry of swimming and newly settled zoospores. Ann Bot 34:451–456
Ferris PJ, Woessner JP, Waffenschmidt S, Kilz S, Drees J, Goodenough UW (2001) Glycosylated polyproline II rods with kinks as a structural motif in plant hydroxyproline-rich glycoproteins. Biochemistry 40:2978–2987
Finlay JA, Callow ME, Ista LK, Lopez GP, Callow JA (2002a) The influence of surface wettability on the adhesion strength of settled spores of the green alga *Enteromorpha* and the diatom *Amphora*. Integr Comp Biol 42:1116–1115
Finlay JA, Callow ME, Schultz MP, Swain GW, Callow JA (2002b) Adhesion strength of settled spores of the green alga *Enteromorpha*. Biofouling 18:251–256
Granhag LM, Finlay JA, Jonsson PR, Callow JA, Callow ME (2004) Roughness-dependent removal of settled spores of the green alga *Ulva* (syn. *Enteromorpha*) exposed to hydrodynamic forces from a water jet. Biofouling 20:117–122
Hayden HS, Blomster J, Maggs CA, Silva PC, Stanhope MJ, Walland RJ (2003) Linnaeus was right all along: *Ulva* and *Enteromorpha* are not distinct genera. Eur. J Phycol 38:277–294
Herrwerth S, Eck W, Reinhardt S, Grunze M (2003) Factors that determine the protein resistance of oliogoether self-assembled monolayers-internal hydrophilicity, terminal hydrophilicity, and lateral packing density. J Am Chem Soc 125:9359–9366
Hoipkemeier-Wilson L, Schumacher JF, Carman ML, Gibson AL, Feinberg AW, Callow ME, Finlay JA, Callow JA, Brennan AB (2004) Antifouling potential of lubricious, micro-engineered, PDMS elastomers against zoospores of the green fouling alga *Ulva* (*Enteromorpha*). Biofouling 20:53–63
Humphrey AJ, Finlay JA, Pettitt ME, Stanley MS, Callow JA (2005) Effect of Ellman's Reagent and dithiothreitol on the curing of the spore adhesive glycoprotein of the green alga *Ulva*. J Adhesion 81:791–803
Ista LK, Callow ME, Finlay JA, Coleman SE, Nolasco AC, Simons RH, Callow JA, Lopez GP (2004) Effect of substratum surface chemistry and surface energy on attachment of marine bacteria and algal spores. Appl Environ Microbiol 70:4151–4157
Joint I, Callow ME, Callow JA, Clarke KR (2000) The attachment of *Enteromorpha* zoospores to a bacterial biofilm assemblage. Biofouling 16:151–158

Joint I, Tait K, Callow ME, Callow JA, Milton D, Williams P, Camara M (2002) Cell-to-cell communication across the prokaryote-eukaryote boundary. Science 298:1207

Kavanagh CJ, Schultz MP, Swain GW, Stein J, Truby K, Darkangelo-Wood C (2001) Variation in adhesion strength of *Balanus eburneus*, *Crassostrea virginica* and *Hydroides dianthus* to fouling-release coatings. Biofouling 17:155–167

Kavanagh CJ, Swain GW, Kovach BS, Stein J, Darkangelo-Wood C, Truby K, Holm E, Montemarano J, Meyer A, Wiebe D (2003) The effects of silicone fluid additives and silicone elastomer matrices on barnacle adhesion strength. Biofouling 19:381–390

Kieslisewski MJ, Lamport DTA (1994) Extensin: repetitive motifs, functional sites, post-translational codes and phylogeny. Plant J 5:157–172

Ostuni E, Chapman RG, Liang MN, Meluleni G, Pier G, Ingber DE, Whitesides GM (2001) Self-assembled monolayers that resist the adsorption of proteins and the adhesion of bacterial and mammalian cells. Langmuir 17:6336–6343

Peters AF, Marie D, Scornet D, Kloareg B, Cock JM (2004) Proposal of *Ectocarpus siliculosus* (Ectocarpales, Phaeophyceae) as a model organism for brown algal genetics and genomics. J Phycol 40:1079–1088

Pettitt M, Henry S, Callow M, Callow J, Clare A (2005) Activity of commercial enzymes on settlement and adhesion of cypris larvae of the barnacle *Balanus amphitrite*, spores of the green alga *Ulva linza*, and the diatom *Navicula perminuta*. Biofouling 20:299–311

Roberts SK, Gillot I, Brownlee C (1994) Cytoplasmic calcium and egg activation. Development 120:155–163

Samuels AL, Bisalputra T (1990) Endocytosis in elongating root cells of *Lobelia erinus*. J Cell Sci 97:157–165

Sigal GB, Mrksich M, Whitesides GM (1998) Effect of surface wettability on the absorption of proteins and detergents. J Am Chem Soc 120:3464–3473

Stanley MS, Callow ME, Callow JA (1999) Monoclonal antibodies to adhesive cell coat glycoproteins secreted by zoospores of the green alga *Enteromorpha*. Planta 210:61–71

Stanley MS, Perry RM, Callow JA (2005) Analysis of expressed sequence tags (ESTs) from the green alga *Ulva linza* (Chlorophyta). J Phycol 41:1219–1226

Sun Y, Guo S, Walker GC, Kavanagh CJ, Swain GW (2004) Surface elastic modulus of barnacle adhesive and release characteristics from silicone surfaces. Biofouling 20:279–289

Swain GW, Schultz MP (1996) The testing and evaluation of non-toxic antifouling coatings. Biofouling 10:187–197

Tait K, Joint I, Daykin M, Milton D, Williams P, Camara M (2005) Disruption of quorum sensing in seawater abolishes attraction of zoospores of the green alga *Ulva* to bacterial biofilms. Environ Microbiol 7:229–240

Walker GC, Sun Y, Guo S, Finlay JA, Callow ME, Callow JA (2005) Surface mechanical properties of the spore adhesive of the green alga *Ulva*. J Adhesion 81:1101–1118

Wheeler GL, Tait K, Taylor A, Brownlee C, Joint I (2006) Acyl-homoserine lactones modulate the settlement rate of zoospores of the marine alga *Ulva intestinalis* via a novel chemokinetic mechanism. Plant Cell Environ doi:10.1111/j.1365–3040.2005.01440.x

5 Diatom Adhesives: Molecular and Mechanical Properties

Anthony Chiovitti, Tony M. Dugdale, and Richard Wetherbee

5.1 Diatoms and Adhesion

5.1.1 Diatom Morphology

Diatoms are a ubiquitous group of unicellular microalgae characterized by their highly ornate, silicified cell walls. They are the major primary producers in most aquatic habitats, responsible for ca. 20% of global carbon fixation, and they are the dominant group of organisms involved in the global turnover of biogenic silica (Mann 1999). The cell wall, or "frustule", of diatoms comprises the silicified wall and associated organic polymers. The silicified portion of the frustule comprises two overlapping halves (or "valves") that fit together like a Petri dish plus several encircling girdle bands that enclose the protoplast (Fig. 5.1a; for a review, see Pickett-Heaps et al. 1990). Diatoms are classified according to their valve symmetry as centric (radial) or pennate (bilateral) (Round et al. 1990). The centric forms are mostly planktonic, whereas the pennate forms are mostly benthic and capable of attachment and motility on natural or artificial substrata. This chapter focuses on the adhesives of benthic forms, which represent a small fraction of the total number of species.

5.1.2 Significance of Diatom Adhesion

Adhesion to a substratum is a well-documented strategy for growth and survival in a range of marine and freshwater organisms, and provides photosynthetic protists with an optimal location to access soluble nutrients and light. The adhesion of benthic diatoms is associated with the secretion of mucilaginous material or extracellular polymeric substances (EPS) (Hoagland et al. 1993). An accumulation of diatom cells and their insoluble EPS (i.e. a biofilm) can beneficially stabilize benthic aquatic habitats by consolidating soft sediments (Paterson 1989; Underwood and Paterson 2003). However, diatoms also cause adverse economic impacts because they are the most frequent and successful microalgal foulers of submerged artificial structures (Bohlander 1991; Alberte

School of Botany, University of Melbourne, Victoria 3010, Australia

Biological Adhesives
(ed. by A.M. Smith and J.A. Callow)

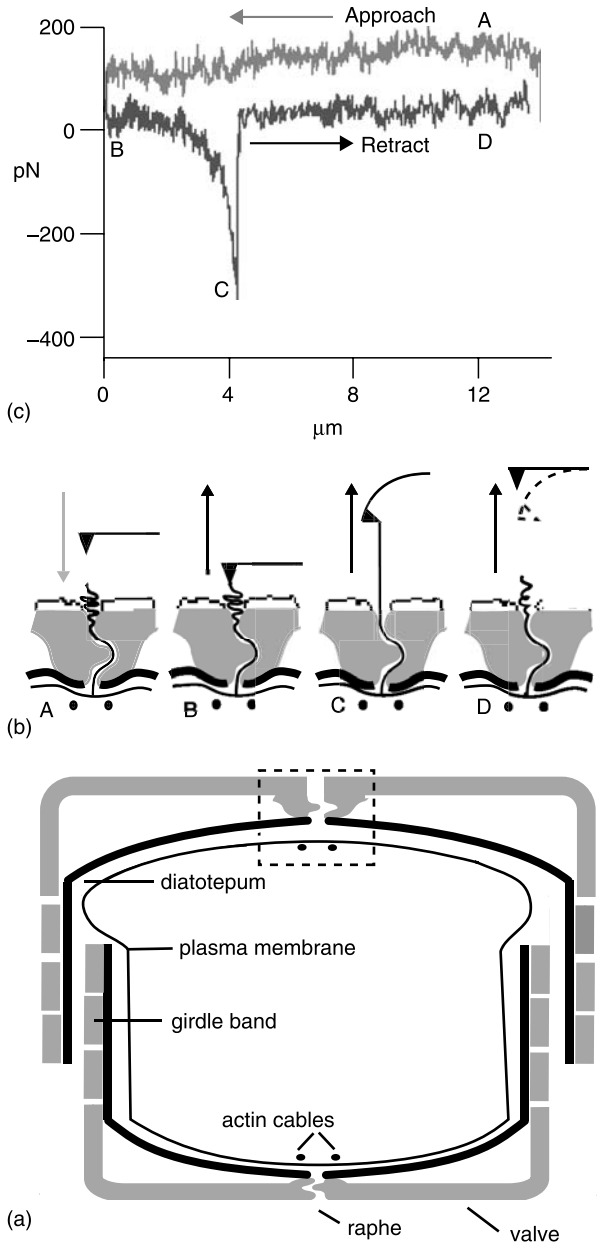

Fig. 5.1. Interaction between the AFM probe and the raphe strands of a diatom: (a) schematic diagram of a raphid diatom in transverse section. The non-driving raphe in the boxed region is expanded in b; (b) diagram depicting the interaction between the AFM cantilever tip and a single adhesive raphe strand; (c) a force-separation curve recorded for the interactions depicted in b. Points A–D in d correspond to those in c. During point A, the cantilever tip approaches the

et al. 1992). Even when diatoms are exposed to biocides that successfully discourage most organisms, such as copper or tributyl tin, surfaces frequently develop thick diatom slimes (Daniel et al. 1980; Callow 1986, 1996). Owing to concerns about environmental toxicity, a worldwide ban has been placed on organotin antifouling paints by the International Maritime Organization and will become fully enforced in 2008 (Omae 2003). These biocidal antifouling paints are gradually becoming replaced by a new generation of environmentally benign antifouling paints based on silicone elastomers with low surface energy (Anderson et al. 2003), yet these paints are also relatively susceptible to fouling by diatoms (Clarkson and Evans 1995a,b; Holland et al. 2004).

5.1.3 Diatom Adhesion Strategies

Diatoms are passively carried to surfaces by the action of currents and localized water movement or by settling under gravity. With the exception of the motile male gametes, diatoms lack flagella throughout their life cycle (Round et al. 1990) and therefore are unable to seek actively a surface to attach to, although a surface-sensing mechanism in diatoms has been postulated (Cooksey and Wigglesworth-Cooksey 1992; Wigglesworth-Cooksey and Cooksey 1992) and may be activated after initial adhesion. Contact with the substratum initiates a set of processes that involve stabilization of initial attachment and re-orientation of the cell (Wetherbee et al. 1998). Following initial adhesion, benthic diatoms generally adopt either of two life-style strategies. Many diatoms use attachment as traction for a form of cell motility termed "gliding" (Edgar and Pickett-Heaps 1984; Wetherbee et al. 1998). Motile diatoms may adjust their position on a substratum or in the sediment in response to a range of stimuli, including tidal fluctuation, diurnal rhythm, nutrient availability, and UV-B irradiation (Cooksey and Cooksey 1988; Serôdio et al. 1997; Smith and Underwood 1998; Moroz et al. 1999). Alternatively, diatoms become sessile, remaining attached to the substratum at one position for an extended period. For both motile and sessile adhesion strategies, cell-substratum adhesion is mediated by the secretion of EPS (Edgar and Pickett-Heaps 1984; Hoagland et al. 1993).

5.1.4 General Composition of Diatom Mucilages

Diatom mucilages are complex, multi-component materials. Many early staining and compositional studies demonstrated that carbohydrates dominate diatom mucilages (for a review, see Hoagland et al. 1993), and during the

raphe without interactions occurring. At point B, the cantilever tip engages the raphe strand. Subsequent retraction of the cantilever tip extends the raphe strand. At point C, the raphe strand is fully extended causing the cantilever tip to deflect downwards (b) and is recorded as an increasingly applied force in the curve (c). The raphe strand detaches from the tip at point D, allowing the cantilever tip to return to the zero deflection line. (Adapted from Higgins et al. 2002)

last decade this principle has shaped the direction and focus of most studies analyzing the EPS chemistry of unialgal diatom cultures (Wustman et al. 1997, 1998; McConville et al. 1999; Staats et al. 1999; Khandeparker and Bhosle 2001; de Brouwer and Stal 2002; Chiovitti et al. 2003b; Bellinger et al. 2005). The data in these studies generally indicate that the carbohydrates comprise complex, anionic polysaccharides with heterogeneous monosaccharide compositions, sulfate ester, and/or uronic acids. Neutral monosaccharides that have been identified include hexoses, pentoses, 6-deoxyhexoses, and O-methylated sugars. The co-occurrence of proteins and carbohydrates was noted in a number of studies (Smestad Paulsen et al. 1978; Bhosle et al. 1995; Lind et al. 1997; Wustman et al. 1997; McConville et al. 1999; Staats et al. 1999; Khandeparker and Bhosle 2001; Chiovitti et al. 2003a, b) but the relationship between the protein and the carbohydrate has been rarely explored (Wustman et al. 1998; Chiovitti et al. 2003a). In contrast to most studies of diatom EPS, biochemical analyses of the extracellular mucilages of *Craspedostaouros australis* (Chiovitti et al. 2003a) and atomic force microscopy (AFM) of the adhesive pads of *Toxarium undulatum* (Dugdale et al. 2005) demonstrated that protein was the fundamental component of the adhesives. For *Achnanthes longipes* stalks, the protein content of the EPS was relatively low but its influence on EPS structure and properties was substantial (Wustman et al. 1998). A role for protein in *Navicula perminuta* adhesion was implied by reduction of adhesion strength by treatment with commercial proteases (Pettitt et al. 2004).

The extracellular location of components extracted from diatoms is often based on inference, and the inherent risk of misinterpreting the origin of nominal EPS was demonstrated recently for water-extractable intracellular glucans (Chiovitti et al. 2004). Localization of structural units in benthic diatom EPS has been probed by labelling with lectins or specific antibodies (Lind et al. 1997; Wustman et al. 1997, 1998; Wigglesworth-Cooksey and Cooksey 2005) or by assessing changes in the appearance and/or properties of diatom EPS by EM or AFM (McConville et al. 1999; Chiovitti et al. 2003b). The composition of various complex diatom EPS has been reviewed by Hoagland et al. (1993) and Underwood and Paterson (2003). The present discussion focuses on recent studies that relate mucilage chemistry to its fine structure and physical properties.

5.2 Adhesion and Gliding of Raphid Diatoms

5.2.1 Adhesion and Gliding Behaviour

In most benthic pennate diatoms, adhesive EPS is secreted from a longitudinal slit in the valve termed the "raphe" (Wetherbee et al. 1998). Most such "raphid" diatoms have a raphe in each valve, although members of the genus *Amphora* differ by having both raphes located on the ventral surface of the

cell (Daniel et al. 1980; Round et al. 1990). When raphid diatoms settle from the water column onto the substratum, they typically land on their girdle surface. Initial adhesion is therefore mediated by cell surface mucilage and the substratum, and it is relatively weak since the diatom may be readily dislodged (Lind et al. 1997; Wang et al. 1997; Higgins et al. 2003a). Following initial adhesion, the cell may rock gently or remain stationary for a short period of time (e.g. 30–90 s in *C. australis*; Lind et al. 1997) before flipping onto one of its valves, bringing the raphe into contact with the substratum. Soon after, the cell typically commences gliding across the substratum parallel to the longitudinal axis of the frustule, simultaneously depositing a trail of adhesive mucilage.

Gliding speeds for raphid diatoms are in the range of 0.1–25 μm/s, but vary substantially depending upon the species, substratum type, and various environmental factors (Edgar and Pickett-Heaps 1984; Webster et al. 1985; Häder and Hoiczyk 1992; Cohn and Weitzell 1996; Lind et al. 1997; Poulsen et al. 1999; Cohn et al. 2003). Gliding diatoms are capable of abrupt reversals in direction, maintaining similar speeds in either direction for prolonged intervals. Rapid, alternating reversals in direction during which the diatom does not shift far from a fixed position have been described as 'shunting' or 'oscillating' (Moroz et al. 1999; Holland et al. 2004). Diatoms often veer from a linear course, forming paths that depict arcs of varying radii (Edgar and Pickett-Heaps 1984; Cohn and Weitzell 1996; Wigglesworth-Cooksey et al. 1999; Higgins et al. 2003a). The path types engaged by gliding diatoms appear to be broadly characteristic for different species but are not apparently related to cell size or shape (Edgar and Pickett-Heaps 1984; Cohn and Weitzell 1996), except for a few asymmetrical species (Edgar and Pickett-Heaps 1984).

5.2.2 Mechanism of Raphid Diatom Adhesion and Gliding

Contemporary models for diatom adhesion and motility (Edgar and Pickett-Heaps 1984; Wetherbee et al. 1998) incorporate the elements of contact between the raphe and substratum, secretion of adhesive mucilage, and the observation that a pair of actin filaments lie beneath the membrane at the raphe (Edgar and Zavortink 1983). By drawing analogies from animal and other protist systems, Wetherbee et al. (1998) elaborated on the earlier proposal of Edgar and Pickett-Heaps (1984) and suggested a detailed model for the Adhesion Complex (AC, Fig. 5.2) and gliding of raphid diatoms. The AC is a polarized continuum of connector molecules that extend from the actin filaments and associated intracellular motor proteins via transmembrane linker molecules to the extracellular adhesives attached to the substratum. The force required to enable gliding is generated by myosin at the actin filaments. As the cell is propelled forward, adhesive EPS are secreted from the raphe and the components of the AC continually assemble at the front boundary of the contact between the moving cell and the substratum. The

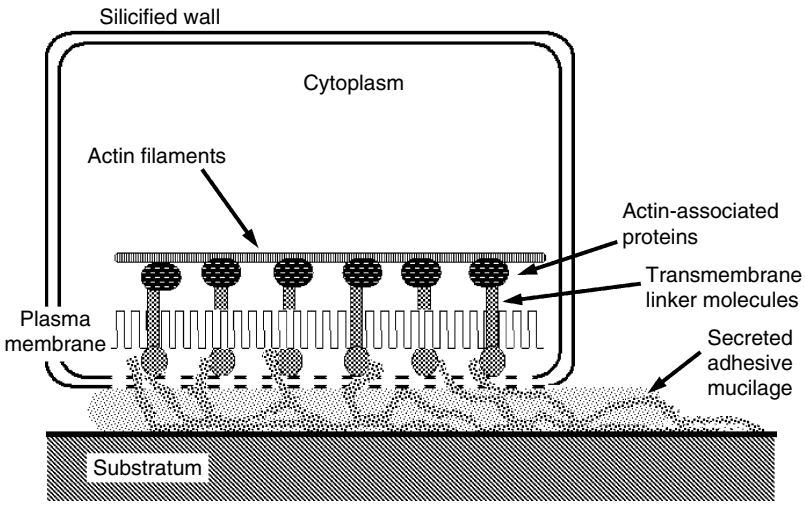

Fig. 5.2. A schematic diagram of a raphid diatom cell with detail of the components of the proposed adhesion complex. (Adapted from Wetherbee et al. 1998)

fluidity of the plasma membrane allows the transmembrane components of the AC to remain fixed in position while the cell is gliding. The AC components continually disassemble at the rear boundary of cell-substratum contact, resulting in deposition of adhesive EPS in the mucilaginous trails. Although the available data on raphid diatom adhesion and gliding are consistent with the AC model, only the actin and extracellular adhesives have been identified so far. Furthermore, an authentic adhesive motif remains unknown.

The functional role of the actin filaments was demonstrated by reversible inhibition of diatom motility with an actin-destabilizing drug, latrunculin A, combined with in situ FITC-phalloidin labeling and Western blotting analysis (Poulsen et al. 1999). Latrunculin also prevented cells that had settled on their girdles from flipping onto their raphes, indicating the dependence of diatom adhesion on the actin filaments of the AC. An alternative hypothesis for raphid diatom locomotion proposes that the propulsive force is generated by the directional secretion and hydration of mucilage (Gordon 1987). However, when synthetic particles are added to the medium, the particles are observed to adhere to and stream back and forth along one of the raphes (Edgar and Pickett-Heaps 1984; Lind et al. 1997; Poulsen et al. 1999). This particle streaming is often bidirectional and reversible, and different particles can move at different speeds simultaneously. This activity is more sophisticated than can be explained by secretion and hydration of mucilage, which would merely repel the particles from the cell, but it can be rationalized as AC elements, including the extracellular adhesive, being driven independently along each of the actin filaments. TEM has shown that secretory vesicles

appear near the raphe, apparently supplying the raphe adhesives (Daniel et al. 1980; Edgar and Pickett-Heaps 1982, 1983, 1984; Wang et al. 2000). Connections were observed between the vesicles and the actin at the raphe in *Navicula cuspidata* (Edgar and Pickett-Heaps 1984), indicating that the actin guides the vesicles into position at the raphe and possibly occurs concomitantly with assembly of the AC.

5.2.3 Fine Structure of Raphid Diatom Mucilages

Imaging by conventional SEM, FESEM, TEM, and AFM have all contributed to developing an understanding of the fine structure of diatom mucilages. The chief advantages of AFM over EM techniques are that it enables imaging of mucilages in their native, hydrated state, as well as measurements of the mechanical properties of mucilages at the molecular scale. The operating principles of the AFM (Binning et al. 1986) rely on there being contact between the AFM probe and the sample. The AFM probe comprises a fine silicon nitride tip (ca. 10–20 nm radius) mounted on a flexible cantilever. During imaging, the cantilever tip is scanned across the surface of the sample with either continuous (contact mode) or intermittent (tapping mode) contact with the sample. The cantilever tip deflects as it encounters topographical changes in the sample and these deflections are used to digitally construct an image.

5.2.3.1 Cell Surface Mucilage

AFM has provided the most realistic images available of the cell surface mucilage of diatoms in its native, hydrated state (Crawford et al. 2001; Higgins et al. 2002, 2003a, b). Tapping-mode images of the girdle and valve regions of *C. australis* cells showed them to be covered in relatively thick mucilage that is mostly smooth and flat but with some regions showing irregularly striated patterns (Fig. 5.3a; Higgins et al. 2002, 2003b). Height images in tapping mode showed the topography of the *C. australis* mucilage varied by up to 25 nm (Higgins et al. 2003b). By using the cantilever tip to scrape surface mucilage away from the siliceous wall, it was shown that mucilage was secreted from the girdle pores of stationary-phase cells but not from those of log-phase cells (Higgins et al. 2002). In contrast, the surface mucilage of *Pinnularia viridis* had the appearance of loosely packed humps which varied by up to 150 nm in height (Fig. 5.3b; Higgins et al. 2003b). Essentially, no surface mucilage was detected for log-phase *Nitzschia navis-varingica* cells, although mucilaginous strands were observed adhering to the valve but not the girdle (Higgins et al. 2003b). These observations demonstrate that the cell surface mucilage of diatoms is not merely an amorphous coating but has distinctive features that vary substantially between species.

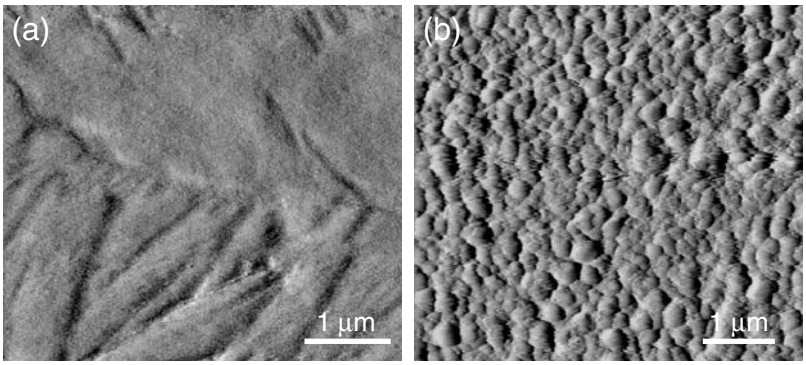

Fig. 5.3. AFM tapping mode images of the cell surface mucilage of raphid diatoms: (a) *Craspedostauros australis*; (b) *Pinnularia viridis*. (From Higgins et al. 2003b, reprinted with permission from the *Journal of Phycology*)

5.2.3.2 Raphe Mucilage

The adhesive raphe strands are yet to be imaged by AFM mainly because the strong binding of raphe strands to the cantilever tip impedes imaging (Higgins et al. 2003a) but probably also because the raphe strands are too mobile in fluid to be imaged. A description of the structure of this mucilage therefore necessarily relies on EM observations of chemically fixed and dehydrated diatom cells. However, the strand-like structure of raphe adhesives indicated by EM is supported by AFM analysis of the properties of native diatom raphe secretions (see Sect. 5.2.4).

SEM of *Navicula* spp., *Pinnularia* spp., and *Amphora coffeaeformis* showed that mucilage strands emerge from along the entire length of both the non-driving raphe and the driving raphe of inverted cells (Rosowski 1980; Edgar 1983; Rosowski et al. 1983; Webster et al. 1985; Higgins et al. 2003a). TEM of thin-sectioned *N. cuspidata* cells attached to a resin and prepared by critical point drying showed the cells to be adhered to the substratum by the raphe secretion (Edgar 1983). Longitudinal sections of these cells show the strands projecting as regular, fine bristles from the driving raphe, with the distal ends deformed as though the strands were under pressure. This suggests that presentation of adhesive strands along the length of the raphe in vivo enables the diatom to anchor to and maintain relatively uniform adhesion over surfaces with nano- and micro-scale roughness since individual strands may be extended or compacted to varying degrees (Jagota and Bennison 2002). TEM of sections of freeze-fractured *N. cuspidata* cells that were rapidly frozen without pretreatment showed that the plasma membrane is closely appressed against the frustule throughout most of the cell, except along the raphe, where it is irregularly wrinkled, indicating that the proximal ends of the secreted adhesive strands retain contact with the plasma membrane (Edgar and Pickett-Heaps 1983, 1984).

SEM of chemically fixed and inverted *P. viridis* cells (exposing the driving raphe) showed distinct, thick mucilaginous strands (ca. 50–100 μm in diameter) protruding from the raphe, some of which were anastomosed (Fig. 5.4a,b; Higgins et al. 2003a). *P. viridis* cells often had a blob of amorphous material at the central nodule of the non-driving raphe that was attached to collapsed raphe strands. In some cells, long tethers were observed extending 40 μm from the valve face to form an attachment with the substratum. The tethers were ca. 1–2 μm in diameter widening to 10–15 μm at the substratum interface (Fig. 5.4c). Similar SEM observations of tethers and tangled bundles of strands (ca. 30 nm in diameter) at the central nodule of the non-driving raphe were made for *C. australis*. The invariant occurrence of adhesive EPS at both the driving and the non-driving raphes supports a model for constitutive, rather than induced, secretion of the raphe adhesive.

SEM of some *P. viridis* cells lying on their girdle region showed they bore mucilaginous sheets originating from the raphe of each valve and extending for 10 μm to the substratum (Fig. 5.4d; Higgins et al. 2003a), an observation which underpins the occasional rocking motion of raphid cells following initial contact. Attachment at both raphes creates a tension between the two competing raphes, essentially resulting in a tug-of-war (Wetherbee et al. 1998). The tension is broken when the force applied at one of the raphes is sufficient to break adhesion at the opposing raphe. However, SEM images, together with light microscopic observations of the occasional jerky movements and flip-flops between raphes of gliding *C. australis* and *P. viridis*, suggest that adhesion at the non-driving raphe is not always broken (Higgins et al 2003a). Instead, the tether at the non-driving raphe remains attached and is stretched as the cell moves on its driving raphe until it eventually detaches and becomes deposited on the substratum surface. Occasionally, detachment occurs at the driving raphe, so that the cell flips over.

5.2.3.3 Secreted Trails

Freshly secreted trails deposited during diatom gliding are readily marked with tracer particles (Edgar and Pickett-Heaps 1984; Lind et al. 1997; Higgins et al. 2003b) or labelled by lectins or specific antibodies (Lind et al. 1997; Wustman et al. 1997; Wigglesworth-Cooksey and Cooksey 2005). However, the trails are difficult to label with conventional stains and it has been suggested that this is probably because they are relatively soluble and disperse readily (Edgar and Pickett-Heaps 1984; Hoagland et al. 1993), although it is no less feasible that trails become cured and consequently resist staining.

Cryo-FESEM images of trails left after gliding *A. longipes* inoculated onto formvar-coated grids revealed a tangle of linear and coiled strands (Wang et al. 2000). These strands covered the substratum surface but "paths" leading to sessile *A. longipes* cells were cleared through them, indicating the

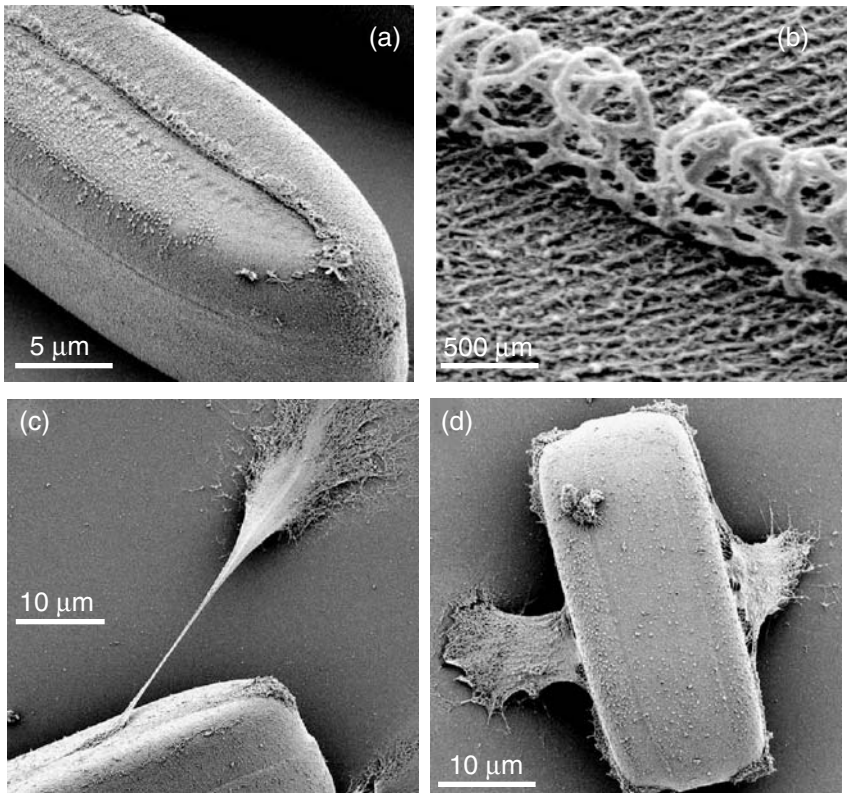

Fig. 5.4. SEM images of the raphe mucilage of *Pinnularia viridis*: (a) the adhesive strands emerge from the driving raphe of a chemically fixed and inverted cell; (b) higher magnification image of entangled raphe strands; (c) a tether formed between the elongated raphe adhesive of a cell and the substratum; (d) a sheet of adhesive extends from each raphe and anchors the cell to the substratum. (From Higgins et al. 2003a, reprinted with permission from the *Journal of Phycology*)

relative ease with which the fresh trails could be displaced. FESEM observations of the trails of *P. viridis* left on glass coverslips showed they were ca. 3 µm wide and extended for several millimeters (Higgins et al. 2000). The trails often appeared as irregular ripples perpendicular to the direction of deposition and composed of short strands lying flat on the substratum. By contrast, tapping-mode AFM images demonstrated that the hydrated trails formed swollen, rounded, continuous ridges that were up to 300 nm high and were well-adhered to the substratum along their entire length (Higgins et al. 2000). These ridges had no apparent substructure or specialized points of attachment, except for a thinner, more diffuse layer of hydrated mucilage either side of the main trail ridges. Some smearing was observed when the trails were imaged in tapping mode within an hour of deposition but the trails were more stable if imaged two to ten days later. These data indicated that the trail

material was initially sticky but cured rapidly after deposition rather than dissolving (Higgins et al. 2000).

The identity of the trail material and the secreted raphe adhesive was indicated by observations of *C. australis* (Lind et al. 1997). Silica microspheres added to the medium became attached to and moved along the driving raphe until they reached the end and remained trapped in the trail secreted behind the cell. Microspheres were rarely seen to attach to any part of the cell other than the raphe. Occasionally, motionless cells with a taut trail of adhesive extending behind the cell recommenced gliding when the trail broke. Like the tethers characterized by SEM for *C. australis* and *P. viridis* (Higgins et al. 2003a), these observations suggest trails are sometimes cable-like and have sufficient tensile strength to arrest cell motility. Similarity between AFM images of the rounded filaments comprising *P. viridis* mucilage trails (Higgins et al. 2000), and SEM images of *P. viridis* tethers suggest they are the same thing (Higgins et al. 2003a). However, differential staining of tethers (positive) and trails (negative) with Stains-All® suggested there are materials in the raphe mucilage that are differentially incorporated into tethers and trails (Higgins et al. 2003a). Alternatively, the staining properties differ if the raphe adhesives coalesce into a tether rather than being deposited as a trail.

5.2.4 Nanomechanical Properties Determined by AFM

The mechanical properties of molecules can be measured by AFM in force mode. During one cycle of force mode, the cantilever tip approaches the sample and is then retracted (Fig. 5.1b,c). Deflections of the cantilever tip during the approach-retraction cycles are recorded and converted to force-distance curves. In conventional force mode, the cantilever tip approaches the sample until the resistance of the sample is detected. In "fly fishing" force mode (Rief et al. 1997b), the AFM probe is allowed to closely approach the sample periphery enabling only the outermost polymers to adsorb to the cantilever tip.

5.2.4.1 Cell Surface Mucilage

AFM experiments showed that the cell surface mucilage of *P. viridis* was relatively soft, cohesive, and only weakly adhesive (Crawford et al. 2001). The mucilage was readily displaced by the sweeping action of the AFM cantilever tip in contact mode and it remained piled up at the periphery of the scan area without deforming for a further 2 h. The extension phase of AFM force-distance curves recorded for the mucilaginous coating of the girdle and the valve regions were non-linear, indicating that the mucilage was soft and compressible (Higgins et al. 2003b), and occasionally showed a peak that indicated the mucilage had a kind of skin which was punctured during the tip's approach to the cell surface (Higgins et al. 2002). The mucilage was therefore

interpreted as having a degree of cross-linking (Crawford et al. 2001; Higgins et al. 2002), although the nature of this cross-linking remains undefined.

The retraction phase of AFM force curves taken on the cell surface mucilage of *C. australis* and *P. viridis* often displayed multiple detachment events and were interpreted as the interaction of many, entangled polymers adsorbed to the cantilever tip, although single detachment events were also detected (Higgins et al. 2002, 2003b). The maximum force required to detach polymers from the cell surface mucilage varied with the loading force of the cantilever tip and was attributed to the depth with which the tip penetrated the mucilage layer. To achieve single binding events in the *C. australis* cell surface mucilage, Higgins et al. (2003b) used a loading force of 1–2 nN with a short contact time. The average maximum force required to detach polymers in the *C. australis* cell surface mucilage (F_{max}) was 203±9 (SD) pN and the average distance required to achieve detachment (D_{max}) was 106±5 (SD) nm. Under the same conditions, no adhesive peaks were observed for *P. viridis*.

The relative elasticity of the surface mucilages of *C. australis* and *P. viridis* was characterized by force-volume mapping (Higgins et al. 2003b). The experimental data fitted the Hertz model well and by making assumptions about tip radius (40 nm) and Poisson's ratio (μ=0.25), the Young's modulus for elasticity was estimated as 0.25±0.01 (SD) MPa in soft regions vs 0.45±0.01 (SD) MPa in hard regions for *C. australis*, and 0.54±0.02 (SD) MPa vs 0.76±0.03 (SD) MPa for *P. viridis*. Despite the uncertainties for precise measurement of Young's modulus, the data suggested the elastic properties of the mucilage of the two diatoms are similar.

5.2.4.2 Raphe Adhesives

AFM force-separation curves recorded at the non-driving raphes of both *C. australis* and *P. viridis* were distinguishable from those recorded for cell surface mucilage and typically displayed multiple but irregular sawtooth patterns and significantly higher detachment forces (Higgins et al. 2003a). From these force curves, average F_{max} for individual detachment events was measured as 4.5±3.6 (SD) nN and average D_{max} as 6.9±3.3 (SD) μm for the raphe strands of *C. australis*, whereas average F_{max} was 3.2±1.9 (SD) nN and average D_{max} was 8.2±2.9 (SD) μm for the raphe strands of *P. viridis* (Higgins et al. 2003a). However, a direct comparison between the average F_{max} values estimated for the two species is not possible because F_{max} is dependent on tip parameters that may differ between experiments and affect the number of strands adhering. A concern with recording conventional force-separation curves was that they measured F_{max} over an area that was determined by the curvature of the cantilever tip, so that the number of strands binding could not be controlled. As a remedy for this, Higgins et al. (2003a) also sought to characterize binding of the raphe strands by the fly-fishing technique (Fig. 5.1b,c). The subsequent retraction phase of the cycle therefore ideally

measured interaction with individual strands. Fly-fishing experiments above the raphe of *C. australis* gave single and/or multiple detachment events with average F_{max} of 197±97 (SD) pN, in the range for those of individual polymers (Zlatanova et al. 2000). However, the average D_{max} of these adhesive strands was 3.5±1.2 (SD) μm, demonstrating that they were highly extensible, even though the estimated value was regarded as less than the true D_{max} because the tip would not necessarily contact the strand at its terminus (Higgins et al. 2003a). Based on these data, it appears that fly-fishing mode measured the force of detachment for individual adhesive strands that comprised single–or at most, a few–polymers. In contrast, the irregular sawtooth patterns of the curves obtained by conventional force mode are suggestive of successive unbinding of clumped adhesive strands from the cantilever tip, and possibly also unbinding between strands and unfolding of domains within strands.

Less commonly, "incessant" S-shaped curves that did not return to the zero deflection line during successive extension-retraction cycles were obtained for the non-driving raphe of both *C. australis* and *P. viridis* (Higgins et al. 2002, 2003a). Although authentic F_{max} and D_{max} values could not be estimated, the energy required to extend and eventually detach these strands was up to 60 nN at distances of up to 15 μm. The attachment of raphe mucilage with the cantilever tip was visualized with Stains-All® and described as a kind of tether (Higgins et al. 2003a). Worm-like chain (WLC) modeling fitted poorly to the data in these incessant curves but persistence length (q) was 0.006±0.005 (SD) nm, about 100 times smaller than that of a simple monomer (0.1–0.5 nm; Higgins et al. 2002). Such persistence length values could arise from multiple chains extending in parallel, each with the same contour length and radius (Kellermeyer et al. 1997; Bemis et al. 1999; Dugdale et al. 2005).

5.2.5 Molecular Composition

5.2.5.1 Craspedostauros australis

Monoclonal antibodies (mAbs) were raised to four high molecular weight frustule-associated components ("FACs") from *C. australis* (Lind et al. 1997). These FACs are estimated to be 87 kDa, 112 kDa, and two >220 kDa, and were visualized by SDS-PAGE with a glycan stain, indicating they were glycoconjugates. In immunolocalization studies, one mAb which had high affinity for all four FACs (StF.H4) labelled the cell surface, the raphe, and the diatotepum (a putative polysaccharide layer between the plasma membrane and the silica wall), whereas another mAb (StF.D5) bound with relatively high affinity to the two smaller FACs and labelled the cell surface only. In addition, cell adhesion and cell motility were inhibited in a concentration-dependent manner when cells were incubated with native StF.H4 or divalent $F(ab)_2$ fragments of StF.H4 but not by monovalent F(ab) StF.H4 fragments or by StF.D5. These observations indicated that inhibition was effected by cross-linking of the

participating FACs recognized by the StF.H4 antibody. The contrasting inhibitory effects, affinities, and labelling patterns of the two mAbs suggested that the two larger FACs form the raphe and trail adhesive, whereas the two smaller FACs contributed to the cell surface mucilage. In contradiction to this interpretation, a third antibody (StF.F3) labelled the 112-kDa FAC with high affinity and immunolocalized to the raphe and girdle region (Lind et al. 1997). However, competitive inhibition assays, periodate treatment, and deglycosylation of the FACs (Lind et al. 1997; Chiovitti et al. 2003a) demonstrated that the antibodies were binding to carbohydrate. The localization data were therefore probably complicated by the antibodies cross-reacting with the same glycan epitopes on different FACs. The three largest FACs were subsequently shown to be high molecular weight glycoproteins decorated with a highly heterogeneous population of xylose-rich glycans, sulfate, and phosphate (Chiovitti et al. 2003a). The protein portions were relatively enriched in small non-polar (Gly and Ala, 22 mol% of total amino acids) and hydroxylated amino acids (Ser, Thr, Tyr, Hyp, 22 mol% of total). The hydroxylated amino acids were proposed to be the main sites of linkage for the glycans. The glycans of the FACs located on the cell surface may function in a manner analogous to those of protistan and mammalian mucins, forcing the glycoproteins to adopt an extended conformation so that they would function as relatively nonadhesive lubricants (Chiovitti et al. 2003a).

5.2.5.2 Pinnularia viridis

Biochemical analysis was combined with AFM to characterize the extracellular polysaccharides of *P. viridis* (Chiovitti et al. 2003b). Polysaccharides were successively extracted from the cells with water at 45 °C, a solution of sodium bicarbonate and EDTA at 95 °C, and hot alkali. AFM demonstrated that warm-water extraction removed an extracellular component that conferred a degree of softness and compressibility to the cell surface mucilage, leaving behind material that was more rigid and less elastic than the original mucilage layer. The rigid material was subsequently extracted with bicarbonate/EDTA, exposing the siliceous cell wall underneath. Carbohydrate analyses detected 19 sugars and 65 linkage and substitution patterns. The warm-water fraction was relatively enriched in fucose residues (and intracellular glucans), whereas the bicarbonate/EDTA fraction was relatively enriched in rhamnose residues, indicating that polymers enriched in fucose or rhamnose, respectively, contributed to the observed changes in the properties of the modified mucilage layer. However, many of the same sugars and a proportion of the linkage patterns were observed in all the fractions, indicating that the *P. viridis* polysaccharides comprised a spectrum of highly heterogeneous but structurally related sulfated polysaccharides. It was proposed that polydisperse molecular weight of the polysaccharides, distribution of residues within the polysaccharides, and covalent and noncovalent intermolecular associa-

tions with protein also affected the properties of the mucilage (Chiovitti et al. 2003b).

5.2.5.3 Amphora coffeaeformis

A. coffeaeformis cells have a tightly bound organic sheath and a loosely associated mucilaginous capsule (Daniel et al. 1980; Wustman et al. 1997). Early histochemical studies strongly indicated that *A. coffeaformis* mucilage was composed of sulfated polysaccharides and uronic acids (Daniel et al. 1980). Mechanically isolated capsules from *A. coffeaeformis* contained 13% sulfate, 6% protein, and a heterogeneous sugar composition consisting of glucose (40%) and nearly equal proportions of glucuronic acid, galactose, mannose, xylose, fucose, and rhamnose (7–13% each; Wustman et al. 1997). Sequential extraction with hot water and hot bicarbonate solution enriched the proportions of fucose and galactose (up to 32% each; Wustman et al. 1997). Surprisingly perhaps, concanavalin A labelled mainly the organic sheaths associated with the frustule, whereas *Abrus precatorius* agglutinin (specific for D-galactose) labelled the loosely associated capsule material (Wustman et al. 1997). However, in a later study, polymers associated with the cell walls, trails, footpads, and intercellular biofilm were all stained with lectins recognizing glucose, mannose, and galactose (Wigglesworth-Cooksey and Cooksey 2005). The apparent differences in staining in the two studies may be due to variations in interpretation, diatom physiology, or strain types. The height of *A. coffeaeformis* footpads estimated from confocal microscopy of FITC-Concanavalin A-labelled footpads is 5–7 μm, indicating the cell is substantially raised above the substratum (Wigglesworth-Cooksey and Cooksey 2005). Apart from an intracellular role in facilitating diatom cell motility (Cooksey 1981; Cooksey and Cooksey 1988), calcium ions apparently also mediate cross-linking of *Amphora* adhesives. Treatment of attached *A. coffeaeformis* with 10 mmol/l EGTA causes "cohesive breaks", with the effect that cells can be freely washed away and the adhesive pads are left behind on the substratum (Cooksey and Cooksey 1980). Similar effects have been described for other diatom species (Geesey et al. 2000). Calcium ions in the pads can be exchanged with strontium ions without any apparent effect on adhesion, although motility is affected (Cooksey and Cooksey 1980).

5.3 Sessile Adhesion

Often, after a period of gliding, benthic diatoms settle and form sessile adhesion structures. These adhesive structures are described primarily as pads and stalks (Daniel et al. 1987; Hoagland et al. 1993). The structures may be intergraded but are differentiated on the basis of relative length (Hoagland

et al. 1993). However, the pads and the stalks of stalk-forming diatoms, such as *A. longipes*, differ in ultrastructure and composition (Daniel et al. 1987; Wang et al. 1997; Wustman et al. 1997). The site of stalk secretion varies for different species and may be the raphe, the mantle edge, or an apical region of the frustule bearing numerous small pores (apical pore field) (Gibson 1979; Pickett-Heaps et al. 1991; Hoagland et al. 1993; Kooistra et al. 2003).

5.3.1 Physical Properties of Adhesive Pads with AFM

Adhesion and motility is normally associated with raphid diatoms but some diatoms that lack a raphe, such as *Ardissonea crystallina* and *T. undulatum*, are also capable of gliding (Pickett-Heaps et al. 1991; Kooistra et al. 2003). This mode of motility is apparently simpler than that of raphid diatoms and propulsion is probably achieved by swelling and hydration of secreted mucilage (Pickett-Heaps et al. 1991). Adhesive mucilage in both species is apparently secreted at the cell apices in the region of the first girdle band. Sessile adhesion is attained by formation of an adhesive pad, described as a "stipe" for *A. crystallina*.

5.3.1.1 Toxarium undulatum

Although the adhesive remains to be characterized biochemically, the properties of the *T. undulatum* adhesive pad have been investigated in substantial detail by AFM (Dugdale et al. 2005). Fly-fishing experiments on native pads with the cells still attached produced force curves displaying regular sawtooth patterns. Like *C. australis* raphe strands (Higgins et al. 2003a, see Sect. 5.2.4.2), but in contrast to most polymers and proteins studied by AFM (Hugel and Seitz 2001), the *T. undulatum* mucilage adsorbed to the cantilever tip without applying detectable force (<5 pN) or pausing. This observation underscores the role of the mucilage as an effective adhesive. The sawtooth pattern was still retained on pads from which cells had been removed for up to 12 h. However, after 48–89 h, these curves were obtained with reduced frequency and the curves sometimes had indistinct peaks or no peaks, indicating that the adhesive slowly underwent degradation and/or curing.

The sawtooth curves of the adhesive nanofibers had regular features (Dugdale et al. 2005). The average distance to the first peak was 201±10.6 (SE) nm, the average distance between each peak was 34.3±1.5 (SE) nm, and the average peak force was 0.801±0.071 (SE) nN. The distance to the last peak varied and was dependent upon the total number of peaks in the curve, which varied from 3 to 27. These data showed that the first ca. 200 nm portion of the adhesive nanofiber invariably unraveled without restriction. This portion must be proximal to the anchor point of the adhesive, probably enabling the adhesive to trawl away from the parent surface. The remainder of the

adhesive nanofiber comprises a backbone of up to 27 domains, each successively unfolding to increase overall length by ca. 34 nm. Most of the peaks were relatively accurately fitted with the WLC model giving a persistence length (q) of 0.036±0.004 (SE) nm. The low average persistence length, together with the high average force for unfolding (0.8 nN) indicated that the adhesive nanofibers are composed of multiple polymer chains that must be aligned in parallel, unfolding and refolding synchronously in order to achieve the observed regular sawtooth patterns.

The adhesive nanofiber of *T. undulatum* also showed very efficient self-healing properties (Dugdale et al. 2005). The regular sawtooth pattern was reproducibly recorded for up to 666 successive approach-retraction cycles of adhesive nanofibers that remained bridged between the pad and the cantilever tip to a distance of 800 nm. The average proportion of domains that refolded decreased as the scan rate increased (from 92% at 0.8 μm/s down to 53% at 7.4 μm/s). However, all the domains refolded if the tip was paused in the extended position for 2 s. These data clearly demonstrated that strong, reversible intradomain bonding was involved in refolding the stretched adhesive nanofiber. It was suggested that hydrogen bonding, which has extremely low activation energies, must facilitate the refolding (Dugdale et al. 2005). The strength and flexibility of the adhesive makes the cells difficult to detach, even in fast moving currents.

The sawtooth pattern of the *T. undulatum* adhesive nanofibers was the characteristic AFM fingerprint for unfolding of modular proteins (Fisher et al. 2000) but this was previously only recorded for purified or recombinant proteins (Rief et al. 1997a; Oroudjev et al. 2002). The multi-cycle sawtooth patterns for bridged adhesive nanofibers were abolished by incubating the *T. undulatum* pads with protease, demonstrating that the backbone of the adhesive nanofiber was composed predominantly of protein (Dugdale et al. 2005). During these experiments, the sawtooth pattern of the initial extension and retraction cycles was the same as those recorded for native bridged adhesive nanofibers. However, the retraction phase of the second and subsequent cycles gave no cantilever deflection. These data indicated that the protease did not interfere with the binding or initial unfolding of the adhesive nanofiber but, when the adhesive nanofiber was extended, it became susceptible to hydrolysis by the protease, resulting in cleavage and rendering it undetectable by AFM.

5.3.1.2 Eunotia sudetica

Irregular unbinding events have been recorded on the adhesive pads of the freshwater diatom, *E. sudetica*. To examine the adhesive, *E. sudetica* cells were dislodged from a glass slide and the adhesive remaining on the substratum was probed with AFM for several hours. Multiple detachment events were recorded in the retraction phase of the cycle with a separation distance of ca. 600 nm (Gebeshuber et al. 2003). The self-healing properties of the

E. sudetica adhesive were not as efficient as those of the *T. undulatum* adhesive. An interval of 30 s was required between successive scanning cycles for the *E. sudetica* adhesive to recover progressively diminished proportions of its relaxed-state structure until, after five scans, the adhesive was undetectable (Gebeshuber et al. 2002).

5.3.2 Molecular Composition and Chemical Properties of Stalks: *Achnanthes longipes*

5.3.2.1 Stalk Formation

The best studied example of stalk formation in a diatom is that of *A. longipes*. Cell density is a key stimulator for stalk production in *A. longipes*, interpreted as a response to crowding by raising cells above the biofilm and possibly triggered by a diffusible autoinducer molecule (Lewis et al. 2002). The adhesion process of *A. longipes* has been described as occurring in four key stages (Wang et al. 1997). In stage 1, cells actively adhere to the substratum via the raphe and glide. Cell motility ceases after ca. 6 h. In stage 2, small globular pad structures are produced from the terminal nodule of the raphe. In stage 3, a flexible, elongated shaft is secreted and elevates the cell above the substratum. The shaft connects the cell to the pad and adhesion of residual pad material to the cell results in formation of a collar at the top of the shaft (Daniel et al. 1987; Wang et al. 1997). Stalk secretion is associated with active vesicle traffic (Daniel et al. 1987; Wang et al. 2000). In stage 4, successive cell divisions lead to formation of filamentous colonies.

Stalk synthesis and cell gliding in *A. longipes*, but not cell division, were reversibly inhibited in a dose-dependent manner by the herbicide, 2, 6-dichlorobenzonitrile (DCB) and four DCB analogues, indicating that events in gliding and stalk secretion are related (Wang et al. 1997). A fluorescent analogue of DCB bound an 18-kDa protein associated with the membrane fraction obtained by detergent extraction of cells that were actively synthesizing adhesives, leading Wang et al. (1997) to postulate that the effect may be sited at the plasma membrane, although the identity of the 18-kDa protein and the mode of DCB action remain unknown.

5.3.2.2 Composition and Properties

The length and diameter of *A. longipes* stalks generally varies depending on the amount of time elapsed since the cells were inoculated (Wang et al. 1997) but, when grown under ideal conditions, stalks are 200–500 μm long and 7–9 μm wide (Johnson et al. 1995). The stalks are composed of four layers identified by TEM of chemically fixed cells (Wang et al. 1997, 2000) or by LM of stained thin sections (Daniel et al. 1987). The core of the shaft comprised a

central ribbon of densely packed fibers surrounded by one layer of perpendicularly arranged fibers, a second layer of fibers arranged parallel to the stalk axis, and a relatively diffuse, outermost layer. The pad and collar are comparatively amorphous.

Based on available data (discussed below), Wustman et al. (1998) proposed a model for *A. longipes* cell adhesion. During sessile adhesion, highly sulfated fucoglucuronogalactans (FGGs) are secreted from the raphe and expand to form a cylinder comprising fibrils that are arrayed perpendicular to the axis of the stalk. This material is assumed to be related to the adhesive used by the cell for motility. The low-sulfate FGGs are secreted from the apical pore field surrounding the raphe pole and form the outer layer of fibrils that run parallel to the stalk axis. Wustman et al. (1998) suggested that the adhesives putatively cure by cross-linking proteins (presumably glycoproteins), polysaccharides, and phenolics through covalent O-linkages.

Mechanically isolated stalks (MIS) of *A. longipes* were composed of carbohydrate (40%), uronic acid (10%, mainly as glucuronic acid), and small amounts of protein (5%) (Wustman et al. 1997). The carbohydrates of MIS and water-insoluble/base-soluble (WIBS) fractions from the stalks were dominated by fucose and galactose (comprising 50–70% of total sugars) with a complex mix of multiple linkage and substitution patterns. ^{13}C-NMR indicated that the fucose was present in the furanosyl form. Differential cytochemical staining and labelling with FITC-lectin conjugates demonstrated that the composition of the pads and collars differed from that of the shaft of the stalk (Wustman et al. 1997). However, a continuity of labelling with some lectins, such as concanavalin A, also showed that related glucose and mannose structural units occurred throughout the stalk.

The WIBS was fractionated by size-exclusion chromatography into three distinct size classes: $F_1 \geq 20{,}000$ kDa, $F_2 \approx 100$ kDa, and $F_3 < 10$ kDa (Wustman et al. 1998). F_1 and F_2 were the major fractions, composed mainly of carbohydrate with small amounts of protein (5% in F_1 and <1% in F_2). F_3 was almost entirely protein and ran as a smear on SDS-PAGE, indicating it was still bound to carbohydrates. Cold NaOH treatment of WIBS led to a decrease in F_1 and an increase in F_2 and F_3, whereas trypsin treatment eliminated F_3, demonstrating that F_1 was a complex of F_2 (mainly polysaccharide) and F_3 (mainly protein). The complexes were likely stabilized by covalent O-linkages between carbohydrates and proteins because chelating agents and imidazole buffers, which disrupt ionic interactions, did not solubilize *A. longipes* stalks (Wustman et al. 1998). CPC-soluble material from WIBS was enriched in protein and contained relatively more terminal and 4-linked mannopyranose and less galactopyranose residues than unfractionated WIBS, suggesting the occurrence of mannoprotein (Wustman et al. 1998). The major amino acids in MIS were the small nonpolar residues (Ala 17 mol%, Gly 13 mol%), together with Ser, Val, and Asx (13 mol% each, Wustman et al. 1997).

High- and low-sulfate FGG fractions of WIBS were isolated by anion-exchange chromatography (Wustman et al. 1998). Both fractions had similar

carbohydrate (80–84%), protein (7–10%), and uronic acid content (18–19%), but differed substantially in sulfate content (11% vs 2 %). Wustman et al. (1998) raised five antibodies that recognized a family of related epitopes with antigenicity dependent upon fucose-containing side chains present on both high- and low-sulfate FGGs. The antibodies differentially localized the high-sulfate FGGs to the shaft core and the low-sulfate FGGs to the outer layers. These observations corroborated earlier cytochemical staining and X-ray microanalysis of sectioned *A. longipes* stalks that indicated that the levels of sulfation were higher in the central core than in the surrounding layers (Daniel et al. 1987; Johnson et al. 1995). Cells grown in media containing methionine in place of sulfate appeared healthy but lacked adhesion and had reduced rates of cell division (Johnson et al. 1995), indicating a crucial role for sulfate in the formation of the stalks. The sulfate may effect cross-linking by divalent cations (Johnson et al. 1995) but may also promote flexibility within the stalk by mutual charge repulsion (Daniel et al. 1987). The mAb with the highest affinity for high-sulfate FGGs (AL.C1) was the only mAb that labelled the inner core of the shaft (Wustman et al. 1998). Interestingly, AL.C1 also labelled the raphe region of motile *A. longipes*. Wustman et al. (1998) concluded that the central core region is raphe-derived and is related to the material exuded during cell gliding.

Bromide is essential for stalk formation in *A. longipes*, with an optimum concentration of 30 mmol/l for maximal stalk production, although bromide was not essential for optimal growth rates (Johnson et al. 1995; Lewis et al. 2002). As bromide concentrations were decreased, stalk morphology became progressively more distorted until only pads were produced (Johnson et al. 1995). Insoluble EPS was not produced in the absence of bromide but cells secreted relatively high levels of soluble carbohydrates, indicating that the EPS were incompletely cross-linked. Increasing iodide concentrations also inhibited the extent and morphological integrity of stalk formation, and only soluble EPS was produced at 67 μmol/l of iodide, even with optimum levels of bromide. Based on their observations, Johnson et al. (1995) proposed that *A. longipes* stalk formation requires the action of a haloenzyme, possibly a vanadate-dependent bromoperoxidase, that stabilizes extracellular matrix components by oxidizing phenolic compounds and effecting their cross-linking to carbohydrates in polysaccharides and glycoproteins. Bromoperoxidase activity has been detected in other chromophytes, mainly representatives of the Phaeophyceae, such as *Ascophyllum* and *Fucus* species (Vilter 1984; Vreeland et al. 1998). Cross-linking of *Fucus serratus* polyphenolics was achieved with an exogenous vanadate-dependent bromoperoxidase from *Ascophyllum nodosum*, and bromide was demonstrated to be essential for the intermolecular cross-linking (Berglin et al. 2004). *A. longipes* stalks autofluoresce when excited at 360 nm, suggesting phenolics are present (Wustman et al. 1997). The inhibitory effect of elevated iodide concentrations on *A. longipes* stalk curing may be due to competitive inhibition of the bromide in the putative bromoperoxidase, with the implication that the binding

pocket of the enzyme is equally accessible to both ions, despite the relative difference in their sizes (Colin et al. 2005).

5.4 Concluding Remarks

The structure, properties, and composition of diatom mucilages vary according to function and include adhesion for motility, sessile adhesion, cell-surface lubrication, and cell elevation. The composition and properties of the adhesives also vary between diatom species and at different sites on the same diatom cell. Disparate data sets for the properties and composition derived for different diatom species could be consolidated by standardizing some model species for complementary studies. The field would benefit, for example, from detailed AFM studies on *A. longipes* stalks, which are well-characterized biochemically (Sect. 5.3.2). However, some tentative principles may be emerging. For example, the very low persistence lengths estimated by AFM for both the *C. australis* raphe strands (Sect. 5.2.4.2) and the *T. undulatum* adhesive nanofibers (Sect. 5.3.1.1) suggest that the adhesive properties of these mucilages derive from the coordinated activity of amalgamated polymers. AFM studies on more diatom species would assist to determine whether these represent isolated observations or a genuine principle underpinning diatom adhesives. Knowledge of the distribution of specific sugar moieties in diatom EPS would enhance understanding of the physical properties of EPS. However, the occurrence of protein in various diatom adhesives highlights a need to focus biochemical studies on characterizing these protein components. With the availability of diatom genomes (Armbrust et al. 2004; Montsant et al. 2005), protein sequences would enable dissection of diatom adhesives with an integrated approach incorporating molecular biology, immunolocalization, and AFM, targeting such goals as determining how adhesives are secreted from the frustule without occluding the secretion sites, characterizing cross-linking processes, and, ultimately, identifying adhesive domains.

References

Alberte RS, Snyder S, Zahuranec BJ, Whetsone M (1992) Biofouling research needs for the United States Navy: program history and goals. Biofouling 6:91–95

Anderson C, Atlar M, Callow M, Candries M, Townsin RL (2003) The development of foul-release coatings for seagoing vessels. J Mar Design Operations 84:11–23

Armbrust EV, Berges JA, Bowler C, Green BR, Martinez D, Putnam NH, Zhou S, Allen AE, Apt KE, Bechner M, Brzezinski MA, Chaal BK, Chiovitti A, Davis AK, Demarest MS, Detter JC, Glavina T, Goodstein D, Hadi MZ, Hellsten U, Hildebrand M, Jenkins BD, Jurka J, Kapitonov VV, Kröger N, Lau WWY, Lane TW, Larimer FW, Lippmeier JC, Lucas S, Medina M, Montsant A, Obornik M, Schnitzler Parker M, Palenik B, Pazour GJ, Richardson PM,

Rynearson TA, Saito MA, Schwartz DC, Thamatrakoln K, Valentin K, Vardi A, Wilkerson FP, Rokhsar DS (2004) The genome of the diatom *Thalassiosira pseudonana*: ecology, evolution, and metabolism. Science 306:79–86

Bellinger BJ, Abdullahi AS, Gretz MR, Underwood GJC (2005) Biofilm polymers: relationship between carbohydrate biopolymers from estuarine mudflats and unialgal cultures of benthic diatoms. Aquat Microbial Ecol 38:169–180

Bemis JE, Akhremitchev BB, Walker GC (1999) Single polymer chain elongation by atomic force microscopy. Langmuir 15:2799–2805

Berglin M, Delage L, Potin P, Vilter H, Elwig H (2004) Enzymatic cross-linking of a phenolic polymer extracted from the marine alga *Fucus serratus*. Biomacromolecules 5:2376–2383

Bhosle NB, Sawant SS, Garg A, Wagh A (1995) Isolation and partial chemical analysis of exopolysaccharides from the marine fouling diatom *Navicula subinflata*. Bot Mar 38:103–110

Binning G, Quate CF, Gerber CH (1986) Atomic force microscope. Phys Rev Lett 56:930–933

Bohlander GS (1991) Biofilm effects on drag: measurements on ships. In: Long DM, Bufton R, Yakimiuk P, Williams K (eds) Polymers in a marine environment. Institute of Marine Engineering, London, pp 135–138

Callow ME (1986) Fouling algae from "in-service" ships. Bot Mar 29:351–357

Callow ME (1996) Ship-fouling: the problem and method of control. Biodeterioration Abstr 10:411–421

Chiovitti A, Bacic A., Burke J, Wetherbee R (2003a) Heterogeneous xylose-rich glycans are associated with extracellular glycoproteins from the biofouling diatom *Craspedostauros australis* (Bacillariophyceae). Eur J Phycol 38:351–360

Chiovitti A, Higgins MJ, Harper RE, Wetherbee R, Bacic A (2003b) The complex polysaccharides of the raphid diatom *Pinnularia viridis* (Bacillariophyceae). J Phycol 39:543–554

Chiovitti A, Molino P, Crawford SA, Teng R, Spurck T, Wetherbee R (2004) The glucans extracted with warm water from diatoms are mainly derived from intracellular chrysolaminaran and not extracellular polysaccharides. Eur J Phycol 39:117–128

Clarkson N, Evans LV (1995a) Further studies investigating a potential non-leaching biocide using the marine biofouling diatom *Amphora coffeaeformis*. Biofouling 9:17–30

Clarkson N, Evans LV (1995b) Raft trial experiments to investigate the antifouling potential of silicone elastomer polymers with added biocide. Biofouling 9:129–143

Cohn SA, Weitzell RE (1996) Ecological considerations of diatom motility. I. Characterization of adhesion and motility in four diatom species. J Phycol 32:928–939

Cohn SA, Farrell, JF, Munro JD, Ragland RL, Weitzell RE, Wibisono BL (2003) The effect of temperature and mixed species composition on diatom motility and adhesion. Diatom Res 18:225–243

Colin C, Leblanc C, Gurvan M, Wagner E, Leize-Wagner E, van Dorsselaer A, Potin P (2005) Vanadium-dependent iodoperoxidases in *Laminaria digitata*, a novel biochemical function diverging from brown algal bromoperoxidases. J Biol Inorg Chem 10:156–166

Cooksey B, Cooksey KE (1980) Calcium is necessary for motility in the diatom *Amphora coffeaeformis*. Plant Physiol 65:129–131

Cooksey B, Cooksey KE (1988) Chemical signal-response in diatoms of the genus *Amphora*. J Cell Sci 91:523–529

Cooksey KE (1981) Requirement for calcium in adhesion of a fouling diatom to glass. Appl Environ Microbiol 41:1378–1382

Cooksey KE, Wigglesworth-Cooksey B (1992) The design of antifouling surfaces: background and some approaches. In: Melo LF, Bott TR, Fletcher M, Capdeville B (eds) Biofilms -science and technology. Kluwer Academic Publ, Dordrecht/Boston, pp 529–549

Crawford SA, Higgins MJ, Mulvaney P, Wetherbee R (2001) Nanostructure of the diatom frustule as revealed by atomic force and scanning electron microscopy. J Phycol 37:543–554

Daniel GF, Chamberlain AHL, Jones EBG (1980) Ultrastructural observations on the marine fouling diatom *Amphora*. Helgoländer Meeresunters 34:123–149

Daniel GF, Chamberlain AHL, Jones EBG (1987) Cytochemical and electron microscopical observations on the adhesive materials of marine fouling diatoms. Br Phycol J 22:101–118

De Brouwer JF, Stal LJ (2002) Daily fluctuations of exopolymers in cultures of the benthic diatoms *Cylindrotheca closterium* and *Nitschia* sp. (Bacillariophyceae). J Phycol 38: 464–472

Dugdale TM, Dagastine R, Chiovitti A, Mulvaney P, Wetherbee R (2005) Single adhesive nanofibers from a live diatom have the signature fingerprint of modular proteins. Biophys J 89:4252–4260

Edgar LA (1983) Mucilage secretions of moving diatoms. Protoplasma 118:44–48

Edgar LA, Pickett-Heaps JD (1982) Ultrastructural localization of polysaccharides in the motile diatom *Navicula cuspidata*. Protoplasma 113:10–22

Edgar LA, Pickett-Heaps JD (1983) The mechanism of diatom locomotion. I. An ultrastructural study of the motility apparatus. Proc R Soc Lond B 281:331–343

Edgar LA, Pickett-Heaps JD (1984) Diatom locomotion. Prog Phycol Res 3:47–88

Edgar LA, Zavortink M (1983) The mechanism of diatom locomotion. II. Identification of actin. Proc R Soc Lond B 218:345–348

Fisher TE, Marszalek PE, Fernandez JM (2000) Stretching single molecules into novel conformations using the atomic force microscope. Nature Struct Biol 7:719–723

Gebeshuber IC, Thompson JB, del Amo Y, Stachelberger H., Kindt JH (2002) *In vivo* nanoscale atomic force microscopy investigation of diatom adhesion properties. Mater Sci Tech 18:763–766

Gebeshuber IC, Kindt JH, Thompson JB, del Amo Y, Stachelberger H, Brzezinski MA, Stucky GD, Morse DE, Hansma PK (2003) Atomic force microscopy study of living diatoms in ambient conditions. J Microsc 212:292–299

Geesey GG, Wigglesworth-Cooksey B, Cooksey KE (2000) Influence of calcium and other cations on surface adhesion of bacteria and diatoms. Biofouling 15:195–205

Gibson RA (1979) Observations of stalk production by *Pseudohimantidium pacificum* Hust. & Krasske (Bacillariophyceae: Protoraphidaceae). Nova Hedwigia 31:899–915

Gordon R (1987) A retaliatory role for algal projectiles, with implications for the mechanochemistry of diatom gliding motility. J Theor Biol 126:419–436

Häder D-P, Hoiczyk E (1992) Gliding motility. In: Melkonian M (ed) Algal cell motility. Chapman and Hall, New York, pp 1–38

Higgins MJ, Crawford SA, Mulvaney P, Wetherbee R (2000) The topography of soft, adhesive diatom 'trails' as observed by atomic force microscopy. Biofouling 16:133–139

Higgins MJ, Crawford SA, Mulvaney P, Wetherbee R (2002) Characterization of the adhesive mucilages secreted by live diatom cells using atomic force microscopy. Protist 153:25–38

Higgins MJ, Molino P, Mulvaney P, Wetherbee R (2003a) The structure and nanomechanical properties of the adhesive mucilage that mediates diatom substratum adhesion and motility. J Phycol 39:1181–1193

Higgins MJ, Sader JE, Mulvaney P, Wetherbee R (2003b) Probing the surface of living diatoms with atomic force microscopy: the nanostructure and nanomechanical properties of the mucilage layer. J Phycol 39:722–734

Hoagland KD, Rosowski JR, Gretz MR, Roener SC (1993) Diatom extracellular polymeric substances: function, fine structure, chemistry, and physiology. J Phycol 29:537–566

Holland R, Dugdale TM, Wetherbee R, Brennan AB, Finlay JA, Callow JA, Callow ME (2004) Adhesion and motility of fouling diatoms on a silicone elastomer. Biofouling 20:323–329

Hugel T, Seitz M (2001) The study of molecular interactions by AFM force spectroscopy. Macromol Rapid Commun 22:989–1016

Jagota A, Bennison SJ (2002) Mechanics of adhesion through a fibrillar microstructure. Integr Comp Biol 42:1140–1145

Johnson LM, Hoagland KD, Gretz MR (1995) Effects of bromine and iodine on stalk secretion in the biofouling diatom *Achnanthes longipes* (Bacillariophyceae). J Phycol 31:401–412

Kellermeyer MSZ, Smith SB, Granzier HL, Bustamante C (1997) Folding-unfolding transitions in single titin molecules characterized with laser tweezers. Science 276:1112–1116

Khandeparker RD, Bhosle NB (2001) Extracellular polymeric substances of the marine fouling diatom *Amphora rostrata* Wm.S. Biofouling 17:117–127

Kooistra WHCF, de Stafano M, Mann DG, Salma N, Medlin LK (2003) Phylogenetic position of *Toxarium*, a pennate-like lineage within centric diatoms (Bacillariophyceae). J Phycol 39:185–197

Lewis R, Johnson LM, Hoagland KD (2002) Effects of cell density, temperature, and light intensity on growth and stalk production in the biofouling diatom *Achnanthes longipes* (Bacillariophyceae). J Phycol 38:1125–1131

Lind JL, Heimann K, Miller EA, van Vliet C, Hoogenraad NJ, Wetherbee R (1997) Substratum adhesion and gliding in a diatom are mediated by extracellular proteoglycans. Planta 203:213–221

Mann DG (1999) The species concept in diatoms. Phycologia 38:437–495

McConville MJ, Wetherbee R, Bacic A (1999) Subcellular location and composition of the wall and secreted extracellular sulphated polysaccharides/proetoglycans of the diatom *Stauroneis amphioxys* Gregory. Protoplasma 206:188–200

Montsant A, Jabbari K, MaheswariU, Bowler C (2005) Comparative genomics of the pennate diatom *Phaeodactylum tricornutum*. Plant Physiol 137:500–513

Moroz AL, Ehrman JM, Clair TA, Gordon RJ, Kaczmarska I (1999) The impact of ultraviolet-B radiation on the motility of the freshwater epipelic diatom *Nitzschia lineariz*. Global Change Biol 5:191–199

Omae I (2003) Organotin antifouling paints and their alternatives. Appl Organmetal Chem 17:81–105

Oroudjev E, Soares J, Arcidiacono S, Thompson JB, Fossey SA, Hansma HG (2002) Segmented nanofibers of spider dragline silk: atomic force microscopy and single-molecule force spectroscopy. Proc Natl Acad Sci USA 99:6460–6465

Paterson DM (1989) Short-term changes in the erodibility of intertidal cohesive sediments related to the migratory behaviour of epipelic diatoms. Limnol Oceanogr 43:223–234

Pettitt ME, Henry SL, Callow ME, Callow JA, Clare AS (2004) Activity of commercial enzymes on settlement and adhesion of cypris larvae of the barnacle *Balanus amphitrite*, spores of the green alga *Ulva linza*, and the diatom *Navicula perminuta*. Biofouling 20:299–311

Pickett-Heaps JD, Schmid A-M, Edgar LA (1990) The cell biology of diatom valve formation. Prog Phycol Res 7:1–168

Pickett-Heaps JD, Hill DRA, Blaze KL (1991) Active gliding in an araphid marine diatom, *Ardissonea* (formerly *Synedra*) *crystallina*. J Phycol 27:718–725

Poulsen NC, Spector I, Spurck TP, Schultz TF, Wetherbee R (1999) Diatom gliding is the result of an actin-myosin motility system. Cell Motility Cytoskeleton 44:23–33

Rief M, Gautel M, Oesterhelt F, Fernandez JM, Gaub HE (1997a) Reversible unfolding of individual titin immunoglobulin domains by AFM. Science 276:1109–1112

Rief M, Oesterhelt F, Heymann B, Gaub HE (1997b) Single molecule force spectroscopy on polysaccharides by AFM. Science 275:1295–1297

Rosowski JR (1980) Valve and band morphology of some freshwater diatoms. II. Integration of valves and bands in *Navicula confervacea* var. *confervacea*. J Phycol 16:88–101

Rosowski JR, Hoagland KD, Roemer SC (1983) Valve and band morphology of some freshwater diatoms. IV. Outer surface mucilage of *Navicula confervacea* var. *confervacea*. J Phycol 19:342–347

Round FE, Crawford RM, Mann DG (1990) The diatoms. Cambridge Univ Press, Cambridge, 747 pp

Serôdio J, da Silva JM, Catarino F (1997) Nondestructive tracing of migratory rhythms of intertidal benthic microalgae using *in vivo* chlorophyll *a* fluorescence. J Phycol 33:542–553

Smestad Paulsen B, Haug A, Larsen B (1978) Structural studies of a carbohydrate-containing polymer present in the mucilage tubes of the diatom *Berkeleya rutilans*. Carbohydr Res 66:103–111

Smith DJ, Underwood GJC (1998) Exopolymer production by intertidal epipelic diatoms. Limnol Oceanogr 43:1578–1591

Staats N, de Winder B, Stal LJ, Mur LR (1999) Isolation and characterization of extracellular polysaccharides from the epipelic diatoms *Cylindrotheca closterium* and *Navicula salinarum*. Eur J Phycol 34:161–169

Underwood GJC, Paterson DM (2003) The importance of extracellular carbohydrate production by epipelic diatoms. In: Callow JM (ed) Advances in botanical research, vol 40. Elsevier Academic Press, Oxford, pp 183–240

Vilter H (1984) Peroxidases from Phaeophyceae -a vanadium (V)-dependent peroxidase from *Ascophyllum nodosum*. 5. Phytochemistry 23:1387–1390

Vreeland V, Waite JH, Epstein L (1998) Polyphenols and oxidases in substratum adhesion by marine algae and mussels. J Phycol 34:1–8

Wang Y, Lu J, Mollet J-C, Gretz MR, Hoagland KD (1997) Extracellular matrix assembly in diatoms (Bacillariophyceae). II. 2,6-dichlorobenzonitrile inhibition of motility and stalk production in the marine diatom *Achnanthes longipes*. Plant Physiol 113:1071–1080

Wang Y, Chen Y, Lavin C, Gretz MR (2000) Extracellular matrix assembly in diatoms (Bacillariophyceae). IV. Ultrastructure of *Achnanthes longipes* and *Cymbella cistula* as revealed by high-pressure freezing/freeze substitution and cryo-field emission scanning electron microscopy. J Phycol 36:367–378

Webster DR, Cooksey KE, Rubin RW (1985) An investigation of the involvement of cytoskeletal structures and secretion in gliding motility of the marine diatom, *Amphora coffeaeformis*. Cell Motility Cytoskeleton 5:103–122

Wetherbee R, Lind JL, Burke J, Quatrano RS (1998) The first kiss: establishment and control of initial adhesion by raphid diatoms. J Phycol 34:9–15

Wigglesworth-Cooksey B, Cooksey KE (1992) Can diatoms sense surfaces? State of our knowledge. Biofouling 5:227–238

Wigglesworth-Cooksey B, Cooksey KE (2005) Use of fluorophore-conjugated lectins to study cell-cell interactions in model marine biofilms. Appl Environ Microbiol 71:428–435

Wigglesworth-Cooksey B, van der Mei H, Busscher HJ, Cooksey KE (1999) The influence of surface chemistry on the control of cellular behaviour: studies with a marine diatom and a wettability gradient. Colloids Surfaces B Biointerfaces 15:71–79

Wustman BA, Gretz MR, Hoagland KD (1997) Extracellular matrix assembly in diatoms (Bacillariophyceae). I. A model of adhesives based on chemical characterization and localization of polysaccharides from the marine diatom *Achnanthes longipes* and other diatoms. Plant Physiol 113:1059–1069

Wustman BA, Lind J, Wetherbee R, Gretz MR (1998) Extracellular matrix assembly in diatoms (Bacillariophyceae). III. Organization of fucoglucuronogalactans within the adhesive stalks of *Achnanthes longipes*. Plant Physiol 116:1431–1441

Zlatanova J, Lindsay SM, Leuba SH (2000) Single molecule force spectroscopy in biology using atomic force microscopy. Prog Biophys Mol Biol 74:37–61

6 Phenolic-based Adhesives of Marine Brown Algae

Philippe Potin and Catherine Leblanc

6.1 Introduction

Brown algae, such as kelps and fucoids, occur over large areas of the subtidal and intertidal rocky shores, including tropical reef habitats, producing high biomass and determining the structure of the ecosystem (i.e. kelp forests). Brown algae live firmly attached to the substratum and are often exposed to high gradients of turbulence. Therefore, they experience drag and lift forces of currents and waves with velocities that may exceed 10 m/s. As other sessile marine organisms, to disperse in certain phases of their life histories and to survive in such a stressful environment, they had to evolve strategies to adhere strongly and durably underwater from the microscopic reproductive cell stages to the large thalli of giant kelps. Brown algal filamentous species such as *Ectocarpus* were also identified as major ship fouling organisms in the 1960s, when the use of anti-fouling paints containing organo-metallic compounds–which was successful against fouling green algae–enabled *Ectocarpus* to bloom (Baker and Evans 1973).

Unfortunately, studies on adhesion mechanisms of marine brown algal adhesives have consisted mostly of analogy and hypothesis (Vreeland et al. 1998). Better characterization of these adhesives will eventually lead to new strategies to prevent biofouling or to produce or design synthetic water-resistant adhesives of commercial value. The properties of the adhesives in terms of spreading and curing underwater are crucial to successful colonization of substrata. However, much of the evidence on the composition of algal adhesives is circumstantial and based on methodologies such as histochemistry (Fletcher and Baier 1984; Gonzales and Goff 1989; Fletcher and Callow 1992; Callow and Callow 2002). These studies indicate that macroalgal adhesion involves carbohydrate and glycoprotein-containing mucilage (Fletcher and Callow 1992) that 'cure' with time after discharge, thereby increasing the strength of attachment to the substratum. In contrast with the progress in the chemical characterization of diatom adhesives (Chamberlain 1976; Stossel 1993; Lind et al. 1997; Wustman et al. 1997; Wetherbee et al. 1998; Higgins et al. 2002), the composition and physicochemical nature of adhesives used by different macroalgae remain unknown. Therefore, it is difficult to infer by which processes they

UMR 7139 CNRS/UPMC, Marine Plants and Biomolecules & LIA-DIAMS, Station Biologique, BP 74, F-29682 Roscoff Cedex, France

Biological Adhesives
(ed. by A.M. Smith and J.A. Callow)

consolidate attachment through 'curing' reactions of adhesives, without knowing their basic components. However, some studies of the formation of adhesives in brown algal zygotes indicated that this mechanism shares common processes with the settlement of intertidal invertebrates such as the oxidase-mediated polymerisation of phenolic compounds (Vreeland et al. 1998).

This chapter summarizes recent work the results of which strengthen the hypothesis that brown algal phlorotannins could be one of the components of the bioadhesive system of brown algae and that vanadium-dependent haloperoxidase may regulate its curing process. It also highlights the recent development of genomic and genetic approaches in brown algae as an inspiring source of new research strategies to understand adhesion processes and to design biomimetic materials.

6.2 Adhesion of Brown Algal Propagules

Brown algae propagate mostly by sexual reproduction with at least swimming male gametes (antherozoids) and by motile spores. Female gametes may be either motile bi-flagellated cells or non-motile eggs in oogamous species (oospheres of the Fucales). The change from a motile to a permanently adhered spore, or the adhesion of a non-motile fertilized egg, is fundamental to the colonization of a new substratum.

6.2.1 Settlement and Attachment of Brown Algal Spores

In kelps, actively swimming spores can choose whether or not to settle and can terminate the settling process after contacting a surface (Reed et al. 1992). In contrast, *Ectocarpus siliculosus* spores do not seem to be attracted (either chemotactically or chemokinetically) nor stimulated to settle by nutrients (Amsler et al. 1999). Nevertheless they did settle differentially to substrates of different surface energy (hydrophobicity or wetability) with fourfold higher rates of settlement on hydrophobic surfaces compared to either positively- or negatively-charged hydrophilic surfaces (Amsler et al. 1999). *Hincksia irregularis* also settles at faster rates on hydrophobic surfaces (Greer and Amsler 2002, 2004; Greer et al. 2003) as do spores of ulvoid green algae (e.g., Callow and Callow 1998a,b, 2000; Ista et al. 2004 and see Chap. 4). Spores attach more readily to hydrophobic surfaces, probably because such a surface more readily allows the exclusion of water molecules from the adhesive/substratum interface (Maggs and Callow 2003, Chap. 4, this volume). However, consistent with most of published data that show that attachment strengths of a range of marine organisms to hydrophobic low-energy surfaces is weakened, most spores appear to be more easily removed from hydrophobic than hydrophilic surfaces. Motile flagellated spores of *E. siliculosus* were also shown to attach to substrata through a mechanism that involves the secretion of a fibrous

material from vesicles (Baker and Evans 1973). After settlement for 1–2 h, the attached cell develops a thin cell wall, but a thin cushion of a fibrillar material underlies the settled cells when viewed by TEM (transmission electron microscopy) (Baker and Evans 1973). The fibrillar nature of this adhesive material is questionable in the light of the recent results obtained with *Ulva* spores using Environmental Scanning EM whereby the adhesive appears as a gel-like material rather than the fibrillar appearance previously shown by TEM, suggesting that the latter may be an artefact of dehydration during specimen preparation (see Chap. 4 in this volume). When combined with cytochemical investigation, this study concluded that most of the *Ectocarpus* spore adhesive seems to be a polysaccharide (Baker and Evans 1973). While we have some information about spore settlement and attachment in brown algae, which allow comparisons with ulvoid spore adhesion processes (see Chap. 4 in this volume), the composition and physicochemical nature of adhesives used by brown algal spores and how they consolidate attachment through 'curing' reactions have been hardly investigated.

6.2.2 Adhesion of Fucoid Zygotes

Since earlier studies like those of Thuret and Bornet (1878) and Levring (1947), the rapid and firm attachment of the zygotes and embryos of fucoid brown algae has been mentioned and it was reinvestigated in the 1970s using scanning electron microscopy techniques (Moss 1981). The non-motile eggs of the Fucales are some of the largest reproductive cells to be found amount seaweeds. As soon as they are released they sink and, immediately after fertilization, the zygotes adhere to the substratum and select a growth axis according to environmental cues (Fig. 6.1). Indeed, fucoid algae exhibit an early developmental pattern in which zygotes generated from symmetric eggs undergo the formation–and eventual fixation–of a polar axis in response to external stimuli, including unilateral light (reviewed in Quatrano 1997; Brownlee et al. 2001). Fucoid zygotes develop cortical and cell surface asymmetries as polar development progresses (Fig. 6.1).

Surprisingly, in this extensively-investigated model, little attention has been paid to the origin and chemical composition of the sticky jelly that surrounds the entire zygote (Fig. 6.1). The chronology of cell adhesion, adhesive deposition, and polar growth axis selection induced by light (photopolarization) have been investigated with regard to zygotes of *Pelvetia fastigiata* (Schröter 1978) and *Silvetia compressa* (Hable and Kropf 1998), respectively. As proposed by Vreeland et al. (1993), the requirements for secreted compounds and the involvement of cytoskeleton in these processes were also confirmed by Hable and Kropf (1998). Adhesive deposition occurred in two distinct stages: a first uniform deposition took place on the outer surface of young zygotes (uniform primary adhesive), simultaneously with cell adhesion and photopolarization, and shortly thereafter an asymmetrical deposition (polar secondary adhesive) occurred at the future growth site of the

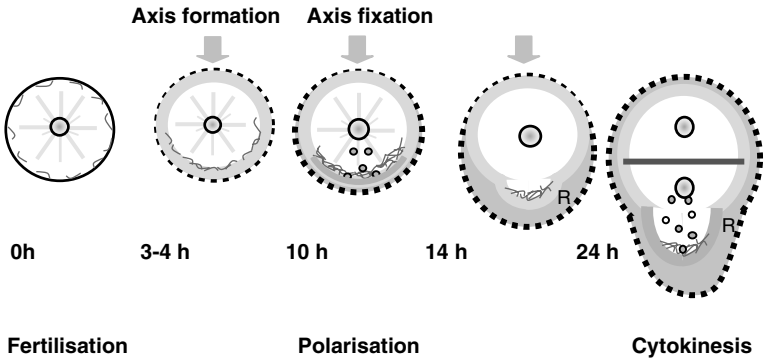

Fig. 6.1. Pattern of adhesive deposition during the early development of fucoid brown algae as revealed by non-fluorescent (Schröter 1978) or fluorescent microbeads (Hable and Kropf 1998) and imaging by light or confocal microscopy. At fertilization (0 h), no adhesive is present. It becomes visible at about 3 h after-fertilization (AF) as a thin layer of uniformly distributed adhesive. From 10 to 14 h AF, adhesive is apparent at both poles of the zygote, but is becoming thicker at the rhizoid pole (R). Cell wall is drawn in *dark line* and the *dotted line* symbolises the microspheres indicating the surface of the adhesive. Some of the key cytological events during the photopolarisation (*arrow*) and asymmetric division of the fucoid zygote are schematized, such as the localisation of actin microfilaments and the targeted secretion of Golgi at the future rhizoid pole

rhizoid cell. Associated with the formation of the polar axis is an asymmetric targeting of molecules, creating a localized accumulation of specific polypeptides (Wagner et al. 1992; Shaw and Quatrano 1996; Pu et al. 2000) and carbohydrates (Quatrano and Crayton 1973; Novotny and Forman 1974; Brawley and Quatrano 1979; Hable and Kropf 1998) at the cell surface prior to the visible morphological changes associated with asymmetric cell growth (Quatrano and Shaw 1997). Based on various cytological methods, it was proposed that some of the components of this jelly are alginate and fucan polysaccharides interacting with other macromolecules (Vreeland et al. 1998).

Following initial adhesion, algae may eventually become tightly bound to the substratum by a range of processes involving complex extracellular polymeric substances or extracellular matrix, including crosslinking mechanisms that have been proposed for diatoms and brown algae (Wang et al. 1996, 1997; Wustman et al. 1997; Vreeland et al. 1998).

A possible mechanism of adhesion, although not directly proved in brown algae, involves a vitronectin-like protein, a so-called Cell Adhesion Molecules (CAM) protein in mammalian adhesion processes (Felding-Habermann and Cheresh 1993). It has been shown that polyclonal antibodies against the human Vitronectin (Vn) recognized a vitronectin-like glycoprotein (Vn-F), exclusively secreted in the cell wall of an elongating rhizoid tip of the zygotes and embryos of *Fucus distichus*. It was also shown in an adhesive assay that, in the presence of the Vn-antibody, the rhizoid was unable to adhere to the

glass substratum, suggesting that the Vn-like glycoprotein might have a functional role in *F. distichus* adhesion (Wagner et al. 1992). If algal adhesion is promoted via a Vn-like glycoprotein, it displays similarities with focal adhesions in animal cells (Yamada and Miyamoto 1995). The heparin binding sequence of this molecule might also interact with the anionic polysaccharides in the adhesive material.

In another study on the adhesion of zygotes of *F. distichus*, it was shown that the primary adhesion was initially noncovalent in nature based on the loss of adhesive properties in high salt or with chelators (Vreeland and Laetsch 1990). Secondary adhesion is thought to involve a number of common processes, including a fiber-phenolic-catalyst mechanism that cross-links extracellular matrix components, including those of the above-mentioned focal adhesion complex (Vreeland et al. 1998). The model of phenolic cross-linking is strengthened by the accumulation of osmiophilic bodies that may contain phenolic compounds, at the site of rhizoid initiation in *Fucus* zygotes (Fig. 6.1).

6.3 Secretion of Brown Algal Phenolics and Adhesion

Brown algal phenolics (Fig. 6.2) are structural analogues of terrestrial condensed tannins. These so-called phlorotannins are known only from brown algae (Phaeophyceae) and are present at detectable concentrations across almost all brown algal orders. Soluble phenolics can constitute up to 25% dry weight (e.g., Targett et al. 1992; van Alstyne et al. 1999). These tannins are acetate-malonate derived polymers of phloroglucinol (1,3,5-trihydroxybenzene). Their chemical structure which is based on aryl-aryl and/or diaryl ether linkages of phloroglucinol units is rather complex and polymerisation processes lead to a wide range of molecular sizes (126 Da to 650 kDa). Depending on the nature of the structural linkages binding the phlorotannin polymers and on the number of hydroxyl groups present, six major groups of structure-based motifs have been defined: fucols, phlorethols, fucophlorethols, fuhalols, isofuhalols and eckols (Ragan and Glombitza 1986). These specific groups are often characteristic of specific algal genera, for example, fucols in *Fucus* and eckols in *Ecklonia*. Phenolic compounds represent about 7–9% of the dry weight of *Fucus* young stages. They are mainly formed of four to seven phloroglucinol units, primarily ether linked with a maximum of three phenyl units per oligomer (Ragan and Glombitza 1986). Branching occurs in about 25% with a degree of polymerization of greater than 100 units. The most striking feature of the polymer in Fucales is that most of the branches terminate with a bi-hydroxyl or tri-hydroxyl phenol group, which could contribute both to the potential oxidative cross-linking of the polymer and to the adhesive properties of the polymer by the ability to replace water at the interface (Waite 1987). It is suggested that they play multiple ecological roles, such as

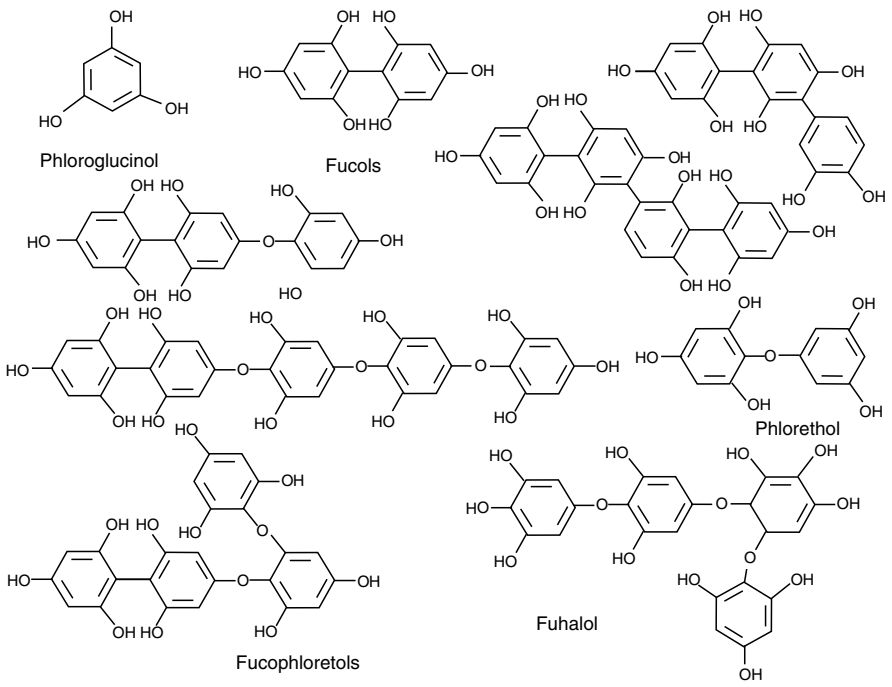

Fig. 6.2. Chemical structure of the main encountered phloroglucinol-based polyphenols in brown algae. Fucols: phloroglucinol units linked through aryl-aryl bonds, occurring in Fucales and in Ectocarpales; Fucophloretols: dehydrooligomers of phloroglucinol which contain both direct carbon-carbon and diaryl ether bond, occurring primarily in Fucales and sporadically in Laminariales. Phlorethols: phloroglucinol units linked through diaryl ether bonds, occurring both in Fucales and Laminariales. Fuhalols: ether-linked phloroglucinol linked through para and ortho ether bonds with an extra hydroxyl group on one unit, occurring primarily in Fucales

antifouling substances and chemical defences against grazers (Arnold and Targett 2002).

Phlorotannins are stored in cell organelles, the so-called physodes, which are round to elliptical, highly mobile, vesicle-like, strongly refractive bodies, observed in the cytoplasm of brown algae (Ragan and Glombitza 1986; Schoenwaelder 2002). Once they have crossed the cell membrane, phenolic bodies break up, presumably because they are no longer bound to the cell membrane, and small particles of phenolic material become embedded in the zygote cell wall. Physodes accumulate at the zygote periphery early in development and are secreted into the primary zygote wall. During germination, physodes accumulate at the rhizoid tip. Phenolic compounds are also involved in the formation of the cell plate and cross-walls of *Hormosira* and *Acrocarpia* (Schoenwaelder and Clayton 1998a) and also in several species of *Fucus* (Schoenwaelder and Wiencke 2000).

It has also been shown in *Fucus* zygotes that the secretion of phenolic polymers correlate with the attachment process (Vreeland and Epstein 1996). The secretion starts a few hours after egg fertilization. Later, after germination, phenolic polymer secretion is localized at the site of attachment. The osmiophilic bodies likely accumulate at the site of rhizoid initiation and one antibody to alginate gelling subunit was shown to label phenolic vesicles, as well as Golgi vesicles in *Fucus* zygotes (Vreeland and Laetsch 1990).

6.4 Curing Mechanisms Involving Brown Algal Vanadium Peroxidases

A model of oxidative cross-linking of secreted phenolics (Fig. 6.3) mediated via the catalysis of a vanadium bromoperoxidase was proposed based on some indirect evidences, such as vHPO immunolocalization in adherent cells

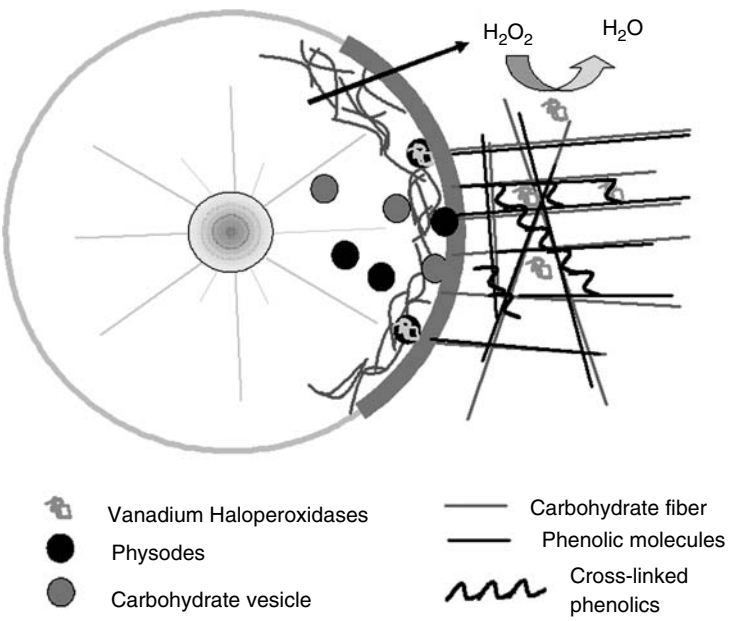

Fig. 6.3. A hypothetical model of adhesive deposition and phlorotannin crosslinks in the adhesive jelly surrounding the cell wall of fucoid zygote at the future rhizoid pole (adapted from Vreeland et al. 1998). This model is not based on the direct testing of cross-links formation, nor on studies of microstructure. It is deduced from the observation of fibrillar material at the site of adhesive deposition in fucoid zygotes by Scanning Electron Microscopy. It takes into account the secretion of phenolic-rich and carbohydrate-containing vesicles and the extracellular location of vanadium haloperoxidases in brown algae. The steady-state release of H_20_2, which is continuously produced during the early development of *Fucus* zygotes and embryos is indicated

of several brown algae (Vreeland and Laetsch 1990; Vreeland and Epstein 1996). Indeed most of our current knowledge is based on this review paper by Vreeland et al. (1998) and on the information displayed in a US Patent (Vreeland and Grotkopp 1996). Simple aggregation experiments were shown, but no details were given on the cross-linking processes.

6.4.1 Brown Algal Vanadium-dependent Haloperoxidase

The first vanadium-dependant haloperoxidase (vHPO) was discovered in *Ascophyllum nodosum*, a brown alga belonging to the Fucales (Vilter 1984). Whereas vHPO activities have been detected in a very large number of the classes of the Phaeophyceae (for a review see Vilter 1995), very few data were available on their biochemical properties notably because of the difficulties in purifying such enzymes from algal matrices extremely rich in anionic polysaccharides and polyphenolic compounds. The improvement of an aqueous two-phase extraction protocol by Jordan and Vilter (1991) for Laminariales, later extended to Fucales (Vilter 1994), allowed the acquisition of biochemical data on some partially- or fully-purified enzymes. At the molecular level, only five cDNAs of vHPOs have been cloned in the three species *A. nodosum*, *F. distichus* and *Laminaria digitata* (Table 6.1).

Haloperoxidases catalyze, in the presence of hydrogen peroxide, the oxidation of halides (X^-: iodide, bromide or chloride) to their corresponding hypohalous acids or a related electron oxidized halogenating intermediate such as OX^-, X_3^- and X^+. A variety of halocarbons can subsequently be generated if the appropriate nucleophilic acceptors are present (for review see Butler and Carter-Franklin 2004). They are named according to the most electronegative halide that they can oxidize: chloroperoxidases can catalyze the oxidation of chloride as well as of bromide and iodide, bromoperoxidases (BPO) react with bromide and iodide, whereas iodoperoxidases (IPO) are specific for iodide. Because of these halogenating properties, extensive research has been conducted on *A. nodosum* vBPO, which has become a laboratory model for understanding catalytic mechanisms of vHPOs (Butler and Carter-Franklin 2004). Its crystal 3D structure has been resolved from native enzyme preparation (Weyand et al. 1999) and compared to those of the vCPO from the fungus *Curvularia inaequalis* and of the vBPO from the red algae *Corallina*, whereas the complete catalytic cycle is still uncertain and the origin of halide selectivity remains one of the unanswered question regarding these enzymes (For reviews see Littlechild and Garcia-Rodriguez 2003; Butler and Carter-Franklin 2004). Very recently, new post-translational bromination and iodination of tyrosine residues of *A. nodosum* vBPO have also been reported (Feiters et al. 2005).

Laminaria digitata features two distinct vanadium-dependent haloperoxidase gene families (Colin et al. 2003, 2005). Iodoperoxidases could be involved in the highly efficient mechanism of iodine accumulation in kelps (Küpper

Table 6.1. Biochemically-characterized vanadium-haloperoxidases in Phaeophyceae

Classification[a]	Species	Activity	References
Order: Fucales	*Ascophyllum nodosum*[b]	vBPO	Vilter (1984); Krenn et al. (1989); Weyand et al. (1999)
	Fucus distichus[c]	vBPO	Soedjak and Butler (1990, 1991); Vreeland et al.[d]
	Pelvetia canaliculata	vIPO	Almeida et al. (2000)
Order: Laminariales	*Macrocystis pyrifera*	vBPO	Soedjak and Butler (1990, 1991)
	Ecklonia stolonifera	vBPO	Hara and Sakurai (1998)
	Laminaria saccharina	vBPO	De Boer et al. (1986); Almeida et al. (2001)
	Laminaria hyperborea	vBPO and vIPO	Almeida et al. (2001)
	Laminaria ochroleuca	vIPO	Almeida et al. (2001)
	Laminaria digitata[c]	vBPO and vIPO	Colin et al. (2003, 2005)
Family: Phyllariaceae	*Phyllariopsis brevipes*	vIPO	Almeida et al. (1996)
	Saccorhiza polyschides	vIPO	Almeida et al. (1998)

vBPO: vanadium-bromoperoxidase; vIPO: vanadium-iodoperoxidase
[a] According to Draisma et al. (2003)
[b] Resolution of the crystal structure from the native protein
[c] Characterization at the molecular level with full-length cDNAs available
[d] Vreeland V, Ng K, Epstein L (unpubl.), GenBank accession no. AF053411

et al. 1998; Colin et al. 2003). The vBPOs form a large multigenic family, whose members should have evolved towards specialized functions such as halocarbon production in relationships with algal chemical defense (Potin et al. 2002) or oxidative detoxification, as seen in protoplasts (Roeder et al. 2005). In the context of cross-linking events, these enzymes should also take part in cell wall assembly during regeneration of protoplasts (Roeder et al. 2005).

6.4.2 *In vitro* Investigations of Haloperoxidase-mediated Oxidative Cross-linking

In fact, vBPO was proven to be involved in the cross-linking of brown algal phlorotannins only very recently (Berglin et al. 2004). Phlorotannins were adsorbed to a quartz crystal sensor and the cross-linking was initiated by the addition of vBPO, KBr and H_2O_2. The decreased dissipation upon addition of the cross-linking agents, as measured with the quartz crystal microbalance

with dissipation monitoring (QCM-D) method, was interpreted as intramolecular cross-links formed between different phloroglucinol units in the phlorotannins. With surface plasmon resonance (SPR) it was shown that no desorption occurred from the sensor surface during the cross-linking. UV/Vis spectroscopy verified the results achieved with QCM-D that all components, i.e. vBPO, KBr and H_2O_2, was necessary in order to achieve intramolecular in vitro oxidative cross-linking of the polymers.

In the light of the recent report that iron is the key reagent in protein cross-linking for mussel adhesive synthesis (Sever et al. 2004), it will be interesting to question the prevalence of this theme of protein-transition metal interactions in marine biomaterials such as those of coral reef structures, kelp adhesives, and barnacle cements. In none of these systems, however, is there available a detailed picture of the bonding schemes employed for material construction. Assuming that the oxidative cross-linking of phlorotannins shares common mechanisms with the bonding of plant phenolics, it may involves a one-electron oxidation and subsequent deprotonation (Oudgenoeg et al. 2002). The formed phenoxyl radical species can combine with other radical species to produce a covalent cross-link (Gross and Sizer 1959). This putative mechanism may also be catalyzed by transition metals in brown algae. Alternatively, considering that the dimerization and rearrangement or fragmentation of phenoxyls is stimulated if the phenols were substituted with a halogen (Eickhoff et al. 2001), a speculative cross-linking mechanism could thus start with the bromination of the phenols (as has been suggested as the main task for vBPO), followed by the oxidation and condensation, and finally, the rearrangement and release of HOBr. Based on the occurrence of halogenated phlorotannins in brown algae, while in low abundance (Ragan and Glombitza 1986), the involvement of a vBPO in the catalysis of phenolic cross-linking is our favourite hypothesis. The occurrence of a transition metal-catalyzed oxidation may eventually lead to the degradation of alginate polymers by generating the Fenton reaction and to the subsequent loosening of attachment (Larsen and Smisrod 1967).

Shear-lap tests have shown that oxidation of the polyphenol is important for the formation of contact points with the surface, thus improving the adhesion strength of the glue (Bitton et al. 2006). However, hardening with alginate and/or calcium is essential for high cohesive strength. Further insight into the spatial arrangement of the glue was obtained from small angle X-ray scattering, light scattering and cryo-Transmission Electron Microscopy (Bitton et al. 2006). The phenolic polymer rearranges and forms flexible chain-like objects. This structure does not change upon oxidation, addition of calcium ions or alginate. However, once the alginate is cross-linked with calcium ions, a rigid network is formed (Fig. 6.4). Presumably this network is responsible for the cohesive strength of the glue. When coupled with results showing that vBPO brings about curing of adhesive extracts more than other catalysts, these data implicate vBPO to be the key reagent in controlling the cross-linking of phenolic polymers for the assembly of brown algal adhesives.

6.4.3 Requirement for an Efficient Oxidation Mechanism *In Situ*

As discussed above, cross-linking of the water-soluble adhesive polymers must take place rapidly or they will be washed away from the site of action. At the interface, all the catalysts of the reaction have therefore to be secreted simultaneously with the phenolic and polysaccharide polymers or already present in the seawater.

In *L. digitata* vBPO, the presence of peptide signal sequences suggested an exportation of the proteins in the cell wall (Colin et al. 2003) and some vBPO were effectively reported to be extracellular in giant kelps (Butler et al. 1990; Jordan et al. 1991). Moreover, in Fucales, an isoenzyme has been more precisely located in the cell wall of surface cells (Krenn et al. 1989). Thus, our observations support a role for haloperoxidase in the differentiation of *Fucus* embryo by cell wall cross-linking. Abnormal localization or excess of

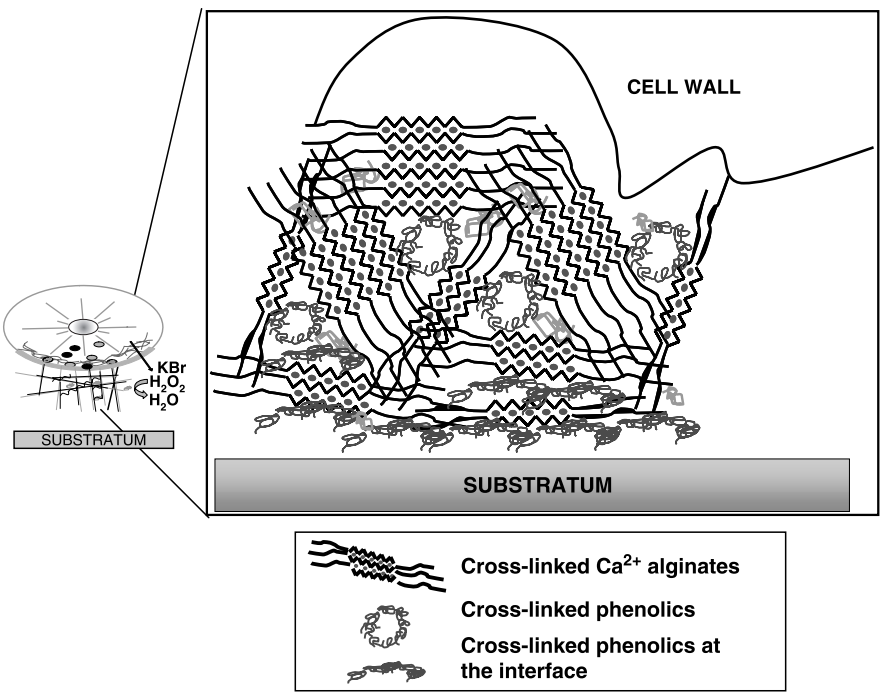

Fig. 6.4. A speculative hypothetical model of spatial arrangement of the deposition of brown algal adhesives at the level of a single vesicle discharged into the extracellular medium. This magnification of a localized region from the model displayed in Fig. 6.3 takes into account the embedding of oxidized phlorotannins in a calcium alginate gel network as deduced from the investigation of microstructure (Bitton et al. 2005) and of surface cross-linking measurements (Berglin et al. 2004). Cross-linked phenolic polymer forms flexible chain-like objects which might form micelles or globular aggregates in aqueous media. We postulate that at the interface with the substratum, these aggregates tend to exclude water and might squash to the surface

exogenous vBPO activity result in preventing cell wall expansion and tip growth initiation (Potin et al., unpubl. res.). The same pattern of abnormal morphogenesis was previously reported in co-cultures of the fucoid alga *A. nodosum* and spores of its endophytic fungus *Mycosphaerella ascophyllii* (Garbary and McDonald 1995). This associated fungus possesses a vanadium-haloperoxidase, which might interfere with normal cross-linking of *A. nodosum* zygote cell walls and prevents wall expansion and consecutive rhizoid emission. In accordance with this precise control of wall assembly by vBPO in *Fucus*, preliminary molecular data have shown a specific expression of a vBPO gene during the first hours after fertilization (Delage et al., unpubl. res.).

Cross-linking of cell wall material by the catalysis of haloperoxidase also requires halogen and H_2O_2. Assuming that the concentrations of halides in the cell wall at the surface of the thallus are close from those found in seawater, the level of bromide (3 mmol/l) should be quite sufficient for the enzymatic reaction, whereas iodide concentration could be limiting (around 0.25 µmol/l) (Saenko et al. 1978). In *Fucus*, we have shown that, during normal embryogenesis, zygotes constitutively secrete H_2O_2 in the extracellular medium (Potin et al., unpubl. res.). This oxidative response was previously reported as an increase in O_2 consumption following fertilization of *Fucus* eggs (Whitaker 1931). Contrarily to the redox changes occurring during fertilization of some marine invertebrates eggs (Schomer and Epel 1998), this ROS (Reactive Oxygen Species) production is not transient but persists for at least 24 h, and then seems to decrease, concomitantly with the elongation of the rhizoid. This steady-state H_2O_2 emission may likewise be under developmental control.

As already mentioned, phenolic compounds are released into the wall of fucoid brown algae from the time of fertilization (Schoenwaelder and Clayton 1998a,b) and then, in *Fucus* zygotes, all the components of the glue are secreted simultaneously under developmental control to permit the efficient attachment of the cells.

6.5 Industrial Potential of Brown Algal Adhesives

The constraints to make an adhesive that can form bonds to a variety of substrates in wet and in high ionic strength environments have led to considerable research in diverse marine organisms (Deming 1999). To date, the mussel adhesive has been most mimicked and several papers investigating such adhesives have been published (Deming 1999; Kitamura et al. 1999; Ninan et al. 2003; Tatehata et al. 2000, 2001; Yamamoto et al. 1995, 2000). The major drawback with the extraction of adhesive proteins directly from the mussel is the cumbersome procedure and the low yield of material. Until recently, the post-translational modification of tyrosine to L-DOPA was con-

sidered as a major challenge affecting the production of recombinant functional adhesive proteins. However, the successful expression in *E. coli* and subsequent modification of two functional mfp5 and mfp3 peptides was recently reported (Hwang et al. 2004, 2005). Therefore synthetic routes to produce peptide mimics are no longer the only alternative for producing mussel adhesives (Statz et al. 2005).

However, alternative marine sources of extracted material with different adhesive properties are suitable. Seaweeds are harvested or maricultured in large quantities and are used as raw material in colloid industry. Therefore, by-products of the seaweed industry are rich in phenolic polymers, inspiring new uses for algae.

Adhesives constitute an important component in the manufacture of a wide array of products derived from the forest industry. At present, most of these adhesives are based on synthetic phenolic compounds cross-linked using toxic catalysts such as formaldehyde. In recent decades, various political, economical and environmental concerns have caused the supply of wood adhesives to decrease dramatically from time to time, producing a concomitant marked increase in price. This situation has led to recognition of the importance of research on alternative sources of starting materials for the production of wood adhesives (Umemura et al. 2003). In general, the materials chosen for study as alternative sources of adhesives feedstock are structurally similar to materials already used for this purpose. For example, tannins and lignins have been studied as replacements for phenol in phenol-formaldehyde adhesives because they contain phenolic moieties within their chemical structures. However, chemical reactivity is dependent in very subtle ways on the chemical structure of a given compounds. Chitosan/phenolics systems were investigated as wood adhesives (Yamada et al. 2000). Adhesion between two pieces of wood veneer developed only when all three components chitosan, a phenolic compound, and laccase (or tyrosinase) were present. The adhesion mechanisms of these chitosan/phenolics systems were proposed to be similar to those of mussel adhesive proteins (Yamada et al. 2000; Peshkova and Li 2003).

When using algal phenolics as adhesives, an industrial catalysis process would require large amounts of enzymes. Similarly, with the mussel adhesive proteins it will require massive production of recombinant enzymes. The heterologous overexpressions have been developed for the vHPO of the fungus *C. inaequalis* (Hemrika et al. 1999) and of the red algae *Corallina* (Carter et al. 2002; Ohshiro et al. 2002). For brown algae, the recombinant expression of an active 198 amino-acid polypeptide derived from *Fucus* vBPO has been described in an international patent (Vreeland 2002). It has already often been reported that the ability of vHPOs to halogenate a broad range of organic compounds of both pharmaceutical and commercial interest as well as their high stability towards high temperatures, oxidative conditions and the presence of organic solvents make them good candidates for use in industrial biotransformations (Littlechild 1999; Dembitsky 2003; Butler and Carter-Franklin 2004). However, given their role in oxidative cross-linking,

they should also be included as strong catalysts in the composition of synthetic polyphenolic adhesives. Another potential application of these enzymes is the development of anti-biofouling processes, which is economically important (Callow and Callow 2002). As seen above, incorporation of vHPO in a product intended for under-seawater uses should prevent the attachment of zygotes thus preventing the growth of brown algae on surfaces.

6.6 Conclusions and Future Prospects

Recent phylogenetic analyses of the eukaryotes have shown that brown algae belong to an independent lineage (Heterokonta) that diverged about one billion years ago during the eukaryotic crown radiation (Baldauf 2003). Phaeophyceae (brown algae) belong in the same lineage as Bacillariophyceae (diatoms) and oomycetes. They are thought to have arisen from a secondary endosymbiosis between a plastid-less protist and an ancestral unicellular red alga. Both Phaeophyceae and oomycetes form the same type of flagellate zoospores displaying the characteristic heterokont paired flagella, one of which is short and smooth and points backwards when swimming, the other being forward-pointing, long and tinsel-like (Maggs and Callow 2003).

Worth noting is that bromide is required for the stalk assembly and the adhesion of the diatom *Achnanthes longipes,* and it could be that haloperoxidases are components in the oxidative cross-linking (Johnson et al. 1995; Wustman et al. 1997). Bromoperoxidase activity was characterized in *Nitzschia* sp., but as a heme-containing enzyme (Moore et al. 1996). Indeed, recent molecular data from the complete genome of *Thalassiosira pseudonana* and EST from *Phaeodactylum tricornutum* do not reveal the presence of vHPO homologues in these two diatom species. Vreeland et al. (1998) also suggested that haloperoxidase-mediated polyphenol-carbohydrate glues could be involved in adhesion of red and green algae. If in *Corallina* red algae, vBPO have been characterized (Shimonishi et al. 1998; Isupov et al. 2000; Ohshiro et al. 2002; Carter et al. 2002), no vHPO activity has been clearly identified in chlorophytes. Adhesion mechanisms are not likely to be conserved processes in the different algal lineages (see Chaps. 4 and 5 in this volume dealing with the chlorophyte *Ulva* and diatoms).

Inside the brown algal phylum, genomic approaches on the newly-established genetic model, *E. siliculosus*, revealed some vHPO homologues in preliminary EST data (Cock et al., pers. comm.). This genetic model could therefore be used to validate the role of vHPO in oxidative cross-linking, using complementary approaches, such as specific invalidation of vHPO genes using RNA interference or general screening of mutants deficient in adhesion processes. Cell adhesion is a criterion of choice to differentiate *E. siliculosus* sporophyte from gametophyte, as the latter floats while the former is attached to the substratum in Petri dishes. A global screen could be con-

ducted on the *Ectocarpus* mutagenised gametes population to examine germination for unattached sporophyte filaments. In these adhesion-deficient mutants, the pattern of vHPO activities, halogen, phenolics and alginate compositions should be modified in comparison with wild type sporophytes. This should allow the identification of new key-actors of the processes involved in biosynthesis and assembly of phlorotannins. They are thought to arise from the condensation of acetate and malonate units via a polyketide synthase enzyme complex although, to date, no such complex has been described in brown algae (Arnold and Targett 2002). It might also point out the key role of vBPO in the control of the oxidative condensation of phlorotannins.

Integrating the data obtained from surface chemistry, physico-chemistry and of knock-down experiments appear to be a necessary strategy to be able one day to elucidate the molecular regulation of cross-linking mechanisms in brown algae.

Acknowledgments. We are grateful to the colleagues of our research group (Ludovic Delage, Carole Colin and Stéphane Labarre) and of the Algal Bioadhesives consortium for stimulating exchanges, and particularly to Mattias Berglin and Havazelet Bianco-Peled, who contributed most of the ideas that gave rise to the hypotheses for mechanisms and to the design of a model for the spatial arrangement of the brown algal phenolic-based adhesives. We also warmly thank Michael Friedlander and Jim Callow for introducing us in the field of algal adhesives. The financial supports by the European Commission "GROWTH" program, Research project; Algal Bioadhesives, Grant G5RD-CT-2001-00542 and CNRS are gratefully acknowledged.

References

Almeida M, Humanes M, Silva JA, Melo R, Frausto da Silva JJR (1996) *Phyllariopsis brevipes* -a brown algae with vanadium-dependent iodoperoxidases. In: Obinger C, Burner U, Ebermann R, Penel C, Greppin H (eds) Plant peroxidases: biochemistry and physiology. University of Geneve, Geneve, pp 146–152

Almeida M, Humanes M, Melo R, Silva JA, Frausto da Silva JJR, Vilter H, Wever R. (1998) *Saccorhiza polyschides* (Phaeophyceae; Phyllariaceae) a new source for vanadium-dependent haloperoxidases. Phytochemistry 48:229–239

Almeida M, Humanes M, Melo R, Silva JA, Frausto da Silva JJR, Wever R (2000) Purification and characterisation of vanadium haloperoxidases from the brown alga *Pelvetia canaliculata*. Phytochemistry 54:5–11

Almeida M, Filipe S, Humanes M, Maia MF, Melo R, Severino N, da Silva JAL, Frausto da Silva, JJR, Wever R (2001) Vanadium haloperoxidases from brown algae of the Laminariaceae family. Phytochemistry 57:633–642

Amsler CD, Shelton KL, Britton CJ, Spencer NY, Greer GP (1999) Nutrients do not influence swimming behavior or settlement rates of *Ectocarpus siliculosus* (Phaeophyceae) spores. J Phycol 35:239–244

Arnold TM, Targett NM (2002) Marine tannins: the importance of a mechanistic framework for predicting ecological roles. J Chem Ecol 28:1919–1934

Baker JR, Evans LV (1973) The ship fouling alga *Ectocarpus*. I. Ultrastructure and cytochemistry of plurilocular stages. Protoplasma 77:1–13

Baldauf SL (2003) The deep roots of eukaryotes. Science 300:1703–1706

Berglin M, Delage L, Potin P, Vilter H, Elwing H (2004) Enzymatic cross-linking of a phenolic polymer extracted from the marine alga *Fucus serratus*. Biomacromolecules 5:2376–2383
Bitton R, Ben-Yehuda M, Davidovich M, Balazs Y, Colin C, Delage L, Potin P, Bianco-Peled H (2005) Properties of algal-born phenolic adhesives. Biomacromolecules (submitted)
Brawley SH, Quatrano RS (1979) Sulfation of fucoidin in *Fucus* embryos. IV. Autoradiographic investigations of fucoidin sulfation and secretion during differentiation and the effect of cytochalasin treatment. Dev Biol 73:193–205
Brownlee C, Bouget F-Y, Corellou F (2001) Choosing sides: establishment of polarity in zygotes of fucoid algae. Semin Cell Dev Biol 12:345–351
Butler A, Carter-Franklin JN (2004) The role of vanadium bromoperoxidase in the biosynthesis of halogenated marine natural products. Nat Prod Rep 21:180–188
Butler A, Soedjak HS, Polne-Fuller M, Gibor A, Boyen C, Kloareg B (1990) Studies of vanadium-bromoperoxidase using surface and cortical protoplasts of *Macrocystis pyrifera* (Phaeophyta). J Phycol 26:589–592
Callow ME, Callow JA (1998a) Attachment of zoospores of the fouling alga *Enteromorpha* in the presence of zosteric acid. Biofouling 13:87–95
Callow ME, Callow JA (1998b) Enhanced adhesion and chemoattraction of zoospores of the fouling alga *Enteromorpha* to some foul-release silicone elastomers. Biofouling 13:157–172
Callow ME, Callow JA (2000) Substratum location and zoospore behaviour in the fouling alga *Enteromorpha*. Biofouling 15:49–56
Callow ME, Callow JA (2002) Marine biofouling: a sticky problem. Biologist 49:10–14
Carter JN, Beatty KE, Simpson MT, Butler A (2002) Reactivity of recombinant and mutant vanadium bromoperoxidase from the red alga *Corallina officinalis*. J Inorg Biochem 91:59–69
Chamberlain AHL (1976) Algal settlement and secretion of adhesive materials. Proc Int Biodegrad Symp 3:417–432
Colin C, Leblanc C, Wagner E, Delage L, Leize-Wagner E, van Dorsselaer A, Kloareg B, Potin P (2003) The brown algal kelp *Laminaria digitata* features distinct bromoperoxidase and iodoperoxidase activities. J Biol Chem 278:23545–23552
Colin C, Leblanc C, Michel G, Wagner E, Leize-Wagner E, van Dorsselaer A, Potin, P (2005) Vanadium-dependent iodoperoxidases in *Laminaria digitata*, a novel biochemical function diverging from brown algal bromoperoxidases. J Biol Inorg Chem 10:156–166
De Boer E, Tromp MGM, Plat H, Kreen BE, Wever R (1986) Vanadium(V) as an essential element for haloperoxidase activity in marine brown algae: purification and characterization of a vanadium(V)-containing bromoperoxidase from *Laminaria saccharina*. Biochem Biophys Acta 872:104–115
Dembitsky VM (2003) Oxidation, epoxidation and sulfoxidation reactions catalysed by haloperoxidases. *Tetrahedron* 59:4701–4720
Deming TJ (1999) Mussel byssus and biomolecular materials. Curr Opin Chem Biol 3:100–105
Draisma SGA, Peters AF, Fletcher RL (2003) Evolution and taxonomy in the Phaeophyceae: effects of the molecular age on brown algal systematics. In: Norton TA (ed) Out of the past. Collected Reviews to Celebrate the Jubilee of the British Phycological Society. British Phycological Society, Belfast, pp 87–102
Eickhoff H, Jung G, Rieker A (2001) Oxidative phenol coupling -tyrosine dimers and libraries containing tyrosyl peptide dimers. Tetrahedron 57:353–364
Feiters MC, Leblanc C, Küpper FC, Meyer-Klaucke W, Michel G, Potin P (2005) Bromine is an endogenous component of a vanadium bromoperoxidase. J Am Chem Soc 127:15340–15341
Felding-Habermann B, Cheresh DA (1993) Vitronectin and its receptors. Curr Opin Cell Biol 5:864–868
Fletcher RL, Baier RE (1984) Influence of surface energy on the development of the green alga *Enteromorpha*. Mar Biol Lett 5:251–254
Fletcher RL, Callow ME (1992) The settlement, attachment and establishment of marine algal spores. Br J Phycol 27:303–329
Garbary DJ, McDonald KA (1995) The *Ascophyllum/ Polysiphonia/ Mycosphaerella* symbiosis IV. Mutualism in the *Ascophyllum/Mycosphaerella* interaction. Bot Mar 38:221–225

Gonzalez MA, Goff LJ (1989) The red algal epiphytes *Microcladia coulterii* and *M. californica* (Rhodophyceae, Ceramicaceae). II. Basiphyte specificity. J Phycol 25:558–567

Greer SP, Amsler CD (2002) Light boundaries and the coupled effects of surface hydrophobicity and light on spore settlement in the brown alga *Hincksia irregularis* (Phaeophyceae). J Phycol 38:116–124

Greer SP, Amsler CD (2004) Clonal variation in phototaxis and settlement behaviors of *Hincksia irregularis* (Phaeophyceae) spores. J Phycol 40:44–53

Greer SP, Iken KB, McClintock JB, Amsler CD (2003) Individual and coupled effects of echinoderm extracts and surface hydrophobicity on spore settlement and germination in the brown alga *Hincksia irregularis*. Biofouling 19:315–326

Gross AJ, Sizer IW (1959) The oxidation of tyramine, tyrosine and related compounds by peroxidase. J Biol Chem 234:1611–1614

Hable WE, Kropf DL (1998) Roles of secretion and the cytoskeleton in cell adhesion and polarity establishment in Pelvetia compressa zygotes. Dev Biol 198:45–56

Hara I, Sakurai T (1998) Isolation and characterization of vanadium bromoperoxidase from a marine macroalga, *Ecklonia stolonifera*. J Inorg Biochem 72:23–28

Hemrika W, Renirie R, Macedo-Ribeiro S, Messerschmidt A, Wever R (1999) Heterologous expression of the vanadium-containing chloroperoxidase from *Curvularia inaequalis* in *Saccharomyces cerevisiae* and site-directed mutagenesis of the active site residues His(496), Lys(353), Arg(360), and Arg(490). J Biol Chem 274:23820–23827

Higgins MJ, Crawford SA, Mulvaney P, Wetherbee R (2002) Characterization of the adhesive mucilages secreted by live diatom cells using atomic force microscopy. Protist 153:25–38

Hwang DS, Yoo HJ, Jun JH, Moon WK, Cha HJ (2004) Expression of functional recombinant mussel adhesive protein Mgfp-5 in *Escherichia coli*. Appl Environ Microbiol 70:3352–3359

Hwang DS, Gim Y, Cha HJ (2005) Expression of functional recombinant mussel adhesive protein type 3A in *Escherichia coli*. Biotechnol Prog 21:965–970

Ista LK, Callow ME, Finlay JA, Coleman SE, Nolasco AC, Simons RH, Callow JA, Lopez GP (2004) Effect of substratum surface chemistry and surface energy on attachment of marine bacteria and algal spores. Appl Environ Microbiol 70:4151–4157

Isupov MN, Dalby AR, Brindley AA, Izumi Y, Tanabe T, Murshudov GN, Littlechild JA (2000) Crystal structure of dodecameric vanadium-dependent bromoperoxidase from the red alga *Corallina officinalis*. J Mol Biol 299:1035–1049

Johnson LM, Hoagland KD, Gretz MR (1995) Effects of bromide and iodide on stalk secretion in the biofouling diatom *Achnanthes longipes* (Bacillariophyceae). J Phycol 31: 401–412

Jordan P, Vilter H (1991) extraction of proteins from material rich in anionic mucilages: partition and fractionation of vanadate-dependent bromoperoxidases from the brown algae *Laminaria digitata* and *L. saccharina* in aqueous polymer two-phases systems. Biochem Biophys Acta 1073:98–106

Jordan P, Kloareg B, Vilter H (1991) Detection of vanadate-dependent bromoperoxidases in protoplasts from the brown algae *Laminaria digitata* and *L. saccharina*. J Plant Physiol 137:520–524

Kitamura M, Kawakami K, Nakamura N, Tsumoto K, Uchiyama H, Ueda Y, Kumagai I, Nakaya T. (1999) Expression of a model peptide of a marine mussel adhesive protein in Escherichia coli and characterization of its structural and functional properties. J Polym Sci Pol Chem 37:729–736

Krenn BE, Tromp MGM Wever R (1989) The brown alga *Ascophyllum nodosum* contains two different vanadium bromoperoxidases. J Biol Chem 32:19287–19292

Küpper FC, Schweigert N, Ar Gall E, Legendre J-M, Vilter H, Kloareg B (1998) Iodine uptake in Laminariales involves extracellular, haloperoxidase-mediated oxidation of iodide. Planta 207:163–171

Larsen B, Smisrod O (1967) The effect of pH and buffer ions on the degradation of carbohydrates by Fenton's reagent. Acta Chem Scand 21:552–564

Levring T (1947) Remarks on the surface layers and the formation of the fertilization membrane in *Fucus* eggs. Göteborg's K. Vetenskaps-Vitterhets-samhäll Handl XVII:97–105
Lind JL, Heimann K, Miller AA, van Vliet C, Hoogenraad NJ, Whetherbee R (1997) Substratum adhesion and gliding in a diatom are mediated by extracellular proteoglycans. Planta 203:213–221
Littlechild JA (1999) Haloperoxidases and their role in biotransformation reactions. Curr Opin Chem Biol 3:28–34
Littlechild JA, Garcia-Rodriguez E (2003) Structural studies on the dodecameric vanadium bromoperoxidase from Corallina species. Coord Chem Rev 237:65–76
Maggs CA, Callow ME (2003) Algal Spores. Encyclopedia of life sciences. Nature Publishing Group, London, version 1.0, pp 1–6
Moore RM, Webb M, Tokarczyk R (1996) Bromoperoxidase and iodoperoxidase enzymes and production of halogenated methanes in marine diatom cultures. J Geophys Res 101:20899–20908
Moss B (1981) Attaching mechanisms of zygotes and embryos of the Fucales. Proc Int Seaweed Symp 8:117–124
Ninan L, Monahan J, Stroshine RL, Wilker JJ, Shi RY (2003) Adhesive strength of marine mussel extracts on porcine skin. Biomaterials 24:4091–4099
Novotny AM, Forman M (1974) The relationship between changes in cell wall composition and the establishment of polarity in *Fucus* embryos. Dev Biol 40:162–173
Ohshiro T, Hemrika W, Aibara T, Wever R, Izumi Y (2002) Expression of the vanadium-dependent bromoperoxidase gene from a marine macro-alga *Corallina pilulifera* in *Saccharomyces cerevisiae* and characterization of the recombinant enzyme. Phytochemistry 60:595–601
Oudgenoeg G, Dirksen E, Ingeman S, Hilhorst R, Gruppen HCGB, Persma SR, van Berkel WJH, Laan C, Voragen AGJ (2002) Horseradish peroxidase-catalyzed oligomerization of ferulic acid on a template of a tyrosine-containing tripeptide. J Biol Chem 277:21332–22134
Peshkova S, Li K (2003) Investigation of chitosan-phenolics systems as wood adhesives. J Biotechnol 102:199–207
Potin P, Bouarab K, Salaün J-P, Pohnert G, Kloareg B (2002) Biotic interactions of marine algae. Curr Opin Plant Biol 5:308–317
Pu R, Wozniak M, Robinson KR (2000) Cortical actin filaments form rapidly during photopolarization and are required for the development of calcium gradients in *Pelvetia compressa* zygotes. Dev Biol 222:440–449
Quatrano RS (1997) Cortical asymmetries direct the establishment of cell polarity and the plane of cell division in the *Fucus* embryo. Cold Spring Harbor Symp Quant Biol 62:65–70
Quatrano RS, Crayton MA (1973) Sulfation of fucoidan in *Fucus* embryos I: possible role in localization. Dev Biol 30:29–35
Quatrano RS, Shaw S (1997) Role of the cell wall in the determination of cell polarity and the plane of cell division in *Fucus* embryos. Trends Plant Sci 2:15–21
Ragan MA, Glombitza KW (1986) Phlorotannins, brown. algal polyphenols. In: Round FE, Chapman DJ (eds) Progress in phycological research, vol 4. Biopress Ltd, Amsterdam, pp 130–241
Reed DC, Amsler CD, Ebeling AW (1992) Dispersal in kelps: factors affecting spore swimming and competency. Ecology 73:1577–1585
Roeder V, Collén J, Rousvoal S, Corre E, Leblanc C, Boyen C (2005) Identification of stress genes transcripts in *Laminaria digitata* (Phaeophyceae) protoplast cultures by expressed sequence tag analysis. J Phycol 41:1227–1235
Saenko GN, Kravtsova YY, Ivanenko VV, Sheludko SI (1978) Concentration of iodine and bromine by plants in the Seas of Japan and Okhotsk. Mar Biol 47:243–250
Schoenwaelder MEA (2002) The occurrence and cellular significance of physodes in brown algae. Phycologia 41:125–139
Schoenwaelder MEA, Clayton MN (1998a) Secretion of phenolic substances into the zygote wall and cell plate in embryos of *Hormosira* and *Acrocarpia* (Fucales, Phaeophyceae). J Phycol 34:969–980

Schoenwaelder MEA, Clayton MN (1998b) The secretion of phenolic compounds following fertilization in *Acrocarpia paniculata* (Fucales, Phaeophyta). Phycologia 37:40–46
Schoenwaelder MEA, Wiencke C (2000) Phenolic compounds in embryos during development of several northern hemisphere fucoids. Plant Biol 2:24–33
Schomer B, Epel D (1998) Redox changes during fertilization and maturation of marine invertebrate eggs. Dev Biol 203:1–11
Schröter K (1978) Asymmetrical jelly secretion of zygotes of *Pelvetia* and *Fucus*. Planta 140:69–73
Sever MJ, Weisser JT, Monahan J, Srinivasan S, Wilker JJ (2004) Metal-mediated cross-linking in the generation of a marine-mussel adhesive. Angew Chem Int Ed 43:448–450
Shaw SL, Quatrano RS (1996) The role of targeted secretion in the establishment of cell polarity and the orientation of the division plane in *Fucus* zygotes. Development 122:2623–2630
Shimonishi M, Kuwamoto S, Inoue H, Wever R, Ohshiro T, Izumi Y, Tanabe T (1998) Cloning and expression of the gene for a vanadium-dependent bromoperoxidase from a marine macro-alga, *Corallina pilulifera*. FEBS Lett 428:105–110
Soedjak HS, Butler A (1990) Characterization of vanadium bromoperoxidase from *Macrocystis* and *Fucus*: reactivity of vanadium bromoperoxidase toward acyl and alkyl peroxides and bromination of amines. Biochemistry 29:7974–7981
Soedjak HS, Butler A (1991) Mechanism of dioxygen formation catalysed by vanadium bromoperoxidase from *Macrocystis pyrifera* and *Fucus distichus*: steady state kinetic analysis and comparison to the mechanism of V-BrPO from *Ascophylum nodosum*. Biochim Biophys Acta 1079:1–7
Statz AR, Meagher RJ, Barron AE, Messersmith PB (2005) New peptidomimetic polymers for antifouling surfaces. J Am Chem Soc 127:7972–7973
Stossel TP (1993) On the crawling of animal cells. Science 260:1086–1094
Targett NM, Coen LD, Boettcher AA, Tanner CE (1992) Biogeographic comparisons of marine algal polyphenolics: evidence against a latitudinal trend. Oecologia 89:464–470
Tatehata H, Mochizuki A, Kawashima T, Yamashita S, Yamamoto H (2000) Model polypeptide of mussel adhesive protein. I. Synthesis and adhesive studies of sequential polypeptides (X-Tyr-Lys)n and (Y-Lys)n. J Appl Polym Sci 76:929–937
Tatehata H, Mochizuki A, Ohkawa K, Yamada M, Yamamoto H (2001) Tissue adhesive using synthetic model adhesive proteins inspired by the marine mussel. J Adhesion Sci Technol 15:1003–1013
Thuret G Bornet E (1878) Études phycologiques. Analyses d'algues marines. Masson, Paris, 105 pp
Umemura K, Inoue A, Kawai S (2003) Development of new natural polymer-based wood adhesives I. Dry bond strength and water resistance of konjac glucomannan and chitosan. J Wood Sci 49:221–226
Van Alstyne KL, Ehlig JM, Whitman SL (1999) Feeding preferences for juvenile and adult algae depend on algal stage and herbivore species. Mar Ecol Prog Ser 180:179–185
Vilter H (1984) Peroxidases from Phaeophyceae: a vanadium(V)-dependent peroxidase from *Ascophyllum nodosum*. Phytochemistry 23:1387–1390
Vilter H (1994) Aqueous two-phase systems. Methods Enz 228:665–672
Vilter H (1995) Vanadium-dependent haloperoxidases. In: Sigel H, Sigel A (eds) Metal ions in biological systems, vol 31. Dekker, New York, pp 325–362
Vreeland V (2002) Recombinant minimal catalytic vanadium haloperoxidases and their uses. International patent no WO 02/00838 A2, 3 Jan
Vreeland V, Epstein L (1996) Analysis of plant-substratum adhesives. In: Linskens HF, Jackson JF (eds) Modern methods of plant analysis, vol 17. Springer, Berlin Heidelberg New York, pp 95–116
Vreeland V, Grotkopp E (1996) Aqueous algal-based phenolic type adhesives and glues. US patent no 5520727, 28 May
Vreeland V, Laetsch WM (1990) A gelling carbohydrate in algal cell wall formation. In: Adair WS, Mecham RP (eds) Organization and assembly of plant and animal extracellular matrix. Academic Press, San Diego, pp 137–171

Vreeland V, Grotkopp E, Espinosa S, Quiroz D, Laetsch WM, West J (1993) The pattern of cell wall adhesive formation by *Fucus* zygotes. Hydrobiologia 261:485–491
Vreeland V, Waite J, Epstein L (1998) Polyphenols and oxidases in substratum adhesion by marine algae and mussels. J Phycol 34:1–8
Wagner VT, Brian L, Quatrano RS (1992) Role of a vitronectin-like molecule in embryo adhesion of the brown alga Fucus. Proc Natl Acad Sci USA 89:3644–3648
Waite JH (1987) Nature's underwater adhesive specialist. Int J Adhes Adhes 7:9–14
Wang J-L, Walling LL, Jauh GY, Gu Y-Q, Lord EM (1996) Lily cofactor-independent phosphoglycerate mutase: purification, partial sequencing, and immunolocalization. Planta 200:343–352
Wang Y, Lu J, Mollet J-C, Gretz MR, Hoagland KD (1997) Extracellular matrix assembly in diatoms (Bacillariophyceae) (II. 2,6-Dichlorobenzonitrile Inhibition of Motility and Stalk Production in the Marine Diatom Achnanthes longipes). Plant Physiol 113:1071–1080
Wetherbee R, Lind JL, Burke J, Quatrano RS (1998) The first kiss: establishment and control of initial adhesion by raphid diatoms. J Phycol 34:9–15
Weyand M, Hecht H-J, Kiess M, Liaud M-F, Vilter H, Schomburg D (1999) X-ray structure determination of a vanadium-dependent haloperoxidase from *Ascophyllum nodosum* at 2.0 A resolution. J Mol Biol 293:595–611
Whitaker DM (1931) On the rate of oxygen consumption by fertilized and unfertilized eggs: I. *Fucus vesiculosus*. J Gen Physiol 15:167–182
Wustman BA, Gretz MR, Hoagland KD (1997) Extracellular matrix assembly in diatoms (Bacillariophyceae) (I. A model of adhesives based on chemical characterization and localization of polysaccharides from the marine diatom achnanthes longipes and other diatoms.) Plant Physiol 113:1059–1069
Yamada KM, Miyamoto S (1995) Integrin transmembrane signaling and cytoskeletal control. Curr Opin Cell Biol 7:681–689
Yamamoto H, Ogawa T, Ohkawa K (1995) Wettability and adhesion of synthetic marine adhesive proteins and related model compounds. J Colloid Interface Sci 176:111–116
Yamamoto H, Sakai Y, Ohkawa K (2000) Synthesis and wettability characteristics of model adhesive protein sequences inspired by a marine mussel Biomacromolecules 1:543–551

7 Chemical Subtleties of Mussel and Polychaete Holdfasts

Jason Sagert, Chengjun Sun, and J. Herbert Waite

7.1 Introduction

Wave and wind-swept rocky shores are turbulent and punishing habitats. Despite this, many organisms prefer to live there, often at extremely high densities. Nutrient mixing, waste product removal, and dissolved gases are important habitat benefits, but the risks include high drag, abrasion, desiccation, and anoxia (Denny 1988). A holdfast for tenacious attachment to the hard substratum is a prerequisite for exposed organisms and the energy allocation for making and maintaining a holdfast can be considerable (Jordan and Valiela 1982).

Holdfast biochemistry as an area of study is still early in its evolution even though it easily goes back as far as the more advanced biochemistry of blood coagulation or connective tissue, for example (Stary and Andratschke 1925). As with other uncharted areas of endeavor, it has appealed to those who seek an untrodden path and come prepared to invent their own methodologies. There are many factors that have contributed to the slow progress of a mechanistic understanding of how marine adhesion works. These include poor protein solubility, changeable or no immunogenicity, repetitive and highly modified primary structures, complex processing by the organism and the absence of a significant protein database.

The purpose of this chapter is to describe better some molecular subtleties of holdfast proteins. These are drawn from our experience with two holdfast structures, mussel byssus and tubeworm cement, which have been previously reviewed (Vovelle 1965; Carrington 2002; Waite et al. 2005; Wiegemann 2005). Both are "permanent holdfasts" in that they cannot be undone by the organisms even though the holdfasts may break, be abandoned, or deteriorate in time. Tubeworm cement is probably the simplest of permanent adhesives in that it has the sole responsibility of holding together sand and shell bits (200–500 μm average diameter) that comprise the tube wall. The worm remains fully mobile within this tube. Mussel byssus is necessarily more complex given that it must mediate attachment of living mussel tissue to the stone surface. To achieve this, byssus consists of a bundle of threads each with four distinct morphological domains: an adhesive plaque, a thread divided

Department of Molecular, Cell & Developmental Biology, University of California, Santa Barbara, CA 93106, USA

Biological Adhesives
(ed. by A.M. Smith and J.A. Callow)

into stiff distal and rubbery proximal portions, and a stem. The threads all converge on the stem, which is contiguous with byssal retractor muscles (within the mussel) used to control thread tension (Waite 1992). The biochemical composition of byssus varies according to its location. *Mytilus edulis* foot proteins (mefps), for example, prevail in the adhesive plaque. The best characterized of these are mefp-2, mefp-3, and mefp-5 (Waite 2002). The thread is dominated throughout by collagen-silk or collagen-elastin hybrids known as preCols (Waite et al. 1998). PreCol-D and a matrix protein, DMP1, occur at the distal end, whereas preCol-P and PMP1 prefer the proximal end. Covering the entire structure is a thin protective cuticle comprised largely of mefp-1 (Waite 2002). Since holdfast tenacity is a complex balance of the adhesive and cohesive properties of molecules throughout the byssus, many aspects of biochemistry must be scrutinized in order to gain a mechanistic understanding of function. We shall discuss three oft-overlooked aspects here: protein deamidation, protein phosphorylation, and the tunable reactivity of 3,4-dihydroxyphenylalanine (Dopa) as they relate to the maturation of a functional holdfast in mussels and worms.

7.2 Protein Deamidation

Acellular structures and extracellular matrices like mussel byssus with little or no protein turnover are particularly vulnerable to the deamidation of asparaginyl residues as well as aspartyl racemization (Fig. 7.1). The tendency of asparagine (Asn) residues in peptides and proteins to undergo spontaneous, nonenzymatic deamidation, resulting in either L- or D-aspartic acid (Asp) or L- or D-isoaspartic acid (isoAsp) has been well documented in vivo and in vitro (Robinson and Rudd 1974). The mechanism involves a nucleophilic attack by the backbone amino group of carbonyl on the N-terminal flanking amino acid side chain, forming a five-member succinimide ring (Fig. 7.1A). The succinimide intermediate is typically short lived and resolved through hydrolysis as either an aspartic acid or the β-linked isoaspartic acid, and in some cases results in cleavage of the peptide bond (Geiger and Clarke 1987). The formation of isoAsp is generally favored over that of Asp at a ratio of approximately 3:1. In tooth enamel and elastin the presence of D-Asp and isoAsp have been correlated with aging (Helfman and Bada 1975; Fujii et al. 2002) while in eye lens, deamidation has been linked to pathogenesis, namely cataract formation (Masters et al. 1977).

Byssal threads of *Mytilus galloprovincialis* contain a family of protein variants named the Distal Matrix Proteins (DMPs) that undergo rapid deamidation at multiple sites (Sagert and Waite 2005). The DMPs have a unique amino acid composition, 65% of which consists of tyrosine (including 1.2–3% Dopa), glycine, and asparagine, and a typical full-length transcript encodes a protein that is 514 amino acids with tandem repeats. The most striking feature of the DMPs is the presence of 43 Asn-Gly sites, which are likely to deamidate rapidly. Indeed, a portion of one of the variants was recombinantly expressed and mass spectrometry was used to show that deamidation

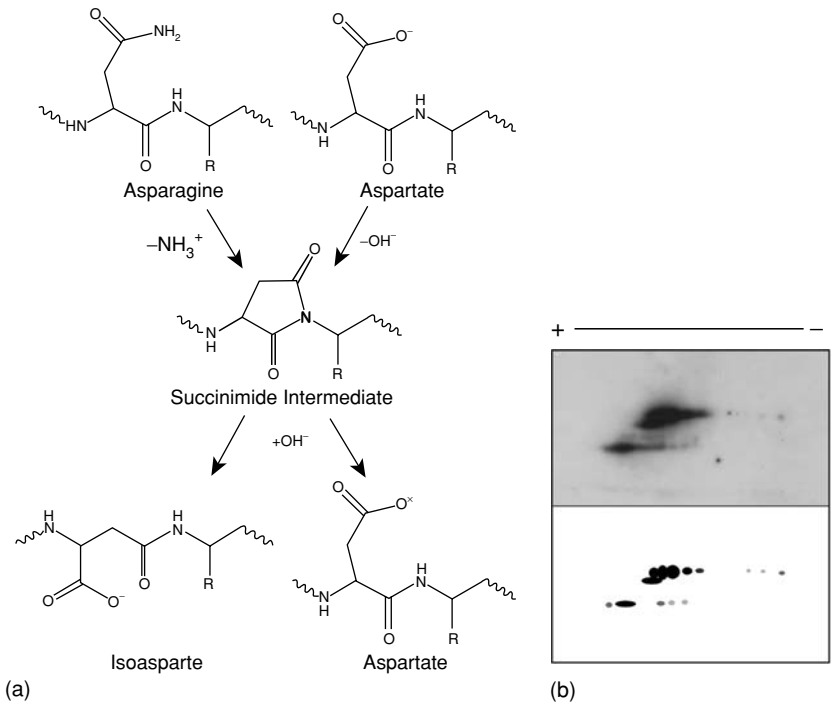

Fig. 7.1. Deamidation of asparagine in the byssal thread: (a) mechanism for the spontaneous deamidation or dehydration of asparagine and aspartate through the succinimide intermediate to generate either isoaspartate or aspartate; (b) Western blot of a two-dimensional gel probed with an anti-DMP antibody. The *top panel* shows the autoradiograph film. The *bottom panel* is a diagram of the spots that are apparent on the autoradiographic film and their relative intensities. Charge heterogeneity moving towards a more acidic pI from the more abundant parent peak is apparent in both proteins

occurred in vitro at multiple sites (n.b. each Asp is 1 Da greater than Asn). In support of the in vivo significance of deamidation of the DMPs, native protein variants extracted from induced threads showed charge heterogeneity when analyzed by 2D electrophoresis and subsequent detection with an antibody. The formation of new threads is typically induced by injecting KCl into the base of the foot (Tamarin et al. 1976), and charge variants were already evident in induced threads in at least two of the DMP polymorphs as detected by western blotting (Fig. 7.1B). Isoaspartate was quantified in extracts which contain the DMPs from distal byssal threads that were less than one week old and was found to be present at concentrations greater than 1 nmol/mg of protein. Determining the rate of deamidation in the thread from the amount of isoAsp is confounded by the fact that not all deamidation events result in isoAsp and that the racemization of Asp can lead to isoAsp as well. However, the presence of charge heterogeneity in DMPs extracted from induced

threads, which consist of neonatal byssal proteins, suggests that deamidation occurs rapidly and is likely to continue to accumulate in mature threads throughout their functional lifetime.

The rate of deamidation has been studied extensively in proteins and model peptides in vitro and has been shown to be dependent on solvent conditions, including the pH, buffering species, and salt concentration (dielectric), and the primary, secondary and tertiary structure of the peptide (reviewed in Brennan and Clarke 1995). In general, the rate of deamidation through a succinimide intermediate increases with pH and salt concentration. The effect that nearest neighbor residues has on the rate of deamidation has led to the identification of sequences that are prone to deamidation. In general, the asparagine's N-terminal neighbor has less of an effect than the amino acid on the C-terminal side, with Asn-Gly, Asn-His, Asn-Ser, and Asn-Ala sequences being particularly labile to deamidation (Robinson and Robinson 2001a). Results obtained for the rate of deamidation in synthetic peptides have been compared with the rate of the same sequences in proteins and has been shown to differ significantly in some cases, suggesting that the three-dimensional structure of a protein influences the deamidation rate of Asn and that flexible sequences are more prone to deamidation (Robinson and Robinson 2001b).

Thus far, the evidence suggests that the DMPs are adaptively prone to deamidate rapidly at many, if not all, Asn sites, making it plausible to propose that the modification serves a functional role in the byssal thread. It has been suggested, for example, that deamidation of Asn could represent an autocatalytic remodeling of proteins, altering their function in some useful way (Robinson 2002; Reissner and Aswad 2003). Although any statement about the function of deamidation in the byssal thread is necessarily speculative, the significant amount of charge heterogeneity observed in DMPs from freshly secreted thread proteins and isoAsp in one-week-old threads supports the idea that deamidation might be necessary in the assembly of the byssal thread. Prior to secretion, protein stockpiled at the acidic pH of the secretory granules would be stable against deamidation; however, upon secretion into the alkaline ocean environment, deamidation of asparagines would be accelerated, thereby lowering protein pI and changing the structure/function relationship in the protein. This in turn would be expected to have an effect on the assembly, mechanics, or obsolescence of the byssal thread. Deamidation could provide a non-reversible, pH dependent switch in the byssal threads. Hassenkam et al. (2004), for example, have proposed that thread formation involves prefabrication of liquid crystalline preCols in smectic arrays, which become "locked" or "frozen" during processing into mature threads. Since the preCols are basic proteins (SwissProt analysis of sequences [http://us.expasy.org] from Waite et al. (1998) gave pIs of 8, 10.3, and 11.5, respectively, for preCol-NG, D, and P), the production of a higher negative charge density on the DMPs could contribute to a structure locking process.

7.3 Protein Phosphorylation

Phosphorylation is a widespread protein modification with an enormous database and, recently, even an "ome", the phosphoproteome. The vast majority of the literature on phosphoproteins has to do with the central role of protein phosphorylation in signal transduction. This, with the exception of casein kinases (enzymes that phosphorylate multiple serines (Veis et al. 1997)), is tangential to the present focus. Protein phosphorylation also emerges as an important theme in the scaffolding proteins of teeth (phosphophoryns), bone, shells, kidney stones, and neurofibrillary tangles (tau). Many amino acids including Ser, Thr, Tyr, His, and Asp can be targets for phosphorylation (Kyte 1995). Only phosphoserine (pSer) has been detected to date in holdfast proteins. pSer is essentially a monophosphoester with two ionizable hydroxyls at pK_1 2.1 and pK_2 6.5 (Kyte 1995). At the pH of seawater (8.2), both are largely charged, rendering this residue and the sequence surrounding it highly polar (Fig. 7.2A).

Mefp-5 is a plaque specific protein in the byssus of *Mytilus edulis* and, among fps, contains the highest Dopa level at 30 mol% (Waite and Qin 2001). It has a pI of 8.3 (with phosphorylation), a mass of about 9.5 kDa and 75 amino acids of which 8 are serines. The serines are variably phosphorylated in that the isolated protein is a mixture of variants having between 0 and 8 phosphoserines. Mefp-5 and other proteins rich in phospho groups can be readily precipitated by addition of Ca^{+2} to solutions (Fujisawa et al. 1987). The protein appears to be distributed near the plaque-substratum interface but the role of phosphoserine in adhesion remains undetermined (Waite 2002). Interestingly, the phosphoprotein, statherin, binds strongly to calcium in hydroxyapatite by way of its phosphoserine groups (Stayton et al. 2003) in a sequence (i.e., pSpSEE) that resembles the N-terminus of mefp-5.

The cement of sabellariids such as the California sandcastle worm *Phragmatopoma californica* contains an unusual hyperphosphorylated protein. In 1988, the cement was reported as extremely serine and glycine rich (each 30 mol%) and compared to silk sericin-like proteins (Jensen and Morse 1988). Reanalysis following short hydrolysis times, however, revealed that phosphoserine and not serine was released during acid hydrolysis (Stewart et al. 2004). Calculations indicated that up to 90% of the serine detected in cement was derived by decomposition from phosphoserine. The two known cement precursors, Pc1 and Pc2, however, did not contain any serine or phosphoserine (Waite et al. 1992), so research was initiated to isolate phosphoserine rich proteins from the cement. The unpredictable solubility of phosphoproteins and the inability to visualize them with standard stains represent the chief factors in their elusiveness to purification (Fisher and Termine 1988). Molecular biology and cloning techniques, however, have allowed a glimpse of putative Pc3 variant sequences, which were serendipitously discovered by 3' untranslated sequences that they share with Pc1. Two

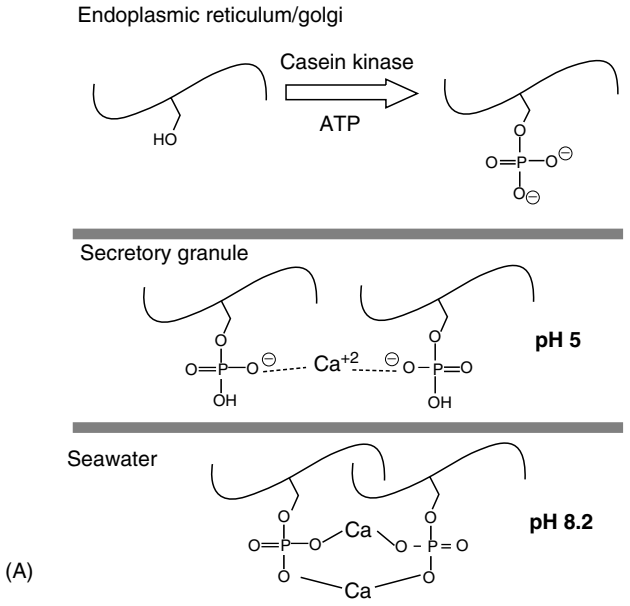

Mytilus foot protein-3 mefp-5 (AF333078)

SSEEYKGGYYPGNAYHY**S**GG**S**YHG**S**GYHGGYKGKYY
GKAKKYYYKYKN**S**GKYKYLKKARKYHRKGYKYYGG**SS**

Phragmatopoma cement protein Pc-3A (AY960618)

D**SSSSSY**SSSSSY**SSSS**Y**SSSS**Y**SSSS**Y**SSSS**Y**SSSS**Y**SSSS
Y**SSSS**Y**SSSS**Y**SSSS**Y**SSSS**Y**SSSS**Y**SSSS**Y**SSSS**Y**S
SSSILSTSTSSSDWKRKVPARRVLRTRRFLKCVTRCT
LRCILFRSAKTCARKCSRRCLKRVF

(B)

Fig. 7.2. Formation of phosphoserine in secreted polyphosphorylated proteins: (a) phosphorylation requires ATP and casein kinases and occurs in the endoplasmic reticulum and perhaps in the Golgi. In the mature secretory granules, H^+ pumping ATPases drop the pH to about 5 and Ca^{+2} is accumulated approaching mmol/l concentrations. Upon secretion into seawater the pH jumps to pH 8.2. The solubility product of $Ca_3(PO_4)_2$ is about 10^{-33} in water but is (Weast 1983) considerably more soluble at low pH. The Ca^{+2} and phosphate interactions thus go from mostly electrostatic at pH 5 to ionic bonds at pH 8; (B) the sequences of two phosphoproteins, mefp-5 and Pc-3A (with GenBank accession numbers). Targeted serines are *highlighted in bold*

types of Pc3 have emerged: Pc3A and Pc3B. Both have runs of serine (four to eleven in a row) separated by tyrosine. The former has a basic, cysteine-rich C-terminus, whereas the latter is serine-rich throughout (Fig. 7.2B). If 90 mol% of the serines are phosphorylated, then pIs are estimated to be between 0.5 and 1.5 (Zhao et al. 2005).

Understandably, there is much curiosity about why such proteins should be present in cement, and here again as in statherin, pSer may function in binding to calcareous minerals. Moreover, Stewart et al. (2004) and Zhao et al. (2005) recently proposed that if cement protein processing depended on complex coacervation, then a phosphoserine-rich protein would be a crucial player. Complex coacervation involves the coalescence of polyelectrolytes in aqueous solution and describes a phase separation in which the polyelectrolytes settle out of equilibrium solution to form a dense partially desolvated liquid coacervate phase. The conditions for this reaction are well documented by the detailed studies of Bungenberg de Jong (1949) with natural polyelectrolytes such as histone, gelatin, casein, and gum arabic. The basis of coacervation is as follows: for every aqueous combination of a polycation with a polyanion (e.g., collagen and gum arabic mixtures), there is some pH at which the two effectively neutralize the charges of each other. At this point there is no repulsion, and many small coacervate droplets form eventually to coalesce into a larger dense phase. Reorganization appears to be driven by coulombic interactions as well as by the low interfacial tension between the equilibrium fluid and coacervate phases.

Careful analysis of *Phragmatopoma* cement has revealed approximately equal amounts of three protein substituents – Pc1, Pc2, and Pc3A/B – having pIs of about 10, 9.7, and 0.5/1.5, respectively (Zhao et al. 2005). At pH 5, for example, Pc1 and Pc2 will be polycations with a charge density of about +0.16/residue and +0.34/residue, respectively. In contrast, the Pc3s will be polyanions with a density between –0.45 to –0.85/residue. Assuming the proteins have similar masses, the polyanions have a far greater charge density to neutralize than Pc1 and Pc2. This requires more positive charges than Pc1 and Pc2 have to offer, particularly when present in equimolar concentrations. The worm appears to get around this impasse by adding micro-ions such as Mg^{+2} and Ca^{+2} as counterions for Pc3 (Stewart et al. 2004). Why not just phosphorylate less? This is always an option, of course, but there may be a further crucial downstream role for the divalent ions. When the coacervate meets seawater, its pH will be re-equilibrated to 8.2. Due to the reduced solubility of the phosphate-Ca^{+2} (or Mg^{+2}) pairs at this pH (Weast 1983), the coacervate will gel into something resembling cheese or tofu. Indeed, calcium ions are exploited to solidify the phosphoproteins in these foods (Nakamura and Niki 1993).

7.4 Dopa Chemistry

7.4.1 Gradients

Dopa is a distinctive functionality of mussel byssus and also, more recently, of the tube cement of polychaete sabellariids. In contrast to initial naïve notions about its role as a protein cross-linker, Dopa biochemistry is turning

out to be complex and full of surprises. One way in which mussels appear to fine-tune Dopa chemistry is by the use of gradients. Protein gradients involving collagenous preCols in mussel byssus have already been much discussed as an adaptive strategy to reduce contact deformation between the soft tissues of the animal and substratum due to their mismatched Young's moduli (Suresh 2001; Waite et al. 2004).

Dopa exhibits its highest molar concentration in the plaque, is somewhat lower in the distal portion of the thread, decreasing in a distal to proximal direction as shown in Fig. 7.3. The plaque contains Dopa as high as 6 mol% (Sun and Waite 2005). In comparison, the exposed distal portion of the thread has Dopa concentrations of nearly 2.5 mol%, whereas the proximal portion, which is normally shielded within the mussel, contains less than 0.5 mol%. As the measured Dopa concentrations represent averages over the volume of sample analyzed, it is crucial to determine where specific Dopa-containing proteins are located within the byssus. All indications point against a uniform distribution. In plaques, Dopa is highest near the plaque/substratum interface. Indeed, those mfps with the highest Dopa levels, mfp-3 (20 mol%) and mfp-5 (30 mol%), are consistently detected near the interface (Floriolli et al. 2000; Waite 2002). The distal portion of *M. edulis* threads is known to contain four proteins: preCol-D, preCol-NG, distal matrix protein (DMP1), and mefp-1. Current models of protein distribution place the preCols in the core separated perhaps by DMP1; mefp-1 in contrast is limited to the outer cuticle, which is only 4–5 μm thick (Benedict and Waite 1986; Qin and Waite 1995; Holten-Andersen et al. 2005).

All known proteins in the distal portion of the thread contain Dopa but content varies from about 15 mol% in mfp-1 to 3 mol% in DMP1, whereas preCol-D and preCol-NG, present in roughly equal parts, have less than 0.4 and 0.6 mol%, respectively (Waite 2002). Given that the preCols comprise the bulk of the thread and DMP1 is present at less than 1 wt%, the Dopa these three would contribute to the thread would be less than 0.6 mol%. Thus, it is probable that the observed ~2.5 mol% Dopa level is derived primarily from mfp-1.

Like the gradient in the mussel foot and thread involving preCols D and P (Qin and Waite 1995), the Dopa gradient is prefabricated in the accessory gland of the foot of *Mytilus* well before it appears in the thread (Fig. 7.3B). Sun and Waite (2005) have shown that the composition of mgfp-1 isolated from successive sections of the foot differs only in its Dopa and Tyr content, suggesting a gradual, modulated, or regulated tyrosylhydroxylase activity along the long axis of the accessory gland. The ratio of Dopa/Tyr ranges from a high of 2 in the distal-most portion to 0.5 at the proximal end – a fourfold decrease. Mfp-1s cannot be extracted from the thread, so we assume that Dopa gradient is derived from secreted, differentially hydroxylated protein according to an injection-molding production process proposed earlier (Fig. 7.3) (Waite 1992). Thus far, the model is consistent with the observations, and the calculations seem reasonable. However, it deals a serious blow to the traditionally assumed function of Dopa whose raison d'etre was given

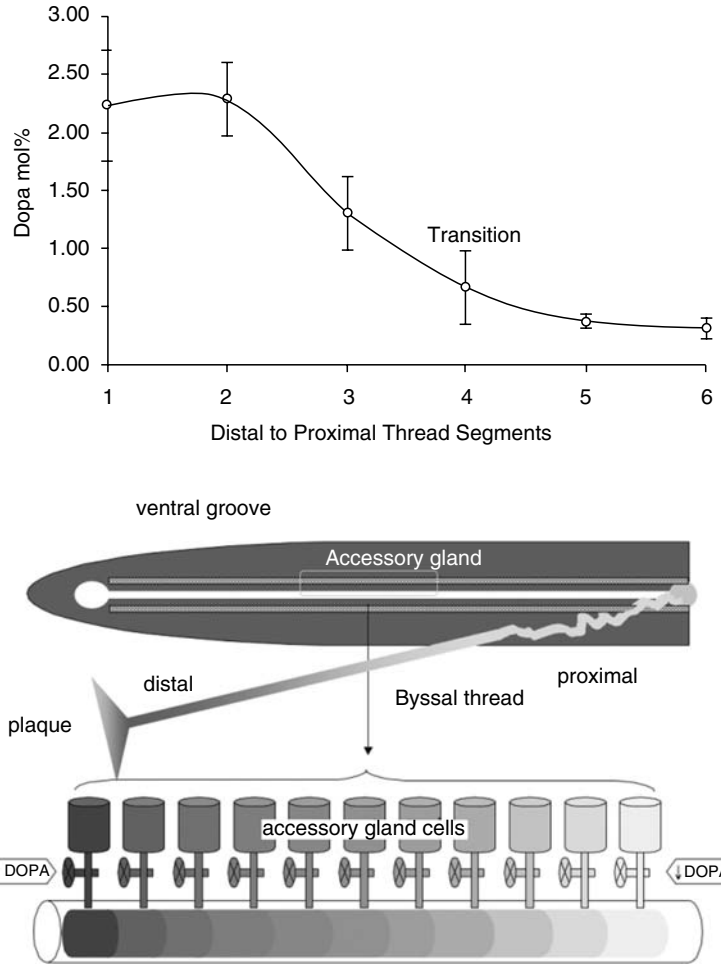

Fig. 7.3. Dopa gradient in byssal threads of *Mytilus galliprovincialis*: (a) all threads were cut into six equally spaced segments excluding plaques and stems. Segments were measured from the transitional region separating the distal and proximal portions, which was bisected precisely between segments 3 and 4. Dopa contents are the average of four measurements (±sd) expressed as mol% or residues per 100 residues (data based on Sun and Waite 2005); (a) model of the mechanism for making Dopa gradients in which the gradient results mostly from the differential modification of Mytilus fp-1 along the distal to proximal axis of the accessory gland of the foot

as cross-linking (quinone tanning)! In other words, if the role of Dopa is to give rise to covalent cross-links in the byssus, how can it persist as Dopa in mature byssal threads? This paradox gets to the heart of the emerging versatility with which Dopa is used in byssus. Clearly, in future endeavors, each occurrence of Dopa must be assumed to possess a distinct reaction pathway that is defined by its local structure.

The local structure of the coating, in which mfp-1 is the major protein component, suggests it might be a composite with knob-shaped 1 μm sized inclusions (Vitellaro-Zucarello 1981). Elemental analyses of the coating indicate much higher levels of Al, Si, Br, and Fe relative to the core (Holten-Andersen et al. 2005; Sun and Waite 2005), and it is in this chemical context in which the Dopa reactivity of mfp-1 must be considered. Since the coating covers and protects the collagenous core, which exhibits strains of up to 70%, the coating too must be extensible. This would not be possible if Dopa cross-linking produced a rigid and noncompliant structure. In the sections below, the chemical diversity of Dopa as a "bridging" or linking functionality is elaborated.

7.4.2 Metal Binding

Although mussel byssus is not mineralized, inorganics are present at up to 1–2 wt% in byssal threads (Coombs and Keller 1981). Fe^{+3} is taken up by filtration and distributed to the threads by way of the byssal glands rather than being passively adsorbed onto the thread surface (George et al. 1976; Sun and Waite 2005). The same seems to be true for distribution of Mn, Co, and Cu in Mytilus and Septifer species (Tateda and Koyanagi 1986). In point of fact, a variety of metals can be accumulated in mussel byssus, particularly in polluted waters (Koide et al. 1982). To date, the exact roles served by the metals in byssus are still debated. Taylor et al. (1994, 1996) showed that Mefp-1 and Dopa-containing peptides derived from Mefp-1 can bind iron(III) reversibly to form ferric catecholate complexes with a stability constant of over 10^{40} in 0.1 mol/l NaCl at neutral pH. Resonance Raman spectra revealed that the complexes formed adopted either bis(μ-oxo/hydroxo)-bridged coordination or tris(catecholato) coordination as shown in Fig. 7.4A with the bis-form being preferred at lower and the tris-form at higher catechol/metal ratios. More recently, Sever et al. (2004) have shown that added Fe^{+3} can cause solutions of mefp-1 to set in vitro but that it may do so either reversibly by the formation of tris-catecholato-iron complexes, or irreversibly, by redox exchange to form Dopa semiquinones to form covalent cross-links.

Catechols such as Dopa have also been shown to interact with solid-state metal/metal oxides having stability constants comparable to those in solution (Fig. 7.4B). X-ray photoelectron spectroscopy, optical wavelength lightmode spectroscopy, and surface induced mass spectroscopy have detected characteristic charge transfer complexes at interfaces between Dopa-containing model compounds and titanium and iron oxides (Dalsin and Messersmith 2005; Dalsin et al. 2005). Coordination of Dopa groups with the Fe(III) in iron oxide requires displacement of the oxy- and hydroxy ligands by the catechol (Fig. 7.4B). This displacement occurs and has important implications for the bioinspired design of underwater adhesives and coatings (Dalsin and Messersmith 2005).

Catechols have significant binding constants to other metals including Al(III), Cu(II), Si(IV), V(IV), and Zn(II) (Waite 1990) as well as oxides of

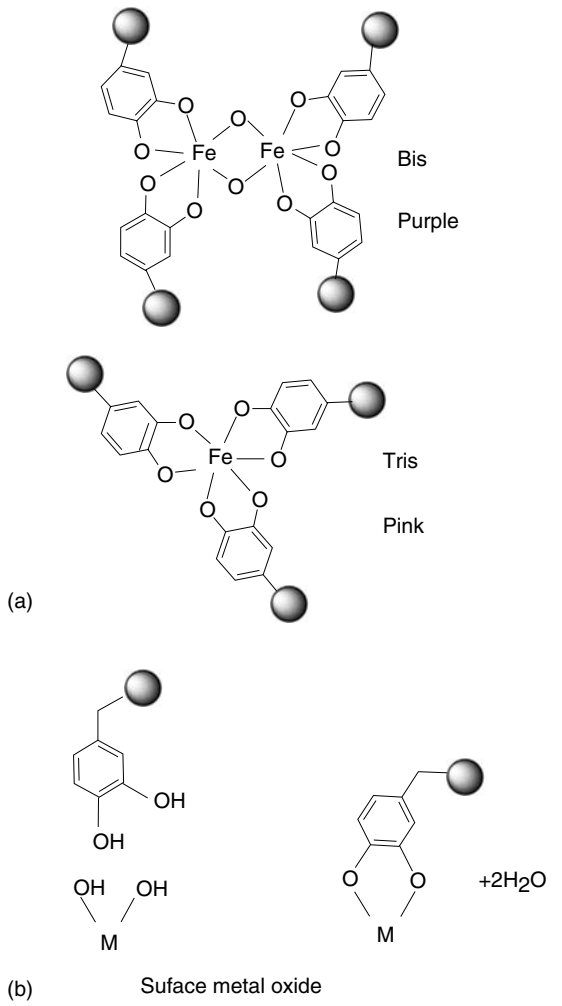

Fig. 7.4. Metal binding of Dopa: (a) being a catechol, peptidyl-Dopa is strongly inclined to form Fe(III) catecholate chelates. The nature of these depends on the relative proportion of the catechol: Fe(III). At low proportions the di-bis form (*upper*) is favored. This is purple and paramagnetic. At higher concentrations, the tris form prevails. It is pink and diamagnetic; (b) chelate binding of metal oxide surfaces. Catecholate functionality has a stronger binding affinity for Fe(III) (for example) than the oxide form (rust) and so displaces the oxy and hydroxy ligands as water. The resulting bonds are reversible, but stronger than noncovalent interactions and independent of the dielectric constant of the medium (Waite et al. 2005)

these metals (reviewed by Waite et al. 2005). Although unequivocal proof of any of these interactions in byssus will be challenging given the complexity of byssus, metallo-Dopa complexes clearly provide an alternative to covalent cross-linking. Metal ions such as Fe^{+3} are polyvalent toward Dopa ligands, the complexes formed are highly stable, and the interactions are reversible. The

latter point is particular relevant to post-hydrolysis detection of Dopa, and the mechanical need for the coating to accommodate the high strains of the thread. Significantly, either Fe^{+3} or inorganic nanoparticles containing ferric iron can provide the surface valency for cross-bridging with Dopa.

7.4.3 Cross-linking

7.4.3.1 Aryl Coupling

Since the identification of peptidyl dihydroxyphenylalanine (DOPA) in the primary sequence of Mytilus edulis foot protein 1 (Mefp-1) (Waite 1983), the sclerotization of byssal threads has been attributed to the ability of Dopa to form oxidatively derived cross-links. Although it was initially assumed that the cross-links would involve a Michael-type addition reaction with primary amines such as lysine (Waite 1983, 1990), these cross-links have so far not materialized from the thread. Insight into the nature of the DOPA derived cross-links in the byssal thread came from work done by Andersen and coworkers (Andersen et al. 1992) on the phenoloxidase activity found in insect cuticle. When 4-methylcatechol was incubated with insect cuticle, the main product identified was 6,6′-di-[1-methylcatechol]. Indeed, the presence of 5,5′-di-dihydroxyphenylalanine (diDOPA) in the adhesive plaques of *Mytilus edulis* was confirmed using rotational-echo double-resonance (REDOR) NMR on plaques produced by mussels grown in the presence of ^{13}C and ^{2}H containing analogs of tyrosine (McDowell et al. 1999) (Fig. 7.5). Confounding the detection of diDOPA, initial REDOR experiments on plaques that were secreted in calm water failed to detect the cross-link (Klug et al. 1996) and only after the plaques were subjected to flow stress were cross-links detectable. DiDOPA is likely present in the thread as well as the adhesive plaque; however, the presence of the cross-link in the thread has not been confirmed, likely due to its low concentration. In support of the in vivo significance of diDOPA, in vitro experiments with the canonical decapeptides from Mefp-1 demonstrated that peptides were covalently cross-linked in the presence of periodate or tyrosinase, and that DOPA was the residue responsible (Burzio and Waite 2000).

Recently, Haemers et al. (2003) have proposed a kinetic model for the rate of diDOPA formation in Mefp-1 that takes into consideration the rate of oxidation of Dopa to quinone and the reverse dismutation of the quinone by an adjacent unoxidized Dopa yielding two highly reactive radicals that couple to form a diDopa cross-link. Depending on the ratio of the rate of oxidation to dismutation, two cross-linking regimes are possible. In the first, the rate of oxidation is much slower than the rate of dismutation, and therefore the rate of oxidation determines the rate of diDopa formation. In the second, the rate of oxidation is much greater than that of dismutation and di-Dopa formation is prevented because once all the Dopa has been oxidized there is nothing left

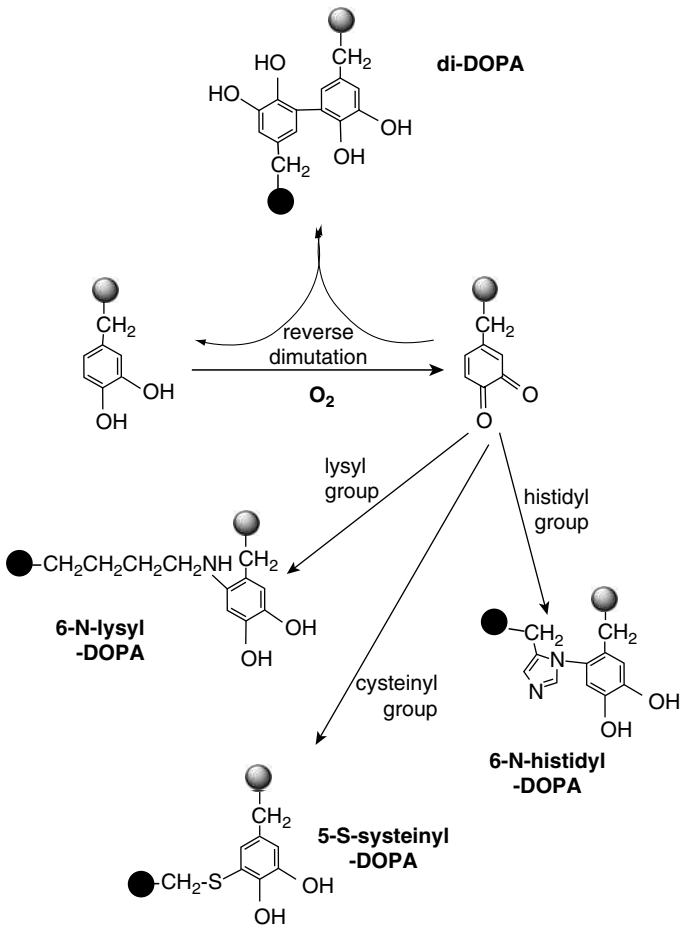

Fig. 7.5. Modes of Dopa-derived cross-links. Dopa is oxidized to Dopaquinone in the presence of catecholoxidase and O_2 (periodate and peroxide are frequently used in vitro). Steady state between the redox pair dictates the type of cross-link formed as does the abundance of and type of nucleophiles present. With equal amounts of Dopa/Dopaquinone, aryl coupling to diDopa takes place. When Dopaquinone prevails, some histidyl and lysyl adducts are expected. However, when cysteinyl groups are present, these overwhelm all other reactions to form cysteinyl-Dopa adducts. True intermolecular cross-linking would occur when the *black and shaded balls* represent different protein backbones

for the Dopaquinone to pair with. Therefore, the ratio of oxidation to dismutation determines the rate of cross-link formation. Both the rate of oxidation and dismutation are determined by the molecular properties of the proteins involved in cross-link formation (Haemers et al. 2002, 2003). The major consequence, as pointed out by Haemers and coworkers, is that the reverse dismutation mechanism provides a way in which nature can gain subtle control of the rate of cross-link formation.

7.4.4 Michael Additions: Amines

Peptidyl Dopaquinone is the two-electron oxidation product of Dopa and typically reacts in three distinctive ways in biological systems: addition, redox exchange, and tautomerism (Land et al. 2004). With regard to addition, the *o*-Dopaquinone is electron-deficient and, given its dual α,β unsaturated bonds, is receptive toward attack by electron-rich nucleophiles via nonenzymatic pathways (Peter 1989). The best known Michael addition of Dopaquinone is the intramolecular addition of the side-chain amine to the 6-ring position yielding the indolic precursors of melanin (Land et al. 2004). Other alkylamines that can add to Dopaquinone include lysine and histidine derivatives. When both the Dopa and amine groups are side-chains of protein backbones there is a distinct potential for cross-linking. ε-*N*-Lysyl-6-Dopaquinone was identified as an active site cofactor in lysyl oxidase (Wang et al. 1996, 1997). A related reaction with an imidazolic N occurs between the quinone of *N*-acetylDopamine and histidine in the sclerotization of insect exoskeleton (Schaefer et al. 1987; Xu et al. 1996). These reactions are simplified in Fig. 7.5 to illustrate the more favorable products. The Michael addition reaction between ortho-quinones and amines is highly dependent upon the pK_a of both primary and secondary amines (Peter 1989); the lower the pK_a, the faster the adducts form. Solvent accessible lysyl and histidyl groups have pK_as of about 10.4 and 6.5, respectively (Kyte 1995); thus only the latter would be expected to react. The presence of Dopaquinone-amine cross-links in marine adhesives remains speculative. Burzio and Waite (2000) found significantly reduced lysine levels in some mefp-1 decapeptides oxidized by tyrosinase, but no cross-links were systematically characterized. Cross-linking in Mytilus byssus seems to be most consistent with aryl coupling at present (Waite 2002), but one hopes that the reason for so much lysine (15–20 mol%) in mfp-1 and -5 will be understood some day.

7.4.5 Michael Thiol Additions

Free Dopaquinone readily undergoes reductive addition with thiols such as cysteine and glutathione. The thiolate form of thiol reacts with the ortho-quinone to give mercapto-catechols (Prota 1992) as shown in Fig. 7.5. The Dopaquinone-cysteine reaction is not very position-specific but 5-*S*-cysteinylDopa appears to be the least sterically impeded form (Land et al. 2004). Dryhurst et al. (1982) showed that thioaddition is one of the most favorable reactions that quinones are capable of. In a comparative analysis, the intramolecular cyclization by the α-amine of free Dopa to form a dihydroxyindole was assigned a relative rate of 1 at pH of 7.4; in relation to this, attack by the ε-amino group of lysine was 0.04, whereas for the thiol of cysteine it was 2100. To this, we can now add aryl coupling reactions since rates have recently been measured at pH 6.5 (van der Leeden 2005): the rank of

Dopa-derived aryl coupling is approximately 70. Thus, if free thiols are about they will scavenge Dopaquinones before anything else. The chemistry described above is entirely associated with free amino acids and melanin formation (Peter 1989; Land et al. 2004). A few studies have extended this to protein-bound cysteinyl and Dopa groups leading to cross-link formation. 5-*S*-CysteinylDopa formation appears in gluten during dough oxidation as well as in the in vitro oxidation of several proteins by tyrosinase (Ito et al. 1984; Takasaki and Kawakishi 1997). CysteinylDopa cross-links have recently been detected in marine holdfasts (Zhao and Waite 2005; Zhao et al. 2005). Significant levels of 5-*S*-cysteinylDopa (≥1 mol%) occur in the byssus of the green shell mussel *Perna canaliculus* and in the cement protein of *Phragmatopoma californica*. The byssus of *M. edulis*, *M. galloprovincialis*, and *M. californianus*, in contrast, contained only traces of cysteinylDopa adducts (Zhao and Waite 2005).

7.5 Conclusion

Holdfast biochemistry in mussels and polychaetes continues to baffle and fascinate. This chapter has examined some subtleties of protein deamidation, phosphorylation, and tyrosine hydroxylation. The degree to which these biochemical transformations are mechanistically understood varies greatly. In the case of Asn deamidation in byssal DMPs, it is completely open to speculation, but it is certainly too fast to be accidental. It could be a programmed trigger for byssus obsolescence or protein stabilization by providing more charges. Future studies will need to explore whether there are detectable mechanical consequences with the accumulation of aspartate and isoaspartate.

In the case of Ser phosphorylation in Pc-3 and mefp-5, the contribution is less ambiguous. Polyphosphoproteins provide effective and versatile macroions for complex coacervation as well as for binding to calcareous mineral surfaces. Complex coacervation in holdfast formation remains to be demonstrated definitively, but its potential contributions to the process are undeniable. Complex coacervation would enable the following: secretion of adhesive in a fluid but phase separated form; adhesive with higher density than sea water; good spreading due to low interfacial tension in water; and a two-step setting process, first by ion bridges, then by covalent cross-links. Additional advantages may emerge.

Finally, Dopa is a particularly revealing example. In the early years after its discovery, Dopa was regarded as the key to understanding quinone tanning in byssus (Waite 1983). This may still be true, but the analysis of Dopa has revealed such diverse reactivity that the meaning of quinone tanning is no longer clear. The catalog of Dopa-derived cross-links includes ring/ring coupling, thiol addition, coordination of multiple ligands by Fe^{+3}, and chemisorption by chelation of surface metal oxides. All of these have been implicated in

some part of the mussel byssus, leading to the suggestion that Dopa may even have "niche specific" chemistry, that is, a reactivity that is locally defined. At first glance this may seem much more complicated than necessary; however, it begs a maxim from structural engineering: the more tunable a joining strategy is, the more design flexibility it offers structures built with it (Kinloch 1980). The adaptive flexibility of mussel byssus, particularly with respect to the role played by Dopa, has spawned a flurry of innovations in hydrogels (Huang et al. 2002), paper products (Li et al. 2004), coatings (Dalsin and Messersmith 2005), and tools for biotechnology (Burdine et al. 2004; Xu et al. 2004).

References

Andersen SO, Jacobson JP, Bojesen G, Roepstorff P (1992) Phenoloxidase catalyzed coupling of catechols. Identification of novel coupling products. Biochim Biophys Acta 1118:134–138

Benedict CV, Waite JH (1986) Location and analysis of byssal structural proteins of Mytilus edulis. J Morphol 189:171–181

Brennan TV, Clarke S (1995) Deamidation and isoaspartate formation in model synthetic peptides: the effect of sequence and solution environment. In: Aswad DW (ed) Deamidation and isoaspartate formation in peptides and proteins. CRC Press, Boca Raton, pp 65–90

Bungenberg de Jong HG (1949) Morphology of coacervates. In: Kruyt HR (ed) Colloid science, vol 2. Elsevier Publ, Amsterdam, pp 433–482

Burdine L, Gillette TG, Lin HJ, Kodadek T (2004) Periodate-triggered cross-linking of DOPA-containing peptide-protein complexes. J Am Chem Soc 126:1142–1143

Burzio LA, Waite JH (2000) Cross-linking in adhesive quinoproteins: studies with model decapeptides. Biochemistry 39:11147–11153

Carrington E (2002) The ecomechanics of mussel attachment: from molecules to ecosystems. Integr Comp Biol 42:846–852

Coombs TL, Keller PJ (1981) Mytilus byssal threads as an environmental marker for metals Aquat Toxicol 1:291–300

Dalsin JL, Messersmith PB (2005) Antifouling polymers inspired by biology. Materials Today (in press)

Dalsin JL, Lin L, Tosatti S, Voros J, Textor M, Messersmith PB (2005) Protein resistance of titanium oxide surfaces modified by biologically inspired mPEG-DOPA. Langmuir 21:640–646

Denny MW (1988) Biology and the mechanics of the wave-swept environment. Princeton Univ Press, Princeton, NJ

Dryhurst G, Kadish KM, Scheller F, Renneberg R (1982) Biological electrochemistry, vol 1. Academic Press, New York, pp 138–139

Fisher LW, Termine JD (1988) Purification of the noncollagenous proteins from bone: technical pitfalls and how to avoid them. In: Ornoy A, Harell A, Sela J (eds) Current advances in skeletogenesis. Elsevier, New York, pp 467–472

Floriolli R, von Langen J, Waite JH (2000) Marine surfaces and the expression of specific byssal adhesive protein variants in Mytilus. Mar Biotech 2:352–363

Fujii N, Tajima S, Tanaka N, Fujimoto N, Takata T, Shimo-Oka T (2002) The presence of D-b-aspartic acid-containing peptides in elastic fibers of sun-damaged skin: a potent marker for ultraviolet-induced skin aging. Biochem Biophys Res Commun 294:1047–1051

Fujisawa R, Kuboki Y, Sasaki S (1987) Effects of dentin phosphophoryn precipitation of calcium phosphate in gel in vitro. Calc Tissue Int 41:44–47

Geiger T., Clarke S (1987) Deamidation, isomerization, and racemization at asparaginyl and aspartyl residues in peptides: succinimide-linked reactions that contribute to protein degradation. J Biol Chem 262:785–794

George SG, Pirie BJS, Coombs TL (1976) The kinetics of accumulation and excretion of ferric hydroxide in Mytilus edulis and its distribution in the tissues. J Exp Mar Biol 23:71–84
Haemers S, van der Leeden MC, Koper GJM, Frens G (2002) Cross-linking and multilayer adsorption of mussel adhesive proteins. Langmuir 18:4903–4907
Haemers S, Koper GJM, Frens G (2003) Effect of oxidation rate on cross-linking of mussel adhesive proteins. Biomacromolecules 4:632–640
Hassenkam T, Gutsmann T, Hansma P, Sagert J, Waite JH (2004) Giant bent core mesogens in the thread forming process of marine mussels. Biomacromolecules 5:1351–1355
Helfman PM, Bada JL (1975) Aspartic acid racemization in tooth enamel from living humans. Proc Natl Acad Sci USA 72:2891–2894
Holten-Andersen N, Slack N, Zok F, Waite JH (2005) Nano-mechanical investigation of the byssal cuticle, a protective coating of a bioelastomer. Mater Res Soc Symp Proc 884:Y3.7.1/R3.7.1
Huang K, Lee BP, Ingram DR, Messersmith PB (2002) Synthesis and characterization of self-assembling block copolymers containing bioadhesive end groups. Biomacromolecules 3:397–406
Ito S, Kato T, Shinpo K, Fujita K (1984) Oxidation of tyrosine residues in proteins by tyrosinase. Detection of protein bonded 3, 4-dihydroxyphenylalanine and 5-S-cysteinylDopa. Biochem J 222:407–411
Jensen R, Morse DE (1988) The bioadhesive of Phragmatopoma californica tubes: a silk-like cement containing L-DOPA. J Comp Phys 158B:317–324
Jordan TE, Valiela I (1982) A nitrogen budget of the ribbed mussel, Geukensia demissa, and its significance in nitrogen flow in a New England saltmarsh. Limnol Oceanog 27:75–90
Kinloch AJ (1980) The science of adhesion, part 1. Surface and interfacial aspects. J Mat Sci 15:2141–2166
Klug CA, Burzio LA, Waite JH, Schaefer J (1996) In situ analysis of peptidyl DOPA in mussel byssus using rotational-echo double-resonance NMR. Arch Biochem Biophys 333:221–224
Koide M, Lee DS, Goldberg ED (1982) Metal and transuranic record in mussel shells, byssal threads and tissues. Estuarine Coast Shelf Sci 15:679–695
Kyte J (1995) Structure in protein biochemistry. Garland Publ, New York
Land EJ, Ramsden CA, Riley PA (2004) Quinone chemistry and melanogenesis. Methods Enzymol 378:88–109
Li K, Geng X, Simonsen J, Karchesy J (2004) Novel wood adhesives from condensed tannins and polyethylenimine. Int J Adhesion Adhesives 24:327–333
Masters P, Bada JL, Zigler JSJ (1977) Aspartic acid racemization in the human lens during aging and in cataract formation. Nature 268:71–73
McDowell LM, Burzio LA et al (1999) Rotational echo double resonance detection of cross-links formed in mussel byssus under high-flow stress. J Biol Chem 274:20293–20295
Nakamura K, Niki R (1993) Rheological properties of casein micelle gels: the influence of calcium concentration on gelation induced by rennet. Biorheology 30:207–216
Peter MG (1989) Chemical modifications of biopolymers by quinones and quinone methides. Angew Chem Int Ed 28:555–570
Prota G (1992) Melanins and melanogenesis, Academic Press, San Diego, CA
Qin X, Waite JH (1995) Exotic collagen gradients in the byssus of the mussel Mytilus edulis. J Exp Biol 198:633–644
Reissner KJ, Aswad DW (2003) Deamidation and isoaspartate formation in proteins: unwanted alterations or surreptitious signals? Cell Mol Life Sci 60:1281–1295
Robinson NE (2002) Protein deamidation. Proc Natl Acad Sci USA 99:5283–5288
Robinson NE, Robinson AB (2001a) Molecular clocks. Proc Natl Acad Sci USA 98:944–949
Robinson NE, Robinson AB (2001b) Prediction of protein deamidation rates from primary and three-dimensional structure. Proc Natl Acad Sci USA 98:4367–4372
Robinson AB, Rudd JC (1974) Deamidation of glutaminyl and asparaginyl residues in peptides and proteins. Curr Top Cell Reg 8:247–295
Sagert J, Waite JH (2005) The unstable functional chemistry of distal matrix protein-1 (submitted)

Schaefer J, Kramer KJ, Garbow JR, Jacob GS, Stejskal EO, Hopkins TL, Speirs RD (1987) Aromatic cross-links in insect cuticle: detection by solid-state ^{13}C and ^{15}N NMR. Science 235:1200–1204

Sever MJ, Weisser JT, Monahan J, Srinivasan S, Wilker JJ (2004) Metal mediated cross-linking in the generation of a marine-mussel adhesive. Angew Chem Int Ed 43:448–450

Stary Z, Andratschke I (1925) Beitrage zur Kenntnis einiger Skleroproteine. Z Physiol Chem 148:83–98

Stayton PS, Drobny GP, Shaw WJ, Long JR, Gilbert M (2003) Molecular recognition at the protein-hydroxyapatite interface. Crit Rev Oral Biol Med 14:370–376

Stewart RJ, Weaver JC, Morse DE, Waite JH (2004) The tube cement of Phragmatopoma californica: a solid foam. J Exp Biol 207:4727–4734

Sun CJ, Waite JH (2005) Mapping chemical gradients within and along a fibrous structural tissue. Mytilus byssal threads (submitted)

Suresh S (2001) Graded materials for resistance to contact deformation and damage. Science 292:2447–2451

Takasaki S, Kawakishi S (1997) Formation of protein-bound 3,4-dihydroxyphenylalanine and 5-S-cysteinyl-3,4-dihydroxyphenylalanine as new cross-linkers in gluten. J Agric Food Chem 45:3472–3475

Tamarin A, Lewis P, Askey J (1976) Structure and formation of byssus attachment plaque in Mytilus. J Morphol 149:199–221

Tateda Y, Koyanagi T (1986) Accumulation of radionuclides by common mussel Mytilus edulis and purplish bifurcate mussel Septifer virgatus. Bull Jap Soc Sci Fish 52:2019–2026

Taylor SW, Luther GW, Waite JH (1994) Polarographic and spectrophotometric investigation of Fe(III) complexation to DOPA-containing peptides and proteins from Mytilus edulis. Inorg Chem 33:5819–5824

Taylor SW, Chase DB, Emptage MH, Nelson MJ, Waite JH (1996) Ferric ion complexes of a DOPA-containing adhesive protein from Mytilus edulis. Inorg Chem 35:7572–7577

Van der Leeden MC (2005) Are conformational changes the underlying mechanism of controlling the adhesive activity of mussel adhesive proteins? Langmuir (in press)

Veis A, Sfeir C, Wu CB (1997) Phosphorylation of the proteins of the extracellular matrix of mineralized tissues by casein kinase-like activity. Crit Rev Oral Biol Med 8:360–379

Vitellaro-Zucarrello L (1981) Ultrastructural and cytochemical study on the enzyme gland of the foot of a mollusc. Tissue Cell 13:701–713

Vovelle J (1965) Le tube de Sabellaria alveolata (L) Annelide Polychaete Hermillidae et son ciment. Étude ecologique, experimentale, histologique, et histochimique. Arch Zool Exp Gen 106:1–187

Waite JH (1983) Evidence for a repeating 3, 4-dihydroxyphenylalanine and hydroxyproline containing decapeptide in the adhesive protein of the mussel Mytilus edulis. J Biol Chem 258:2911–2915

Waite JH (1990) Marine adhesive proteins: natural composite thermosets. Int J Biol Macromol 12:139–144

Waite JH (1992) Anatomy of a natural manufacturing process. In: Case ST (ed) Results and problems in cell differentiation, vol 19. Springer, Berlin Heidelberg New York, pp 27–54

Waite JH, (2002) Adhesion a la moule. Integr Comp Biol 42:1172–1180

Waite JH, Qin XX (2001) Polyphenolic phosphoprotein from the adhesive pads of the common mussel. Biochemistry 40:2887–2893

Waite JH, Jensen R, Morse DE (1992) Cement precursor proteins of the reef-building polychaete Phragmatopoma californica (Fewkes). Biochemistry 31:5733–5738

Waite JH, Qin XX, Coyne KJ (1998) The peculiar collagens of mussel byssus. Matrix Biol 17:93-108

Waite JH, Lichtenegger HC, Stucky GD, Hansma P (2004) Exploring molecular and mechanical gradients in structural bioscaffolds. Biochemistry 43:7653–7662

Waite JH, Holten-Andersen N, Jewhurst S, Sun CJ (2005) Mussel adhesion: finding the tricks worth mimicking. J Adhesion 81:297–317

Wang SX, Mure M, Medzihradsky KF, Burlingame AL, Brown DE, Dooley DM, Smith AJ, Kagan HK, Klinman JP (1996) A cross-linked cofactor in lysyloxidase: redox function for amino acid side chains. Science 273:1078–1084

Wang SX, Nakamura N, Mure M, Klinman JP, SandersLoehr J (1997) Characterization of the native lysine tyrosylquinone cofactor in lysyl oxidase by Raman spectroscopy. J Biol Chem 272:28841–28844

Weast RC (ed) (1983) Handbook of chemistry and physics. CRC Press, Boca Raton

Wiegemann M (2005) Adhesion in blue mussels (Mytilus edulis) and barnacles (genus Balanus): Mechanisms and technical applications. Aquat Sci 67:166–176

Xu C, Xu K, Gu H, Zheng R, Liu H, Zhang X, Guo Z, Xu B (2004) Dopamine as a robust anchor to immobilize functional molecules on the iron oxide shell of magnetic nanoparticles. J Am Chem Soc 126:9938–9939

Xu R, Huang X, Morgan TD, Prakash O, Kramer KJ, Hawley MD (1996) Characterization of products from the reactions of N-acetyldopamine quinone with N-acetylhistidine. Arch Biochem Biophys 329:56–64

Zhao H, Waite JH (2005) Plant cell wall-like protein from the green shell mussel Perna canaliculus. Biochemistry 44:15915–15923

Zhao H, Sun CJ, Stewart RJ, Waite JH (2005) Cemented sandcastles of Phragmatopoma californica. J Biol Chem (in press)

8 Barnacle Underwater Attachment

Kei Kamino

8.1 Introduction

Biological localization at an interface is ubiquitous behavior. An organism at an interface benefits from access to resources, protection from predators, and improved gene transfer. Many aquatic organisms specialize in localization at a liquid-solid interface, and to do so utilize a specific molecular system for underwater attachment. The mussel, a bivalve, and barnacle, a crustacean, are models for molecular research on underwater fixation by a permanent cement. In general, studies on underwater cement are hampered by such obstacles as the insoluble and/or sticky nature of the sample and poor development of micro-analytical methods for identifying the functions of underwater attachment. The multi-functionality of underwater attachment (Waite 1987) also complicates analyses, this multi-functionality referring to the cement being a complex structure consisting of many different parts, each of which may contribute in a different way.

Both model organisms employ a proteinaceous substance for underwater attachment, with the mussel byssus consisting of more than 95% protein and the barnacle cement consisting of more than 90%, and both being a multi-protein complex. The biochemical structure of each is quite different though. Recent work on barnacle cement has characterized the multi-functionality, and enabled a model for the molecular events to be proposed. Identification of the multi-functionality might be useful for protein/peptide-based material research (Sarikaya et al. 2003; Zhang 2003) and may also allow unknown functions in underwater attachment to be found. Furthermore, barnacle studies have suggested the significance of intermolecular non-covalent interaction, which is a likely trend in material science, i.e., supra-molecular chemistry (Whitesides and Boncheva 2002).

This chapter summarizes barnacle underwater attachment and the biochemistry of the underwater cement. Perspectives in material science are also discussed.

Marine Biotechnology Institute, 3-75-1 Heita, Kamaishi, Iwate 026-0001, Japan

Biological Adhesives
(ed. by A.M. Smith and J.A. Callow)

8.2 Barnacle Attachment

8.2.1 A Unique Sessile Crustacean

The barnacle is the only sessile crustacean. The adult acorn-type barnacle is covered with calcareous shell plates which are generally composed of four to six peripheral plates, four opercular valves, and a base plate (Fig. 8.1). All the shell plates are tightly pulled by a retractor muscle, making the barnacle look like a "pot". The adult firmly fixes its base to a foreign surface in the water via an underwater adhesive called "cement" (Walker 1972). This cement permanently bonds together two different materials, i.e., the base plate and the foreign material, in water. Once attached, neither the juvenile nor adult moves or self-detaches. The attachment strength is remarkably high, although an accurate survey of the strength on a naturally occurring substratum is difficult, because the body structure is destroyed by any attempt to dislodge it. In the case of attachment to the surface of a man-made anti-fouling coating, however, the animal has been dislodged from the substratum with a force of $0.1–0.3\times10^5$ (Nm^{-2}) (Watermann et al. 1997; Berglin et al. 2001; Kavanagh et al. 2003). Although the attachment strength of a small adult with a membranous base has also been determined to be 9.252×10^5 (Nm^{-2}) (Yule and Walker 1984), the strength of the adult barnacle with a calcareous base on a natural surface would be much more than those values.

Cirripedia are, in general, grouped into stalk and acorn types by their morphology, the acorn barnacle including both the calcareous and membranous

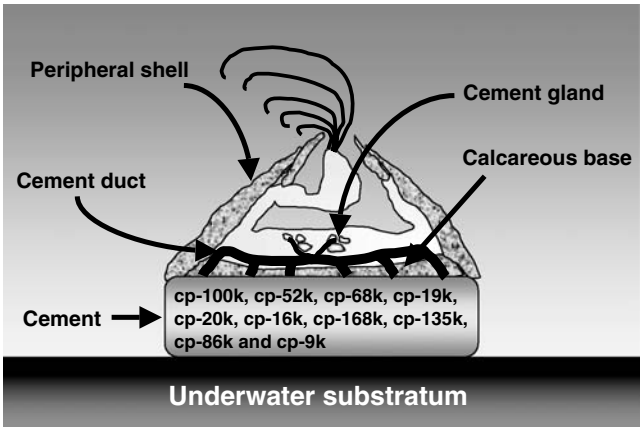

Fig. 8.1. Barnacle underwater attachment (Kamino, in press). The cross-section of a barnacle on a foreign substratum is shown schematically. The calcareous base is fixed to the foreign material via an underwater adhesive called cement. This cement is biosynthesized by the cement gland and transported through the duct to an interface filled with seawater. The cement permanently bonds together the two different materials. Once attached, the adult never moves or self-detaches. The cement layer in the illustration has been drawn thickly for emphasis

bases. This present review is concerned with the calcareous base acorn barnacle unless otherwise noted.

8.2.2 Attachment in the Life Cycle

After its metamorphosis from the nauplius larva, the cypris larva initiates exploring behavior for settlement, appearing to "walk on stilts"; a pair of antennules corresponds to the stilts. This behavior results in the cypris larva secreting mucous material from the tips of the antennules, leaving footprints on the surface (Walker and Yule 1984). Once the larva has settled, it undergoes metamorphosis and initiates the calcification process to form the shell plates. The juvenile develops into an adult with repetitive molting, calcification, and cementing.

There are three attachment processes in the barnacle life cycle: temporary attachment during the cypris exploring behavior, attachment with cypris cement for settlement, and permanent fixation by adult cement (Walker 1981). Cypris cement is secreted from a pair of larval cement glands. It passes through the collecting canal, cement duct and on to the adhesive disk, whereby the adhesive disk and fourth segment of the antennules are embedded by the cypris cement and attached to the foreign substratum. Adult cement glands start to secrete adult cement approximately 40 days later (Yule and Walker 1987). Although it has not been completely elucidated whether cypris cement and adult cement are heterogeneous, the lack of expression of adult cement protein genes (Sect. 8.3.5) in cypris larvae suggests that these are different substances. In this chapter, "barnacle" and "cement" refer to "adult" and "adult cement" respectively, unless otherwise stated.

8.2.3 Biosynthesis and Secretion of Underwater Cement

Histological studies (Lacombe 1970; Saroyan et al. 1970; Walker 1970; Fyhn and Costlow 1976) have identified the cement glands to be giant cells (200–300 μm in diameter) which are laid on connective tissue in close association with ovarian tissue and joined together by ducts. These ducts eventually lead to the base of the animal. A pushing action to secrete the cement has been suggested by the observation of a node-like structure at the joint of the duct. It has occasionally been observed that double or triple "dumpling"-like secondary cement gel (Sect. 8.3.2) was piled up on the barnacle calcareous base. This observation probably means that the first secretion is puffed out by the second secretion after rapid hardening of the first secretion, supporting the hypothesis of a pushing action for cement secretion.

The hypothesis that the cement gland biosynthesizes the cement proteins is supported by a northern blotting analysis using isotope-labeled DNA probes. This has indicated that the cement protein genes (Sect. 8.3.5) are only

expressed in the basal portion, where the cement gland is located, and not in the upper portion, where almost all the viscera is located (Kamino et al. 2000; Urushida et al., submitted; Kamino et al., submitted; Urushida Y, Yoshida M, Mori Y, Kado R, Kamino K, unpubl.). Both portions include body fluids, so expression in the body fluid cells is negligible.

While the soft tissue grows with repetitive molting, the peripheral and base plates grow by the calcification process. The enlarged marginal area in the calcareous base should be further fixed to the substratum, so it is assumed that the timing of cement secretion and/or cement gene-expression is tuned to the molting cycle. A histological study (Fyhn and Costlow 1976) has confirmed that a positive region of nucleic acid staining in the cement gland cell, i.e., a possible biosynthesis region, became enlarged immediately after molting, and subsequently reduced in size. It was also confirmed that the expression level of cement protein genes (Sect. 8.3.5) in a barnacle that has naturally attached to the substratum was higher after molting, before subsequently dropping to the base level (Urushida Y, Yoshida M, Kado R, Kamino K, unpubl.). The biosynthesis of cement proteins and molting are probably controlled together. However, if the barnacle has been carefully dislodged from the substratum without damage, the expression patterns of the cement protein genes seem not to be always guided in this manner. This is probably supported by the observation of individual differences in secondary cement secretion (Saroyan et al. 1970). More comprehensive studies into molting, calcification, and cementing are required.

8.3 Barnacle Underwater Cement

8.3.1 Cement Layer

The cement layer between the calcareous base and foreign substratum has been reported to be approximately 5 μm in thickness (Saroyan et al. 1970). However, the cement layer formed on an anti-fouling coating, i.e., poly(dimethylsiloxane) [PDMS], is thicker. The formation of this thick cement layer has been explained by Wiegemann and Watermann (2003). At the time of cement secretion, the retractor muscle pulls the peripheral shell plate downward. Since the fixation of the base shell plate to the anti-fouling coating is much weaker than to the natural substratum, this pulling action partially separates the base plate from the coating. The cement permeates to either the newly formed inter-space or to the separated old cement layer, with repeated cementing making the cement layer thicker. The cement layer seems not to have a macroscopic type of structure like the mussel holdfast called byssus, but instead a microscopic type. This latter type of structure will be discussed in Sect. 8.3.3.

8.3.2 Cement Sample

The cement has historically been characterized into two types, primary and secondary, based on the mode of formation (Saroyan et al. 1970). Primary cement is a material found in the narrow gap at the joint between the calcareous base and substratum when the animal is naturally attached in the water (Fig. 8.1). Secondary cement is an underwater secretion by the intact barnacle through the calcareous base after it has been dislodged from the substratum and is usually hardened, resulting in a white opaque jelly-like material. Both types of cement have been found to be proteinaceous substances (Walker 1972; Kamino et al. 1996). Primary cement is difficult to collect for detailed analysis, because the joint is usually less than 5 μm in thickness (Saroyan et al. 1970). Secondary cement, however, is much easier to collect. Correct identification of these two types of cement is essential for their study. The reattachment of a dislodged barnacle is accomplished by the secondary cement (Saroyan et al. 1970; Dougherty 1990), and the similarity in amino acid composition (Naldrett 1993), the similarity of peptide maps by cyanogen bromide (CNBr)-protein fragmentation (Kamino et al. 1996), and cross-reactivity of an antibody have enabled the secondary cement to be identified as almost the same as the primary cement in its protein composition, thus simplifying further biochemical analyses.

8.3.3 Cement Nature

The cement is primarily a proteinaceous substance. Quantification by an amino acid analysis has revealed the cement to consist of more than 90% protein (Walker 1972; Yan and Tang 1981; Kamino et al. 1996). Crude cement samples from several barnacle species have shown a similar amino acid composition (Walker 1972; Naldrett 1993; Kamino et al. 1996), such that an average composition can be applied (Nakashima et al. 1990). 3,4-Dihydroxy phenylalanine (DOPA), which is a common component in the foot proteins of the mussel, has not been found in barnacle cement (Naldrett 1993; Kamino et al. 1996). Several studies have focused on rendering the cement soluble for further analysis. Approaches to render soluble an insoluble proteinaceous substance would mainly be classified into partial proteolytic and non-proteolytic methods. Although it still remains to be fully accomplished, some researchers have nearly achieved it (Barnes and Blackstock 1976; Yan and Pan 1981; Naldrett 1993; Kamino et al. 1996; Naldrett and Kaplan 1997). Kamino et al. persevered with a development of the non-proteolytic method, whereby more than 90% of *M. rosa* cement could be rendered soluble without any hydrolysis of the proteins (Kamino et al. 2000). The method depends on heat-denaturation with higher concentrations of dithiothreitol and guanidine hydrochloride, both being indispensable to rendering soluble the cement proteins. The method has not been used on cement from species other than

M. rosa and *Amphibalanus amphitrite*, but there seems to be no reason why it should not be possible. This last method revealed the cement to be a multi-protein complex for the first time. The treatment has so far enabled three major cement proteins (CPs) and three minor CPs to be identified (Kamino and Shizuri 1998), while a further four CPs await identification. The six identified CPs each have characteristics distinct from each other, five of them being novel in their primary structure (see Sect. 8.3.5). These results have confirmed the cement to be a unique protein complex.

Differences in the microscopic structure of the cement according to the characteristics of the substratum, roughly equating to a "non-stick" surface or "easy-to-attach-to" surface have been noted (Wiegemann and Watermann 2003). The cement secreted by a barnacle attached to a "non-stick" surface such as PDMS is a swollen substance, and is formed by a loose network of hydrated adhesive threads. The cement from a barnacle on an "easy-to-attach-to surface" such as aluminum foil or polycarbonate is a dense sheet formed by a closely woven network of threads. The former has much lower adhesive strength than the latter. The difference in structure may be due to failure to form a strong attachment on the non-stick surface, thus leading to an artifactual structure.

8.3.4 Multi-functionality in Underwater Attachment (Kamino, in press)

Underwater attachment is actually a rapid multi-step process (Waite 1987), and can only be accomplished by fulfilling all the requirements in the correct order with proper timing (Fig. 8.2). An underwater cement needs the

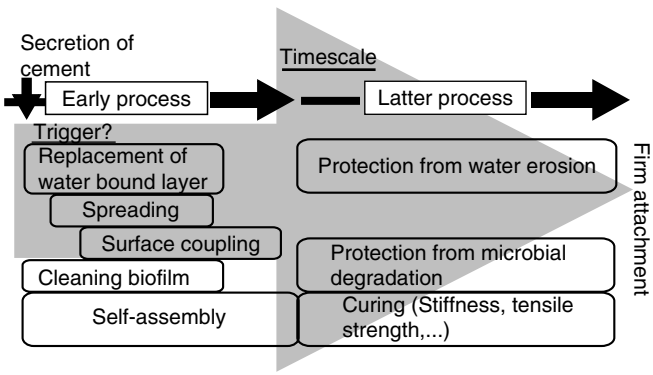

Fig. 8.2. Multi-functionality in underwater attachment (Kamino 2005). Underwater attachment can only be accomplished by fulfilling all the requirements in the correct order with proper timing. The principle of underwater attachment cannot be expected to be analogous to that of a man-made synthetic adhesive. Each function involved in underwater attachment is attractive for developing material science

ability to prevent random aggregation during transport via the duct, to displace sufficient seawater to prime and spread on the surface without being dispersed in the water, to couple strongly with a variety of material surfaces, and to self-assemble itself to join the calcareous base and the substratum. After the initial process, it is then necessary to cure the cement so that the holdfast remains stiff and tough, and to protect it from continuous water penetration/erosion and microbial degradation. The underwater cement can orchestrate all these requirements, thus allowing the barnacle to inhabit the liquid-solid interface. This orchestration distinguishes the barnacle cement from man-made cements. Since underwater attachment is only possible by accomplishing all the functions in the correct order with proper timing, and the cement is a multi-protein complex, proper micro-analytical methods for each function need to be developed before there can be any research advances. These two current obstacles are common to biotic underwater adhesive studies. Each cement protein has unique characteristics as described in the next section. The individual cement proteins are presumed to cooperate for underwater attachment, each protein specializing in at least one of the functions required to achieve underwater attachment. The cement is therefore a self-organizing, multi-protein and multi-functional complex.

8.3.5 Cement Proteins and Possible Functions

The cement is composed of more than 10 cement proteins (CPs), of which four have not yet been identified. Five of the six identified CPs are novel in respect of their primary structure, and the six CPs can be classified into four categories. The cement proteins are identified by their apparent molecular weight, as estimated by SDS-PAGE, and the unique characteristics of these six CPs are summarized next.

8.3.5.1 CP-100k and CP-52k

CP-100k and CP-52k are two major proteins in the cement with similar protein contents (Kamino et al. 2000). Both proteins also have similar behavior during solubilization, as the DTT/GdnHCl-denaturing treatment is the only non-hydrolytic method known to render these proteins soluble. Both cement proteins were first isolated from *M. rosa* cement. Further isolation of CP-100k in *A. amphitrite* cement allowed universal PCR primers to be designed, whereby several CP-100k homologous genes were isolated from species including *Fistrulobalanus albicostatus, B. trigonus, B. rostratus, and Semibalanus cariosus* (Urushida Y, Syougaki N, Kasai H, Kado R, and Kamino K, unpubl.). cDNA cloning indicated both CP-100k and CP-52k to be novel from database searches, and to have low homology to each other. The primary structure of

CP-52k contains an approximately 120 amino acid-long low-homologous repetitive sequence, while there is no repetitive sequence in CP-100k. CP-100k and CP-52k are both highly hydrophobic, and composed of a relatively low number of Cys residues (1.4% and 1.1%, respectively). Although the reason why an excess amount of reductant is required to render these proteins soluble is not yet known, it may be due to disulfide bonds that hold the individual protein molecule in a shape that strengthens intermolecular non-covalent bonding such as that involved in hydrophobic interaction. A denaturation treatment by using GdnHCl and heating would loosen the intermolecular hydrophobic barrier, whereby an excess amount of a reductant could cleave the disulfide bonds. Cleavage of the disulfide bonds may make the molecular conformation flexible, thus further weakening the intermolecular interaction and finally rendering these proteins soluble. Although there are no data to indicate whether the disulfide bonds in these CPs are intramolecular or intermolecular, this author leans toward the hypothesis that intermolecular non-covalent interaction is the major contributor in initial self-assembly of the cement and that intramolecular disulfide bonds in CP-100k and CP-52k contribute to the stability of each molecular conformation. Intermolecular non-covalent interaction is unusually strong when the molecular conformation is optimized for mutual interaction. This has particularly been shown in the assembly of beta-sheet protein (Otzen et al. 2000). This hypothesis does not exclude further intermolecular cross-linking, including other types and exchange of disulfide bonds in the curing process. Such cross-linking could account for the proteinaceous fraction amounting to about 10% in the cement, named the GdnHCl-insoluble fraction (GIF) (Kamino et al. 2000), which is not soluble with repeated DTT/GdnHCl treatment. Moreover, biochemical analyses have been mainly focused on freshly collected secondary cement, so the degree of curing may have been insufficient.

The similarities in solubility, contents, and high hydrophobicity have suggested that both CP-100k and CP-52k play a similar role in underwater attachment. They may provide an insoluble framework for other proteins; for example, while the CP-68k and CP-19k cement proteins are partially soluble in a GdnHCl solution, they are completely soluble in DTT/GdnHCl, possibly due to destruction of the insoluble framework formed by CP-100k and CP-52k. Thus, CP-100k and CP-52k are the bulk materials in the cement, and are thought to tie up other cement proteins and give the framework that provides adhesive strength. Although the involvement of CP-100k and CP-52k in the curing process is likely, there have only been limited studies on the process as already mentioned. There has long been speculation about the involvement of DOPA-mediated cross-linking (Lindner and Dooley 1973) similar to that in mussel byssus (Deming 1999), but the absence of DOPA from barnacle cement is now evident (Naldrett 1993; Kamino et al. 1996). Elucidation of the curing process, including unknown types of cross-linking and the contribution of inorganic ions, should be continued.

8.3.5.2 CP-68k

Another major cement protein is CP-68k (Kamino et al. 2000). CP-68k is not extractable from the cement in pure water, but is partially soluble in a GdnHCl solution, and rendered completely soluble by the DTT-GdnHCl treatment which rendered CP-100k and CP-52k soluble for the first time. Therefore, CP-68k is presumed not to be covalently connected to CP-100k and CP-52k, but to be embedded in their framework. CP-68k is known to be glycosylated (Kamino et al., submitted), and is characterized by an amino acid composition of Ser, Thr, Ala, and Gly evenly comprising 60% (Kamino et al. 1996). CP-68k has been isolated from both *M. rosa* and *A. amphitrite*, each with a similar amino acid composition (Fig. 8.3), although the sequence homology was low (47% identical, and 65% similar). Naldrett and Kaplan (1997) have found a 58-kDa protein in *Amphibalans eburneus* cement that had a similar amino acid composition, and may have been a CP-68k homologue. An attempt to design a universal PCR primer failed, probably due to the high amino acid exchange rate in the protein. It is likely that the functional significance of CP-68k is based on the content of the four amino acids.

The alignment of the two CP-68ks indicates that the primary structure is divided into two regions: a long Ser-, Thr-, Ala-, and Gly-rich N-terminal region, and a short C-terminal region composed of much less of these four amino acids and more of such amino acids as Lys, Pro, Trp, Cys, and hydrophobic types

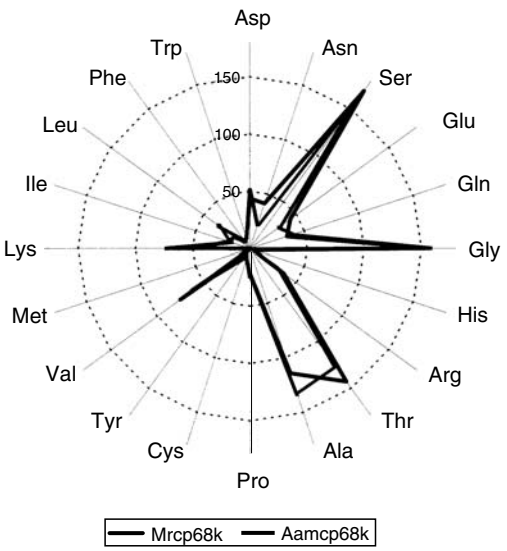

Fig. 8.3. Similarity between CP-68k and CP-19k in their amino acid bias and segment structure (Kamino, in press): (a) Ser, Thr, Gly, and Ala are predominant in CP-68k, and represent the outstanding components. CP-68k from *M. rosa* and *B. amphitrite*, although each had a similar amino acid composition, had low sequence homology (47% identical, and 65% similar);

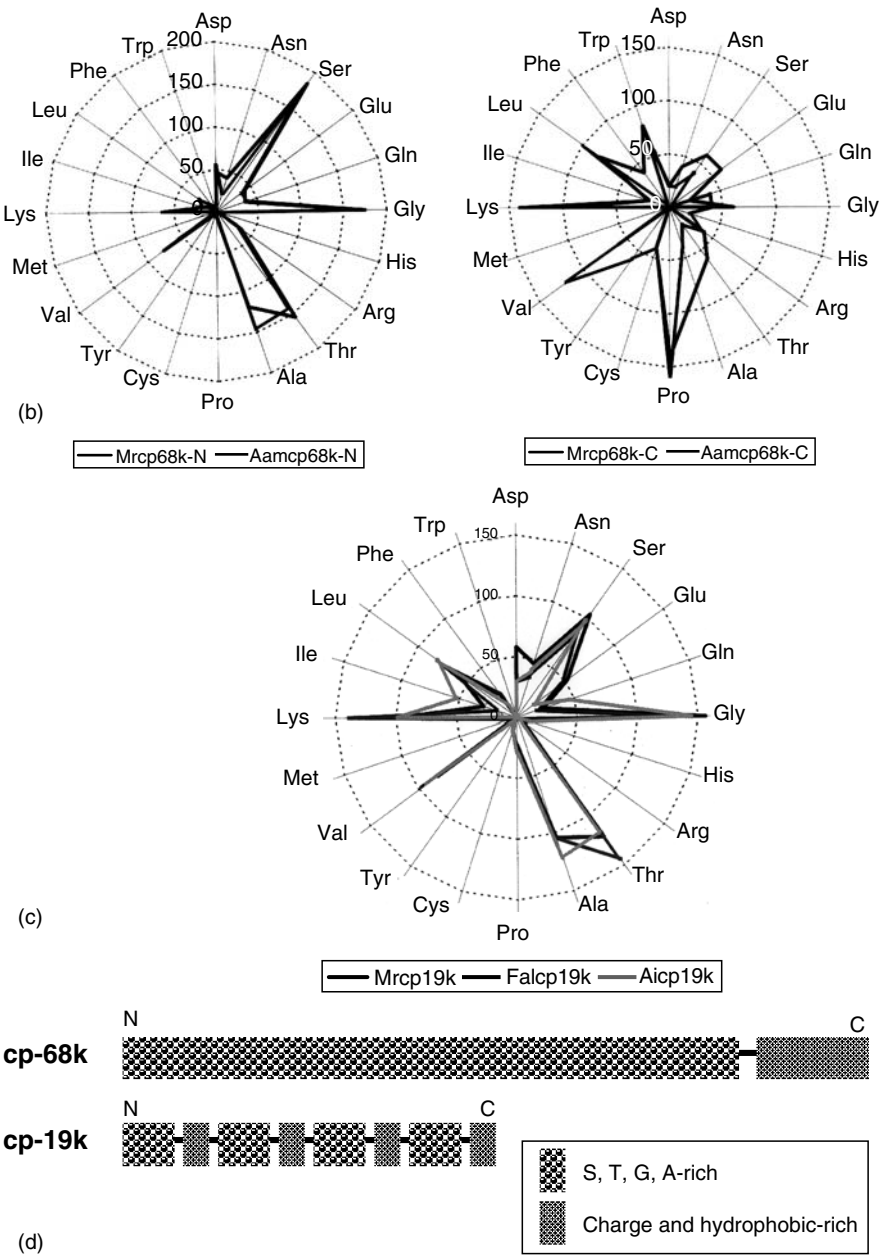

Fig. 8.3. (b) the primary structure of CP-68k is divided into two regions: a long Ser, Thr, Ala, and Gly-rich N-terminal region, and a short C-terminal region composed of much less of the four dominant amino acids in the N-terminal region and of such amino acids as Lys, Pro, Trp, Cys, and hydrophobic amino acids; (c) the high-content amino acids were the same in both the CP-68k and CP-19k proteins, indicating that these proteins probably contribute to a similar function. There was no homology between CP-19k and CP-68k in their primary structures;

(Fig. 8.3). The C-terminal region may have a compact conformation, because Pro, Trp, and the hydrophobic amino acids are generally advantageous for packing into this structure by their backbone fixation, pi-pi stacking, and hydrophobic core formation. If we accept the hypothesis that those amino acids contribute to structural stabilization, the molecular surface would be covered with a strong charge due to the Lys residues, and this charge might be essential to the function of the C-terminal region. The N-terminal region has a thin polypeptide chain whose surface is probably covered with such amino acids as Ser and Thr residues and the glycosyl moiety. It may be thought that many of the Ser and Thr residues would contribute to *O*-linked glycosylation sites; however, SDS-PAGE of a bacterial recombinant, which would not be post-translationally modified, gave only slightly higher gel-migration than that of the protein purified from the cement. This suggests that the glycosyl moiety in MrCP-68k was limited in amount, so that the hydroxyl groups in almost all Ser and Thr were probably free. An essential element in the CP-68k protein for its function might therefore be the dominant hydroxyl group on the molecular surface of the N-terminal region and the charge on that of the C-terminal region. Ala is also common in CP-68k. In the anti-freeze protein, which is a binding protein to the ice nucleus to inhibit crystal growth in the cytosolic space of several organisms (Fletcher et al. 2001), the Ala and/or methyl group of Thr on the molecular surface are known to be essential in the process of binding to the ice nucleus (Zhang and Laursen 1998; Jia and Davies 2002), although the role of the amino acids is not yet clearly understood. Analogously, the hydrophobicity of the side chains on abundant Ala and part of Thr may play a pivotal role in interacting with the aqueous layer bound to the material surface.

A possible function of CP-68k is as a priming and surface-coupling molecule. An underwater glue is first required to approach the liquid-solid interface without being dispersed in the surrounding seawater. Functions called “priming”, “spreading”, and “condensation” are the most elusive functions in underwater attachment, and we have not yet been able to elucidate the mechanism for these functions. Waite has attempted to explain the molecular event with the primer by classifying the targeted solid surfaces as non-polar and polar (Waite 1987). Water would weakly bind to an underwater non-polar surface, and a macromolecule with many hydroxyl groups may be a good primer to displace this water. Such a molecule, however, may not have sufficient ability to displace any water that is strongly bound to an underwater polar surface; therefore, additional guidance would be required in the molecular event. In the case of mussel foot proteins (FPs), the catechol moiety of DOPA residues is a possible activator for priming the polar surface by its strong surface-coupling ability. In respect

(d) CP-68k is composed of a long [Ser, Thr, Gly, and Ala]-rich segment and short [charged and hydrophobic amino acid]-rich one. Careful observation and a bioinformatic analysis of CP-19k suggested four alternating repetitions of two short segments: a [Ser, Thr, Gly, and Ala]-rich segment and [charged and hydrophobic amino acid]-rich one. The segmental structure is similar in the two proteins

of CP-68k, the dominant hydroxyl group on the molecular surface of the N-terminal region may be useful for priming activity. The strong charge on the molecular surface of the C-terminal region may contribute to surface coupling with the polar surface, and may also assist with priming to an underwater polar surface.

8.3.5.3 CP-20k

Several other proteins are also present in small amounts in the underwater cement, although their content does not directly suggest any functional significance in underwater attachment. CP-20k has been identified as a simple 20-kDa protein and a minor cement protein (Kamino 2001). This protein is characterized by the abundance of charged amino acids and Cys residues. Of these charged amino acids, Asp, Glu, and His comprise 32% and Cys comprises 17% of the protein. Time-of-flight mass spectrometry has shown the protein recovered in the GdnHCl-soluble fraction designated GSF1 or in the pure-water extract to have the mass of a monomer, thus precluding any intermolecular disulfide bond formation in CP-20k. The fact that this protein has not been recovered in the DTT/GdnHCl-treated soluble fraction designated GSF2 also indicates no formation of intermolecular disulfide bonds among the other cement proteins. If anything, the lack of reactivity with alkylating agents suggests that all Cys in the protein has formed intramolecular disulfide bonds. Our recent NMR analysis of the recombinant in *E. coli* has indicated that an intramolecular disulfide bond in the protein was essential for stabilizing the conformation (Suzuki et al. 2005). Thus, the abundant Cys in CP-20k was more essential for the structure than for the function. Since the protein was composed of a much lower number of hydrophobic amino acids than usual, many intramolecular disulfide bonds may have been introduced to compensate for the poor hydrophobic core formation. Although polymerization by CP-20k based on intermolecular disulfide bonds has been discussed for cement curing elsewhere (Wiegemann and Watermann 2003), experimental data do not support this hypothesis for the function of this protein.

The primary structure of CP-20k was found to comprise six repetitions when the Cys residues were appropriately aligned. However, except for Cys and Pro, the amino acids were not at all conserved among the repetitive modules. The results of an NMR study seem to support the notion of three units being the minimum structural unit (Suzuki et al. 2005).

Such abundant charged amino acids as Glu, Asp, His, Lys, and Arg would be positioned on the molecular surface and would thus be essential for the function in underwater attachment. The isolation of a homologous gene from *B. albicostatus* has revealed the high content of charged amino acids and Cys to be of conserved chemical character, although the homology between MrCP-20k and the *B. albicostatus*-homologous protein was remarkably low

(Mori et al., in prep.). These results confirm the functional significance of the charged amino acids in CP-20k. Our recent analysis of the bacterial MrCP-20k recombinant has indicated that the protein had no adsorption activity to a glass surface in seawater, but had adsorption activity to calcite in seawater and formed an oligomer in seawater. Since the base and periphery of a barnacle shell are composed of calcite, CP-20k may be a specific coupling agent to the barnacle's own calcareous base and to another barnacle shell. Lateral interaction among the CP-20k molecules on a calcite surface may assist in the "spreading" action by surface-effective alignment, while oligomerization of CP-20k in seawater may indicate something of a function.

8.3.5.4 CP-19k

CP-19k (Urushida et al., submitted) is a minor cement protein and a simple protein. Like CP-68k, this protein has been recovered in the solubilization process from cement in both GSF1 and GSF2. CP-19k is characterized by a similar amino acid bias to that of CP-68k (Fig. 8.3), with the six amino acids, Ser, Thr, Gly, Ala, Lys, and Val, comprising more than 67% of the total. The development of a universal PCR primer has allowed us to amplify homologous cDNA from other species, whereby the primary structures from *M. rosa, B. albicostatus,* and *B. improvisus* have so far been elucidated. The homology among the three CP-19ks is as follows: 51% for the *Mr* vs *Bal* proteins, 54% for the *Mr* vs *Bi* proteins, and 60% for the *Bal* vs *Bi* proteins. No simple repetitive sequence could be found in the primary structures. This bias in the contents of the six amino acids in CP-19k is probably of functional significance. There is no homology between CP-19k and CP-68k in their primary structures, although the high-content amino acids are the same in both proteins. This may indicate that these proteins probably contribute to a similar function. Careful observation and a bioinformatics analysis have suggested four alternating repetitions of two short segments, these being a [Ser, Thr, Gly, and Ala]-rich segment and [charged and hydrophobic amino acid]-rich one (Fig. 8.3).

CP-19k has been successfully expressed in the soluble fraction of *E. coli*. Purification of the recombinant allowed it to be characterized, and adsorption to a glass surface (Urushida et al., submitted), SiO_2-modified surface, and TiO_2-modified surface (Urushida Y, Sano K, Shiba K, Kamino K, unpubl.) in seawater has been demonstrated. How CP-19k couples to different surfaces is intriguing, and is now under investigation. Thus, the possible function of CP-19k is coupling to a foreign material surface, although other surface activity, including priming and spreading, also needs to be carefully considered. Although CP-68k and CP-19k are different proteins, they should strictly play similar but distinct roles in underwater attachment. Finding the difference between these proteins awaits a detailed analysis.

8.3.5.5 CP-16k

CP-16k is a minor cement protein, and can be extracted in GSF1 from the cement. The primary structure shares 47% homology with lysozyme-P in *Drosophila melanogaster*, with all catalytic amino acids and Cys being conserved. The crude cement shows lytic activity to the *Micrococcus luteus* membrane fraction, so CP-16k is probably a lysozyme (Kamino and Shizuri 1998). Its possible sub-functions include removing biofilm from the substratum and/or protecting the cement from microbial degradation.

Both primary and secondary cement is usually collected by very gently scraping the surface of the calcareous base. Some may raise the possibility of contamination by calcification proteins. If this were so, this protein should also be contained in the peripheral shell. In contrast, if the protein cannot be found in the peripheral shell, this would confirm it to be a cement protein. The peripheral shell and base shell were each decalcified and subjected to western blotting. All CPs, except for CP-16k (the antibody for CP-16k was not then available), were conclusively confirmed to be cement proteins (Urushida Y, Yoshida M, Kado R, Kamino K, unpubl.).

As briefly mentioned in Sect. 8.2.3, five CP genes, excepting CP-16k, were highest in their expression level just after molting, before decreasing to the basic level. The expression patterns of these five genes were consistent in a northern blotting analysis, confirming that at least five CPs were part of a multi-protein complex.

8.3.6 Possible Molecular Model for Barnacle Underwater Attachment

Adhesion would begin with cement being extruded from the duct to seawater, filling the narrow inter-space between the calcareous base and the substratum. Several functions in underwater attachment would then need to be fulfilled as molecular-guided events. The target molecules for cement proteins can be placed in these categories: the foreign material surface, water molecules, and homogenous/heterogeneous cement protein molecules. Thus, each cement protein contributes to underwater attachment via interaction with some of the targets (Fig. 8.2). The amino acid bias seems to be ubiquitous in cement proteins, and the biased amino acids are presumed to be essential for interaction with the target. Taken together with recombinant characterization and indirect evidence, the model shown in Fig. 8.4 is suggested for the molecular events in underwater attachment.

The instantaneous function would include the displacement of water bound to the material surface, and spreading and coupling after the extrusion of cement from the duct. CP-68k and CP-19k are candidates for these functions. The characterization of the bacterial CP-20k recombinant suggests a specific coupling agent to its own base or to the peripheral shell of another barnacle. Homo-interaction among the CP-20k molecules may also be

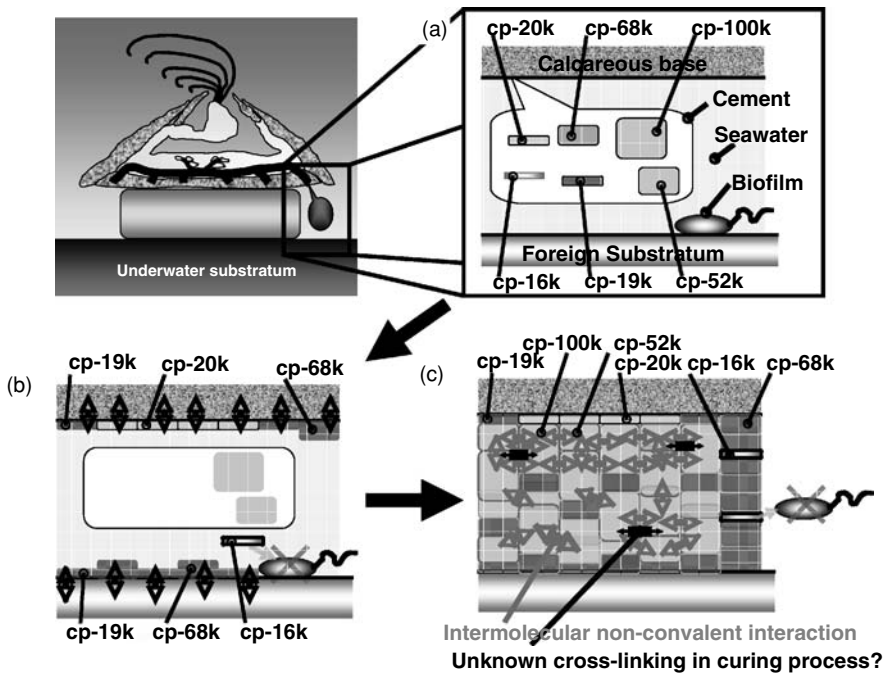

Fig. 8.4. Hypothetical model for molecular events in barnacle underwater attachment: (a) cement is secreted into the seawater-filled space between the calcareous base and foreign substratum; (b) the possible primer and coupling agents, CP-19k, CP-20k, and CP-68k, form a layer on both surfaces of the calcareous base and foreign substratum. CP-16k may also remove the bio-film layer almost simultaneously; (c) CP-100k and CP-52k form a network by intermolecular non-covalent interaction, and other CPs are associated together. Following self-assembly, curing may occur to make the holdfast stiff and tough, whereby further intermolecular cross-linking may be involved in the process. Daily protection from bacterial degradation might also be significant for the formation of a long, stable holdfast, with CP-16k being a candidate for this function

involved with the spreading function on to the substratum. CP-16k may also help spreading and adsorption by removing the layer of organic substances and biofilm that cover almost all material surfaces in the environment.

Almost simultaneously or immediately after successful coupling between the substratum and its own calcareous base, cement proteins must be self-assembled together to join the two materials. CP-100k and CP-52k might quickly form a network by intermolecular hydrophobic interaction or by another mechanism, so that other CPs are associated together. Following this self-assembly, curing may occur to make the holdfast stiff and tough, whereby further intermolecular cross-linking may be involved in the process. Daily protection from bacterial degradation might also be significant for forming a durable holdfast, and CP-16k is a likely candidate for this function. It is

uncertain if there is a protein that is necessary to protect from continuous water penetration. A man-made synthetic adhesive usually relies on water being absent. If we consider the design criteria for a man-made synthetic adhesive, the function against water penetration is assumed to be vital. However, barnacle underwater cement is protein-made, and constitutive water molecules would be essential to stabilize the molecular conformation. It is therefore likely that a biotic underwater adhesive works in concert with water. This may be an element common to the structure of all cement proteins.

During transportation through the duct in the animal, the function of the CP mixture may be controlled or the mixture may be a precursor, because the narrow duct could become clogged by premature initiation of the functions. Although the trigger factor is not yet known, there are several possible mechanisms for this, including conformational change of each protein molecule and processing by proteolysis or protein modification. In either case, a salinity change, specific metal interaction, and extrusion pressure may each be candidates for triggering the conformational change or activation of the processing enzyme. Dougherty has reported possible exo-carboxypeptidase activity in the cement of *Chthamalus fragilis* (Dougherty 1997). The trigger mechanism is not necessarily a single activity and might depend on the protein. In any case, the conformational change is very rapid, being fascinating as an instantaneous function.

8.4 Comparison with Other Holdfast Proteins

The counterpart to consider in a biotic underwater cement study is the mussel foot protein (Rzepecki and Waite 1995; Taylor and Waite 1997; Waite 1999; Sagert et al., this volume), although no homology at all has been found in the primary structures between mussel foot proteins and barnacle cement proteins. The mussel holdfast, the byssus, is composed of macroscopically or microscopically separate modular structures. The adhesive plaque is distally coupled with the foreign surface. The bulk of the plaque consists of a solid foam-like structure composed primarily of Cys-rich DOPA-containing foot proteins. The boundary between the plaque and substratum consists of small DOPA-containing foot proteins, while the thread consists of a collagenous material forming a stiff distal zone and an elastic proximal zone. The surface of the byssus is coated with a thin layer (5–10 μm) that is also rich in DOPA-containing foot proteins. A mussel holds itself with byssus as a whole against strong and repeated shock by waves and currents. On the other hand, a barnacle attaches directly to the substratum by its whole base via cement, this cement seeming not to have a macroscopically modular structure. This difference is also apparent from the distribution of the secretory glands. In the mussel foot, several glands specializing in the biosynthesis of individual foot proteins are appropriately aligned along the longitudinal

axis of the ventral groove in the foot (Waite 1992), making possible a macroscopically modular structure. In the barnacle, however, only the cement gland has been found so far, and all cement proteins seem to be secreted together via the duct system.

The mussel adhesive proteins found at the interface (FP-3 and FP-5) are typically small (6–10 kD) with substantial post-translational modification to DOPA, *O*-phosphoserine, and 4-hydroxyarginine. These proteins are probably involved in the displacement of the water layer, and spreading and/or surface coupling. Many studies have shown the catechol group in the DOPA residue to be versatile, and it is speculated to be involved in such functions as surface coupling (Fant et al. 2002; Hansen et al. 1998; Suci and Geesey 2001), curing (Ooka and Garrel 2000; McDowell et al. 1999; Sever et al. 2004; Deming 1999; Holl et al. 1993) and fiber elasticity (Sun and Waite 2005). *O*-Phosphoserine might have the special function of coupling to calcareous material such as the shell surface of other mussels and barnacles (Waite and Qin 2001). Such remarkable and attractive individuality as DOPA and *O*-phosphoserine in the mussel is not apparent in barnacle cement proteins. However, characterization of the bacterial recombinants of CP-20k has suggested this to be a calcite-specific coupling protein. The characterization of the bacterial CP-19k recombinant and its similarity to CP-68k has suggested that these proteins are possible coupling and/or priming agents. In the case of barnacle cement proteins, orientation of the side chain in the common amino acids may be optimized by the protein-molecular conformation to perform the same functions as the versatile modified amino acid residues in the mussel.

CP-100k and CP-52k of the barnacle cement proteins are hydrophobic, resulting in the formation of an insoluble framework, and these proteins are probably involved in the association of cement and/or curing. The bulk of the adhesive plaque in the mussel is formed by FP-2 and FP-4. No hydrophobic protein has so far been found in mussel foot proteins, so cross-linking has been suggested as the major contributor to the organization of FPs. A single thread is formed at a time in producing the mussel byssus. Thus, all functional processes including curing must be completed at once, very rapid processing being required to achieve this. In contrast, most barnacle cement is added to the enlarged marginal area as the animal grows or repairs the cement layer that has already been formed. Curing may not be urgent with barnacle cement, because the cement layer which has already been formed would assist the holdfast. The curing process for barnacle cement may therefore be relatively slow, and studies should pay further attention to this aspect.

Protection from bacterial degradation is a possible function required by an extra-cellular proteinaceous structure. The mussel byssus is evidently protected by being varnished with FP-1 which is cross-linked via the DOPA residue. Barnacle cement provides lytic activity originating from CP-16k, a lysozyme homologue, and this is probably useful for protecting the cement.

These two typical sessile organisms, the mussel and barnacle, have evidently evolved individually in respect of their molecular systems for cementing.

8.5 Applications to Material Science

In contrast to mussel byssus studies, barnacle cement studies have had less impact on material science, probably due to the absence of a versatile modified amino acid residue such as DOPA. The characterization of each bacterial recombinant suggested that the multi-functionality in cement can be dissected. The functions involved in underwater attachment are attractive to material science, making each cement protein a possible model for developing a protein/peptide-based material.

Molecular self-assembly is one of most attractive events in supramolecular chemistry (Whitesides and Boncheva 2002), nano-scale technology (Zhao and Zhang 2004), and tissue engineering. Peptide-based materials offer great advantages in interdisciplinary biotechnological material science due to their huge molecular diversity, simple design from protein-based biomolecular materials, easy insertion of a biological motif, and freedom from contamination of viral and prion origin in their production. Although several peptide self-assemblies have so far been designed, amphiphilicity and a beta-sheet structure have been preferentially studied (Zhang 2003).

Peptides whose primary structures have been designed from the repetitive sequences in CP-20k were chemically synthesized, and their ability for self-assembly under several salt concentrations was evaluated by using dynamic light scattering (DLS) measurement, atomic force microscopic (AFM) imaging, and SEM observation (Nakano et al., submitted). The DLS measurements suggested an increase in the apparent molecular size of a peptide with the addition of several kinds of salt. The peptide was soluble in water, and self-assembly was suddenly triggered by more than 0.4 mol/l of NaCl. AFM imaging indicated that the peptide assembly had a consistent rod shape of 100 nm in width. A similar molecular assembly was also confirmed by SEM observation. A higher peptide concentration resulted in the formation of macroscopically observable and handleable membranous material. Peptides designed from the CP-20k underwater adhesive protein had self-assembly activity with a threshold near 0.5 mol/l of NaCl concentration, which is close to that of seawater. The consistent diameter of the peptide suggests its ordered self-assembly. An analysis of the self-assembly process indicated that self-assembly upon the addition of salt was based on non-covalent molecular interaction. The peptides examined in this study contained numerous charged amino acids, few hydrophobic amino acids, had no simple amphiphilicity and had no beta-sheet structure; therefore, self-assembly of these peptides may lead to novel principles for peptide self-assembly. Images indicating extension of the long axis were also captured, and it is suggested that improving the peptide

sequence by molecular engineering and different self-assembly conditions might lead to the development of various peptide-based materials. Peptide-based design of materials from underwater cement proteins with individual underwater attachment functions is a promising future application.

8.6 Concluding Remarks

Barnacle underwater attachment is basically a molecular-led event. A multi-protein complex handles the multi-functionality of this underwater attachment, which is based on a different principle from that of man-made adhesives. A detailed analysis of the multi-protein complex and future reconstruction study would help to elucidate the specific functions involved in underwater attachment, and might lead to the future design of novel materials. The study of barnacle cement has also suggested the significance of non-covalent molecular interaction, and highlighted the importance of identifying the orientation of the functional group, i.e., solving the protein structure-function relationships. In contrast, finding a novel functional group, e.g., DOPA in a mussel study, has had a direct impact on material science. Efforts to find such a versatile structural unit, i.e., post-translational modification in the curing process, are to be encouraged. Further research objectives also include the cell biology, adaptability to various material surfaces, and mesoscopic structure of the cement layer. Recent barnacle studies have enabled the initial molecular model for underwater attachment to be designed, although verification and repeated refining of this model are essential. The doorway to molecular studies on barnacle underwater attachment has now been reached.

Acknowledgments. Some of this work was performed as part of The Industrial Science and Technology Project entitled "Technological Development for Biomaterials Design Based on Self-organizing Proteins" supported by New Energy and Industrial Technology Development Organization (NEDO).

References

Barnes H, Blackstock J (1976) Further observations on the biochemical composition of the cement of *Lepas Fascicularis Ellis* & *Solander*; electrophoretic examination of the protein moieties under various conditions. J Exp Mar Biol Ecol 25:263–271

Berglin M, Larsson A, Jonsson PR, Gatenholm P (2001) The adhesion of the barnacle, *Balanus improvisus*, to poly(dimethylsiloxane) fouling-release coatings and poly(methyl methacrylate) panels: the effect of barnacle size on strength and failure mode. J Adhesion Sci Technol 15:1485–1502

Deming TJ (1999) Mussel byssus and biomolecular materials. Curr Opin Chem Biol 3:100–105

Dougherty WJ (1990) Barnacle adhesion: reattachment of the adult barnacle *Chthamalus fragilis* Darwin to polystyrene surfaces followed by centrifugational shearing. J Crustacean Biol 10:469–478

Dougherty WJ (1997) Carboxypeptidase activity of the zinc metalloprotease in the cement precursor secretion of the barnacle, *Chthamalus fragilis* Darwin. Comp Biochem Physiol 117B:565–570

Fant C, Elwing H, Höök F (2002) The influence of cross-linking on protein-protein interactions in a marine adhesive: the case of two byssus plaque proteins from the blue mussel. Biomacromol 3:732–741

Fletcher GL, Hew CL, Davies PL (2001) Antifreeze proteins of teleost fishes. Annu Rev Physio 63:359–390

Fyhn UE, Costlow JD (1976) A histochemical study of cement secretion during the intermolt cycle in barnacles. Biol Bull 150:47–56

Hansen DC, Corcoran SG, Waite JH (1998) Enzymatic tempering of a mussel adhesive protein film. Langmuir 14:1139–1147

Holl SM, Hansen D, Waite JH, Scaefer J (1993) Solid-state NMR analysis of cross-linking in mussel protein glue. Arch Biochem Biophys 302:255–258

Inoue K, Takeuchi Y, Miki D, Odo S, Harayama S, Waite JH (1996) Cloning, sequencing and sites of expression of genes for the hydroxyarginine-containing adhesive-plaque protein of the mussel *Mytilus galloprovincialis*. Eur J Biochem 239:172–176

Jia Z, Davies PL (2002) Antifreeze proteins: an unusual receptor-ligand interaction. Trends Biochem Sci 27:101–106

Kamino K (2001) Novel barnacle underwater adhesive protein is a charged amino acid-rich protein constituted by a Cys-rich repetitive sequence. Biochem J 356:503–507

Kamino K (2005) Barnacle underwater adhesive: complexity from multi-functionality in a multiprotein complex. In: Nagabhushanam R, Fingerman M (eds) Recent advances in marine biotechnology. Science Publ, Enfield, New Hampshire, USA, pp 537–557

Kamino K, Shizuri Y (1998) Structure and function of barnacle cement proteins. In: Le Gal Y, Halvorson H (eds) New developments in marine biotechnology. Plenum Press, New York, pp 77–80

Kamino K, Odo S, Maruyama T (1996) Cement proteins of the acorn barnacle, *Megabalanus rosa*. Biol Bull 190:403–409

Kamino K, Inoue K, Maruyama T, Takamatsu N, Harayama S, Shizuri Y (2000) Barnacle cement proteins. J Biol Chem 275:27360–27365

Kamino K, Sasaki F, Urushida Y, Shizuri Y, Inoue N, Kanai S Barnacle underwater adhesive protein, cement protein (cp)-68k, is a four-amino-acid-biased novel glyco-protein with adsorption activity in seawater (submitted for publication)

Kavanagh CJ, Swain GW, Kovach BS, Stein J, Darkangelo-Wood C, Truby K, Holm E, Montemarano J, Meyer A, Wiebe D (2003) The effects of silicone fluid additives and silicone elastomer matrices on barnacle adhesion strength. Biofouling 19:381–390

Lacombe D (1970) A comparative study of the cement glands in some balanid barnacles (cirripedia, balanidae). Biol Bull 139:164–179

Lindner E, Dooley CA (1973) Chemical bonding in cirripede adhesive. In: Acker RF, Floyd Brown B, DePalma JR, Iverson WP (eds) Proceedings of the third international congress on marine corrosion and fouling. Northwestern University Press, Evanston, IL, USA, pp 653–673

McDowell LM, Bursio LA, Waite JH, Schaefer J (1999) Rotational echo double resonance detection of cross-links formed in mussel byssus under high-flow stress. J Biol Chem 274:20293–20295

Mori Y, Urushida Y, Shen JR, Suzuki R, Kamino K Manuscript in preparation

Nakano M, Shen JR, Kamino K Self-assembling peptide from a biotic underwater adhesive protein. Submitted for publication

Nakashima H, Nishikawa K, Ooi T (1990) Distinct character in hydrophobicity of amino acid composition of mitochondrial proteins. Proteins 8:173–178

Naldrett MJ (1993) The importance of sulphur cross-links and hydrophobic interactions in the polymerization of barnacle cement. J Mar Bio Assoc UK 73:689–702

Naldrett MJ, Kaplan DL (1997) Characterization of barnacle (*Balanus eburneus* and *B. crenatus)* adhesive proteins. Mar Biol 127:629–635

Otzen DE, Kristensen O, Oliveberg M (2000) Designed protein tetramer zipped together with a hydrophobic Alzheimer homology: a structural clue to amyloid assembly. Proc Natl Acad Sci USA 97:9907–9912
Ooka AA, Garrell RL (2000) Surface-enhanced Raman spectroscopy of DOPA-containing peptides related to adhesive protein of marine mussel, *Mytilus edulis*. Biopolymers 57:92–102
Rzepecki LM, Waite JH (1995) Wresting the muscle from mussel beards: research and applications. Mol Mar Biol Biotech 4:313–322
Sarikaya M, Tamerler C, Jen AK, Schulten K and Baneyx F (2003) Molecular biomimetics: nanotechnology through biology. Nat Biotech 2:577–585
Saroyan JR, Lindner E, Dooley CA (1970) Repair and reattachment in the balanidae as related to their cementing mechanism. Biol Bull 139:333–350
Sever MJ, Weisser JT, Monahan J, Srinivasan S, Wilker JJ (2004) Metal-mediated cross-linking in the generation of a marine-mussel adhesive. Angew Chem Int Ed 43:448–450
Suci PA, Geesey GG (2001) Use of attenuated total internal reflection Fourier transform infrared spectroscopy to investigate interactions between *Mytilus edulis* foot proteins at a surface. Langmuir 17:2538–2540
Sun CJ, Waite JH (2005) Mapping Chemical Gradients within and along a Fibrous Structural Tissue, Mussel Byssal Threads. J Biol Chem 280:39332–39336
Suzuki R, Mori Y, Kamino K, Yamazaki T (2005) NMR assignment of the barnacle cement protein Mrcp-20k. J Biomol NMR 32:257
Taylor SW, Waite JH (1997) Marine adhesives: from molecular dissection to application. In: McGrath K, Kaplan D (eds) Protein-based materials. Birkhauser, Boston, pp 217–248
Urushida Y, Sasaki F, Nakano M, Inoue N, Kanai S, Kitamura N, Nishino T, Kamino K, Novel barnacle underwater adhesive protein has a six-amino-acid bias in content and has solid-surface adsorption activity. Submitted for publication
Waite JH (1987) Nature's underwater adhesive specialist. Int J Adh Adhesives 7:9–14
Waite JH (1992) Results and problems in cell differentiation. In: Case ST (ed) Biopolymers, vol 19. Springer, Berlin Heidelberg New York, pp 27–53
Waite JH (1999) Reverse engineering of bioadhesion in marine mussels. Ann NY Acad Sci 875:301–309
Waite JH, Qin XX (2001) Polyphosphoprotein from the adhesive pads of *Mytilus edulis*. Biochemistry 40:2887–2893
Walker G (1970) The histology, histochemistry and ultrastructure of the cement apparatus of three adult sessile barnacles, *Elminius modestus, Balanus balanoides* and *Balanus haemri*. Mar Biol 7:239–248
Walker G (1972) The biochemical composition of the cement of two barnacle species, *Balanus hameri* and *Balanus crenatus*. J Mar Biol Assoc UK 52:429–435
Walker G (1981) The adhesion of barnacles. J Adhesion 12:51–58
Walker G, Yule AB (1984) Temporary adhesion of the barnacle cyprid: the existence of an antennular adhesive secretion. J Mar Biol Assoc UK 64:679–686
Watermann B, Berger H-D, Sönnichsen H, Willemsen P (1997) Performance and effectiveness of non-stick coatings in seawater. Biofouling 11:101–118
Wiegemann M, Watermann B (2003) Peculiarities of barnacle adhesive cured on non-stick surfaces. J Adhesion Sci Technol 17:1957–1977
Whitesides GM, Boncheva M (2002) Beyond molecules: self-assembly of mesoscopic and macroscopic components. Proc Natl Acad Sci USA 99:4769–4774
Yan W, Pan S (1981) The solubilizing effect of denaturation chemicals on the cement of *Balanus reticulates* Utinomi. Oceanologica et Limnologia Sinica 12:125–132
Yan W, Tang Y (1981) The biochemical composition of the secondary cement of *Balanus reticulates* Utinomi and *Balanus amaryllis* Darwin. Nanhai Studia Marina Sinica 2:145–152
Yule AB, Walker G (1984) The adhesion of the barnacle, *Balanus balanoides,* to slate surfaces. J Mar Biol Assoc UK 64:147–156
Yule AB, Walker G (1987) Adhesion in barnacles. In: Southward AJ (ed) Barnacle biology. Balkema, Rotterdam, pp 389–402

Zhang S (2003) Fabrication of novel biomaterials through molecular self-assembly. Nat Biotech 21:1171–1178
Zhang W, Laursen RA (1998) Structure-function relationships in a type I antifreeze polypeptide. The role of threonine methyl and hydroxyl groups in antifreeze activity. J Biol Chem 273:34806–34812
Zhao X, Zhang S (2004) Fabrication of molecular materials using peptide construction motifs. Trends Biotech 22:470–476

9 The Biochemistry and Mechanics of Gastropod Adhesive Gels

Andrew M. Smith

9.1 Introduction

A wide variety of organisms attach to surfaces using gels as glues, but the mechanism by which a gel can form a strong attachment has only recently been studied in depth. The adhesive gels used by animals are unusual biomaterials. Their structure and properties are strikingly different from common commercial glues. Commercial glues are generally solids; they may be applied in liquid form and then solidify, or they may be deformable, tacky solids (Wake 1982). In either case, their final form consists entirely of polymers or crosslinked material. In contrast, adhesive gels typically consist of dilute polymer networks that contain more than 95% water. These gels are highly deformable. One would not expect such a dilute hydrogel to be suited for adhesion. In fact, dilute polymer gels are often excellent lubricants. Nevertheless, a wide array of animals use such gels as powerful glues (Smith 2002).

Because they are gels, these glues have a variety of interesting and useful properties. Foremost among these are their great flexibility and their ability to bond to wet, untreated surfaces. Furthermore, despite being dilute and easily deformable, these adhesive gels provide surprisingly strong attachments. Snails such as limpets can be extraordinarily difficult to detach by hand. They use gels to create tenacities (attachment force per unit area) ranging from 100 to 500 kPa (Branch and Marsh 1978; Grenon and Walker 1981; Smith 1992; Smith and Morin 2002). This approaches the adhesive strength of the solid cements of mussels and barnacles, which is typically 500–1000 kPa (Waite 1983; Yule and Walker 1987).

Since the adhesive gels have unusual properties that would not be predicted for such dilute polymer mixtures, the mechanism by which they work should be interesting. What features of these gels make them such strong adhesives instead of lubricants? The goal of this chapter is to describe the structure and mechanics of adhesive gels focusing on those of gastropod molluscs. Gastropods are particularly interesting because of the diversity and impressive performance of their adhesive gels. They are also notable because a key structural feature has been discovered that appears to control the mechanics of the gels; this is the presence of specific glue proteins that are not found in the

Department of Biology, Ithaca College, Ithaca, New York 14850, USA

Biological Adhesives
(ed. by A.M. Smith and J.A. Callow)

non-adhesive forms of the gels. These glue proteins may crosslink other polymers, thus strengthening the gel and possibly contributing to interfacial adhesion.

9.2 Background

A key step in understanding how snails such as limpets can create strong adhesion with a gel was the recognition that the glue was a different form of gel than the normal mucous gel. It is now becoming clear that there are many ways to construct gels, and these differences give rise to substantial functional differences (Smith 2002). As anyone who has handled an invertebrate can appreciate, the normal mucus covering their outer surface is not inherently sticky. This type of mucus appears to be used during suction adhesion of limpets. If suction is eliminated through a leak, or because the animal is not forcibly contracting the musculature that creates suction, the adhesive strength in shear is low to non-existent (Smith 1991b, 2002). Thus, the mucus that the animals normally crawl on provides virtually no adhesive strength on its own. The mucus that is used in adhesion, though, is different. When limpets glue down in an aquarium, they are easily distinguished from limpets that are not glued down (Smith 1992). In addition to having a high shear tenacity, detachment of limpets that are glued down occurs abruptly and usually leaves a thin film of gel stuck firmly to the glass. One can remove this gel with a razor blade to get an elastic mass that is unlike the loose slime that many snails produce across their general body surface. Thus, it is likely that there are substantial structural differences between these gels. Indeed, there are probably a wide variety of invertebrate gels. The use of the term mucus, therefore, is probably misleading in that it implies a unity of structure that does not appear to exist.

9.3 Adhesive Gels Used by Different Animals

There are probably a wide variety of animals that use adhesive gels. Many echinoderms adhere using secretions that are described as containing either mucopolysaccharides or protein (Flammang 1996; Chap. 10, this volume). A wide variety of worm-like invertebrates also adhere using such viscous secretions (Hermans 1983). Any time a polymeric adhesive secretion contains a high percentage of water and is easily deformable but strikingly viscous and even elastic, it is likely to be a gel. Some species of frogs can produce a sticky gel that is markedly different from common mucous secretions (Graham et al., Chap. 11, this volume). Many microscopic organisms also adhere with gels (Callow and Callow. Chap. 4, this volume).

Adhesive gels have been studied in depth for four gastropod molluscs. These represent a range of habitats and functions. Of these, the attachment of limpets has been studied for the greatest length of time. Most limpets live on rocky intertidal coasts. Limpets in the genus *Lottia* use their adhesive gel to glue down when they are exposed and inactive during low tide (Smith 1992). The adhesive strength protects them from dislodgement by predators such as shorebirds (Hahn and Denny 1989). When the tide returns, the limpets typically become active and at this point rely on suction for adhesion (Smith 1992). The adhesive might also be used instead of suction to attach when wave surge is particularly strong. It is likely that other limpets also alternate between attachment mechanisms, though the cues may be different.

The marsh periwinkle, *Littoraria irrorata,* can also produce adhesive and non-adhesive gels. These snails forage along mud flats, but when the tide returns they climb marsh grass stems and glue the lip of their shell down. In this way, they avoid aquatic predators such as crabs and fish (Warren 1985; Vaughn and Fisher 1988). When the tide recedes they break their adhesion and return to the mud flats. The shear tenacity created by their adhesive gel can exceed 100 kPa. This is an order of magnitude greater than the tenacity these snails create using suction and any viscous contributions from the mucus they crawl upon (Smith and Morin 2002). As with limpets, the adhesive gel is surprisingly elastic, and significantly firmer than the mucus the animal crawls upon (Fig. 9.1A,B). One difference from limpets is that the glue forms a thin strip along the edge of the shell, while limpets secrete the glue under the sole of the foot. This means that periwinkle glue, unlike limpet glue, is exposed to the elements. Thus, it may dry into a solid sheet in warm, dry weather. In some species of periwinkle, such as *L. aspera*, the glue may always dry (Denny 1984) while in others it may typically stay gelled. The peak force required to detach marsh periwinkles using the gelled glue, though, is not significantly different from that of the dried film (Smith, unpublished). If anything, the flexibility of the gel may provide better adhesive performance by absorbing energy during detachment rather than failing as a brittle solid. While *L. irrorata* has been studied in depth, many other periwinkles also use glues to attach to rocks or vegetation, often switching between active and inactive states.

Some land snails such as *Helix aspersa* also glue the lip of their shell onto the substrate during periods of inactivity. In this case they stay glued for longer periods, sometimes months, estivating until conditions are sufficiently moist (Wells 1944; Campion 1961; Barnhart 1983). Unlike marsh periwinkles, the glue always seems to dry into a tough film. It also forms a seal around the entire circumference of the opening instead of just the anterior end. Whereas the marsh periwinkle glue functions solely in holding the animal's position above the water, the land snail's glue also plays an important role in desiccation resistance by limiting airflow into the area under the shell (Campion 1961; Barnhart 1983). As with limpets and marsh periwinkles, adhesion is not immediate. Marsh periwinkles take roughly 10 min to form the glue (Bingham 1972). The

limpets and land snails that have been studied seem to take at least that long to form the fully functional adhesive bond (personal observation), though limpet feet can become tacky to the touch within seconds (Smith 1991b).

Finally, many terrestrial slugs, such as *Arion subfuscus*, use an adhesive gel as a defensive secretion (Mair and Port 2002). When disturbed, *A. subfuscus* secretes a markedly sticky, orange gel from its dorsal surface. This typically appears as a liquid on the dorsal surface but soon stiffens into a rubbery mass (Fig. 9.1C–E). Like the glues of limpets and marsh periwinkles, it is a gel. It may be slightly more concentrated, but is still roughly 95% water. When used to glue acrylic disks together, it sets within seconds and creates tenacities up to 100 kPa (Smith, unpubl.). As with the other gastropods, the glue was distinct from the normal mucus used in locomotion and lubrication.

It is interesting to note the substantial functional variation among the adhesive gels. Analysis of the adhesive gels of other animals will likely show further variation. In order to understand this variation, it is first necessary to understand gel mechanics in general.

9.4 Principles of Gel Mechanics

A gel is a dilute polymer network within a liquid (Tanaka 1981). The liquid, which is water in biological systems, keeps the polymer network from collapsing. The polymers trap the liquid so that it cannot easily flow. Thus, a gel has solid properties, despite its high water content. Gels are typically viscoelastic; when a stress is applied to them, they have a viscous and an elastic resistance

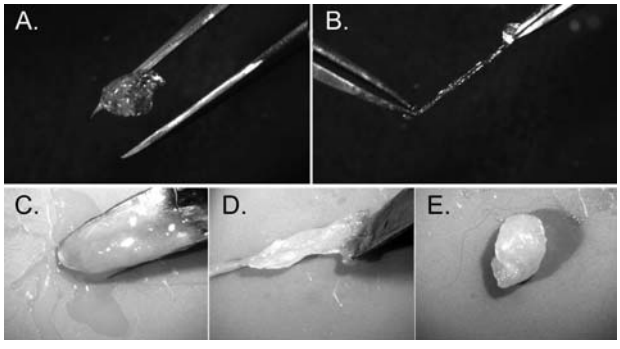

Fig. 9.1. The physical characteristics of two gastropod adhesive gels: **A,B** the glue from the marsh periwinkle *L. irrorata* forms an irregular mass (a) that can be stretched extensively (b). This deformation is reversible. The glue in A and B is held by fine-tip forceps; **C–E** the glue from the slug *A. subfuscus* is often secreted in a form that appears fairly fluid (c), but which sets into an elastic gel that sticks strongly to most surfaces, and can also be stretched extensively (d). This deformation is also reversible (e). In C and D the glue is attached to a metal spatula

to deformation. For a full description of viscosity and elasticity see Wainwright et al. (1976) or Denny and Gosline (1980). In brief, a purely viscous material will flow in response to an applied stress, resulting in a permanent deformation. Higher viscosities give more resistance to flow. A purely elastic material will not flow. Instead, it will deform in proportion to the applied stress and will maintain that stable deformation as long as the force is applied. When the force is removed, the material will spring back to its original configuration. A viscoelastic material may resist deformation elastically at first, but over time the molecules rearrange and flow in response to the stress. Note that these properties depend on the rate of deformation (Wainwright et al. 1976). Gels range from highly viscous secretions that have little elasticity to elastic materials that barely flow (Tanaka 1981).

The ability to gel and the mechanics of the gel depend largely on interactions between polymers (Williams and Phillips 2000). Polymers can entangle or crosslink to form a network that will not dissolve in water. Only certain kinds of polymers are likely to interact in this way, though. If each polymer occupies a relatively small volume because of its size and configuration, it is unlikely to interact with its neighbors, and the solution will not have elasticity (Fig. 9.2A). In contrast, if a polymer occupies a large volume, it may begin to overlap its neighbors at low concentrations (Fig. 9.2B). There will be a critical concentration at which this overlap begins. Once there is overlap, the viscosity of the solution increases markedly and begins to depend on the rate of shear (Williams and Phillips 2000). Very large, extended molecules may begin to overlap near a concentration of 1%, while similar-sized molecules that fold into a compact shape may not overlap until the concentration reaches 20% or higher. Smaller compact molecules may not interact at all even though they become noticeably more viscous (Williams and Phillips 2000). Thus, most gels contain molecules that take on an extended configuration in order to occupy a large volume and achieve overlap. In many cases, these molecules will be unusually large, but that is not always so.

If the only interactions among polymers are through physical entangling due to overlap, the polymer solution will be viscoelastic, but may not solidify to form a classic gel. The behavior is dominated by reptation, which is the untangling process that occurs in response to stress (Doi and Edwards 1988; deGennes and Leger 1982). Initially, the stress deforms the polymers elastically as each polymer is stretched against the resistance of its neighbors. The polymers can flow, though, creeping through the boundaries imposed by their neighbors. The ability of the polymers to move in this way determines the mechanics of the material. To form a more elastic gel, polymers generally form intermolecular crosslinks (Williams and Phillips 2000). When the material is strained, the polymers are deformed, but the crosslinks prevent them from flowing appreciably to alleviate the stress. In this case, the elastic contribution to the mechanics is greater than the viscous contribution, and neither depends much on shear rate (Williams and Phillips 2000). Thus, the material may behave more like a solid, even though it may still consist of over 95% water.

Thus, two major characteristics of polymers that affect the mechanics of the gel are the following; (1) the size and configuration of the polymers, and (2) the ability of the polymers to crosslink. Large, extended molecules entangle to a greater extent and thus have greater difficulty working their way through the twisted path imposed by the network (Fig. 9.2C) (Doi and Edwards 1988). Branching also impedes this flow. Increased concentration also increases the extent of entangling, restricting the movements of the polymers further (Doi and Edwards 1988). If a gel is crosslinked (Fig. 9.2D), the size of the individual polymers does not matter as much. For example, with gelatin, the strength of the gel increases as the gelatin fragments get bigger, up to 100 kD. Increasing the size of the polymers beyond this does not strengthen the gel further (Williams and Phillips 2000). Instead, the elasticity of the gel would depend on the number and strength of the crosslinks (Denny 1983).

The final aspect of gel mechanics to consider is the mode of failure. Because gels are highly deformable, brittle failure through simple crack propagation is less likely than with solids. As cracks form, their leading edges are usually blunted by flow. Thus, a major component of the energy required to break the attachment goes towards deforming the gel (Wainwright et al. 1976). When one of the adhering surfaces is flexible, as is the case with gastropod feet, failure would often occur by peeling (Gay 2002). Even if the surfaces are sufficiently rigid, and pulled directly apart, failure will often not occur uniformly. If cracks do not form and propagate within the glue or along

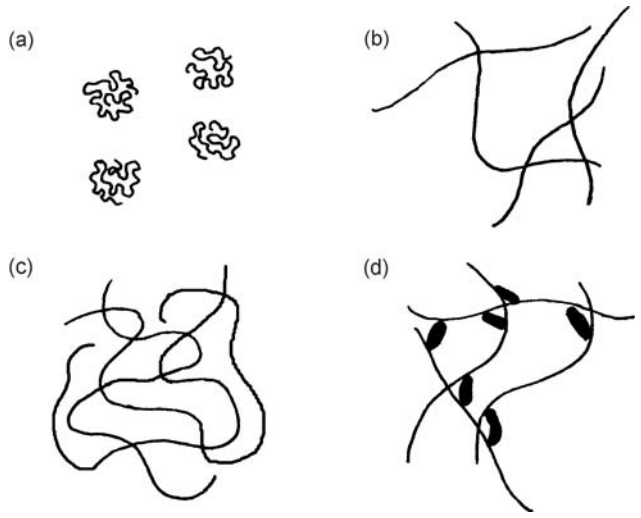

Fig. 9.2. The effect of size, configuration and interactions of polymers on gel mechanics: (a) compact polymers do not interact at low concentrations; (b) if the polymers take on an extended configuration, they are more likely to entangle, increasing viscosity and stiffness; (c) longer polymers entangle to a greater extent, creating a stiffer, more viscous material; (d) crosslinks between polymers can dramatically increase the stiffness of the material

the adhesive interface, failure typically occurs when regions of instability trigger localized flow, resulting in "fingers" of air or water being sucked between the surfaces (Gay 2002). The glue would deform dramatically during this process, dissipating a great deal of energy. In addition, bubble formation by cavitation can occur (Gay 2002). In cavitation, the detaching force creates a reduced pressure in the water that makes up the gel. This may be sufficient to trigger the expansion of microscopic air pockets (Smith 1991a). As with fingering, cavitation would initiate failure, but in doing so would create scattered regions of high deformation and thus energy dissipation. Because of the mechanical strength of the gel, the bubbles would not expand rapidly and form one large bubble, as would happen in pure water (Gay 2002).

An interesting feature of gastropods is that a number of them can use either suction or glue (Smith 1991b, 1992). During suction, the muscles of the foot create a reduced pressure in the water under their foot. Of course, the water is presumably in the mucus layer between the foot and substratum. It is clearly suction, though, as shown by direct pressure measurements and the effect of leaks (Smith 1991b). During suction, the mechanics of the gel do not appear to play a role in adhesion. When the same gastropods glue themselves down, though, the mechanical properties of the gel dominate and failure is more typical of a viscoelastic solid. There will also likely be forms of adhesion that are intermediate between suction and glue, as observed by Smith (1992). For example, when animals use suction, they could easily strengthen the seal with the adhesive gel.

9.5 Adhesive Gel Structure

Unlike most mucus-like secretions, which appear to consist primarily of giant protein-carbohydrate complexes (Denny 1983; Davies and Hawkins 1998), molluscan adhesive gels contain a substantial fraction of smaller proteins. The term "giant polymers" will be used to describe molecules with an apparent size of roughly 1000 kD or more that do not dissociate into subunits under heat and dissociating conditions. Such molecules should tangle easily to form a loose network, and are common in mucus. The importance of smaller proteins, though, has often been overlooked; these proteins appear to play a major role in controlling gel mechanics. The size of these proteins and their amount relative to the giant polymers differs among molluscan adhesive gels (Fig. 9.3). In some cases there are no giant polymers, and only smaller proteins that presumably crosslink. In other cases there is a mixture of giant polymers that may contribute by entangling and smaller proteins that may be involved in crosslinking. In all four species studied, though, the primary characteristic that distinguished the adhesive gel from the non-adhesive mucus was the presence of specific proteins (Fig. 9.4). These were named glue proteins (Pawlicki et al. 2004).

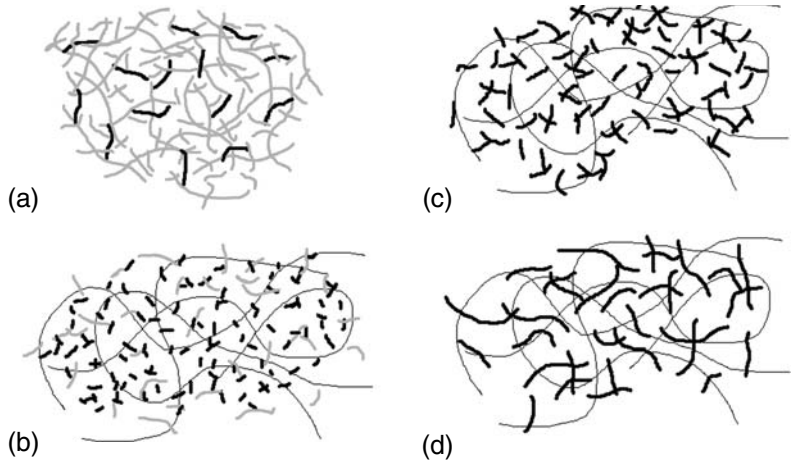

Fig. 9.3. Schematic illustrations of the relative size and abundance of the components of adhesive gels from: (a) the limpet *L. limatula*; (b) the periwinkle *L. irrorata*; (c) the slug *A. subfuscus*; (d) the land snail *H. aspersa*. Polymers of roughly 1000 kD or larger are drawn as *thin black lines*, smaller proteins (10–200 kD) are drawn as *thicker lines*, with glue proteins in *black* and other proteins in *gray*. The size of the polymers and relative amounts of each are depicted to scale using data from Smith et al. (1999), Smith and Morin (2002) and Pawlicki et al. (2004)

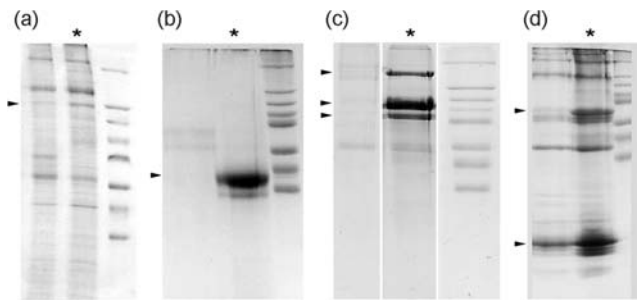

Fig. 9.4. Sodium dodecyl sulfate polyacrylamide gel electrophoresis comparison of non-adhesive (*left lanes*) and adhesive mucus (*) from four molluscs: (a) the limpet *L. limatula*; (b) the marsh periwinkle *L. irrorata*; (c) the land snail *H. aspersa*; (d) the slug *A. subfuscus*. Note the difference in specific proteins (*arrowheads*) between the adhesive and non-adhesive lanes. These are identified as glue proteins. MW markers (*right lanes*) are 205, 116, 97, 84, 66, 55, 45 and 36 kD. For each species, the same amount of dried sample was present in the adhesive and non-adhesive lanes. From Smith et al. (1999), Smith and Morin (2002), and Pawlicki et al. (2004)

Limpet glue appears to be constructed primarily of 20–200-kD proteins (Figs. 9.3A and 9.4A) (Grenon and Walker 1980; Smith et al. 1999). In order for proteins of this size to form a gel, it is highly likely that they take on an extended configuration and interact with each other. Compact proteins of this size that did not crosslink would be incapable of gelling. The non-adhesive

mucus from *L. limatula* is structurally similar to the glue, but the glue has a 118-kD glue protein in addition to the other proteins.

Unlike limpets, the glues of the marsh periwinkles, land snails, and terrestrial slugs that have been studied consist of roughly equal parts giant polymers (≥1000 kD) and smaller proteins (Figs. 9.3 and 9.4) (Smith and Morin 2002; Pawlicki et al. 2004). In the marsh periwinkle (*L. irrorata*) and land snail (*H. aspersa*) glues, two or three glue proteins make up most of the protein content. The trail mucus has giant polymers, but almost no small proteins. In the slugs (*A. subfuscus*) there are a significant number of proteins besides the glue proteins. Among the three different gastropods, the giant polymers differ in their carbohydrate content, with marsh periwinkle giant polymers consisting primarily of carbohydrate (Smith and Morin 2002), and land snail and slug giant polymers appearing to consist mostly of protein with much less carbohydrate (Pawlicki et al. 2004).

The glue proteins of all four species may be structurally similar. They typically have acidic isoelectric points and a large proportion of charged and polar amino acids. For the limpet *L. limatula*, the proteins have isoelectric points that are typically between 4.7 and 5.3, and 65% of the amino acids would be polar or charged at neutral pH (Smith et al. 1999). For marsh periwinkles the two glue proteins have an isoelectric point of 4.75 and contain 49 and 52% charged or polar amino acids (Smith and Morin 2002). For land snails (*H. aspersa*) and slugs (*A. subfuscus*), the isoelectric points fall in the same range (Smith, unpubl.). The glue proteins differ in size, which is likely to be functionally significant. The glue proteins range in mass from 14 kD for the primary slug glue protein to 118 kD for the primary limpet glue protein (Smith et al. 1999; Pawlicki et al. 2004). The land snail also has a glue protein with a mass of roughly 175 kD (Pawlicki et al. 2004). Note that these molecular masses are based on gel electrophoresis, and may not be precise.

Little is known at present about the giant polymers. They are defined primarily by their size; in Sephacryl S-400 gel filtration they elute in the void volume, implying a mass greater than 1000 kD (Smith and Morin 2002; Pawlicki et al. 2004). In most invertebrate mucus, such polymers are carbohydrate-rich and anionic. The charge typically comes from sulfated or carboxylated sugars, with the former more common in seawater (Denny 1983). A large amount of negative charge would generally cause the polymers to take on an extended configuration, which would assist gel formation. The fact that the giant polymers from land snail glue do not appear to have much carbohydrate is surprising. The assay used for carbohydrates in the work of Pawlicki et al. (2004) would not have detected amino sugars, and may miss other sugar derivatives. Smith and Morin (2002) addressed this, estimating that the carbohydrate concentrations may be as much as 50% greater than assayed, based on the relative proportions of different types of sugars in other molluscs. Even considering this, the giant polymers of land snails appear to be mostly protein. It is possible that they consist of smaller proteins that are

covalently crosslinked or associated into tight complexes as collagen fibers are. The same may be true of the giant polymers from slug glue.

9.6 The Role of Different Proteins in Adhesion

Because a major difference between the adhesive gels and non-adhesive mucus from the same animal was the presence of glue proteins, these proteins are likely to play a central role in adhesion. This was confirmed by Pawlicki et al. (2004), who purified the glue proteins from different molluscs and showed that they are potent gel-stiffeners. They are able to stiffen non-specifically gels formed from large, negatively charged polymers (Fig. 9.5). Their effect was weak or absent on similar, neutral polymers, which suggested that electrostatic interactions may play a role. Other proteins found in the gel did not have this stiffening effect.

The experiments of Pawlicki et al. (2004) suggest that the glue proteins crosslink the other polymers in the gel. This is the most likely way that they could stiffen gels. Without crosslinking, a dilute gel will lack the stiffness necessary to maintain a strong adhesive bond for an extended period (Eagland 1990). In order to demonstrate crosslinking directly, an important step is to show that the glue proteins bind to other proteins in the secretion. The behavior of the glue proteins in a variety of biochemical techniques suggests a strong tendency to aggregate with themselves and other polymers in the secretion, particularly the giant polymers (Smith et al. 1999; Pawlicki et al. 2004). Most notably, the glue proteins tend to coelute with other polymers in gel filtration chromatography, even under dissociating conditions (Pawlicki et al. 2004).

The relative insolubility of the adhesive gels also suggests that crosslinking occurs. These gels are difficult to dissolve, unlike most mucous secretions (Smith et al. 1999). To dissolve them, a combination of shear and dissociating agents such as urea and non-ionic detergents are typically used (Smith et al. 1999; Smith and Morin 2002; Pawlicki et al. 2004). Milder treatments

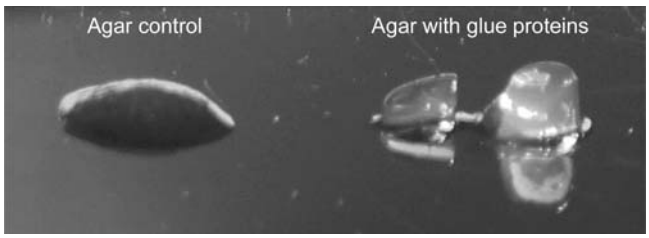

Fig. 9.5. The gel-stiffening effect of gastropod glue proteins. The following shows 0.6% agar with either bovine serum albumen (*left*) or glue proteins from *L. irrorata* (*right*) added. The control is a viscous liquid, while the glue proteins stiffen the agar into a firm gel. From Pawlicki et al. (2004)

extract the same proteins, but at much lower concentrations. These observations suggest that typical covalent bonds are not essential, as they would not be broken under these conditions, but there must be strong non-covalent bonds. The relative insolubility of the gels makes sense for an adhesive that must maintain its integrity underwater.

While an ability to crosslink and stiffen a gel would be a key step in adhesion, that alone is not sufficient. In addition, the gel must adhere to the surfaces to which it is exposed. This aspect has not yet been studied in gastropod adhesive gels. If the glue proteins are capable of non-specifically binding to polymers in the gel, it is likely they can also bind to molecules on the substrate. Surfaces in the ocean are typically covered with an organic film that would be rich in negatively charged molecules (Kamino, Chap.8, this volume). These molecules are probably quite diverse structurally, though, and the mechanism of interaction may not be the same. It is possible that other molecules in the glue are responsible for interfacial adhesion. It is intriguing, though, that Pawlicki et al. (2004) note that the glue proteins increase the ability of solutions to wet surfaces.

In addition to the glue proteins, another difference between non-adhesive and adhesive mucus is the overall concentration (Smith et al. 1999; Smith and Morin 2002). The concentration of the adhesive may be twice the concentration of the non-adhesive mucus, though still less than 3% organic material by weight. An increased concentration would increase tangling interactions, and thus strengthen the glue. This may play a role in addition to the glue proteins, but it is unlikely to be sufficient without crosslinking. Data from Smith (2002) and Ben-Zion and Nussinovitch (1997) for a wide variety of polymers show that increased concentration can improve adhesive strength somewhat, but even a much greater change in concentration would not come close to accounting for the great adhesive strength of molluscan adhesive gels.

The other proteins that are present in the glue of slugs and limpets may play a role in attachment as well. Recent work with barnacles (Kamino, Chap. 8, this volume) and mussels (Sagert et al., Chap. 7, this volume) has made it clear that adhesion in animals often depends on the action of a variety of proteins, each with somewhat different functions. While most of the proteins in limpet glue share similar amino acid compositions, Smith et al. (1999) found other differences between them. One of the two most common proteins in limpet glue, the 140-kD protein, is glycosylated, unlike the other proteins in the glue. It also has substantially more proline than the other proteins. One relatively less common protein, at 53 kD, has a basic isoelectric point (8.6), while the pIs of the other proteins typically fall between 4.7 and 5.3. These differences may relate to their function, but further research would need to be done to elucidate this.

It is also worth noting that there are often several glue proteins in each adhesive gel. Usually there is one that is noticeably more common, but there are often others that are also characteristic of the glue. The evidence suggests that these are related, and in some cases may just be different size variants of

the same protein. The 41- and 36-kD glue proteins from marsh periwinkles, for example, have strongly similar amino acid compositions and the same isoelectric point (Smith and Morin 2002). In limpets, the 118- and 80-kD glue proteins behave similarly in a number of biochemical procedures. For example, they both transfer substantially slower than other proteins in electrophoretic blotting procedures (Smith et al. 1999). It is still possible, though that each protein has slightly different functions.

The mechanism of detachment of these animals may or may not involve biochemical changes. In periwinkles it has been reported that the animal simply eats the glue or tears it down with its radula (Bingham 1972). In other snails, the detachment mechanism has not been tested. In *H. aspersa*, it has been suggested that a protease present in the mucus breaks down the glue (Campion 1961). In limpets, the glue forms a thin layer between the foot and substratum, so one possibility is that they secrete a layer of non-adhesive mucus over the top of the glue. This mucus could include molecules that compete for binding sites and block them, or it could include an enzyme that breaks bonds in the glue. Alternatively, the animal may break the bonds mechanically, by generating sufficient shear. It is worth noting that there is a 68-kD protein that is unique to the non-adhesive mucus of the limpet *L. limatula* (Smith et al. 1999). This may play a role in detachment, though it is found in the pedal mucus used during locomotion, not solely during detachment.

9.7 Mechanisms of Crosslinking

While Pawlicki et al. (2004) suggested that electrostatic crosslinks were important for glue proteins, the actual nature of the crosslinks is likely to be more complex. A key factor is that the glue proteins operate in an aqueous environment. Water has a high dielectric constant; it interacts strongly with charges on the polymers, effectively weakening the electrical field between them (Waite et al. 2005). In essence, water masks the charges. Anything that removes this water would strengthen the interactions between charged groups. Given the usefulness of detergents in solubilizing the adhesive gels, it is possible that hydrophobic interactions assist bonding. They may contribute by excluding water from certain regions, thus allowing the formation of stronger ionic interactions. The charged regions may also be involved in forms of bonding that involve more than simple electrostatic interactions.

The use of a combination of bonding mechanisms is not unusual for gels. A variety of different types of interactions have been demonstrated in commercially used gels (Phillips and Williams 2000). Hydrogen bonding and hydrophobic interactions between helical regions are important in gels such as agar and gelatin. Electrostatic bonding using divalent ions to bridge polymers is common among gels such as pectins. Recently, a number of researchers have synthesized gels with controllable mechanical properties.

These have used a variety of different mechanisms to cross-link the gels. Miyata et al. (1999) used antigen-antibody interactions to crosslink gels. These would presumably depend on several different types of interactions. Several groups have used coiled-coil interactions to link together chains (Petka et al. 1998; Wang et al. 1999, 2001). Coiled-coil interactions depend on hydrophobic interactions between helices that wind around each other. These are sometimes stabilized by electrostatic interactions. Nowak et al. (2002) used polypeptides whose ability to gel depended on having separate hydrophobic and charged regions, both of which presumably contribute to bonding. Alternatively, some researchers have used covalent bonds to crosslink gels. Lee et al. (2002, 2004) incorporated the amino acid dihydroxyphenylalanine (DOPA) into polymer hydrogels in order to form crosslinks. Hu and Messersmith (2003) also created hydrogels with the crosslinking enzyme transglutaminase.

These mechanisms suggest the breadth of ways that gels can be crosslinked. Based on the type of treatments used to solubilize molluscan adhesive gels and keep the proteins from aggregating during chromatography, gastropod glue proteins may depend on similar types of non-covalent interactions. Another possibility is that metal ions could be involved in crosslinking. Multivalent ions typically have large effects on the mechanics of gels (Tanaka 1981). Metals such as iron are also able to form other types of bonds, such as coordinate covalent bonds. Interactions involving metal ions appear to play a key role in mussel adhesion (Sagert et al., Chap. 7, this volume).

9.8 Comparison of Gel Structure Among Gastropods

It is interesting to consider possible explanations for the differences in adhesive gel structure among gastropods. It is possible that the different structures merely reflect evolutionary heritage, where animals evolved glue proteins to work with whatever polymers were present in the trail mucus. In this case, the differences may be unrelated to adhesive performance. Alternatively, they may reflect adaptations for different performance requirements.

One factor that could have a functional impact is the relative sizes of the molecules in the glue. Limpet glue is interesting because it does not appear to contain any giant polymers. Both the non-adhesive and adhesive gels are built primarily of smaller proteins. Given that the limpet is most well-known among gastropods for its adhesive strength, and has produced the highest recorded adhesive strengths for gels, this may suggest that a network of smaller, crosslinked proteins is stronger. It is difficult to compare adhesive strengths among these gastropods, though, as the geometry of detachment varies markedly. Interestingly, Williams and Phillips (2000) note that the strength of crosslinked commercial gels typically reaches a maximum when

the polymer size is near 100 kD. This may also be relevant to the fact that the primary glue proteins of the land snail *H. aspersa* and the limpet *L. limatula* are 97 and 118 kD.

At 14 kD, the glue protein from the slug *A. subfuscus* is markedly smaller than the other glue proteins. The slug glue appears to be defensive, and its most notable characteristic is its ability to set rapidly and generate interfacial adhesion. Perhaps the small size of the glue proteins facilitates this speed, forming interactions more rapidly than the bulkier glue proteins of other species. It is often advantageous to make glues out of smaller polymers that can flow more readily to interact with the adhering surfaces before crosslinking (Bikerman 1958; Wake 1982; Waite 1983).

The land snail and marsh periwinkle glues are both interesting in that they have a substantial amount of giant polymer, and there are no other proteins besides the glue proteins. Thus, the proportion of glue proteins to other components in these two species is also typically higher. A functional difference that may correlate with this is that these glues sometimes (marsh periwinkles) or always (land snails) dry into tough films.

9.9 Conclusion

The adhesive gels produced by molluscs have unusual and potentially useful properties. They are highly flexible, strong and adhere well underwater. Thus, it will be interesting to determine how they function. There are a variety of ways of making a gel, and the mechanics of the resulting gels will vary considerably. Often unusually large molecules (>1000 kD) play a role, but crosslinking by much smaller proteins seems to be a central factor in creating adhesive strength. Specific glue proteins have been identified, and these have a gel-stiffening action that is relatively non-specific. The mechanism by which they do this is probably non-covalent. There are a number of non-covalent interactions that could create stiff gels, but at present it is unclear which mechanism the glue proteins use. In the long run, determining the nature of these interactions and characterizing the functional effects of different gel structures should lead to useful insights into gel design.

Acknowledgments. I would like to thank R. Shadwick for comments on the manuscript, and J.H. Waite and S. Werneke for helpful discussions. This work was supported in part by an Ithaca College summer research grant.

References

Barnhart MC (1983) Gas permeability of the epiphragm of a terrestrial snail, *Otala lactea*. Physiol Zool 56:436–444

Ben-Zion O, Nussinovitch A (1997) Hydrocolloid wet glues. Food Hydrocolloids 11:429–442
Bingham FO (1972) The mucus holdfast of *Littorina irrorata* and its relationship to relative humidity and salinity. Veliger 15:48–50
Bikerman JJ (1958) The rheology of adhesion. In: Eirich FR (ed) Rheology: theory and applications, vol III. Academic Press, New York, pp 479–503
Branch GM, Marsh AC (1978) Tenacity and shell shape in six *Patella* species: adaptive features. J Exp Mar Biol Ecol 34:111–130
Campion M (1961) The structure and function of the cutaneous glands in *Helix aspersa*. Quart J Microscop Sci 102:195–216
Davies MS, Hawkins SJ (1998) Mucus from marine molluscs. Adv Mar Biol 34:1–71
deGennes PG, Leger L (1982) Dynamics of entangled polymer gels. Annu Rev Phys Chem 33:49–61
Denny MW (1983) Molecular biomechanics of molluscan mucous secretions. In: Wilbur K, Simkiss K, Hochachka PW (eds) The mollusca, vol I. Academic Press, New York, pp 431–465
Denny MW (1984) Mechanical properties of pedal mucus and their consequences for gastropod structure and performance. Am Zool 24:23–36
Denny MW, Gosline JM (1980) The physical properties of the pedal mucus of the terrestrial slug *Ariolimax columbianus*. J Exp Biol 88:375–393
Doi M, Edwards SF (1988) The theory of polymer dynamics. Clarendon Press, Oxford
Eagland D (1990) What makes stuff stick? Chemtech (April):248–254
Flammang P (1996) Adhesion in echinoderms. In: Jangoux M, Lawrence JM (eds) Echinoderm studies, vol 5. Balkema, Rotterdam, pp 1–60
Gay C (2002) Stickiness -some fundamentals of adhesion. Integr Comp Biol 42:1123–1126
Grenon JF, Walker G (1980) Biomechanical and rheological properties of the pedal mucus of the limpet, *Patella vulgata* L. Comp Biochem Physiol B 66:451–458
Grenon JF, Walker G (1981) The tenacity of the limpet, *Patella vulgata* L.: an experimental approach. J Exp Mar Biol Ecol 54:277–308
Hahn T, Denny M (1989) Tenacity-mediated selective predation by oystercatchers on intertidal limpets and its role in maintaining habitat partitioning by *'Collisella' scabra* and *Lottia digitalis*. Mar Ecol Prog Ser 53:1–10
Hermans CO (1983) The duo-gland adhesive system. Oceanogr Mar Biol Annu Rev 21:283–339
Hu BH, Messersmith PB (2003) Rational design of transglutaminase substrate peptides for rapid enzymatic formation of hydrogels. J Am Chem Soc 125:14298–14299
Lee BP, Dalsin JL, Messersmith PB (2002) Synthesis and gelation of DOPA-modified poly(ethylene glycol) hydrogels. Biomacromolecules 3:1038–1047
Lee BP, Huang K, Nunalee FN, Shull KR, Messersmith PB (2004) Synthesis of 3,4-dihydroxyphenylalanine (DOPA) containing monomers and their co-polymerization with PEG-diacrylate to form hydrogels. J Biomater Sci Polym Ed 15:449–64
Mair J, Port GR (2002) The influence of mucus production by the slug, *Deroceras reticulatum*, on predation by *Pterostichus madidus* and *Nebria brevicollis* (Coleoptera: Carabidae). Biocontrol Sci Technol 12:325–335
Miyata T, Asami N, Uragami T (1999) A reversibly antigen-responsive hydrogel. Nature 399:766–769
Nowak AP, Breedveld V, Pakstis L, Ozbas B, Pine DJ, Pochan D, Deming TJ (2002) Rapidly recovering hydrogel scaffolds from self-assembling diblock copolypeptide amphiphiles. Nature 417:424–428
Pawlicki JM, Pease LB, Pierce CM, Startz TP, Zhang Y, Smith AM (2004) The effect of molluscan glue proteins on gel mechanics. J Exp Biol 207:1127–1135
Petka WA, Harden JL, McGrath KP, Wirtz D, Tirrell DA (1998) Reversible hydrogels from self-assembling artificial proteins. Science 281:389–392
Phillips GO,Williams PA (2000) Handbook of hydrocolloids. Woodhead Publ, Cambridge
Smith AM (1991a) Negative pressure generated by octopus suckers: a study of the tensile strength of water in nature. J Exp Biol 157:257–271
Smith AM (1991b) The role of suction in the adhesion of limpets. J Exp Biol 161:151–169

Smith AM (1992) Alternation between attachment mechanisms by limpets in the field. J Exp Mar Biol Ecol 160:205–220
Smith AM (2002) The structure and function of adhesive gels from invertebrates. Integr Comp Biol 42:1164–1171
Smith AM, Morin MC (2002) Biochemical differences between trail mucus and adhesive mucus from marsh periwinkles. Biol Bull 203:338–346
Smith AM, Quick TJ, St. Peter RL (1999) Differences in the composition of adhesive and non-adhesive mucus from the limpet *Lottia limatula*. Biol Bull 196:34–44
Tanaka T (1981) Gels. Sci Am 244:124–138
Vaughn CC, Fisher FM (1988) Vertical migration as a refuge from predation in intertidal marsh snails: a field test. J Exp Mar Biol Ecol 123:163–176
Wainwright SA, Biggs WD, Currey JD, Gosline JM (1976) Mechanical design in organisms. Princeton Univ Press, Princeton
Waite JH (1983) Adhesion in bysally attached bivalves. Biol Rev Camb Philos Soc 58:209–231
Waite JH, Andersen NH, Jewhurst S, Sun C (2005) Mussel adhesion: finding the tricks worth mimicking. J Adhesion 81:1–21
Wake WC (1982) Adhesion and the formulation of adhesives. Applied Science Publ, London
Wang C, Stewart RJ, Kopeček J (1999) Hybrid hydrogels assembled from synthetic polymers and coiled-coil protein domains. Nature 397:417–420
Wang C, Kopeček J, Stewart RJ (2001) Hybrid hydrogels cross-linked by genetically engineered coiled-coil block proteins. Biomacromolecules 2:912–920
Warren JH (1985) Climbing as an avoidance behaviour in the salt marsh periwinkle, *Littorina irrorata* (Say). J Exp Mar Biol Ecol 89:11–28
Wells GP (1944) The water relations of snails and slugs III. Factors determining activity in *Helix pomatia* L. J Exp Biol 20:79–87
Williams PA, Phillips GO (2000) Introduction to food hydrocolloids. In: Phillips GO, Williams PA (eds) Handbook of hydrocolloids. Woodhead Publ, Cambridge, pp 1–20
Yule AB, Walker G (1987) Adhesion in barnacles. In: Southward AJ (ed) Crustacean issues: barnacle biology, vol 5. Balkema, Rotterdam, pp 389–402

10 Adhesive Secretions in Echinoderms: An Overview

PATRICK FLAMMANG

10.1 Introduction

Members of the phylum Echinodermata are among the most familiar sea creatures, and representatives, such as the sea stars, have become virtually a symbol of sea life. The phylum contains about 7000 living species of relatively large invertebrates, all being exclusively marine and largely bottom-dwellers (Ruppert and Barnes 1994). There are five extant classes of echinoderms: the crinoids (sea lilies and feather stars), the asteroids (sea stars), the ophiuroids (brittle stars), the echinoids (sea urchins and sand dollars), and the holothuroids (sea cucumbers). The most striking characteristics of the group are the pentamerous radial symmetry and the presence of a unique system of coelomic canals and surface appendages composing the water-vascular system.

Echinoderms are also quite exceptional in the sense that most species belonging to this group use adhesive secretions extensively. Moreover, according to the species or to the developmental stage considered, different adhesive systems may be recognized. These include: (1) tube feet or podia, organs involved in attachment to the substratum, locomotion, food capture or burrowing; (2) larval adhesive organs allowing attachment of larvae during settlement and metamorphosis; and (3) Cuvierian tubules, sticky defence organs occurring in some holothuroid species. All these systems rely on different types of adhesion and therefore differ in the way they operate, in their structure and in the composition of their adhesive.

10.2 Tube Feet

Being exclusively benthic animals, echinoderms have activities and adaptations that are correlated with a relationship with the sea bottom. Most of these activities, such as attachment to the substratum, locomotion, handling of food, and burrow-building, rely on adhesive secretions allowing the animal to stick to or to manipulate a substratum. In post-metamorphic echinoderms,

Université de Mons-Hainaut, Laboratoire de Biologie marine, Académie Universitaire Wallonie-Bruxelles, Mons, Belgium

Biological Adhesives
(ed. by A.M. Smith and J.A. Callow)

these adhesive secretions are always produced by specialized organs, the podia or tube feet. These are the external appendages of the water-vascular system and are also probably the most advanced hydraulic organs in the animal kingdom. Tube foot attachment is typically temporary adhesion. Indeed, although tube feet can adhere very strongly to the substratum, they are also able to detach easily and voluntarily from the substratum before reinitiating another attachment-detachment cycle (Thomas and Hermans 1985; Flammang 1996).

Tube feet have diversified into a wide variety of morphotypes, which were classified by Flammang (1996) into disc-ending, penicillate, knob-ending, lamellate, ramified, and digitate. In terms of adhesion, however, for practical considerations only disc-ending tube feet involved in attachment to the substratum and locomotion have been studied in detail. These tube feet consist of a basal hollow cylinder, the stem, and an enlarged and flattened apical extremity, the disc (Fig. 10.1A). The stem is extensible and flexible and allows the movements of the tube foot, whereas the disc makes contact with the substratum and releases the adhesive secretion (Fig. 10.1) (Flammang 1996).

Tube foot adhesive strength has been evaluated by measuring their tenacity, which is the adhesion force per unit area and is expressed in Pascals (Pa). Tenacity of single tube feet has been quantified in several species of asteroids and echinoids. The mean normal tenacity measured on a glass substratum is 170 kPa in *Asterias vulgaris* (Paine 1926), 198 kPa in *A. rubens* (Flammang and Walker 1997), and 59, 120 and 290 kPa in *Arbacia lixula*, *Sphaerechinus*

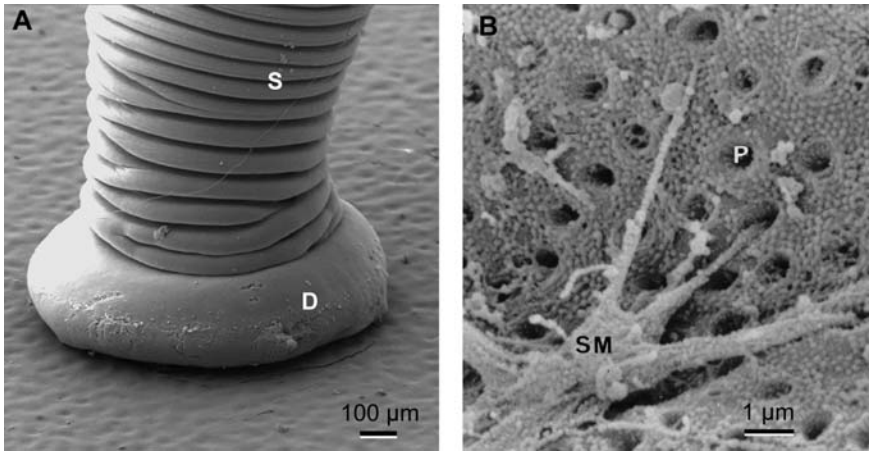

Fig. 10.1. Tube foot adhesion and adhesive in the asteroid *Asterias rubens*: (a) SEM photograph of a disc-ending tube foot attached to a textured polymer substratum (original); (b) detailed view of the distal surface of the disc showing the release of adhesive secretion (from Flammang et al. 1994). D disc, P secretory pore, S stem, SM secreted adhesive material

granularis, and *Paracentrotus lividus*, respectively (Flammang et al. 2005). On polymer substrata, the tube feet of *P. lividus* presented a mean tenacity of 340 and 140 kPa on polymethyl methacrylate (PMMA) and polypropylene, respectively; and the tube feet of *A. rubens* adhered to PMMA with a tenacity of 180 kPa (Santos et al. 2005a). All these values are in the same range as those observed in other marine invertebrates known to adhere very strongly to polymer and glass substrata, e.g., 170 and 230 kPa in limpets (Grenon and Walker 1981), 80 and 230 kPa in barnacles (Yule and Walker 1987), 120 and 750 kPa in mussels (Waite 2002), respectively). Moreover, it was recently demonstrated that asteroid and echinoid tube feet show increased adhesion on a rough substratum in comparison to its smooth counterpart (Santos et al. 2005a). This is because the disc adhesive surface is highly compliant, replicating the substratum profile. The increase in contact area between the disc and the substratum leads to a higher adhesion force (Santos et al. 2005a). Tube foot discs and their adhesive secretions therefore appear to be well-tailored to provide an efficient attachment to natural rocky substrata, allowing echinoderms to resist hydrodynamically generated forces.

The histological structure of the tube feet is remarkably constant for all echinoderm species. Their tissue stratification consists of four layers: an inner myomesothelium surrounding the water-vascular lumen, a connective tissue layer, a nerve plexus, and an outer epidermis covered externally by a cuticle (Flammang 1996). At the level of the tube foot tip, these tissue layers are specialized in adhesion and sensory perception: the connective tissue layer and the nerve plexus are thickened, and the epidermis is differentiated into a well-developed sensory-secretory epithelium. The latter comprises two types of secretory cells: non-ciliated secretory cells (NCS cells) enclosing large heterogeneous granules and ciliated secretory cells (CS cells) enclosing small homogeneous electron-dense granules (Fig. 10.2) (see Flammang 1996 for review). In some species, two types of NCS cells co-occur in the sensory-secretory epidermis. The study of the ultrastructure of the CS and NCS cells during a complete cycle of attachment-detachment of the tube foot in *A. rubens* (Fig. 10.2) demonstrated that they function as a duo-gland adhesive system as originally proposed by Hermans (1983), and in which NCS cells (types 1 and 2) release an adhesive secretion and CS cells a de-adhesive secretion (Flammang et al. 1994, 2005; Flammang 1996). The adhesive is present as a thin film between the tube foot cuticle and the substratum and, when detachment occurs, it takes place at the level of the outermost layer of the cuticle, the fuzzy coat, leaving the adhesive material strongly attached to the substratum as a footprint (Fig. 10.2) (Flammang 1996). In *A. rubens*, polyclonal antibodies have been raised against footprint material and were used to locate the origin of footprint constituents in the tube feet (Flammang et al. 1998a). Extensive immunoreactivity was detected in the secretory granules of both NCS1 and NCS2 cells, suggesting that their secretions make up together the bulk of the adhesive material. No immunoreactivity was detected in the secretory granules of CS cells and the only other structure strongly labelled

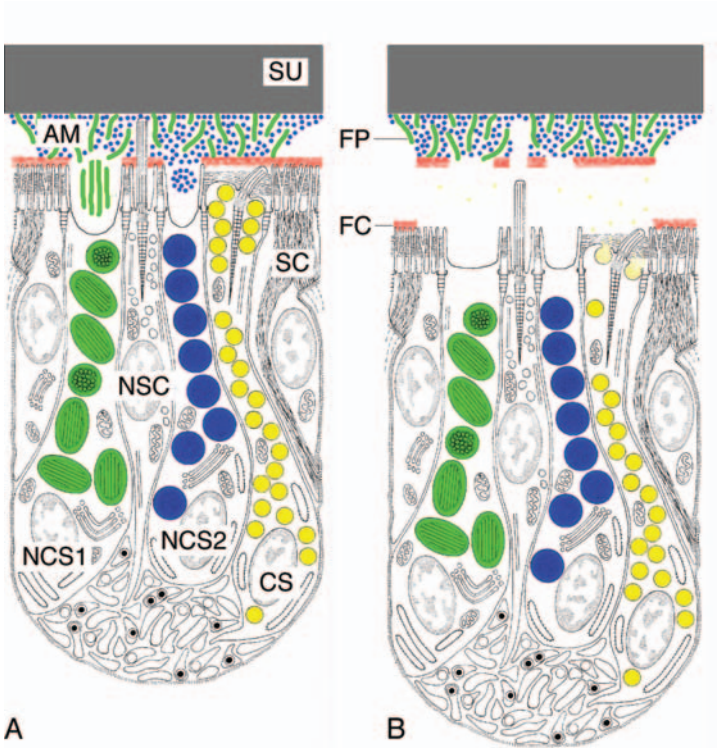

Fig. 10.2. Diagrammatic representation of the duo-gland model proposed for the attachment and detachment of a tube foot of the asteroid *Asterias rubens* using reconstructions of longitudinal sections through the disc epidermis (from Flammang et al. 1998a): (a) during attachment to the substratum, the two types of non-ciliated secretory cells (NCS1, *in green*, and NCS2, *in blue*) release some of their granules whose contents coalesce and mix to form the adhesive material; (b) during detachment from the substratum, ciliated secretory cells release their secretion (*in yellow*) which would function to jettison the fuzzy coat (*in red*) thereby allowing the podium to detach. The adhesive footprint left on the substratum after detachment thus comprises adhesive secretions and fuzzy coat material, but no de-adhesive secretion. AM adhesive material, CS ciliated secretory cell, FC cuticle fuzzy coat, FP footprint, NCS1 type 1 non-ciliated secretory cell, NCS2 type 2 non-ciliated secretory cell, NSC non-secretory ciliated cell, SC support cell, SU substratum

was the fuzzy coat. This pattern of immunoreactivity suggests that secretions of CS cells are not incorporated into the footprints, but instead might function enzymatically to jettison the fuzzy coat thereby allowing the tube foot to detach (Fig. 10.2B) (Flammang 1996; Flammang et al. 1998a).

Although the ultrastructure of the de-adhesive cell granules is remarkably constant from one echinoderm taxon to another, that of the adhesive cell granules varies extensively. The secretory granules of NCS cells are usually made up of at least two materials of different electron density which gives them a complex ultrastructure. Five broad categories can be recognized

(Flammang 1996): (1) homogeneous granules apparently made up of only one material, (2) heterogeneous granules in which two different materials are mixed in an irregular pattern (Fig. 10.3A), (3) dense-cored granules consisting of an electron-denser core surrounded by less dense material (Fig. 10.3B), (4) granules with a central filamentous bundle resembling granules of the previous group but in which the core is made up of a parallel arrangement of fibrils or rods (Fig. 10.3C), and (5) capped granules in which an electron-lucent material is covered, on one side, by a cap of electron-dense material (Fig. 10.3D). The significance of these ultrastructural differences between different echinoderm taxa is unknown at present. However, in asteroids, Engster and Brown (1972) pointed out a relationship between the internal organization of adhesive cell secretory granules and species habitat: asteroids confined to hard rocky substratum have complex granules enclosing a highly organized

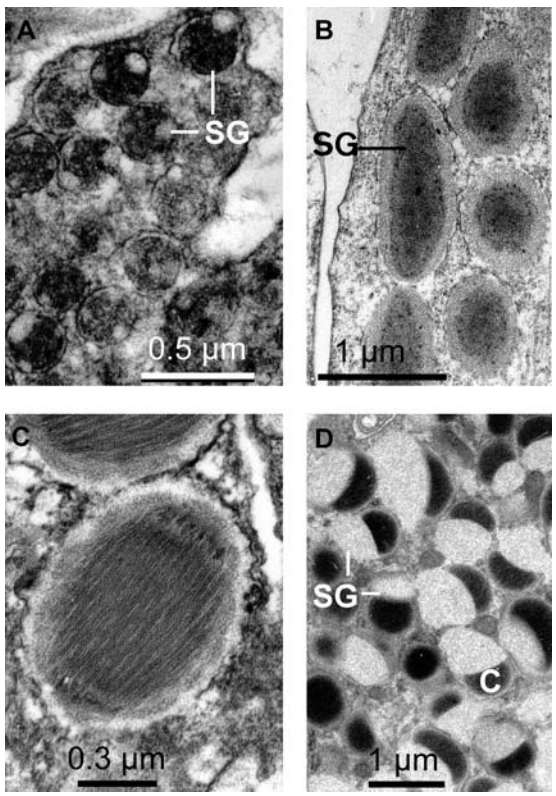

Fig. 10.3. Ultrastructure of the secretory granules of the adhesive cells from echinoderm tube feet (originals): (a) heterogeneous granules in the echinoid *Sphaerechinus granularis*; (b) dense-cored granules in the ophiuroid *Asteroxyx loveni*; (c) granules with a central filamentous bundle in the asteroid *Asterias rubens*; (b) capped granules in the holothuroid *Holothuria forskali*. C cap of electron-dense material, SG secretory granules

core whereas soft substratum dwelling species have granules of considerably simpler ultrastructure. They suggested that the different substructure of the adhesive cell granules would depend on the nature and composition of their contents that, in turn, could be related to the possible adhesive strength of the tube feet. In histochemistry, the adhesive cell secretory granules stain for both proteins and acid mucopolysaccharides, the former being predominant in some species and the latter in others (see Flammang 1996 for review).

In all echinoderm species investigated so far, after detachment of the tube foot, the adhesive secretion remains firmly bound to the substratum as a footprint. Although footprint diameter is easily measured after staining of the adhesive material (Flammang 1996), footprint thickness is difficult to estimate. Using an interference-optical profilometer, which generated three-dimensional images of the footprint surface, the mean maximum thickness of dry footprints was found to be 100 nm in the echinoid *P. lividus* and 230 nm in the asteroid *A. rubens* (Flammang et al. 2005). On the other hand, based on TEM observations, the thickness of fixed footprints in *A. rubens* ranges between 1 and 5 µm (Fig. 10.4C) (Flammang et al. 1994; Flammang 1996). Footprints appear as a foam-like material deposited as a thin layer on the substratum (Fig. 10.4A–C) (Thomas and Hermans 1985; Flammang 1996; Flammang et al. 1998a). This cellular aspect has been observed on fresh (Fig. 10.4A), freeze-dried (Fig. 10.4B), and fixed (Fig. 10.4C) footprints, and therefore is presumably not an artifact. In the asteroid *A. rubens*, the footprint adhesive material has the ultrastructure of a fibre-reinforced composite (Fig. 10.4D,E), which is able to fill out the very small surface irregularities – in the nanometer range – of the substratum (e.g., around the bacterium in Fig. 10.4E). The TEM study of the adhesive cells during tube foot attachment suggests that the electron-dense fibres present in the adhesive material derive directly from the rods described in their secretory granules (Figs. 10.2 and 10.3C). The chemical composition of the footprint material was analysed in *A. rubens*. Leaving inorganic residue apart, this material is made up mainly of proteins and carbohydrates, representing about 20 and 10% of the material's dry weight, respectively (Flammang et al. 1998a). The protein moiety contains significant amounts of both charged (especially acidic) and uncharged polar residues. Moreover, it has somewhat higher levels of glycine, proline, isoleucine and cysteine than the average eukaryotic protein (Table 10.1), this latter amino acid being presumably involved in intermolecular disulphide bonds reinforcing the cohesive strength of the adhesive (Flammang et al. 1998a). The carbohydrate moiety is also acidic, comprising both uronic acids and sulfate groups. So far, *A. rubens* is the only species in which the tube foot adhesive has been studied biochemically and nothing is known on other echinoderm species. Regarding the asteroids, however, a comparative immunohistochemical study of the tube feet from 14 species representing 5 orders and 10 families revealed that the adhesives of all these species are at least partly related, and this independently of the taxon considered, of the species habitat, of the tube foot morphotype or function, and of the adhesive cell secretory granule ultrastructure (Santos et al. 2005b).

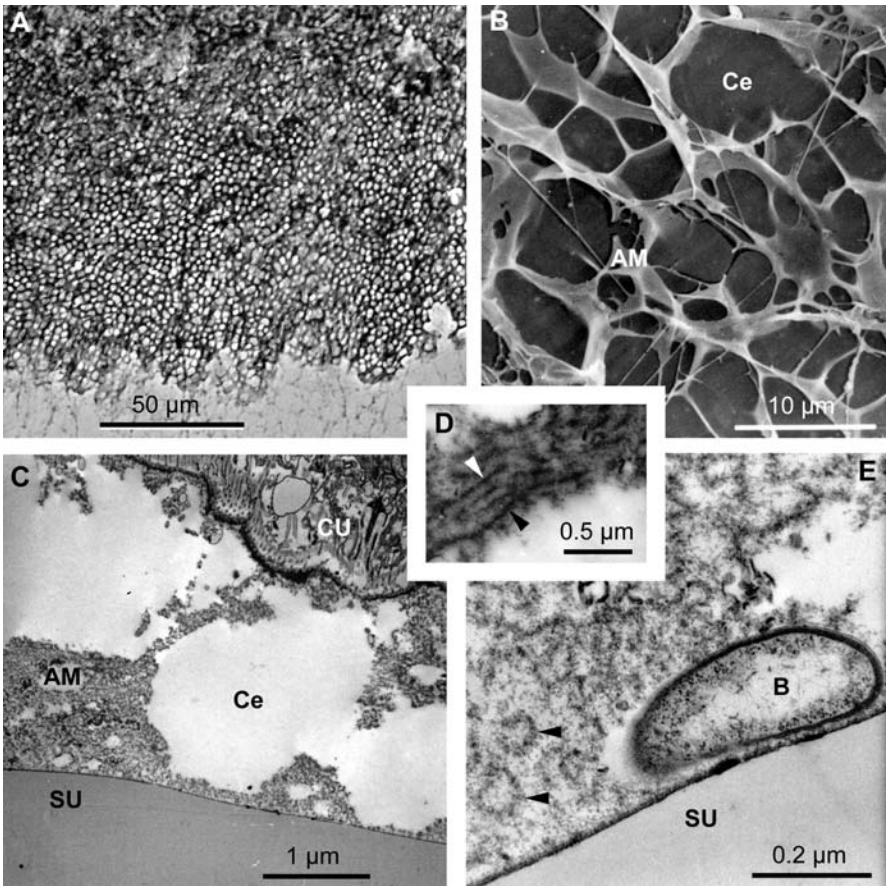

Fig. 10.4. Adhesive footprints and attached tube feet of the asteroid *Asterias rubens* (originals): (a) light microscopy photograph of a fresh footprint stained with a 0.05% aqueous solution of Crystal Violet; (b) detail of a freeze-dried footprint in SEM; (c) TEM photograph of a tube foot disc bond to the substratum by adhesive material; (d,e) details of the ultrastructure of the adhesive material (*arrowheads* indicate electron-dense fibre-like structures). AM adhesive material, B bacterium surrounded by the adhesive material, Ce cell in the foam-like adhesive, CU tube foot disc cuticle, SU substratum

10.3 Larval Adhesive Organs

For most echinoderms, metamorphosis transforms a bilaterally symmetrical and pelagic larva into a radially symmetrical and benthic postmetamorphic individual. Settlement always takes place during the so-called perimetamorphic period (Gosselin and Jangoux 1998; Haesaerts et al. 2003), but either before or after the metamorphic stage according to the class considered (Strathmann 1978). In both cases, adhesive organs attach either the competent

Table 10.1. Amino acid composition of the adhesive secretion from the tube feet of the sea star *Asterias rubens* (values in residues per thousand; from Flammang et al. 1998a)

Amino acid	
ASX	118
THR	78
SER	76
GLX	102
PRO	61
GLY	97
ALA	62
CYS/2	32
VAL	67
MET	17
ILE	45
LEU	61
TYR	27
PHE	38
HIS	56
LYS	21
ARG	41

larva or the postlarva to the substratum during settlement. In three of the five extant echinoderm classes, these organs are the tube feet, viz. the five primary tube feet of competent echinoplutei in echinoids, the five primary tentacles (and, for some species, two posterior tube feet) of pentactulae in holothuroids, the five primary tube feet and the five first pairs of tube feet of ophiuroid postlarvae (Strathmann 1978). These tube feet are similar in structure and function to tube feet of adults (Cameron and Fankboner 1984; Flammang et al. 1998b). Larval adhesive organs of crinoids and asteroids are, on the other hand, unique and have no equivalent in the postmetamorphic stage (Strathmann 1978).

The perimetamorphic period of crinoids comprises three stages: the doliolaria (free swimming larval stage), the cystidean (attached metamorphic stage), and the pentacrinoid stages (attached postlarval stage) (Mladenov and Chia 1983; Lahaye and Jangoux 1987; Nakano et al. 2003). Competent doliolariae are small barrel-shaped larvae. They possess an attachment complex at their anterior end which consists of a ciliary cap surrounding an apical tuft of elongated cilia and a ventrally located and slightly depressed adhesive pit (Fig. 10.5A,B). The ultrastructure of this attachment complex has been studied in comatulids (Chia et al. 1986; Jangoux and Lahaye 1990). It is strictly epidermal and made up of elongated ciliated cells associated with a thick basiepider-

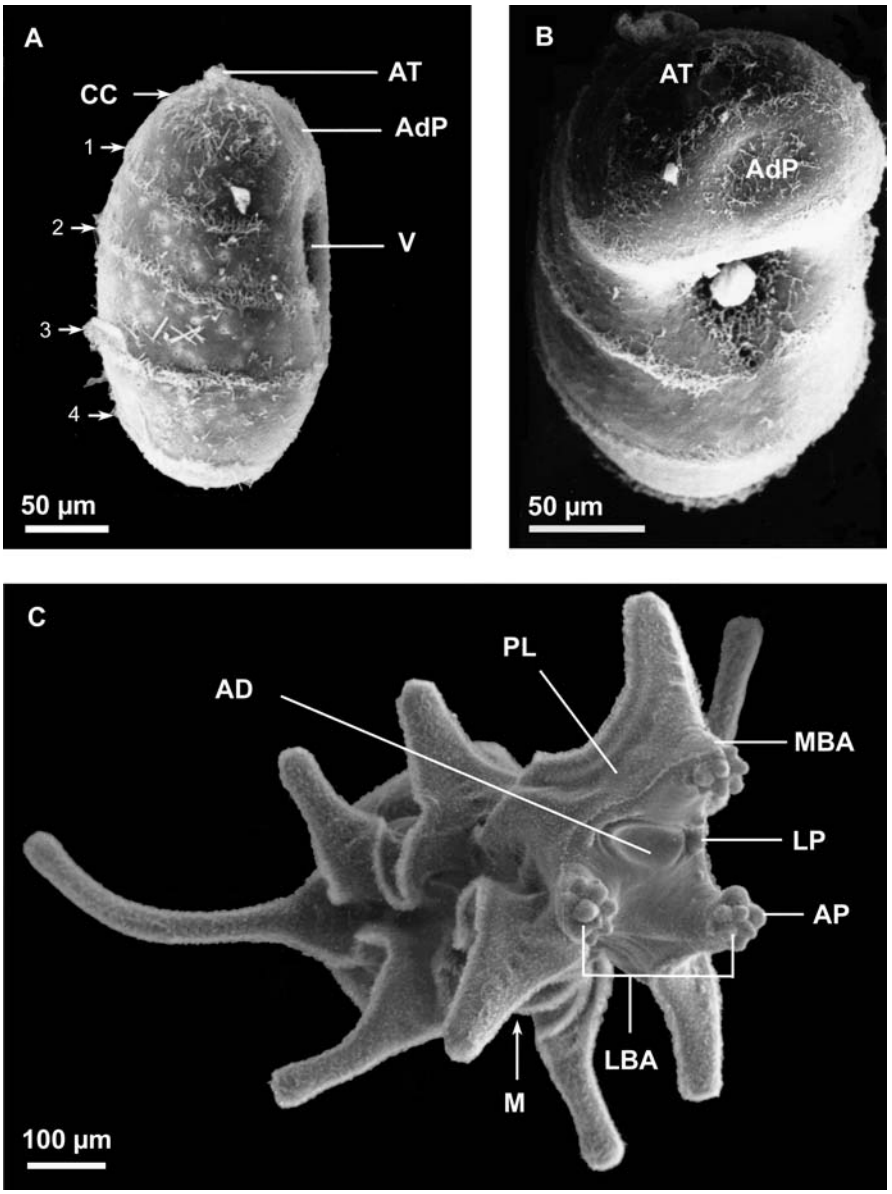

Fig. 10.5. Larval adhesive organs of crinoids and asteroids. SEM photographs of: (a) the doliolaria larva of *Antedon bifida*; (b) its anterior adhesive pit (from Lahaye 1987); (c) the brachiolaria larva of *Asterias rubens* (from Flammang et al. 2005). AD adhesive disc, AdP adhesive pit, AP apical papilla, AT apical tuft, CC ciliary cap, LBA lateral brachiolar arm, LP lateral papilla, M mouth, MBA median brachiolar arm, PL preoral lobe, V vestibule, 1–4 ciliary bands

mal nerve plexus. The four cell types forming the complex are sensory cells, covering cells and two types of secretory cells. Sensory cells and secretory cells of the first type occur exclusively in the ciliary cap. The former bear a long vibratile cilium whereas the latter are filled with secretory granules, which contain a flocculent mucopolysaccharidic material. Secretory cells of the second type are restricted to the adhesive pit where they are the most abundant cell type. These cells are filled with secretory granules with an electron dense fibrillar proteinaceous content. At the beginning of the settlement phase, the doliolaria becomes demersal and brushes the substratum with its apical tuft (sensory structure) (Mladenov and Chia 1983; Lahaye and Jangoux 1988). This implies the occurrence of a mechanism allowing the larva to combine loose adhesion to the substratum with movement. This transitory adhesion is achieved by the combined action of the secretory cells of the ciliary cap that produce a thin mucous film retaining the larva at the water-substratum interface, and of the covering cells whose cilia beat in this mucus (Jangoux and Lahaye 1990; Flammang 1996). When reaching a suitable site, the larva stops moving and turns itself round to have its body directed obliquely (the adhesive pit facing the substratum). It then becomes permanently fixed and transforms into a cystidean larva (Mladenov and Chia 1983; Lahaye and Jangoux 1988). Permanent adhesion starts with the release of the proteinaceous cement by the secretory cells of the adhesive pit and continues during both cystidean and pentacrinoid stages (Chia et al. 1986; Jangoux and Lahaye 1990). After development of the cirri during this last stage, the juvenile detaches from its cemented stalk (Lahaye and Jangoux 1987).

Competent larvae in asteroids are called brachiolariae because they possess a specialized attachment complex on their anterior part comprising three brachiolar arms and an adhesive disc (Fig. 10.5C) (Barker 1978; Haesaerts et al. 2003). Brachiolar arms are hollow tubular structures occupied by an extension of the larval anterior coelom. Their histological organisation comprises four tissue layers: an inner myomesothelium, a connective tissue layer, a subepidermal nerve plexus, and an outer epidermis. Each brachiolar arm is tipped by several sensory-secretory areas named papillae, where both the epidermis and the nerve plexus are greatly thickened (Fig. 10.6A). The papillary epidermis encompasses two types of secretory cells (adhesive and de-adhesive cells), sensory cells, and support cells (Barker 1978; Haesaerts et al. 2005a). Adhesive cells bear an apical cilium and contain large ovoid granules that enclose an electron-dense heterogeneous material staining histochemically as neutral mucopolysaccharides. De-adhesive cells bear a sub-cuticular cilium and are filled with small granules containing an homogeneous electron-dense material. The adhesive disc is a round, concave structure lying between the brachiolar arms. It is an epidermal structure composed of two main cell types (Fig. 10.6B): ciliated cement-secreting cells and support cells (Barker 1978; Haesaerts et al. 2005a). The former are full of large secretory granules enclosing a fibrous proteinaceous content of woven aspect. When exploring the substratum, the competent larva orients itself ventral side down and successively attaches and

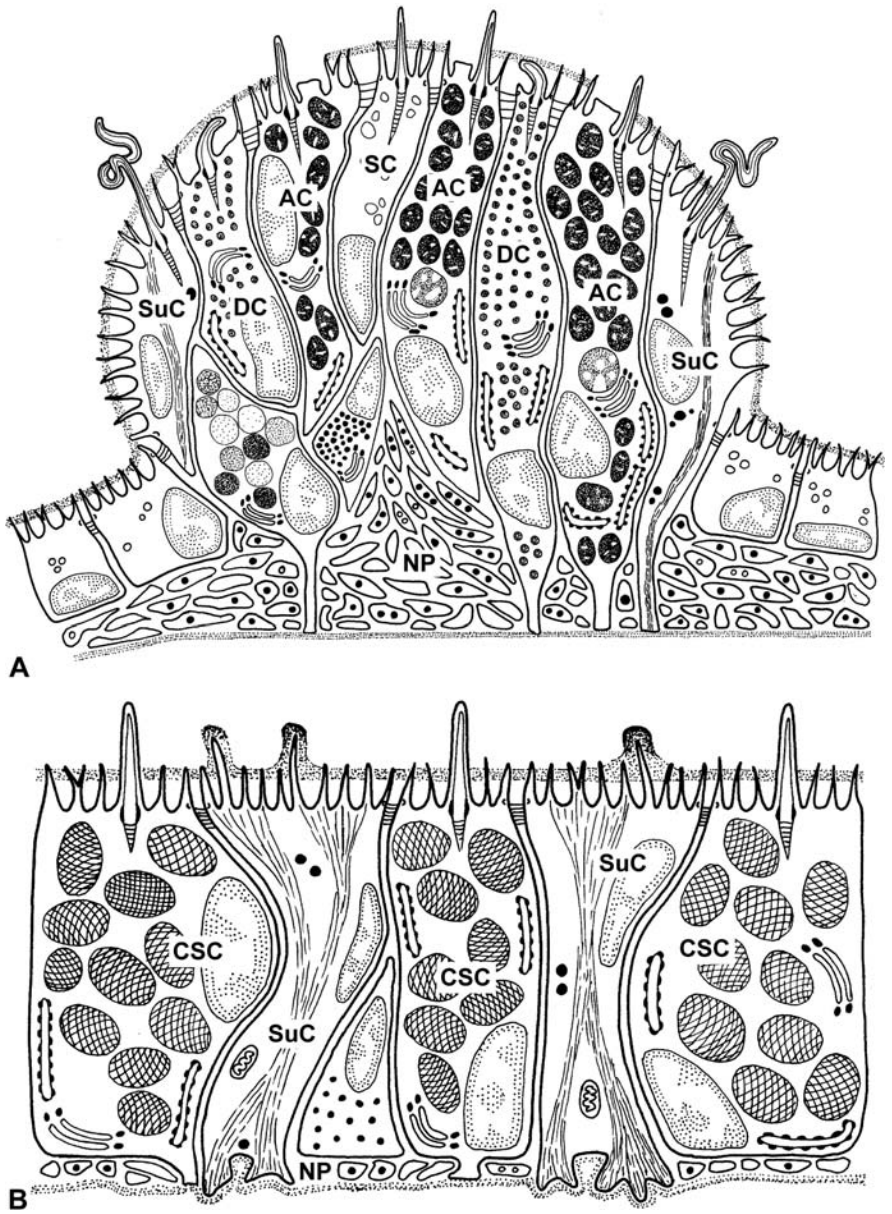

Fig. 10.6. Adhesive organs of the brachiolaria larva of the asteroid *Asterias rubens*. Schematic drawings of: (a) a longitudinal section through the papilla epidermis of a brachiolar arm; (b) a section through the adhesive disc epidermis (from Haesaerts et al. 2005a). AC adhesive cell, CSC cement secreting cell, DC de-adhesive cell, NP nerve plexus, SC sensory cell, SuC support cell

detaches its brachiolar arms (Barker 1978; Strathmann 1978; Haesaerts et al. 2003). Papillae, when making contact with the substratum, are responsible for sensory testing and temporary adhesion. Like adult tube feet, they function as a duo-gland system (Hermans 1983; Flammang 1996; Haesaerts et al. 2005a). In addition, the contents of brachiolar arm adhesive cells cross-react with antibodies raised against tube foot adhesive of *A. rubens*, indicating that temporary adhesives from larvae and adults are related to each other and probably share identical molecules, or, at least, identical epitopes on their constituents (Haesaerts et al. 2005a). Once the larva has found a suitable site for metamorphosis, brachiolar arms are gradually splayed out, enabling the disc to release its cement (Barker 1978; Haesaerts et al. 2003). This attaches the larva permanently to the substratum and marks the onset of the metamorphic stage. During this stage, tube feet become functional and ultimately help the newly formed postlarva to detach from the cemented disc (Haesaerts et al. 2003). In the species *Asterina gibbosa*, a turbulent channel flow apparatus has been used to evaluate the attachment strength of the different developmental stages (Haesaerts et al. 2005b). Using this technique, the nominal wall shear stresses needed to dislodge temporarily attached individuals are similar: about 1 Pa for brachiolariae attached by the arms and 7 Pa for postmetamorphic individuals attached by tube feet. On the other hand, a nominal wall shear stress of about 40 Pa is needed to detach metamorphic individuals permanently attached by the disc, showing the higher adhesive strength of the cement.

10.4 Cuvierian Tubules

Cuvierian tubules are peculiar organs found in several species of holothuroids (sea cucumbers), all belonging exclusively to the family Holothuriidae. Tubules (Fig. 10.7A) occurring in holothuroids of the genera *Bohadschia*, *Holothuria* and *Pearsonothuria* are expelled as sticky white threads that function as a defence mechanism against predators (Hamel and Mercier 2000; Flammang et al. 2002). Cuvierian tubule adhesion is a typical example of instantaneous adhesion, adhesion being achieved in a matter of seconds (less than 10 s; Zahn et al. 1973).

Cuvierian tubules occur in great numbers (between 200 and 600 in *H. forskali*; VandenSpiegel and Jangoux 1987) in the posterior part of the body cavity of the holothuroid. Proximally they are attached to the basal part of the left respiratory tree and their distal, blind end floats freely in the coelomic fluid. When disturbed, the sea cucumber directs its aboral end toward the stimulating source and undergoes a general body contraction. The anus opens, the wall of the cloaca tears, and the free ends of a few tubules (usually 10 to 20 in *H. forskali*; VandenSpiegel and Jangoux 1987), together with coelomic fluid, are expelled through the tear and the anus. As water from the respiratory tree is forcefully injected into their lumen, the emitted tubules elongate up to 20 times their

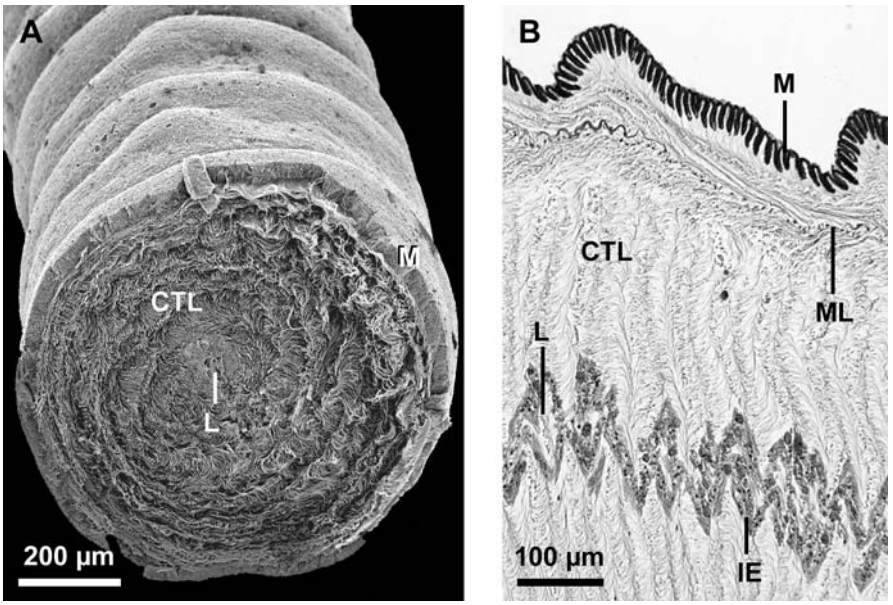

Fig. 10.7. Morphology of the Cuvierian tubules of *Holothuria impatiens* (from Flammang et al. 2005): (a) SEM photograph of a transversally-sectioned tubule; (b) longitudinal histological section showing the arrangement of the tissue layers. CTL connective tissue layer, IE inner epithelium, L lumen, ML muscle layer, M mesothelium

original length (VandenSpiegel and Jangoux 1987). Upon contact with any surface, the elongated tubules instantly become sticky. The adhesiveness of Cuvierian tubules combined with their tensile properties make them very efficient for entangling and immobilizing most potential predators (VandenSpiegel and Jangoux 1987; Hamel and Mercier 2000). Finally, the expelled tubules autotomize at their attachment point on the left respiratory tree and are left behind as the holothuroid crawls away (VandenSpiegel and Jangoux 1987). After expulsion and autotomy, Cuvierian tubules are readily regenerated. Cuvierian tubules thus constitute an efficient defensive mechanism. Their large number, sparing use and regeneration dynamics make them a formidable line of defense (Hamel and Mercier 2000; VandenSpiegel et al. 2000).

Cuvierian tubule adhesive strength on glass has been measured in seven species of sea cucumbers belonging to the genera *Bohadschia*, *Holothuria* and *Pearsonothuria* (Flammang et al. 2002). The mean normal tenacity observed varies from about 30 to 135 kPa. These values fall within the range of adhesive strengths described for marine organisms. They lie, however, among the lowest observed values (Flammang 2003). Tubule tenacity is influenced by the nature of the substratum: tubules adhere more strongly to polar than to non-polar substrata, indicating the importance of polar interactions in adhesion (Flammang et al. 2002).

Cuvierian tubules consist of, from the inside to the outside, an epithelium surrounding the narrow lumen, a thick connective tissue layer, and a mesothelium lining the surface of the tubule that is exposed to the coelomic cavity (Fig. 10.7). The mesothelium is responsible for adhesion. In quiescent tubules, it is a pseudostratified epithelium made up of two superposed cell layers – an outer layer of peritoneocytes and an inner layer of granular cells which is highly folded along the long axis of the tubule (Fig. 10.7B). Granular cells are filled with densely packed membrane-bound granules enclosing a proteinaceous material (Endean 1957; VandenSpiegel and Jangoux 1987). During elongation, the structure of the mesothelium is modified: the protective outer layer of peritoneocytes disintegrates and the granular cell layer, now unfolded, thus becomes outermost on the tubule. Granular cells empty the contents of their granules when the elongated tubule comes into contact with a surface, resulting in adhesion (VandenSpiegel and Jangoux 1987; De Moor et al. 2003).

In *H. forskali*, tubule print material – i.e., the secreted adhesive left on the substratum after mechanical detachment of the tubule – is composed of 60% protein and 40% neutral carbohydrate (De Moor et al. 2003). The proteinic nature of the adhesive material is confirmed by the observation that proteolytic enzymes reduce the adhesive strength of Cuvierian tubules in *H. forskali* (Zahn et al. 1973). The amino acid compositions of the protein fraction in *H. forskali*, *H. leucospilota*, *B. subrubra*, and *P. graeffei* indicate that their adhesives are closely related (Tables 10.2 and 10.3). All are rich in small side-chain amino acids, especially glycine, and in charged and polar amino acids. Only a small fraction of the secreted Cuvierian tubule adhesive (tubule prints) can be extracted using denaturing buffers containing both chaotropic and reducing agents. This soluble fraction contains about ten different proteins with molecular masses ranging from 10 to 220 kDa, but with closely related amino acid compositions, resembling that of the whole adhesive (De Moor et al. 2003). Non-secreted Cuvierian tubule adhesive has been directly extracted from isolated granular cells (adhesive cells). These cells were enzymatically dissociated from whole tubules and purified by density gradient centrifugation (Leclercq, Waite and Flammang, unpubl. data). Transmission electron microscopy demonstrated that granular cells were readily purified by this method (Fig. 10.8A). Extraction of the cells with the denaturing buffer used on tubule prints showed that their contents were much more easily solubilized than the secreted adhesive. Electrophoretic analyses revealed a very abundant low molecular weight protein (about 10 kDa) (Fig. 10.8B). The amino acid composition of this protein is almost identical to the one of the whole adhesive and to those of the proteins extracted from the tubule print material. The 10-kDa protein could therefore be the constitutive monomer of the adhesive. In this hypothesis, most of the proteins extracted from the secreted adhesive would be polymers of this 10-kDa protein. The chemical mechanism by which the adhesive monomer instantly polymerize upon release in sea water so far remains unknown.

Table 10.2. Amino acid compositions of adhesive secretions from the Cuvierian tubules of several species of holothuroids (values in residues per thousand)

Amino acid	*Holothuria forskali*[a]	*Holothuria leucospilota*[b]	*Bohadschia subrubra*[b]	*Pearsonothuria graeffei*[b]
HYP	0	24	8	8
ASX	78	74	64	62
THR	87	69	65	80
SER	60	42	58	58
GLX	91	122	106	124
PRO	55	74	69	63
GLY	266	267	298	254
ALA	88	115	91	85
CYS/2	14	3	9	4
VAL	38	29	35	37
MET	10	9	1	9
ILE	28	24	25	32
LEU	37	31	37	38
TYR	20	14	17	17
PHE	20	16	20	20
HIS	26	13	8	20
HLYS	0	5	12	3
LYS	31	12	29	22
ARG	50	57	46	63

[a] De Moor et al. (2003)
[b] Flammang et al. (2005)

10.5 Comparisons of Echinoderm Adhesives with Other Marine Bioadhesives

The density of seawater denies gravity the power to hold organisms to the bottom; thus, if they want to withstand the hydrodynamic forces, marine organisms must have adhesive mechanisms. Attachment to the substratum is therefore the most important use of adhesion by marine invertebrates, but other functions such as handling of food or building of tubes or burrows are also widespread in the marine fauna (Walker 1987; Tyler 1988; Flammang 1996; Whittington and Cribb 2001). Adhesion to the substratum may be permanent, transitory, or temporary (Tyler 1988; Flammang 1996; Whittington and Cribb 2001). Permanent adhesion involves the secretion of a cement and is characteristic of sessile organisms staying at the same place throughout their adult life (e.g., the attachment of barnacles on rocks). Transitory adhesion allows

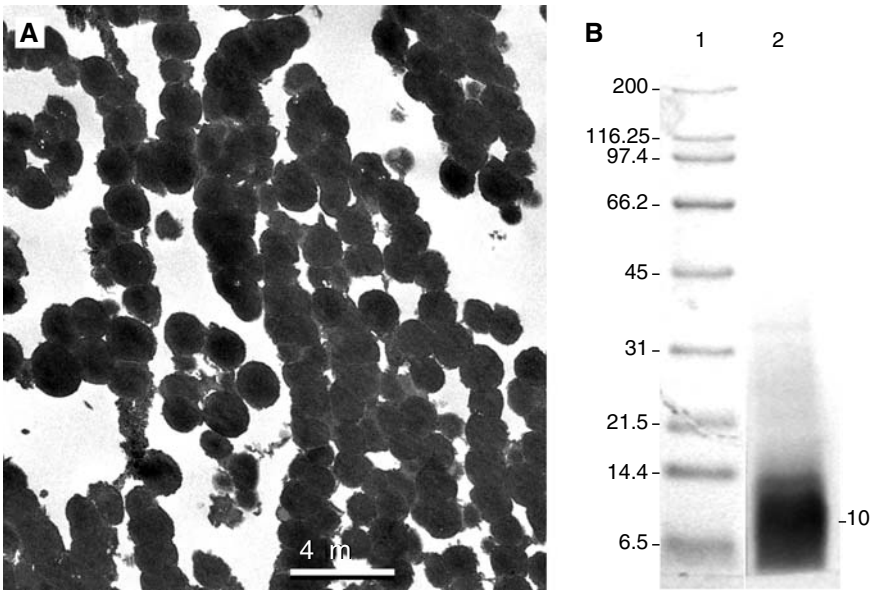

Fig. 10.8. Purification of the adhesive proteins from the Cuvierian tubules of *Holothuria forskali* (Leclercq, Waite and Flammang, unpubl. data): (a)transmission electron micrograph of a section through a pellet of purified granular cells; (b) electrophoresis (SDS-PAGE) of the proteins extracted from this pellet: *Lane 1*, molecular weight markers; *Lane 2*, extract from the granular cells showing a single abundant protein band at 10 kDa

simultaneous adhesion and locomotion: the animals attach by a viscous film they lay down between their body and the substratum, and creep on this film which they leave behind as they move (e.g., the ventral secretions of turbellarian platyhelminths). Temporary adhesion allows organisms to attach firmly but momentarily to a substratum (e.g., the adhesion of echinoderm podia). The boundary between transitory and temporary adhesion is not always clear, however. Indeed, gastropod molluscs may use either transitory adhesion (in conjunction with suction) when they are moving, or temporary adhesion when stationary for a long period of time, the latter giving by far the greatest adhesive strength to the animal (see, e.g., Smith et al. 1999a). A fourth type of adhesion, instantaneous adhesion, comprises invertebrate adhesive systems that do not fit into the three types of adhesion described above. These adhesive systems rely on single-use organs or cells and are used in functions other than attachment to the substratum requiring a very fast formation of adhesive bonds. Prey capture by collocyte-bearing tentacles of ctenophorans and defence reaction involving Cuvierian tubules in holothuroids are typical examples of this type of adhesion (Flammang et al. 2005).

In marine invertebrates, adhesive secretions are always predominantly made up of proteins. Yet their biochemical composition varies from one taxonomic group to another (Flammang et al. 1998a; Smith et al. 1999a;

Flammang 2003). As a general rule, permanent adhesives consist almost exclusively of proteins. On the other hand, non-permanent adhesives (transitory as well as temporary) are made up of an association of proteins and carbohydrates, the latter being mostly in the form of acid and sulfated sugars (see Whittington and Cribb 2001 for review). The ratio of proteins to carbohydrates is usually about 2:1 but there may be substantial variation on this figure though there is typically more protein than carbohydrate (Grenon and Walker 1980; Davies et al. 1990; Flammang et al. 1998a; Smith et al. 1999a; Smith and Morin 2002). The composition of the instantaneous adhesive of the Cuvierian tubule adhesive is reminiscent of non-permanent adhesives by its association of proteins and carbohydrate in a 3:2 ratio (De Moor et al. 2003). However, it differs from them by the fact that the carbohydrate fraction is in the form of neutral sugars and not acidic sugars.

As far as the amino acid composition of the protein fraction is concerned, all the marine bioadhesives characterized so far have in common their richness in small side-chain amino acids as well as in charged and polar amino acids. These characteristics were indeed observed in flatworms (Hamwood et al. 2002), mussels (Benedict and Waite 1986; Waite et al. 1989), limpets (Grenon and Walker 1980; Smith et al. 1999a), tubeworms (Jensen and Morse 1988; Stewart et al. 2004), barnacles (Walker 1972; Naldrett and Kaplan 1997; Kamino et al. 1996), sea stars (Flammang et al. 1998a), and sea cucumbers (De Moor et al. 2003). Charged and polar amino acids are probably involved in adhesive interactions with the substratum through hydrogen and ionic bonding (Waite 1987). Small side-chain amino acids, on the other hand, are often found in large quantities in elastomeric proteins (Tatham and Shewry 2000). These proteins are able to withstand significant deformations without rupture before returning to their original state when the stress is removed (Smith et al. 1999b). Marine glues thus appear to be tailored for both high adhesive strength and high cohesive strength.

Despite these similarities, the composition of marine invertebrate adhesives is variable from one species to another. To quantify this variability, the method of Marchalonis and Weltman (1971) was used. It allows the determination of relatedness among proteins based upon statistical analysis of differences in their amino acid composition. A parameter called $S\Delta Q$ is calculated by pairwise comparison of the percentages of each amino acid constituting the proteins. Marchalonis and Weltman (1971) reported that values of $S\Delta Q \leq 100$ indicate relatedness. Here, this method has been extended to whole adhesives, which are usually blends of different proteins, based on the assumption that if they include closely related proteins their whole amino acid compositions will be similar too. The values of $S\Delta Q$ for comparisons between the adhesives of 15 invertebrate species belonging to seven taxonomic groups are given in Table 10.3. Three amino acids (i.e., half-cystine, hydroxyproline and di-hydroxyphenylalanine [DOPA]) that were not considered by Marchalonis and Weltman (1971) have been taken into account because they are important constituents of some marine adhesives (Taylor

Table 10.3. SΔQ for comparison among adhesives in marine invertebrates (modified from Flammang 2003). Values in bold indicate relatedness; solid-line boxes frame species belonging to a same taxonomic group (i.e., mussels, barnacles, limpets and sea cucumbers, respectively)

		Permanent adhesion						Non-permanent adhesion				Instantaneous adhesion			
	Pc	Gd	Me	Bc	Be	Bh	Mr	Ll	Pv	Es	Ar	Hf	Hl	Bs	Pg
Pc	**0**	-	-	-	-	-	-	-	-	-	-	-	-	-	-
Gd	714	**0**	-	-	-	-	-	-	-	-	-	-	-	-	-
Me	706	**90**	**0**	-	-	-	-	-	-	-	-	-	-	-	-
Bc	989	191	348	**0**	-	-	-	-	-	-	-	-	-	-	-
Be	1038	263	430	**107**	**0**	-	-	-	-	-	-	-	-	-	-
Bh	888	216	383	**97**	**97**	**0**	-	-	-	-	-	-	-	-	-
Mr	907	160	364	**72**	**76**	**64**	**0**	-	-	-	-	-	-	-	-
Ll	1130	214	480	151	213	139	**77**	**0**	-	-	-	-	-	-	-
Pv	1093	176	385	**99**	128	**93**	**39**	**60**	**0**	-	-	-	-	-	-
Es	971	124	357	186	222	195	**78**	**105**	**96**	**0**	-	-	-	-	-
Ar	1007	116	323	**74**	148	**82**	**34**	**34**	**32**	**62**	**0**	-	-	-	-
Hf	818	145	131	433	580	457	427	445	406	345	345	**0**	-	-	-
Hl	1005	214	189	518	672	539	510	527	462	391	422	**40**	**0**	-	-
Bs	832	209	176	568	722	591	571	599	553	440	484	**28**	**34**	**0**	-
Pg	882	157	175	421	546	438	405	426	376	301	335	**20**	**23**	**34**	**0**

Tube-dwelling worm: Pc *Phragmatopoma californica*, Jensen and Morse 1988
Mussels: Gd *Geukensia demissa*, Waite et al. 1989; Me *Mytilus edulis*, Benedict and Waite 1986
Barnacles: Bc *Balanus crenatus*, Walker 1972; Be *Balanus eburneus*, Naldrett and Kaplan 1997; Bh *Balanus hameri*, Walker 1972; Mr *Megabalanus rosa*, Kamino et al. 1996
Limpets: Ll *Lottia limatula*, Smith et al. 1999; Pv *Patella vulgata*, Grenon and Walker 1980
Flatworm: Es *Entobdella soleae*, Hamwood et al. 2001
Sea star: Ar *Asterias rubens*, Flammang et al. 1998a
Sea cucumbers: Hf *Holothuria forskali*, De Moor et al. 2003; Hl *Holothuria leucospilota*, Bs *Bohadschia subrubra*, Pg *Pearsonothuria graeffei*, Flammang et al. 2005

and Waite 1997; Kamino et al. 2000). Aspartic acid and asparagine, glutamic acid and glutamine were taken as Asx and Glx respectively as in the original method. The level of significance was also set at 100, but two values just above 100 were also considered as indicating relatedness (Table 10.3). Values given in Table 10.3 show that the adhesives of every species within a same taxonomic group are related, suggesting, as expected, that they are homologous. More interesting is the relationship between the adhesives of all the species using non-permanent adhesion, despite the fact that they belong to very disparate phyla (i.e., platyhelminthes, mollusks and echinoderms; dotted-line box; Table 10.3). This relationship indicates convergence in composition because of common function and selective pressures. On the other hand, such an analogy is not observed for the adhesives of sessile invertebrates using permanent adhesion. Indeed, the adhesives from mussels, tubeworms and barnacles differ one from another (Table 10.3). The protein fractions of mussel byssal plaque and polychaete cement have in common the presence of DOPA in their composition (Benedict and Waite 1986; Jensen and Morse 1988; Waite et al. 1989). However, the tubeworm adhesive stands apart from any other adhesive by its very high content of phosphoserine (Stewart et al. 2004). Barnacle cement, on the other hand, contains no DOPA and appears to be closer to non-permanent adhesives (Table 10.3). They have in common the importance of disulfide bonds in their insolubilization (Flammang et al. 1998a; Smith et al. 1999a; Kamino et al. 2000; Hamwood et al. 2002). These disulfide bonds may be intermolecular, providing cross-linking between the adhesive proteins (Flammang et al. 1998a; Hamwood et al. 2002), or intramolecular, holding proteins in the specific shape required for interaction with their neighbors (Kamino 2001; Smith and Morin 2002). As for the instantaneous adhesive from holothuroid Cuvierian tubules, it differs from every other marine bioadhesive by its amino acid composition (Table 10.3). The protein fraction of this adhesive is particularly rich in glycine (De Moor et al. 2003; Flammang et al. 2005), resembling in this way mussel adhesives (Benedict and Waite 1986; Waite et al. 1989). To complete this comparison, marine invertebrate adhesives were plotted as a function of the hydrophobicity and polarity of their amino acids (Fig. 10.9) (Vincent 1980). Hydrophobicity was calculated using the method of Bigelow (1967). In this method, each amino acid that requires energy for transfer from a hydrophobic to an aqueous environment is assigned a value equal the energy of transfer minus the energy of transfer for glycine. The mole percent of each amino acid for which the free energy of transfer is positive is then multiplied by this free energy of transfer, and all the values are summed. Polarity is expressed as the percentage of polar amino acids in the composition. Once again, the non-permanent adhesives cluster together (except for the adhesive of *Patella vulgata* which has a lower percentage of polar amino acids) and are close to most barnacle adhesives (Fig. 10.9). With this representation, they are also close to mussel adhesives. The permanent adhesives from mussels, tubeworms, and barnacles largely differ one from another, and the instantaneous

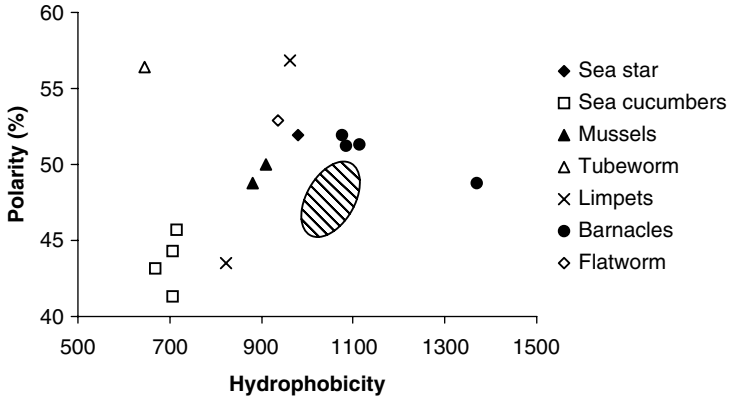

Fig. 10.9. Variation in hydrophobicity and polarity of amino acids in adhesives from marine invertebrates. The graph is based on the same amino acid compositions as those used in Table 10.3. The *striped area* represents average protein compositions compiled from different internet sources

adhesives from sea cucumbers stand apart from all other adhesives. Among marine bioadhesives, those of barnacles are the most hydrophobic and those of tubeworms and sea cucumber the least hydrophobic. Marine adhesives are blends of many different proteins and they are therefore compared to an average protein rather than to an arbitrarily selected protein (Fig. 10.9). As should be expected for an underwater glue, the different adhesives are either more polar (tubeworm, limpet, flatworm, sea star, barnacles) or more hydrophilic (sea cucumbers, limpets, mussels, flatworm, tubeworm) than the average protein composition, the two conditions not being mutually exclusive.

10.6 Conclusion

In addition to fundamental interests in marine bioadhesives, a substantial impetus behind understanding these adhesives are the potential technological applications that can be derived from their knowledge. These applications cover two broad fields of applied research: design of water-resistant adhesives and development of new antifouling strategies. The challenge with all of the biological adhesives is therefore to understand their mode of action sufficiently well that their essential features can be mimicked, in the case of the design of new adhesives, or inhibited, in the case of biofouling control. This will require a detailed knowledge of their physico-chemical characteristics (e.g., protein composition, sequences of these proteins, identification of their post-translational modifications), in order to relate them to their properties (e.g., specificity towards vari-

ous substrata, speed of action, insolubilization of the adhesive, life-expectancy of the attachment, etc.). This detailed information is progressively becoming available for the adhesive systems of several types of organisms (see the other chapters in this book). So far, however, none is available for any echinoderm adhesive secretion. Work is currently in progress to identify, purify, and characterize the different molecules involved in the reversible attachment of tube feet, the powerful fixation of asteroid larvae, and the instantaneous adhesion of Cuvierian tubules. Only the complete elucidation of their structure and characteristics will allow valid comparisons with the other biological adhesives.

Acknowledgments. This work was supported in part by the U.S. Office of Naval Research (Grant n ° N00014-99-1-0853). P.F. is Research Associate of the National Fund for Scientific Research of Belgium (FNRS). This study is a contribution from the "Centre Interuniversitaire de Biologie Marine" (CIBIM; http://www.ulb.ac.be/sciences/biomar/).

References

Barker MF (1978) Structure of the organs of attachment of brachiolaria larvae of *Stichaster australis* (Verrill) and *Coscinasterias calamaria* (Gray) (Echinodermata: Asteroidea). J Exp Mar Biol Ecol 33:1–36

Benedict CV, Waite JH (1986) Composition and ultrastructure of the byssus of *Mytilus edulis*. J Morphol 189:261–270

Bigelow CC (1967) On the average hydrophobicity of proteins and the relation between it and protein structure. J Theor Biol 16:187–211

Cameron JL, Fankboner PV (1984) Tentacle structure and feeding processes in life stages of the commercial sea cucumber *Parastichopus californicus* (Stimpson). J Exp Mar Biol Ecol 81:193–209

Chia FS, Burke RD, Koss R, Mladenov PV, Rumrill SS (1986) Fine structure of the doliolaria larva of the feather star *Florometra serratissima* (Echinodermata: Crinoidea), with special emphasis on the nervous system. J Morphol 189:99–120

Davies MS, Jones HD, Hawkins SJ (1990) Seasonal variation in the composition of pedal mucus from *Patella vulgata* L. J Exp Mar Biol Ecol 144:101–112

De Moor S, Waite JH, Jangoux M, Flammang P (2003) Characterization of the adhesive from the Cuvierian tubules of the sea cucumber *Holothuria forskali* (Echinodermata, Holothuroidea). Mar Biotechnol 5:37–44

Endean R (1957) The Cuvierian tubules of *Holothuria leucospilota*. Q J Micros Sci 98:455–472

Engster MS, Brown SC (1972) Histology and ultrastructure of the tube foot epithelium in the phanerozonian starfish, *Astropecten*. Tiss Cell 4:503–518

Flammang P (1996) Adhesion in echinoderms. In: Jangoux M, Lawrence JM (eds) Echinoderm studies, vol 5. Balkema, Rotterdam, pp 1–60

Flammang P (2003) The glue of sea cucumber Cuvierian tubules: a novel marine bioadhesive. In: Colliec-Jouault S, Bergé JP, Guézennec J, Fleurence J, Le Gal Y, Roy P (eds) Marine biotechnology: an overview of leading fields. Actes Colloq Ifremer 36:176–185

Flammang P, Walker G (1997) Measurement of the adhesion of the podia in the asteroid *Asterias rubens* (Echinodermata). J Mar Biol Assoc UK 77:1251–1254

Flammang P, Demeuleneare S, Jangoux M (1994) The role of podial secretions in adhesion in two species of sea stars (Echinodermata). Biol Bull 187:35–47

Flammang P, Michel A, van Cauwenberge A, Alexandre H, Jangoux M (1998a) A study of the temporary adhesion of the podia in the sea star *Asterias rubens* (Echinodermata, Asteroidea) through their footprints. J Exp Biol 201:2383–2395

Flammang P, Gosselin P, Jangoux M (1998b) The podia, organs of adhesion and sensory perception in larvae and postmetamorphic stages of the echinoid *Paracentrotus lividus* (Echinodermata). Biofouling 12:161–171

Flammang P, Ribesse J, Jangoux M (2002) Biomechanics of adhesion in sea cucumber Cuvierian tubules (Echinodermata, Holothuroidea). Integr Comp Biol 42:1107–1115

Flammang P, Santos R, Haesaerts D (2005) Echinoderm adhesive secretions: From experimental characterization to biotechnological applications. In: Matranga V (ed) Marine molecular biotechnology: Echinodermata. Springer, Berlin Heidelberg New York, pp 201–220

Gosselin P, Jangoux M (1998) from competent larva to exotrophic juvenile: a morphofunctional study of the perimetamorphic period of *Paracentrotus lividus* (Echinodermata, Echinoidea). Zoomorphology 118:31–43

Grenon JF, Walker G (1980) Biochemical and rheological properties of the pedal mucus of the limpet, *Patella vulgata* L. Comp Biochem Physiol 66B:451–458

Grenon JF, Walker G (1981) The tenacity of the limpet, *Patella vulgata* L.: an experimental approach. J Exp Mar Biol Ecol 54:277–308

Haesaerts D, Jangoux M, Flammang P (2003) Study of the perimetamorphic period of the sea star *Asterias rubens* by scanning electron microscopy. In: Féral JP, David B (eds) Echinoderm research 2001. Balkema, Lisse, pp 155–159

Haesaerts D, Jangoux M, Flammang P (2005a) The attachment complex of brachiolaria larvae of the sea star *Asterias rubens* (Echinodermata): an ultrastructural and immunocytochemical study. Zoomorphology 124:67–78

Haesaerts D, Finlay JA, Callow ME, Callow JA, Grosjean P, Jangoux M, Flammang P (2005b) Evaluation of the attachment strength of the perimetamorphic stages of *Asterina gibbosa* (Echinodermata, Asteroidea). Biofouling (in press)

Hamel J-F, Mercier A (2000) Cuvierian tubules in tropical holothurians: usefulness and efficiency as a defence mechanism. Mar Fresh Behav Physiol 33:115–139

Hamwood TE, Cribb BW, Halliday JA, Kearn GC, Whittington ID (2002) Preliminary characterization and extraction of anterior adhesive secretion in monogenean (Platyhelminth) parasites. Folia Parasitol 49:39–49

Hermans CO (1983) The duo-gland adhesive system. Oceanogr Mar Biol Annu Rev 21:281–339

Jangoux M, Lahaye M-C (1990) The attachment complex of the dololaria larvae of *Antedon bifida* (Echinodermata, Crinoidea). In: De Ridder C, Dubois P, Lahaye M-C, Jangoux M (eds) Echinoderm research. Balkema, Rotterdam, pp 99–105

Jensen RA, Morse DE (1988) The bioadhesive of *Phragmatopoma californica* tubes: a silk-like cement containing L-DOPA. J Comp Physiol 158B:317–324

Kamino K (2001) Novel barnacle underwater adhesive protein is a charged amino acid-rich protein constituted by a Cys-rich repetitive sequence. Biochem J 356:503–507

Kamino K, Odo S, Maruyama T (1996) Cement proteins of the acorn barnacle, *Megabalanus rosa*. Biol Bull 190:403–409

Kamino K, Inoue K, Maruyama T, Takamatsu N, Harayama S, Shizuri Y (2000) Barnacle cement proteins. Importance of disulfide bonds in their insolubility. J Biol Chem 275:27360–27365

Lahaye M-C (1987) Comportement larvaire et ontogénèse postembryonnaire chez la comatule *Antedon bifida* (Echinodermata, Crinoidea). PhD Thesis, Université Libre de Bruxelles, Belgium

Lahaye M-C, Jangoux M (1987) The skeleton of the stalked stages of the comatulid crinoid *Antedon bifida* (Echinodermata). Fine structure and changes during growth. Zoomorphology 107:58–65

Lahaye M-C, Jangoux M (1988) Morphologie externe et comportement des larves doliolaria d'*Antedon bifida* (Echinodermata, Crinoidea). Ann Soc R Zool Belg 118:183–189

Marchalonis JJ, Weltman JK (1971) Relatedness among proteins: a new method of estimation and its application to immunoglobins. Comp Biochem Physiol 38B:609–625

Mladenov PV, Chia FS (1983) Development, settling behaviour, metamorphosis and pentacrinoid feeding and growth of the feather star *Florometra serratissima*. Mar Biol 73: 309–323
Nakano H, Hibino T, Oji T, Hara Y, Amemiya S (2003) Larval stages of a living sea lily (stalked crinoid echinoderm). Nature, Lond 421:158–160
Naldrett MJ, Kaplan DL (1997) Characterization of barnacle (*Balanus eburneus* and *B. crenatus*) adhesive proteins. Mar Biol 127:629–635
Paine VL (1926) Adhesion of the tube feet in starfishes. J Exp Zool 45:361–366
Ruppert EE, Barnes RD (1994) Invertebrate zoology, 6th edn. Saunders College Publishing, Fort Worth, 1056 pp
Santos R, Gorb S, Jamar V, Flammang P (2005a) Adhesion of echinoderm tube feet to rough surfaces. J Exp Biol 208:2555–2567
Santos R, Haesaerts D, Jangoux M, Flammang P (2005b) Comparative histological and immunohistochemical study of sea star tube feet (Echinodermata, Asteroidea). J Morphol 263:259–269
Smith AM, Morin MC (2002) Biochemical differences between trail mucus and adhesive mucus from marsh periwinkle snail. Biol Bull 203:338–346
Smith AM, Quick TJ, St Peter RL (1999a) Differences in the composition of adhesive and non-adhesive mucus from the limpet *Lottia limatula*. Biol Bull 196:34–44
Smith BL, Schäffer TE, Viani M, Thompson JB, Frederick NA, Kindt J, Belcher A, Stucky GD, Morse DE, Hansma PK (1999b) Molecular mechanistic origin of the toughness of natural adhesives, fibres and composites. Nature 399:761–763
Stewart RJ, Weaver JC, Morse DE, Waite JH (2004) The tube cement of *Phragmatopoma californica*: a solid foam. J Exp Biol 207:4727–4734
Strathmann RR (1978) Larval settlement in echinoderms. In: Chia FS, Rice ME (eds) Settlement and metamorphosis of marine invertebrate larvae. Elsevier-North Holland, New York, pp 235–246
Tatham AS, Shewry PR (2000) Elastomeric proteins: biological roles, structures and mechanisms. Trends Biochem Sci 25:567–571
Taylor SW, Waite JH (1997) Marine adhesives: From molecular dissection to application. In: McGrath K, Kaplan D (eds) Protein-based materials. Birkhäuser, Boston, pp 217–248
Thomas LA, Hermans CO (1985) Adhesive interactions between the tube feet of a starfish, *Leptasterias hexactis*, and substrata. Biol Bull 169:675–688
Tyler S (1988) The role of function in determination of homology and convergence-examples from invertebrates adhesive organs. Fortsch Zool 36:331–347
VandenSpiegel D, Jangoux M (1987) Cuvierian tubules of the holothuroid *Holothuria forskali* (Echinodermata): a morphofunctional study. Mar Biol 96:263–275
VandenSpiegel D, Jangoux M, Flammang P (2000) Maintaining the line of defense: regeneration of Cuvierian tubules in the holothuroid *Holothuria forskali* (Echinodermata). Biol Bull 198:34–49
Vincent JFV (1980) Insect cuticle: a paradigm for natural composites. In: Vincent JFV, Currey JD (eds) The mechanical properties of biological materials. Symp Soc Exp Biol 34. Cambridge Univ Press, Cambridge, pp 183–210
Waite JH (1987) Nature's underwater adhesive specialist. Int J Adhesion Adhesives 7:9–14
Waite JH (2002) Adhesion à la moule. Integr Comp Biol 42:1172–1180
Waite JH, Hansen DC, Little KT (1989) The glue protein of ribbed mussels (*Geukensia demissa*): a natural adhesive with some features of collagen. J Comp Physiol B159:517–525
Walker G (1972) The biochemical composition of the cement of two barnacle species, *Balanus hameri* and *Balanus crenatus*. J Mar Biol Assoc UK 52:429–435
Walker G (1987) Marine organisms and their adhesion. In: Wake WC (ed) Synthetic adhesives and sealants. Wiley, Chichester, pp 112–135
Whittington ID, Cribb BW (2001) Adhesive secretions in the Platyhelminthes. Adv Parasitol 48:101–224

Yule AB, Walker G (1987) Adhesion in barnacles. In: Southward AJ (ed) Crustacean issues, vol 5: biology of barnacles. Balkema, Rotterdam, pp 389–402

Zahn RK, Müller WEG, Michaelis M (1973) Sticking mechanisms in adhesive organs from a *Holothuria*. Res Mol Biol 2:47–88

11 An Adhesive Secreted by Australian Frogs of the Genus *Notaden*

Lloyd D. Graham[1], Veronica Glattauer[2], Yong Y. Peng[2], Paul R. Vaughan[2], Jerome A. Werkmeister[2], Michael J. Tyler[3], and John A.M. Ramshaw[2]

11.1 Introduction

The main body of research into skin secretions from amphibians has been directed towards biologically active compounds responsible for the various toxic, pharmacological, antimicrobial and poisonous nature of various amphibian granular secretions. A very important difference between amphibian skin and that of other vertebrates is the diversity of glandular structures that are found. Significant bioactivity has been found within the secretions of amphibious skins. For example, pharmacological activity testing of Australian frog skins over a period of more than 30 years has shown the presence of an extensive array of simple and complex aliphatic, aromatic and heterocyclic molecules, as well as a range of small and large peptides (Doyle et al. 2003; Apponyi et al. 2004).

There has been little research into adhesive exudates. The scarcity of research in this area has been attributed to the difficulty of getting the adhesive gland products into a solution for analysis (Williams 1994), even though the adhesives of these amphibians generally do not seem to entail a covalent curing step to give tenacity of adhesion. Brodie and Gibson (1969) were unable to analyze the granular gland secretions of a salamander, *Ambystoma gracile*, due to difficulties in dissolving the adhesive secretions. Williams and Larsen (1986) used histological methods to show that the adhesive secretions from *A. macrodactylum* were proteinaceous. More recently, Williams (1994) examined the secretions of three species of salamander known to secrete an adhesive. Stimulating the animals both above and under water revealed that the skin secretions only became adhesive when exposed to air. Also, Evans and Brodie (1994) examined the tensile strength of the adhesive secretions from 12 species of amphibian, including 5 frog species. Frogs that produce secretions with tenacious adhesive properties include those from a South African species, *Breviceps poweri* (Channing 2001).

[1] CSIRO Molecular & Health Technologies, Sydney Laboratory, P.O. Box 184, North Ryde, NSW 1670, Australia
[2] CSIRO Molecular & Health Technologies, Ian Wark Laboratory, Bag 10, Clayton South, Victoria 3169, Australia
[3] School of Earth & Environmental Sciences, University of Adelaide, South Australia 5005, Australia

Biological Adhesives
(ed. by A.M. Smith and J.A. Callow)

Recently, we have initiated studies on the adhesives produced by members of the genus of Australian fossorial frogs, *Notaden*. These produce an exudate, secreted by glands on their backs, that quickly sets into an adhesive and elastic material. Three Australian frogs have so far been identified as producing adhesive, these being *N. melanoscaphus*, *N. bennetti* and *N. nichollsi*. Initial observations on adhesive efficacy were made using the exudates of *N. melanoscaphus*. More recently, however, studies have used the exudates from *N. bennetti*. Commonly known as the "Holy Cross Frog" (Fig. 11.1), *N. bennetti* is found on plains near larger rivers, in savannah woodland and in mallee areas across central New South Wales and the interior of southern Queensland (Barker et al. 1995). There appears to be little, if any, difference between the properties of the adhesive from these two species.

Notaden frogs secrete the sticky material from their dorsal skin when they are provoked, probably in an attempt to deter potential predators (Evans and Brodie 1994). The frogs typically live 1 m underground in dried mud for nine months of the year, emerging only during torrential rain. On these occasions they are vulnerable to insect attacks and so a possible use of the exudate may be to jam the jaws of biting insects like ants, sticking them to the frog's skin, which it later sheds and eats. The exudate sets rapidly as a yellow-coloured tacky elastic solid, and sticks well even in the frog's moist habitat.

11.2 Preliminary Field and Laboratory Data

The potential of the *Notaden* exudate as a novel adhesive system was first identified during field studies (M.J. Tyler, unpubl.). These data indicated that the liquid exudate had a fast setting time, ~10 s to ~3 min, giving a strong adhesive bond. The adhesion worked on moist surfaces, for example where moisture had

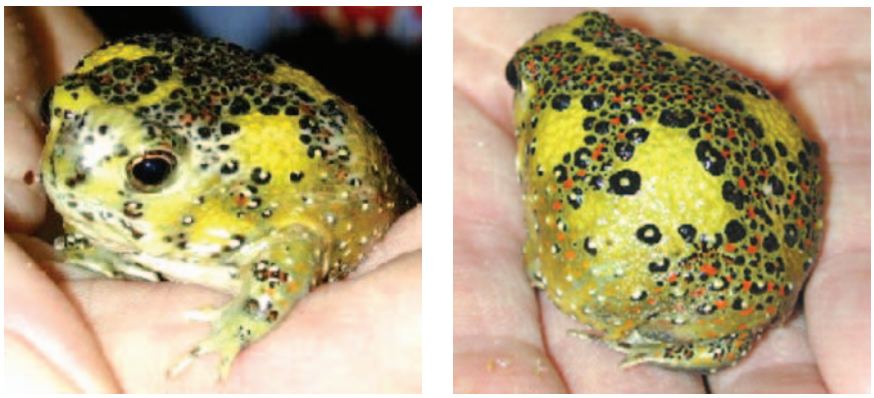

Fig. 11.1. The "Holy Cross Frog", *Notaden bennetti*

condensed onto a cool surface, and worked in these cool conditions. It adhered to a wide range of both hydrophilic and hydrophobic surfaces, including metal, wood, paper, plastics and glass. Subsequent preliminary laboratory trials confirmed the field observations that the *Notaden* exudate adheres tightly and with comparable affinity to a wide variety of surfaces such as glass, metal, wood, and plastic including polypropylene, polystyrene and even the 'non-stick' polymer Teflon® (Tyler and Ramshaw 2002), and also to biological tissues such as soft tissue, cartilage and bone. Further data indicated that the adhesive remained flexible in an indoor environment for over six months, and that it was resistant to many solvents and to mild abrasion (Tyler and Ramshaw 2002).

11.3 Adhesive Collection

Skin secretions are elicited once the frog is provoked. In the field, simply approaching the frogs is generally sufficient to elicit secretion. However, for laboratory studies, a small number of frogs are held in captivity, where they become accustomed to handling and the frog no longer secretes the adhesive exudate when approached. In these cases mild stimulation is required. A method for achieving this is to wash the animals briefly in water to remove debris and then stimulate the back of the frog with a mild electrical discharge to contract the dermal muscles. The magnitude and time of the pulse should lead to contraction of only the dermal muscles, including glandular muscles, and thereby empty the glands of their contents onto the surface of the frog. This can be achieved by using a two-pole electrode and a physiological stimulator that provides a square wave output. At low voltage (<20 V) and frequencies of up to 60 Hz (Tyler et al. 1992) the secretion is readily induced.

The skin secretion can be harvested by taking the liquid from the back of the frog by dipping an article such as a spatula into the liquid. The secretions also accumulate on the electrodes and can be removed by scraping from the metal, for example, with a spatula. The quantity of skin secretion that is harvested varies with the size of the frog, the length in captivity and the species, but a quantity in the range of 20 to 100 mg can be collected. This process needs to be carried out with speed as the exudate rapidly starts to become more viscous and harder to handle. The time period between effective collections of reasonable amounts of material has not been established, but our experience suggests that generally the frog exudate can be harvested about once a month in captivity.

The skin secretion can also be collected by washing the material from the skin into a collection vessel using an aqueous washing solution that is not harmful to the frog. For example, the washing solution could be phosphate buffered saline (PBS), or PBS containing other solutes. Thus, washing the backs of exudate-producing frogs under argon in PBS/10 mmol/l Cys.HCl, pH 4.5, emulsified the solids which, on settling, consolidated into a sticky and

elastic plug of translucent yellow solid (Fig. 11.2A) (Graham et al. 2005). When the frogs were irrigated using 20 mmol/l phosphate buffer, pH 6.2, the solids were not emulsified but rather formed aggregates of translucent yellow elastic solid. Irrigation with 50 mmol/l ascorbic acid resulted in clear viscous solutions (pH ~2.5) rather than the formation of any solid material. For samples collected without irrigation, the material typically bonded avidly to the metal electrode poles or other sample collecting devices and the solid that formed was typically much more cohesive (i.e., firmer or more rubber-like) and much less tacky than the adhesive that was collected by emulsification followed by settling (Graham et al. 2005).

The frog adhesive binds most avidly to the surface on which it first solidifies. It is likely that the adhesive determinants in the newly-secreted material seek interaction partners and, in the absence of suitable adherends they simply interact with each other and/or the buffer components, resulting in a solid that is still sticky but not nearly as adhesive as the nascent exudate. In all cases the collected material is a yellow-orange colour and is initially pliable and compressible, for example using a finger, and is elastic in that it can stretch when adhered between two surfaces. Samples of solid that were stored at −70 °C in their cognate washings (if any) appeared to retain all the functionality of the unfrozen solid (Graham et al. 2005).

11.4 Solubilisation and Solidification

Initial studies had suggested that the frog exudate, once it had formed a firm, dehydrated product, was not readily dissolved by a number of solvents, including water, hexane, xylene, hydrochloric acid and sulfuric acid. However, it was subsequently found that the solid material obtained both from undiluted exudates and those collected with irrigation could be fully dissolved at room temperature in 5 vol.% acetic acid (Fig. 11.2B). This could be achieved in a matter of hours for samples that had not become fully dehydrated and was slower (but still possible) for material that had been dried. Sometimes a small proportion of the sample would remain insoluble, in which case the trace solids could be removed by brief centrifugation. Other solvent systems that have similar effects include 10% (w/v) SDS, 5 mol/l guanidinium hydrochloride, pH 5, and 10 mmol/l H_3PO_4 (Graham et al. 2005). Thus, the solubility of frog material appears to be greater than that of marine mussel plaque (Burzio et al. 1997; Deming 1999) and much greater than that of barnacle cement (Burzio et al. 1997; Naldrett and Kaplan 1997; Kamino et al. 2000). As a routine solvent 5 vol.% acetic acid is preferred, and this permits concentrations of up to 10 mg protein/ml to be obtained. Although 0.05 vol.% acetic acid was not effective at dissolving the adhesive, concentrated solutions in this solvent could be achieved by dissolving the adhesive in 5 vol.% acetic acid and then dialysing the solution against 0.05 vol.% acetic acid at 4 °C (Graham et al. 2005).

It was particularly interesting to find that lumps of frog adhesive could be dissolved and then resolidified in a functionally adhesive form (Graham et al. 2005). For example, raising the ionic strength of solutions of dissolved material caused the components to self-assemble spontaneously into a tacky and elastic solid which retained most of the functionality of the original adhesive. Thus, if a small volume of 5 mol/l NaCl solution was gradually dispensed to a final concentration of 0.8–1.0 mol/l NaCl into a solution of ≥4 mg protein/ml in 5 vol.% or 0.05 vol.% acetic acid, then adhesive formed as fibrils or particles that could be grown or harvested as a translucent yellow sticky solid (Fig. 11.2C). Removing trapped acetic acid and salt from reconstituted adhesive by washing in water increased the translucence and adhesiveness of the solid, although it seemed to remain softer and less adhesive than the adhesive collected directly from the frogs (Graham et al. 2005).

11.5 Mechanical Properties

To provide an initial assessment on the strength of the adhesion provided by the *Notaden* adhesive, a simple test involving wooden craft stick pairs that were bonded in an in-line lap-joint configuration was used. Moist adhesive pieces were sandwiched between the overlapped ends of the craft sticks and the joint was allowed to dry completely while being held in mild compression.

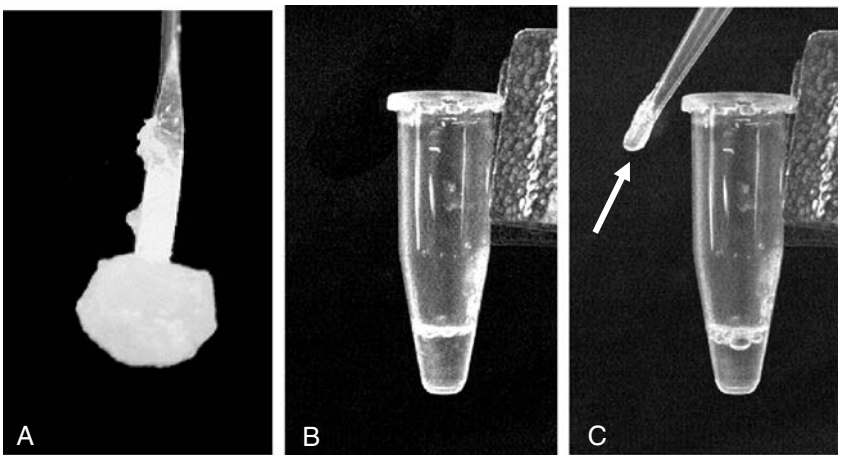

Fig. 11.2. (a) *Notaden* adhesive solids, after collection by washing the backs of exudate-producing frogs under argon in PBS/10 mmol/l Cys.HCl, pH 4.5, have consolidated into a sticky yellow solid. (b) A clear yellow solution obtained by dissolving *Notaden* adhesive in 5 vol.% acetic acid. (c) Reconstituted adhesive (harvested onto a disposable pipette tip, as indicated by the *arrow*) recovered from solution by adding 5 mol/l NaCl solution to a final concentration of about 0.8–1.0 mol/l NaCl

The test samples, along with joints formed using readily available commercial glues, were then examined using an Instron testing machine. The area of the zone of adhesion in each case (about 6 mm diameter) was measured by image analysis after testing (Image Pro Plus, MediaCybernetics). These bond strength data (Table 11.1) showed that the *Notaden* adhesive gave a mean shear strength of 1.7±0.3 MPa (n=6), which was greater than that observed for both PVA and UHU® Stick glues, while comparable to cyanoacrylate (n-butyl-2-cyanoacrylate) adhesive. Overall, in these strength tests of the *Notaden* adhesive there seemed to be no difference between adhesive sourced from different frogs. Also, adhesive that had been dissolved and reconstituted before use provided dry bond strengths similar to adhesive that had not (L.D. Graham, unpubl.). Possibly the most striking property of the *Notaden* adhesive is its capability to adhere to many diverse materials. Indeed, when the adhesive was used to bond a nickel spatula to a hard surface bound with Teflon® tape and allowed to dry, the spatula could not be removed without tearing a hole in the tape (L.D. Graham, unpubl.).

The strength tests were expanded to include data for moist frog adhesive as a bonding agent for polypropylene, tests that were designed to be comparable to those used in assessment of other amphibian secretions (Evans and Brodie 1994). Freshly secreted neat exudate was observed to bond 10 mm diameter polypropylene discs in an elastic manner with a prompt tensile strength of 57±6 kPa (n=8). On testing, each separated joint showed a mixture of adhesive and cohesive failure. When separated discs were re-jointed and stored humidified for 24 h at 4 °C, they were found to have a tensile strength of 78±8 kPa (n=8). When the joints were again re-formed and stored humidified for a further 1 h at 21 °C, they were found to have a tensile strength of 64±5 kPa (n=8). These three sets of tensile strength data were statistically indistinguishable (Graham et al. 2005). It is clear from these data that reforming separated joints by hand rapidly restores most of their strength, with more than 80% of the original bond strength returning within 1 h. The elastic modulus was also unaffected by breaking and reforming of the joint (Graham et al. 2005).

As the *Notaden* adhesive may have biomedical applications, its adhesive properties were also examined using biological adherends and compared with various commercial surgical adhesives. The method selected was a tear propa-

Table 11.1. Shear strength of wood bonded using selected adhesives (n=6, all cases)

Adhesive	Shear strength Mean±SD (MPa)
Notaden	1.7±0.3
Cyanoacrylate glue	1.7±0.7
PVA glue	1.3±0.2
UHU® Stic	0.9±0.4

gation test on longitudinal bonded tears using sheep menisci. This method was preferred as it was considered that a longitudinal meniscal tear is a prevalent injury in humans (Roeddecker et al. 1994). In this method, fresh medial menisci were dissected from intact sheep joints and a longitudinal cut (2–3 mm in from the meniscal periphery) was created which extended from the posterior horn to the anterior horn, leaving a 1.5-cm anterior region intact. Holding sutures were inserted into the free end of the meniscal fragments. Fresh *Notaden* adhesive (from *N. melanoscaphus*) was applied to one side of the cut and the fragments pressed firmly together for 90 s. For comparisons, a similar approach was used, with gelatin/resorcinol/formaldehyde (GRF: Implants Chirurgicaux) glue being held for 90 s, fibrin (Beriplast HS: fibrinogen/thrombin; CenteonPharma GmbH) for 60 s and cyanoacrylate (*n*-butyl-2-cyanoacrylate: Indermil Tissue Adhesive: Loctite Ireland Ltd) for 30 s. Glued samples were incubated in humid conditions at room temperature for 24 h (Szomor et al. 2001). A tear propagation method, at a constant rate of displacement (40 mm/min), was then used to determine the peel strength of each adhesive, with the total area of the glued region determined using image analysis software after the test. In all cases, tearing occurred along the tissue-adhesive interface. Cyanoacrylate formed a hard, brittle film on the glued surfaces, while the other glues remained rubbery. The peel strengths (Table 11.2) show that the cyanoacrylate was the strongest, followed by the *Notaden* adhesive, which was significantly stronger than both the GRF and fibrin adhesives.

Overall, it appears that moist *Notaden* adhesive functions as a pressure-sensitive adhesive whose bond strength is largely unaffected by breaking and re-forming of the joint. Like other pressure-sensitive adhesives, the frog adhesive is most effective at bonding rigid surfaces which can be placed under pressure. In tests similar to our studies with polypropylene discs other researchers determined tensile strengths of ~100 kPa for freshly secreted Tomato Frog exudate and 20–63 kPa for freshly secreted adhesives from other frogs and salamanders (Evans and Brodie 1994). With a tensile strength of 57–78 kPa, freshly secreted *N. bennetti* exudate sets with a bond strength comparable to those for adhesive secretions from other amphibians. The *N. bennetti* values are intermediate between the tensile strengths reported for the adhesion of marine mussel plaque to hydrophobic substrates (~13 kPa) and to hydrophilic ones (320–860 kPa) (Crisp et al. 1985).

Table 11.2. The average peel strengths of selected adhesives (n=11–12)

Adhesive	Peel strength Mean±SD (N mm^{-1})
Cyanoacrylate	0.149±0.034
Notaden	0.097±0.032
Gelatin	0.039±0.026
Fibrin	0.020±0.010

11.6 Biocompatibility

Another feature of this adhesive is that it appears to be biocompatible, in that it does not, in a general sense, evoke an adverse reaction and appears to be non-toxic. Material collected by water washing was applied at approximately 1 μg/ml to toad *rectus abdominis* muscle preparation (striated muscle), guinea pig ileum, vas deferens from rats, and isolated rabbit ear artery preparations. No activity was observed with any of these tissue preparations, not even when the secretions were tested on the very sensitive rabbit ear artery model (Tyler and Ramshaw 2002).

The adhesive was also assessed in cell and organ culture experiments. Before these experiments could be undertaken it was essential to find an effective means of sterilizing the adhesive. Many standard treatments were ineffective. For example, dissolved adhesive could not be filter-sterilised because the material blocked 0.2-μm filters. Chemical sanitisation (e.g. acid treatment plus germicidal UV irradiation) did not kill all of the bacteria present. High pressure treatments of solid samples were also unsuccessful: subjecting the material to 400 MPa for 2 min did not kill fungal contaminants, and although treatment at 600 MPa for 5 min appeared to sterilize the sample it adversely affected the functionality of the adhesive. Likewise, autoclave treatments sterilized the adhesive but rendered it non-functional. However, gamma irradiation at 25 kGy sterilised the adhesive without causing structural or functional damage (Fig. 11.3), although higher levels of irradiation (35 kGy) did impair the stickiness and elasticity of the adhesive (L.D. Graham, unpubl.).

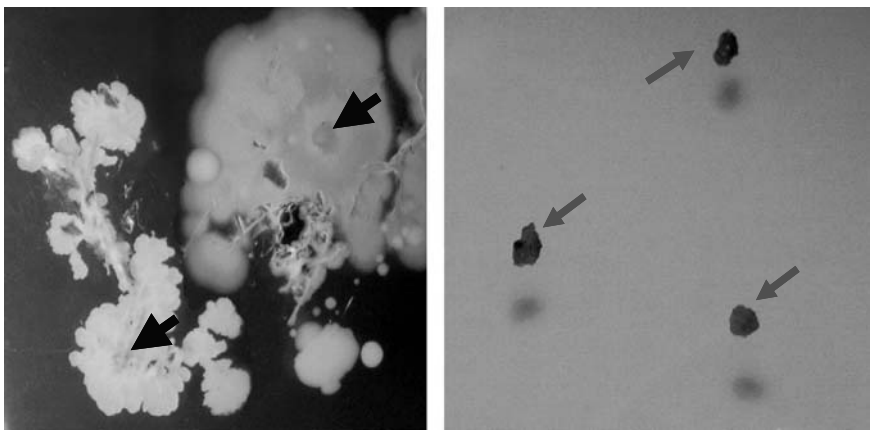

Fig. 11.3. (a) Unsterilised *Notaden* adhesive pieces (shown by *arrows*) on nutrient agar, showing growth of micro-organisms after three days at 37 °C. (b) *Notaden* adhesive pieces (shown by *arrows*) that had been sterilized with 25-kGy γ-irradiation, showing no growth of micro-organisms under similar culture conditions

In organ culture experiments, it was found that collagen-coated plastic lenticules could be adhered effectively to debrided bovine corneas using material dissolved in 0.05% (w/v) acetic acid. Epithelial regrowth was not inhibited by exposure to the solution, and regrowth proceeded smoothly over the lenticule-cornea junction even where the corneal edge was uneven. Paraffin histology of corneal sections stained with H&E stain confirmed that epithelium had successfully mounted the edge of the lenticule in all cases (L.D. Graham, S. Taylor and M.D.M. Evans, unpubl.).

Tissue culture plates were coated with the adhesive by allowing the material to adsorb from solution and then rinsing the plates with sterile PBS. Bovine corneal epithelial cells attached and proliferated well on these coated plates, with no impairment relative to uncoated surfaces, while the migration of these cells from a tissue explant was ~75% of that observed on uncoated surfaces (L.D. Graham and G. Johnson, unpubl.). The edge of the migrating cell sheets appeared thickened (Fig. 11.4), in the manner typical of how these cells respond to hydrophobic surfaces. No cytotoxicity was detected from dissolved frog adhesive at concentrations up to ~8 μg protein/ml, beyond which the acetic acid present in the stock solution began to adversely affect cell viability (L.D. Graham and G. Johnson, unpubl.).

Despite these encouraging findings on the biocompatibility of the *Notaden* adhesive, other issues such as resorption rate and immunological reactivity need to be ascertained.

11.7 Biochemical Studies

General biochemical analyses have shown the *Notaden* adhesive to be a protein-based hydrogel. Vacuum drying of fully hydrated adhesive pellets suggested

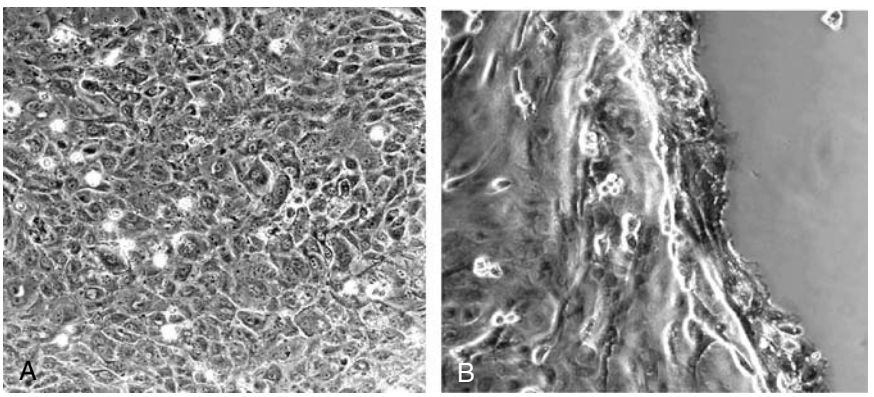

Fig. 11.4. Culture of bovine corneal epithelial cells on tissue culture plates that had been coated with *Notaden* adhesive (by adsorption from solution, followed by rinsing with sterile PBS): (a) confluent cells attached to the surface; (b) migrating cells on the surface, showing a thickened layer at the leading edge of migration

that the fully hydrated adhesive contained around 85–90 wt% water, while a colorimetric assay indicated that the hydrated adhesive contained ~10 wt%. Despite the very high water content of fully hydrated adhesive, the material handled more like an elastic solid than a viscous dilute hydrogel (Graham et al. 2005). For simplicity, and to distinguish it from liquid and emulsion forms, we will refer to the set adhesive as a solid. A colorimetric assay for carbohydrate, using the phenol-sulfuric acid assay (Dubois et al. 1956) with D-glucose as standard, indicated that vacuum-dried material contained only 0.75 wt% glucose equivalents (Graham et al. 2005). This assay detects individual aldoses, ketoses, deoxy-sugars and sugar acids with somewhat different efficiencies, but is still one of the best general purpose biochemical assays for carbohydrate content.

11.7.1 Colour

Some of the yellow-orange colour can be removed from the *Notaden* adhesive by organic solvents, and the UV-visible absorbance spectrum of the resulting extracts is characteristic of carotenoid chromophores (Schmidt-Dannert et al. 2000). Such compounds are known to contribute to the colour of amphibian skin (Frost-Mason et al. 1994). De-pigmented *Notaden* adhesive is translucent and white but otherwise seems to be fully functional (L.D. Graham, unpubl.).

11.7.2 CD Spectra

Since protein was the major non-water component of the *Notaden* adhesive, CD spectroscopy was used to examine the overall secondary structure of the exudate. The CD spectrum of the adhesive dissolved in 10 mmol/l H_3PO_4 at 0.1 mg protein/ml is shown in Fig. 11.5. Deconvolution of the spectrum (Greenfield and Fasman 1969) indicated a poorly structured system, dominated by random coil and/or containing non-standard elements, with the presence of little or no alpha helix, about 36% β-elements, and the remainder as 64% random coil (Graham et al. 2005).

11.7.3 Amino Acid Analysis

Amino acid analysis of the *Notaden* adhesive indicated that the material was rich in Gly, Pro and Glx compared to other vertebrate proteins (Doolittle 1986), but was low in Ala, Ser and Met. Structural proteins often have high levels of Gly and Pro, while elastomeric proteins show compositions that may be rich in Gly, in Gly and Pro, or in Gly, Pro and Gln (Tatham and Shewry 2000). It was of interest that there was a significant 4-hydroxyproline (Hyp)

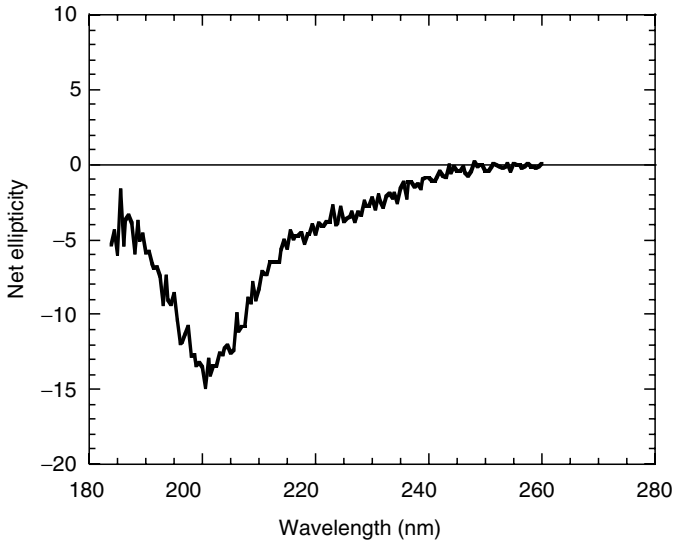

Fig. 11.5. Circular dichroism (CD) spectrum of *Notaden* adhesive dissolved in 10 mmol/l H_3PO_4 at 0.1 mg protein/ml. The spectrum indicates a relatively unstructured system dominated by random coil and/or containing non-standard elements

content (Table 11.3) (Graham et al. 2005). This imino acid, which is obtained by post-translational modification of proline, is characteristically found in collagens or other proteins that form triple-helical structures (Brodsky and Ramshaw 1997). It is also seen in adhesive plaque proteins from the mussel, *Mytilus edulis* (Waite 1983; Burzio et al. 1997; Deming 1999). Specific analyses for dihydroxyphenylalanine (L-Dopa), which is obtained by post-translational modification of tyrosine, were done using modified hydrolysis conditions (Gieseg et al. 1993) but no L-Dopa was detected in the *Notaden* adhesive (Table 11.3) (Graham et al. 2005). The presence of this amino acid is a key part of the adhesive mechanism of the glues from several organisms, including *M. edulis* (Waite 1983; Monahan and Wilker 2004).

11.7.4 Protein Fractionation

Various electrophoretic methods have been used to examine the protein components of the *Notaden* adhesive. It was found that sodium dodecyl sulfate-polyacrylamide gel electrophoresis (SDS-PAGE) using pre-cast Tricine or Tris/Glycine 10–20% gradient gels gave good resolution of the proteins found in *Notaden* exudates (Fig. 11.6). The gel pattern was essentially the same for reduced and unreduced samples except for one key difference: material that in non-reduced samples could not enter the gel migrated in

Table 11.3. Amino acid composition of *Notaden* adhesive (mol%)

Asx[a]	7.2
Thr	4.4
Ser	3.8
Glx[a]	14.1
Gly	15.8
Ala	2.8
Cys/2	0.7
Val	6.2
Met	1.1
Ile	4.8
Leu	6.9
Tyr	2.2
Phe	3.8
Lys	5.8
His	3.1
Arg	3.8
Pro	8.8
Hyp	4.6
L-Dopa	0
Trp	n.d.

[a] Deamidation during acid hydrolysis means that Asn cannot be distinguished from Asp and Gln cannot be distinguished from Glu; the two groups are presented together as Asx and Glx respectively
n.d., not determined

reduced samples as the most abundant and slowest-moving component, Nb-1R (Fig. 11.6). The characteristic pattern of proteins has apparent molecular masses ranging from ~15 to ~400 kDa. Other electrophoretic separations were attempted, including native gels run in both acidic and basic conditions, acid urea gels, and isoelectric focusing. These separated some components, but did not give the full resolution afforded by the SDS-PAGE gradient gels (V. Glattauer and L.D. Graham, unpubl. res.).

Various approaches for larger scale fractionation of the protein components have also been examined. These included fractional precipitation with various agents, including ammonium sulfate, PEG, NaCl, EtOH, but none gave well-resolved components. Similarly, attempts to fractionate using column chromatography approaches, including gel permeation and ion-exchange chromatography, were also not as successful as had been hoped. In many cases, the adhesive components bound irreversibly to the chromatography matrices and rendered the columns inoperable, even when strong

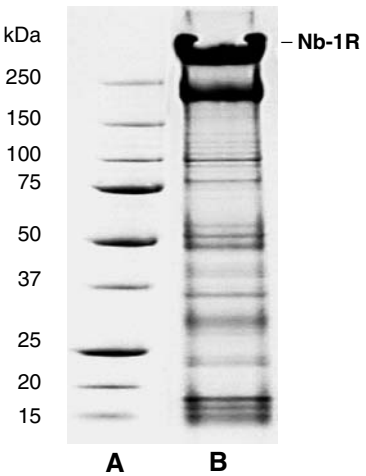

Fig. 11.6. SDS-PAGE of reduced *Notaden* adhesive, showing a range of protein components: (a) electrophoretic markers, with the molecular masses (kDa) shown at the *left*; (b) the characteristic pattern of proteins, with the largest and most abundant protein, Nb-1R, indicated

solvents containing high concentrations of denaturants were used (Graham et al. 2005; L.D. Graham and V. Glattauer, unpubl. res.).

Thus, although attempts at larger scale fractionation were unsatisfactory and do not permit the immediate examination of the adhesive effects of individual components or specific mixtures, SDS-PAGE does provide a convenient approach to resolve the mixture. Given the sensitivity of present analytical methods, including gas-phase Edman degradation and sequence analysis of tryptic peptides by mass spectrometry, it is anticipated that much structural information on the individual components will be obtained from material separated by SDS-PAGE.

11.8 Applications

The adhesive from *Notaden* has several useful properties compared with other materials. These include its ability to bond to moist surfaces or those covered by water droplets. It is also very adaptable in the types of surfaces to which it can effectively bond, including metals, glass, plastics and biological tissues. Although for convenience we have been referring to the set adhesive as a solid, the moist material is actually a hydrogel containing a large proportion of trapped water. Examination of the set adhesive by scanning electron microscopy (Fig. 11.7) shows an open, porous structure formed by a meshwork of fibres and sheets. The pores in this structure can exceed 5–10 μm. The sponge-like network of pores and channels within the adhesive explains how the moist solid can accommodate a water content of 85–90 wt%. Along

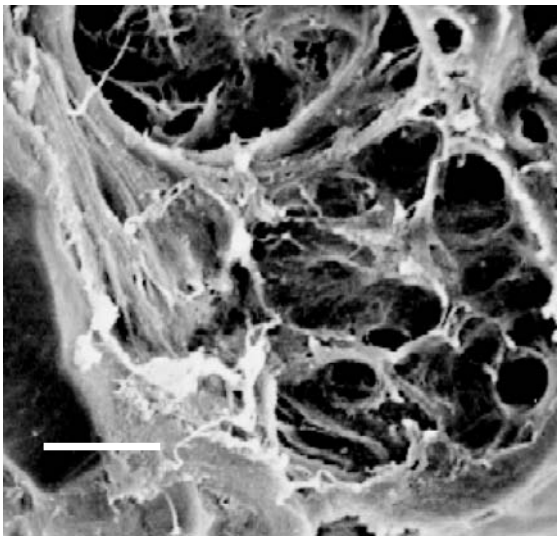

Fig. 11.7. Scanning electron microscopy of the *Notaden* adhesive. *Bar*=5 μm

with the adhesive's ability to bond biological tissues, this porosity suggests that the adhesive could potentially be useful in biomedical applications, as the porosity will allow the diffusion of nutrients, gases and waste products and may also allow the migration and infiltration of cells.

If the *Notaden* adhesive is to be developed into a medical product, then we must be able to produce a sterile material that is reproducible in composition and available in sufficient quantity. This strongly suggests that the natural extract, which has collection difficulties (due to seasonal availability and environmental concerns) and which is difficult to harvest and sterilize, would not be the material of choice. Rather, if we can arrive at an understanding of which protein(s) represent the key structural agent(s), then production of a recombinant version of the adhesive may present an excellent option. Such material would be very well defined and highly reproducible. Further, the knowledge of the key component(s) and the mechanism of adhesion could then lead to recombinant versions that are modified forms of the natural material or artificial mimics produced by synthetic organic chemistry. These could minimize immunogenicity issues or other adverse phenomena and prove easier to progress through to regulatory approval.

A novel adhesive for medical applications would be particularly useful as there is a significant unmet clinical need for a strong and flexible surgical adhesive that is highly biocompatible (MedMarket 2002). Current biological adhesives (e.g. fibrin, albumin, gelatin-resorcinol-formaldehyde, etc.) typically suffer from low bond strength and in some cases are derived from blood products, with associated risk of viral or prion contamination. On the other

hand, synthetic glues (e.g. cyanoacrylate adhesives) are very strong but they are also toxic to living tissues and form rigid, non-porous films that can hinder wound healing. The tear propagation method of mechanical testing using meniscal tissue provided consistent and reproducible data and showed that the *Notaden* adhesive performed very well compared to other current surgical adhesives (Szomor et al. 2001). Further, preliminary studies using an in vivo meniscal defect model in sheep have suggested the usefulness of the adhesive in meniscal repair, and show the potential for development of a chemical or recombinant mimic of this material as a novel medical adhesive. A study using ten test and six control animals with artificial meniscal tears showed after ten weeks that the adhesive could hold the torn fragments together, especially if the meniscal fragments were not completely separated, and that tissue repair had commenced with new fibrous tissue present (cited in Tyler and Ramshaw 2002). These data seem promising as the meniscus is the most commonly injured and torn structure of the body. The limitations of current treatments of the meniscus are most evident in those parts of the tissue that are poorly vascularised, and where it is difficult to keep the meniscus fragments in good contact for the healing procedure.

11.9 Conclusions

The yellow adhesive material that frogs of the genus *Notaden* secrete on their dorsal skin when provoked provides a new material that could be developed into a specialty adhesive. This adhesive bonds rapidly to a wide range of polar and non-polar materials, including moist and cool surfaces. Mechanical tests indicated that the bonding was not as strong as cyanoacrylate, but was superior to various medical adhesives, such as fibrin glue. Preliminary experiments have shown that the glue is compatible with cell attachment and growth, while forming an open porous structure that could allow cell infiltration. Biochemical studies have shown that the adhesive is a highly hydrated protein material that is rich in Gly, Pro and Glx residues, with small amounts of bound carbohydrate. The protein components can be readily separated for further analysis by SDS-PAGE. The glue can be dissolved in dilute acetic acid and then re-solidified by addition of NaCl. The largest and most abundant protein in the adhesive, Nb-1R, appears to be the key structural component. While small quantities of adhesive can be collected in the laboratory, other strategies such as recombinant protein production will be needed for larger scale trials. The properties of the adhesive suggest that it has potential for medical applications.

Acknowledgments. The authors wish to thank Joel Mackay (Sydney University) for the CD spectrum, Raju Adhikari, Lawry McCarthy, Helmut Thissen and Tony Cripps (CSIRO) for help with the adhesive strength tests, and Graham Johnson and Meg Evans (CSIRO) for the bovine corneal organ culture and epithelial cell culture tests.

References

Apponyi MA, Pukala TL, Brinkworth CS, Maselli VM, Bowie JH, Tyler MJ, Booker GW, Wallace JC, Carver JA, Separovic F, Doyle J, Llewellyn LE (2004) Host-defence peptides of Australian anurans: structure, mechanism of action and evolutionary significance. Peptides 25: 1035–1054

Barker J, Grigg GC, Tyler MJ (1995) A field guide to Australian frogs. Surrey Beatty, Chipping Norton, Australia

Brodie ED, Gibson LS (1969) Defensive behaviour and skin glands of the northwestern salamander, *Ambystoma gracile*. Herpetologica 25:187–194

Brodsky B, Ramshaw JAM (1997) The collagen triple-helix structure. Matrix Biol 15:545–554

Burzio LO, Burzio VA, Silva T, Burzio LA, Pardo J (1997) Environmental bioadhesion: themes and applications. Curr Opin Biotechnol 8:309–312

Channing A (2001) Amphibians of central South Africa. Comstock, Ithica

Crisp DJ, Walker G, Young GA, Yule AB (1985) Adhesion and substrate choice in mussels and barnacles. J Colloid Interface Sci 104:40–50

Deming TJ (1999) Mussel byssus and bimolecular materials. Curr Opin Chem Biol 3:100–105

Doolittle RF (1986) Of URFs and ORFs: a primer on how to analyze derived amino acid sequences. University Science Books, California, p 55

Doyle J, Brinkworth CS, Wegener KL, Carver JA, Llewellyn LE, Olver IN, Bowie JH, Wabnitz PA, Tyler MJ (2003) nNOS inhibition, antimicrobial and anticancer activity of the amphibian skin peptide, citropin 1.1 and synthetic modifications. The solution structure of a modified citropin 1.1. Eur J Biochem 270:1141–1153

Dubois M, Gilles KA, Hamilton JK, Rebers PA, Smith F (1956) Colorimetric method for determination of sugars and related substances. Anal Chem 28:350–356

Evans CM, Brodie ED (1994) Adhesive strength of amphibian skin secretions. J Herpetol 28:502–504

Frost-Mason S, Morrison R, Mason K (1994) Pigmentation. In: Heatwole H, Barthalmus GT (eds) Amphibian biology, vol 1. Surrey Beatty, Chipping Norton, Australia, pp 64–97

Gieseg SP, Simpson JA, Charlton TS, Duncan MW, Dean RT (1993) Protein-bound 3,4-dihydroxyphenylalanine is a major reductant formed during hydroxyl radical damage to proteins. Biochemistry 32:4780–4786

Graham LD, Glattauer V, Huson MG, Maxwell JM, Knott RB, White JF, Vaughan, PR, Peng Y, Tyler MJ, Werkmeister JA, Ramshaw JAM (2005) Characterization of a protein-based adhesive elastomer secreted by the Australian frog *Notaden bennetti*. Biomacromolecules 6:3300–3312

Greenfield N, Fasman GD (1969) Computed circular dichroism spectra for the evaluation of protein conformation. Biochemistry 8:4108–4116

Kamino K, Inoue K, Maruyama T, Takamatsu N, Harayama S, Shizuri Y (2000) Barnacle cement proteins. J Biol Chem 275:27360–27365

MedMarket (2002) MedMarket Diligence Report #S120, Worldwide Wound Sealant Market, Medmarket Diligence, Foothill Ranch, CA

Monahan J, Wilker JJ (2004) Cross-linking the protein precursor of marine mussel adhesives: bulk measurements and reagents for curing. Langmuir 20:3724–3729

Naldrett MJ, Kaplan DL (1997) Characterization of barnacle (*Balanus eburneus* and *B. cenatus*) adhesive proteins. Marine Biol 127:629–635

Roeddecker K, Muennich U, Nagelschmidt M (1994) Meniscal healing: a biomechanical study. J Surg Res 56:20-27

Schmidt-Dannert C, Umeno D, Arnold FH (2000) Molecular breeding of carotenoid biosynthetic pathways. Nat Biotechnol 18:750–753

Szomor ZL, Appleyard R, Tyler MJ, Murrell GAC (2001) Meniscal repair with a new biologic glue. 47th annual meeting, Orthopaedic Research Society, San Francisco, CA, p 47

Tatham AS, Shewry PR (2000) Elastomeric proteins: biological roles, structures and mechanisms. Trends Biochem Sci 25:567–571

Tyler MJ, Ramshaw JAM (2002) International patent application WO02/22756
Tyler MJ, Stone DJ, Bowie JH (1992) A novel method for the release and collection of dermal, glandular secretions from the skin of frogs. J Pharmacol Toxicol Methods 28:199–200
Waite JH (1983) Evidence for a repeating 3,4-dihydroxyphenylalanine- and hydroxyproline-containing decapeptide in the adhesive protein of the mussel, *Mytilus edulis* L. J Biol Chem 258:2911–2915
Williams TA (1994) Technique to isolate salamander granular gland products with a comment on the evolution of adhesiveness. Copeia 1994:540–541
Williams TA, Larsen JH (1986) New function for the granular skin glands of the eastern long-toed salamander, *Ambystoma macrodactylum columbianum*. J Exp Zool 239:329–333

12 Properties, Principles, and Parameters of the Gecko Adhesive System

Kellar Autumn

> "The designers of the future will have smarter adhesives that do considerably more than just stick" (Fakley 2001)

12.1 Introduction

Gecko toe pads are sticky because they feature an extraordinary hierarchy of structure that functions as a smart adhesive. Gecko toe pads (Russell 1975) operate under perhaps the most severe conditions of any adhesives application. Geckos are capable of attaching and detaching their adhesive toes in milliseconds (Autumn et al. 2006) while running with seeming reckless abandon on vertical and inverted surfaces, a challenge no conventional adhesive is capable of meeting. Structurally, the adhesive on gecko toes differs dramatically from that of conventional adhesives. Conventional pressure sensitive adhesives (PSAs) such as those used in adhesive tapes are fabricated from materials that are sufficiently soft and sticky to flow and make intimate and continuous surface contact (Pocius 2002). Because they are soft and sticky, PSAs also tend to degrade, foul, self-adhere, and attach accidentally to inappropriate surfaces. Gecko toes typically bear a series of scansors covered with uniform microarrays of hair-like setae formed from β-keratin (Wainwright et al. 1982; Russell 1986), a material orders of magnitude stiffer than those used to fabricate PSAs. Each seta branches to form a nanoarray of hundreds of spatular structures that make intimate contact with the surface.

Functionally, the properties of gecko setae are as extraordinary as their structure: the gecko adhesive is 1) directional, 2) attaches strongly with minimal preload, 3) detaches quickly and easily (Autumn et al. 2000; Autumn and Peattie 2002), 4) sticks to nearly every material, 5) does not stay dirty (Hansen and Autumn 2005) or 6) self-adhere, and 7) is nonsticky by default. While some of the principles underlying these seven functional properties are now well understood, much more research will be necessary to fully map out the parameters of this complex system.

Department of Biology, Lewis & Clark College, Portland, OR 97219-7899, USA

Biological Adhesives
(ed. by A.M. Smith and J.A. Callow)

Over two millennia ago, Aristotle commented on the ability of the gecko to "run up and down a tree in any way, even with the head downwards" (Aristotle 1918). How geckos adhere has attracted substantial and sustained scientific scrutiny (Cartier 1872a; Gadow 1901; Schmidt 1904; Hora 1923; Dellit 1934; Mahendra 1941; Maderson 1964; Ruibal and Ernst 1965; Hiller 1968, 1969, 1975; Gennaro 1969; Russell 1975, 1986; Williams and Peterson 1982; Stork 1983; Schleich and Kästle 1986; Weitlaner 1902; Irschick et al. 1996; Autumn et al. 2000, 2002b; Autumn and Peattie 2002; Arzt et al. 2003; Huber et al. 2005a; Hansen and Autumn 2005). The unusual hairlike microstructure of gecko toe pads has been recognized for well over a century (Cartier 1872a,b, 1874; Braun 1878). Setal branches were discovered using light microscopy (Schmidt 1904), but the discovery of multiple split ends (Altevogt 1954) and spatular nanostructure (Ruibal and Ernst 1965) at the tip of each seta was made only after the development of electron microscopy.

A single seta of the tokay gecko is approximately 110 μm in length and 4.2 μm in diameter (Ruibal and Ernst 1965; Russell 1975; Williams and Peterson 1982) (Fig. 12.1). Setae are similarly oriented and uniformly distributed on

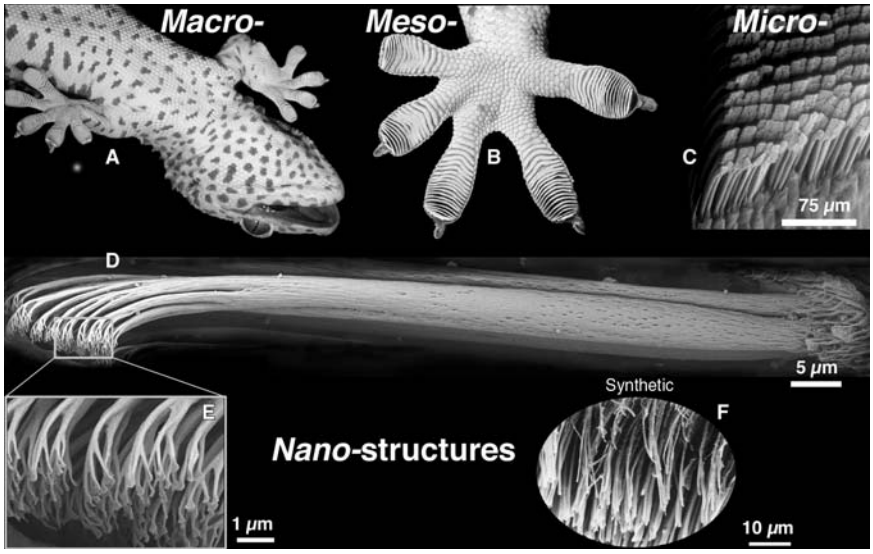

Fig. 12.1. Structural hierarchy of the gecko adhesive system: (a) ventral view of a tokay gecko (*Gekko gecko*) climbing a vertical glass surface; (b) ventral view of the foot of a tokay gecko, showing a mesoscale array of seta-bearing scansors (adhesive lamellae) (images A and B by Mark Moffett); (c) microscale array of setae are arranged in a nearly grid-like pattern on the ventral surface of each scansor. In this scanning electron micrograph, each diamond-shaped structure is the branched end of a group of four setae clustered together in a tetrad; (d) micrograph of a single gecko seta assembled from a montage of five Cryo-SEM images (image by Stas Gorb and K. Autumn). Note individual keratin fibrils comprising the setal shaft; (e) nanoscale array of hundreds of spatular tips of a single gecko seta; (f) synthetic spatulae fabricated from polyimide at UC Berkeley in the lab of Ronald Fearing using nanomolding (Campolo et al. 2003)

the scansors. Setae branch at the tips into 100–1000 more structures (Ruibal and Ernst 1965; Schleich and Kästle 1986) known as spatulae. A single spatula consists of a stalk with a thin, roughly triangular end, where the apex of the triangle connects the spatula to its stalk. Spatulae are approximately 0.2 μm in length and also in width at the tip (Ruibal and Ernst 1965; Williams and Peterson 1982). While the tokay is currently the best studied of any adhesive gecko species, there are over a thousand species of gecko (Han et al. 2004), encompassing an impressive range of morphological variation at the spatula, seta, scansor, and toe levels (Maderson 1964; Ruibal and Ernst 1965; Russell 1975, 1981, 1986; Peterson and Williams 1981; Williams and Peterson 1982; Stork 1983; Schleich and Kästle 1986; Russell and Bauer 1988, 1990a,b; Roll 1995; Irschick et al. 1996; Autumn and Peattie 2002; Arzt et al. 2003). Setae have even evolved on the tails of some gecko species (Bauer 1998). Remarkably, setae have evolved convergently in iguanian lizards of the genus *Anolis* (Braun 1879; Ruibal and Ernst 1965; Peterson and Williams 1981), and in scincid lizards of the genus *Prasinohaema* (Williams and Peterson 1982; Irschick et al. 1996). This chapter aims broadly at identifying the known properties of the gecko adhesive system, possible underlying principles, and quantitative parameters that affect system function. However, much of what is known is based on studies of a single species–the tokay gecko (*Gekko gecko*)–and the degree of variation in function among species remains an open question that should be kept in mind.

12.2 Adhesive Properties of Gecko Setae

Two front feet of a tokay gecko (*Gekko gecko*) can withstand 20.1 N of force parallel to the surface with 227 mm^2 of pad area (Irschick et al. 1996). The foot of a tokay bears approximately 3600 tetrads of setae per mm^2, or 14,400 setae per mm^2 (Schleich and Kästle 1986; pers. obs.). Consequently, a single seta should produce an average force of 6.2 μN, and an average shear stress of 0.090 N mm^{-2} (0.9 atm). However, single setae proved both much less sticky and much more sticky than predicted by whole animal measurements, under varying experimental conditions, implying that attachment and detachment in gecko setae are mechanically controlled (Autumn et al. 2000).

12.2.1 Properties (1) Anisotropic Attachment and (2) High Adhesion Coefficient (μ′)

Using a newly developed micro-electromechanical systems (MEMS) force sensor (Chui et al. 1998), Autumn et al. (2000) measured the adhesive and shear force of a single isolated gecko seta. Initial efforts to attach a single seta failed to generate forces above that predicted by Coulomb friction because of

the inability to achieve the proper orientation of the seta in six degrees of freedom. The angle of the setal shaft was particularly important in achieving an adhesive bond. Strong attachment occurred when using proper orientation and a motion based on the dynamics of gecko legs during climbing (based on force plate data; Fig. 12.2; Autumn et al. 2006). A small normal preload force yielded a shear force of ~40 μN, six times the force predicted by whole-animal measurements (Irschick et al. 1996). The small normal preload force, combined with a 5-μm proximal shear displacement yielded a very large shear force of 200 μN, 32 times the force predicted by whole-animal measurements (Irschick et al. 1996) and 100 times the frictional force measured with the seta oriented with spatulae facing away from the surface (Autumn et al. 2000). The preload and drag steps were also necessary to initiate significant adhesion in isolated gecko setae, consistent with the load dependence and directionality of adhesion observed at the whole-animal scale by Haase (1900) and Dellit (1934). The ratio of preload to pulloff force is the adhesion coefficient, μ′, which represents the strength of adhesion as a

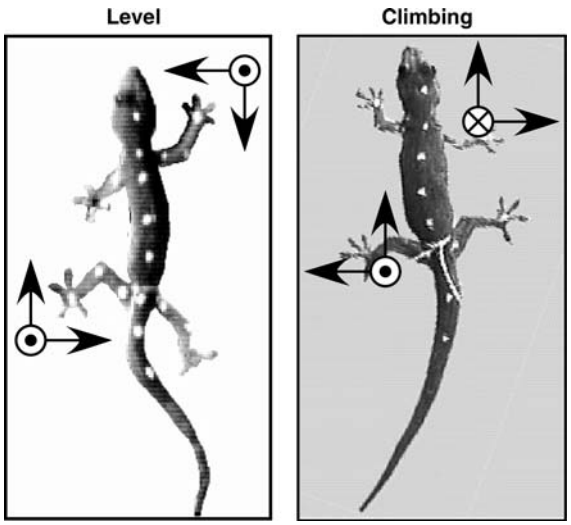

Fig. 12.2. Single-leg ground reaction forces in running geckos (*Hemidactylus garnotii*): (a) during level running, geckos' front legs produce deceleratory ground reaction forces while their hind legs produce acceleratory forces (Autumn et al. 2006). All legs push away from the body, producing ground reaction forces aimed through the joints toward the center of mass, minimizing joint moments, and possibly stabilizing the animal as it runs. *Circles with dots* represent positive ground reaction forces normal to the surface. During level running these represent the forces that support the animal's weight; (b) during vertical climbing, geckos have similar kinematics, but alter dramatically their kinetics in comparison to level running (Chen et al. 2006). While climbing, all legs accelerate the body up the wall, and all legs pull in toward the center of mass, engaging the adhesive setae and claws. Front limbs pull away from the surface and hind limbs push into the surface, producing a torque that tips the head toward the wall, counteracting the tendency of the animal's head to pitch back as it climbs

function of the preload (Bhushan 2002). In isolated gecko setae, a 2.5-μN preload yielded adhesion between 20 μN (Autumn et al. 2000) and 40 μN (Autumn et al. 2002b) and thus a value of μ′ of between 8 and 16.

12.2.1.1 Large Safety Factor for Adhesion and Friction?

All 6.5 million (Schleich and Kästle 1986; Irschick et al. 1996) setae of a 50-g Tokay gecko attached maximally could theoretically generate 1300 N (133 kg force) of shear force–enough to support the weight of two humans. This suggests that a gecko need only attach 3% of its setae to generate the greatest forces measured in the whole animal (20 N; Irschick et al. 1996). Only less than 0.04% of a gecko's setae attached maximally are needed to support its weight of 50 g on a wall. At first glance, gecko feet seem to be enormously overbuilt by virtue of a safety margin of at least (20 N/0.5 N)−1=3900%. However, it is unlikely that all setae are able to achieve the same orientation simultaneously. The proportion of spatulae attached may be greatly reduced on rough surfaces (particularly those with roughness on the same scale as spatulae or setae) (Persson and Gorb 2003). On dusty or exfoliating surfaces, attachment to a well-anchored substrate will not be possible for every seta. Geckos may use a significant portion of their safety margin while withstanding high winds during tropical storms, resisting predator attack, or recovering adhesion after a fall (Hecht 1952; Vinson and Vinson 1969; Russell 1976; Autumn and Peattie 2002; Pianka and Sweet 2005).

Geckos have been observed to recover from a fall by re-attaching their toes to leaves or branches as they plummet (Vitt and Zani 1997; Pianka and Sweet 2005). A simple calculation suggests that recovery from a fall may require a large proportion of a gecko's safety margin of adhesion or friction. Consider a 50-g gecko falling from rest. If the gecko attaches a foot to a vertical surface after it has fallen 10 cm (neglecting air resistance) it will be moving at 1.4 m/s. If the foot is able to produce 5 N of friction, the gecko will be able to come to a stop in 15 ms after sliding 1.1 cm. In this theoretical example, recovering from a fall of the very modest distance of 10 cm would require 50% of the shear capacity of one foot based on whole animal measurements (Irschick et al. 1996) but still less than 4% of the theoretical maximum shear stress calculated for single setae (Autumn and Peattie 2002).

12.2.2 Property (3) Low Detachment Force

The surprisingly large forces generated by single setae raised the question of how geckos manage to detach their feet in just 15 ms (Autumn et al. 2006) with no measurable detachment forces (Autumn et al. 2006). We discovered that simply increasing the angle that the setal shaft (α) makes with the substrate to 30° causes detachment (Autumn et al. 2000). We proposed that as the angle of the setal shaft increases, sliding stops and stress increases at the trailing edge

of the seta, causing fracture of the seta-substrate bonds (Autumn et al. 2000) and returning the seta to the unloaded default state. This scenario is supported by models of setae as cantilever beams (Sitti and Fearing 2003; Gao et al. 2005; Spolenak et al. 2005) and by finite element modeling (FEM) of the seta (Gao et al. 2005). FEM simulation of the single seta pulloff experiment in Autumn et al. (2000) revealed more than an order of magnitude decrease in adhesive force as α increased from 30° to 90°. The FEM simulation also identified a transition from sliding to peeling that occurs at α=30°, consistent with cantilever beam-based models (Sitti and Fearing 2003) and empirical observations that setae slide at α<30° but detach at α>30° (Autumn et al. 2000). Thus the gecko adhesive can be thought of as the first known *programmable adhesive*. Preload and drag steps turn on and modulate stickiness while increasing the shaft angle to 30° turns off stickiness.

12.2.3 Integration of Body and Leg Dynamics with Setal Attachment and Detachment

How attachment and detachment of millions of setae during locomotion are integrated with the function of the scansor, toe, foot, leg, and body remains a topic of interest and ongoing research (Russell 1986, 2002; Autumn and Peattie 2002; Autumn et al. 2005a,b; Gao et al. 2005). Since gecko setae require a preload in the normal axis for adhesion, large forces could potentially be associated with attachment of the foot. The tremendous adhesive capacity of gecko setae suggests that large forces could also occur during detachment. In fact, no measurable ground reaction forces were associated with either attachment or detachment during vertical climbing on a force plate of the house gecko *Hemidactylus garnotii* (Autumn et al. 2006), indicating that these actions are either mechanically decoupled from the center of mass in this species, or result in forces so small as to be undetectable. Russell (2002) suggested that in the tokay (*Gekko gecko*), the perpendicular preload and 5 μm drag requirements (Autumn et al. 2000; Autumn and Peattie 2002) are controlled by hydrostatic pressure in the highly derived blood sinuses, and lateral digital tendon system, respectively. However, control of inflation and deflation of the sinuses remains to be demonstrated. This mechanism would not be available to those species that lack blood sinuses.

Setal preload and drag could also be a consequence of force development during the stride (Fig. 12.2). The force necessary to bend even thousands of setae into an adhesive orientation is probably quite small (at most 10 mN; Autumn and Peattie 2002) and possibly below the threshold of the force plate used (Autumn et al. 2006). Another possibility is that attachment is a reversal of the peeling process of toe detachment, which may be decoupled from the center of mass. The gecko's foot may approach the substrate without pressing into it and re-apply the adhesive by unrolling its toes like a new year's party favor. This process is called digital hyperextension (Russell 1975,

2002). In this case, setal preload forces would be spread out over time, and would likely be far below the 1 mN resolution of force plates used in measurements of whole body and single leg dynamics of small animals (Biewener and Full 1992).

Peeling may reduce detachment and attachment forces, but may limit speed during vertical climbing. If toe peeling and uncurling in climbing geckos requires some minimum time, then speed cannot be increased by reducing contact time as is typical in level running. *Hemidactylus garnotii* increased velocity by increasing stride length (Autumn et al. 2006). Attachment and detachment occupied a constant value of approximately 20 ms.

12.2.4 Molecular Mechanism of Gecko Adhesion

While setal structures of many gecko species are well documented, a complete understanding of what makes them adhere has been more elusive. At the turn of the twentieth century, Haase (1900) noted that attachment is load-dependent and only occurs in one direction: proximally along the axis of the toe. Haase was also the first to suggest that geckos stick by intermolecular forces (*Adhäsion*), noting that under this hypothesis the attractive force should increase as the space between the feet and the substrate decreases. However, at least seven possible mechanisms for gecko adhesion have been discussed over the past 175 years.

12.2.4.1 Unsupported Mechanisms: Glue, Suction, Electrostatics, Microinterlocking, and Friction

Since geckos lack glandular tissue on their toes, sticky secretions (Dewitz 1882) were ruled out early in the study of gecko adhesion (Wagler 1830; Cartier 1872b; Simmermacher 1884). The hypothesis that the toe pads acted as suction cups was first proposed by Wagler (1830), who classified geckos as amphibians. The hypothesis that individual setae act as miniature suction cups was first under debate in the insect adhesion literature (Blackwall 1845; Hepworth 1854). Dewitz argued against suction as an explanation for gecko adhesion (1882), but Simmermacher (1884) considered suction to be the most likely mechanism. However, there are no data to support suction as an adhesive mechanism, and the adhesion experiments carried out in a vacuum by Dellit (1934) suggest that suction is not involved. Measurements of 9 atm of adhesive stress (Autumn et al. 2002b) strongly contradict the suction hypothesis. Despite substantial evidence against it, the suction hypothesis has been surprisingly tenacious in the popular literature (e.g. Gennaro 1969). Electrostatic attraction (Schmidt 1904) was another hypothesized mechanism for adhesion in gecko setae. Experiments using X-ray bombardment (Dellit 1934) eliminated electrostatic attraction as a necessary mechanism for setal adhesion since geckos could still

adhere to metal in ionized air. However, electrostatic effects could enhance adhesion even if another mechanism is operating (Maderson 1964).

Setae are recurved such that their tips point proximally, leading Dellit (1934) to hypothesize that setae act as micro- or nanoscale hooks, catching on surface irregularities (microinterlocking). Mahendra (1941) suggested that setae were analogous to the Crampon of a climbers boot. Microinterlocking was challenged by the ability of geckos to adhere while inverted on polished glass. This mechanism could play a secondary role under some conditions, but the presence of large adhesive forces on a molecularly smooth SiO_2 MEMS semiconductor (Autumn et al. 2000) demonstrates that surface irregularities are not necessary for adhesion. The friction hypothesis (Hora 1923) can be dismissed since, by definition, friction only acts in shear (Bhushan 2002), and therefore cannot in itself explain the adhesive capabilities of geckos on inverted surfaces.

12.2.4.2 Potential Intermolecular Mechanisms: van der Waals and Capillary Forces

Using the greatly enhanced resolution of electron microscopy, Ruibal and Ernst (1965) described the spatular structures at the setal tips. They concluded that spatulae were unlikely to function like the spikes on climbing boots and postulated that the spatulae lie flat against the substrate while the seta is engaged. It was clear to them that these flattened tips increased the realized contact area. Ruibal and Ernst (1965) concluded that gecko adhesion was the result of molecular interactions, not mechanical interlocking. The turning point in the study of gecko adhesion came with a series of experiments (Hiller 1968, 1969) that suggested that the surface energy of the substrate, rather than its texture, determined the strength of attachment. By providing evidence that intermolecular forces were responsible, Hiller paved the way for the application of modern methods of surface science (Israelachvili 1992) in studies of gecko adhesion (Autumn et al. 2000, 2002b; Autumn and Peattie 2002; Huber et al. 2005a; Hansen and Autumn 2005).

Hiller (1968, 1969, 1975) showed that shear force was correlated with the water droplet contact angle of the surface, and thus with the surface energy of the substrate, providing the first direct evidence that intermolecular forces are responsible for attachment in geckos.

Intermolecular capillary forces are the principal mechanism of adhesion in many insects (Gillett and Wigglesworth 1932; Edwards and Tarkanian 1970; Lee et al. 1986; Lees and Hardie 1988; Brainerd 1994), frogs (Emerson and Diehl 1980; Green 1981; Hanna and Barnes 1991) and even mammals (Rosenberg and Rose 1999). Unlike many insects, geckos lack glands on the surface of their feet (Cartier 1872a; Bellairs 1970). However, this does not preclude the role of capillary adhesion (von Wittich 1854, quoted directly in Simmermacher 1884; Baier et al. 1968; Israelachvili 1992; Stork 1980) since layers of water molecules are commonly present on hydrophilic surfaces at

ambient humidities, and can cause strong attraction between surfaces. The observation (Hiller 1968, 1971, 1975) that geckos cannot adhere to polytetrafluoroethylene (PTFE; Teflon) is consistent with the capillary hypothesis, since PTFE is strongly hydrophobic. Indeed, the apparent correlation between adhesive force and hydrophobicity (water contact angle) (Hiller 1968, 1971, 1975) suggested that the polarity of the surface might be an important factor in the strength of adhesion (Autumn and Peattie 2002).

A non-mutually-exclusive alternative mechanism is van der Waals force (Stork 1980; Autumn et al. 2000). van der Waals force is strongly dependent on the distance between surfaces, increases with the polarizability of the two surfaces, and is not related directly to surface polarity (Israelachvili 1992). The observation (Hiller 1968) that geckos cannot adhere to PTFE is consistent with both van der Waals and capillary hypotheses, since PTFE is weakly polarizable and hydrophobic.

12.2.4.3 Contact Angle Estimates of Surface Energy

Hiller's experiments (Hiller 1968, 1969, 1975) were groundbreaking because they provided the first direct evidence for adhesion *sensu stricto*. The precise nature of the adhesion remained unknown until 2002 (Autumn and Peattie 2002; Autumn et al. 2002b). The intermolecular attraction between any fluid droplet and a surface is due to a combination of dispersive (van der Waals) and polar components (Israelachvili 1992; Pocius 2002). Water contact angle by itself cannot be used to determine the relative contributions of van der Waals and polar interactions. Complete liquid droplet contact angle analyses require a series of fluids ranging from dispersive (e.g. methylene iodide) to primarily polar (e.g. water) in order to partition the relative contributions of the different intermolecular forces (Baier et al. 1968; Israelachvili 1992; Pocius 2002). However, it is possible to test the hypothesis that van der Waals forces are sufficient for gecko adhesion by reanalyzing Hiller's data to linearize the relationship between water contact angle and adhesion energy (Autumn and Peattie 2002). Hiller's data (Hiller 1968, 1969, 1975) when linearized (Autumn and Peattie 2002), yield a strong correlation between force and adhesion energy for $\theta > 60^\circ$, consistent with the van der Waals hypothesis.

12.2.5 Property (4) Material Independent Adhesion

12.2.5.1 Testing the van der Waals and Capillary Adhesion Hypotheses

To test directly whether capillary adhesion or van der Waals force is a sufficient mechanism of adhesion in geckos, Autumn and colleagues (2002b) measured the hydrophobicity of the setal surface and measured adhesion and friction on two polarizable semiconductor surfaces that varied greatly in hydrophobicity.

If capillary adhesive forces dominate, we expected a lack of adhesion on the strongly hydrophobic surfaces. In contrast, if van der Waals forces are sufficient, we predicted large adhesive forces on the hydrophobic, but polarizable GaAs and Si MEMs surfaces. In either case we expected strong adhesion to the hydrophilic SiO_2 control surfaces. We showed that tokay gecko setae are ultrahydrophobic (160.9°; Autumn et al. 2002b; Autumn and Hansen 2005), probably a consequence of the hydrophobic side groups of β-keratin (Bereiter-Hahn et al. 1984). The strongly hydrophobic nature of setae suggests that they interact primarily via van der Waals forces whether water is present or not.

Shear stress of live gecko toes on GaAs (θ=110°) and SiO_2 (θ=0°) semiconductors was not significantly different, and adhesion of a single gecko seta on the hydrophilic SiO_2 and hydrophobic Si cantilevers differed by only 2%. These results reject the hypothesis that polarity (as indicated by θ) of a surface predicts attachment forces in gecko setae, as suggested by Hiller (1968, 1969), and are consistent with reanalysis of his data using adhesion energies (Autumn and Peattie 2002). Since van der Waals force is the only mechanism that can cause two hydrophobic surfaces to adhere in air (Israelachvili 1992), the GaAs and hydrophobic semiconductor experiments provide direct evidence that van der Waals force is a sufficient mechanism of adhesion in gecko setae, and that water-based capillary forces are not required. Setal adhesion is strong on polar and nonpolar surfaces, perhaps because of the strongly hydrophobic material they are made of, and due to the very large contact areas made possible by the spatular nanoarray. Gecko setae thus have the property of *material independence*: they can adhere strongly to a wide range of materials, largely independently of surface chemistry.

12.2.5.2 The Role of Water in Gecko Adhesion

Property (4), material independent adhesion, does not preclude an effect of water on gecko adhesion under some conditions. Water is likely to alter contact geometry and adhesion energies when present between hydrophobic (e.g. spatula) and hydrophilic (e.g. glass) surfaces, but it is exceedingly difficult to predict what the effect will be in gecko setae because of the complexity of the system. An excellent example of the difficulty of interpreting the effect of water on gecko adhesion is a study by Sun et al. (2005) that used a model of interaction of two hydrophilic surfaces as a function of humidity to predict greatest adhesion due to capillary forces at 70–80% relative humidity (RH). Sun et al. measured greater adhesion in gecko spatulae at 70% RH than in dry air. However, the theory and methods of this study leave room for interpretations other than that favored by its authors. While the parameters and assumptions of the capillary model were not presented in their paper, it is clear that a hydrophilic-hydrophilic model is not applicable to gecko setae since they are strongly hydrophobic (Autumn et al. 2002b; Autumn and

Hansen 2005). This raises the question of how to explain the apparent effect of humidity on gecko adhesion by Sun et al. (2005).

It is interesting to consider the possibility that adsorbed water could act as an interlayer, with van der Waals forces acting between setae and water, while polar interactions could dominate between water and the substrate. Water could reduce adhesion on rough surfaces by preventing spatular penetration into gaps, thus decreasing the contact fraction (Persson and Gorb 2003). Alternatively, a fluid interlayer could enhance adhesion on rough surfaces by filling in gaps and increasing the contact fraction. The property of material independence predicts that the primary effect of water would be to alter the contact fraction, not adhesion energy. This is supported by measurements of spatular adhesion using AFM (Huber et al. 2005b). Huber et al. (2005b) confirmed that humidity can have a significant effect on adhesion. However, in contrast to the conclusions of Sun et al. (2005), Huber et al. (2005b) rejected "true" capillary forces involving a water bridge since only a few monolayers of water were present at the spatula-substrate interface – even at high humidity. Instead, they concluded that humidity 1) modifies the contact geometry, increasing adhesion, and 2) decreases the van der Waals Hamaker constant (A), reducing adhesion. These two effects balanced each other to yield an increase in adhesion from 7nN at low humidity to 12nN at high humidity. Thus van der Waals interactions not capillary forces best explain the results of Sun et al. (2005). These results support prior work (Autumn et al. 2002) showing that geckos can adhere solely by van der Waals forces.

It is well known that hydrophobic-hydrophobic interactions in air are due solely to van der Waals force. Since plant surfaces are generally hydrophobic (Holloway 1969; Jeffree 1986), as are gecko setae, it remains unclear whether the effect of humidity is important in nature. An additional potential effect of humidity would be to alter material properties or surface chemistry of the setal protein, but this remains theoretical at this point. The effect of water on adhesion and friction in gecko setae will be a challenging and productive research area.

12.2.5.3 Dominance of Geometry in VdW Interactions

The theoretical magnitude of van der Waals force between a planar substrate and a circular planar spatula of radius R (Israelachvili 1992) is $F_{vdw} = \frac{AR^2}{6D^3}$, and for a planar substrate and a curved spatula of radius R, $F_{vdw} = \frac{AR}{6D^2}$, where A represents the Hamaker constant, D is the gap distance (typically 0.2 nm for solids in contact). A is a function of the volume and polarizability of the molecules involved.

A, the Hamaker constant, for materials interacting in dry air is typically approx. 10^{-19} J. Altering the chemical composition of one or both surfaces

can alter A, which can be as low as approx. one-half to one-third this value for some polymer-polymer interactions (e.g. PTFE or polystyrene), and as high as five times this value for some metal-on-metal interactions. In water, A can be reduced by an order of magnitude. Nevertheless, the variation in A is only about an order of magnitude while gap distance and contact area may vary by six or more orders of magnitude without macroscopically visible changes at the interface. Moreover, the effects of gap distance are exponential to a power of at least two. Thus adhesive surface effects due to van der Waals interactions are a function primarily of geometry, not of chemistry. A van der Waals mechanism for adhesion in gecko setae suggests that continuum theory models of the mechanics of surface contact (Johnson 1985) may be applicable. Then again, since the complex structure of setae and spatulae differs dramatically from the ideal curved and planar surfaces used in contact mechanics models, one might question the validity of models based on simple geometries to the function of gecko setae.

12.2.5.4 JKR Model of Spatulae

The mechanics of contact have been modeled using continuum theory and highly simplified geometries. For example the Johnson, Kendall, Roberts (JKR; Johnson et al. 1973) model considers the force F required to pull an elastic sphere of radius R from a planar surface. The predicted adhesion force is given by, $F=(3/2)\pi R\gamma$, where γ is the adhesion energy between the sphere and the surface. Using values of R=100 nm and γ=50 mJ/m^2, the predicted force for a gecko spatula is F=23.6 nN, approx. twice the value measured by AFM (Huber et al. 2005a) (Table 12.1).

Another test of the validity of the JKR model is to begin with the forces measured in single setae, and then calculate the size of the JKR sphere (Autumn et al. 2002b). Adhesion is ~40 μN per seta on silicon cantilever surfaces (Table 12.1). The setal tip is approximately 43 μm^2 in area, and therefore the adhesive stress (σ) was ~917 kPa. If the spatulae are packed tightly, $\sigma \approx (3/2)\pi R\gamma / \pi R^2 = (3/2)\gamma/R$. Using a typical adhesion energy for van der Waals surfaces (γ=50–60 mJ/m^2), solving for the predicted radii (R) of individual spatulae using empirical force measurements: $R=(3/2)\gamma/\sigma$=82–98 nm, (164–196 nm in diameter). This value is remarkably close to empirical measurements of real gecko spatulae (200 nm in width) (Ruibal and Ernst 1965; Autumn et al. 2000) yet obviously spatulae are not spherical (Fig. 12.1E). Note that the preceding estimate of R using the JKR model differs from that of Autumn and colleagues (Autumn et al. 2002b) in that they estimated the area of one seta using setal density, and arrived at a similar but somewhat lower value for σ. The confirmation that the JKR model predicts similar magnitudes of force as observed in setae suggested the extraordinary conclusion that adhesion can be enhanced simply by splitting a surface into

Table 12.1. Scaling of adhesion and friction stresses in tokay gecko setae. Shear stress decreases approximately exponentially (Fig. 12.6), or approximately linearly on a log-log scale. The Kendall peel model prediction uses a square spatula of 100 nm on a side. The JKR model prediction uses a spherical spatula with 100 nm radius. Both predictions use an adhesion energy of $W=50$ mJ/m^2. Note that the similarity of area between single toe and single foot is due to the use of larger geckos in the single toe measurements

Scale	Mode	Force	Area	Stress (kPa)	Stress (atm)
Single spatula (Huber et al. 2005a)	Adhesion	10 nN	0.02 μ^2	500	4.9
JKR model prediction for single spatula	Adhesion	23.56 nN	0.0314 μ^2	750	7.4
Kendall peel model prediction for single spatula	Adhesion	10.00 nN	0.04 μ^2	250	2.5
Single seta (Autumn et al. 2000)	Adhesion	20 μN	43.6 μ^2	458	4.5
Single seta (Autumn et al. 2002a,b)	Adhesion	40 μN	43.6 μ^2	917	9.0
Single seta (Autumn et al. 2000)	Friction	200 μN	43.6 μ^2	4585	45.2
Setal array (Hansen and Autumn 2005)	Friction	0.37 N	0.99 mm^2	370	3.7
Single toe (Hansen and Autumn 2005)	Friction	4.3 N	0.19 cm^2	226	2.2
Single foot (Autumn et al. 2002a, b)	Friction	4.6 N	0.22 cm^2	186	1.8
Two feet (Irschick et al. 1996)	Friction	20.4 N	2.27 cm^2	90	0.9

small protrusions to increase surface density (Autumn et al. 2002b) and that adhesive stress is proportional to $1/R$ (Arzt et al. 2002). This model is supported by a comparative analysis of setae in lizards and arthropods (Arzt et al. 2003) (see Sect. 12.5.1).

12.2.5.5 Kendall Peel Model of Spatulae

Spatulae may also be modeled as nanoscale strips of adhesive tape (Huber et al. 2005a; Spolenak et al. 2004; Hansen and Autumn 2005). Using the approach of Kendall (1975), $F=\gamma w$, assuming there is negligible elastic energy storage in the spatula as it is pulled off, and where w is the width of the spatula, and γ is the adhesion energy as for the JKR model. Empirical measurements of spatular adhesion (Huber et al. 2005a) suggest that each spatula

adheres with approximately 10 nN force. Using a value of γ=50 mJ/m^2, typical of van der Waals interactions the Kendall peel model predicts a spatular width of 200 nm, remarkably close to the actual dimension (Ruibal and Ernst 1965; Autumn et al. 2000).

Theoretical considerations suggest that generalized continuum models of spatulae as spheres or nanotape are applicable to the range of spatula size and keratin stiffness of setae found in reptiles and arthropods (Spolenak et al. 2004). Interestingly, at the 100 nm size scale the effect of shape on adhesion force may be relatively limited (Gao and Yao 2004; Spolenak et al. 2004). However, at sizes above 100 nm and especially above 1 μm, Spolenak et al. (2004) concluded that shape should have a very strong effect on adhesion force. A phylogenetic comparative analysis of attachment force in lizards and insects will be an important test of this hypothesis.

12.3 Anti-adhesive Properties of Gecko Setae

Paradoxical as it may seem, there is growing evidence that gecko setae are strongly anti-adhesive. Gecko setae do not adhere spontaneously to surfaces, but instead require a mechanical program for attachment (Autumn et al. 2000). Unlike adhesive tapes, gecko setae do not self-adhere. Pushing the setal surfaces of a gecko's feet together does not result in strong adhesion. Also unlike conventional adhesives, gecko setae do not seem to stay dirty.

12.3.1 Properties (5) Self-cleaning and (6) Anti-self-adhesion

Dirt particles are common in nature (Little 1979), yet casual observation suggests that geckos' feet are quite clean (Fig. 12.1B). Sand, dust, leaf litter, pollen, and plant waxes would seem likely to contaminate gecko setae. Hair-like elements on plants accumulate micron-scale particles (Little 1979) that could come into contact with gecko feet during climbing. Indeed, insects must cope with particulate contamination that reduces the function of their adhesive pads (Gorb and Gorb 2002), and spend a significant proportion of their time grooming (Stork 1983) in order to restore function. On the other hand, geckos have not been observed to groom their feet (Russell and Rosenberg 1981), yet apparently retain the adhesive ability of their setae during the months between shed cycles. How geckos manage to keep their toes clean while walking about with sticky feet has remained a puzzle until recently (Hansen and Autumn 2005). While self-cleaning by water droplets has been shown to occur in plant (Barthlott and Neinhuis 1997) and animal (Baum et al. 2002) surfaces, no adhesive had been shown to self-clean.

Gecko setae are the first known self-cleaning adhesive (Hansen and Autumn 2005). Tokay geckos with 2.5 μm radius microspheres applied to their feet

recovered their ability to cling to vertical surfaces after only a few steps on clean glass. We contaminated toes on one side of the animal with an excess of 2.5 μm radius silica-alumina microspheres and compared the shear stress to that of uncontaminated toes on the other side of the animal. Prior researchers had suggested that geckos' unique toe peeling motion (digital hyperextension) might aid in cleaning of the toe pads (Russell 1979; Bauer et al. 1996), so we immobilized the geckos' toes and applied them by hand to the surface of a glass force plate to determine if self-cleaning could occur without toe peeling. After only four simulated steps on a clean glass surface, the geckos recovered enough of their setal function to support their body weight by a single toe (Hansen and Autumn 2005). To test the hypothesis that self-cleaning is an intrinsic property of gecko setae and does not require a gecko, we isolated arrays of setae and glued them to plastic strips. We simulated steps using a servomanipulation system we called RoboToe. We compared shear stress in clean setal arrays to that in the same arrays with a monolayer of microspheres applied to their adhesive surfaces. Self-cleaning of microspheres occurred in arrays of setae isolated from the gecko. Again as for live gecko toes, isolated setal arrays rapidly recovered the shear force lost due to contamination by microspheres. We hypothesized that the microspheres were being preferentially deposited on the glass substrate, and did not remain strongly attached to the setae.

Contact mechanical models suggest that it is possible that self-cleaning occurs by an energetic disequilibrium between the adhesive forces attracting a dirt particle to the substrate and those attracting the same particle to one or more spatulae (Fig. 12.3) (Hansen and Autumn 2005). The models suggest that self-cleaning may in fact require γ of spatulae to be relatively low (equal to or less than that of the wall), perhaps constraining the spatula to be made of a hydrophobic material. So, geckos may benefit by having setae made of an anti-adhesive material: decreasing γ decreases adhesion energy of each spatula but promoting self-cleaning should increase adhesion of the array as a whole by maximizing the number of uncontaminated spatulae. If γ were to be increased by supplementing van der Waals forces with stronger intermolecular forces such as polar or H-bonding, it is likely that self-cleaning and anti-self properties would be lost. Thus the self-cleaning and anti-self properties may represent a sweet spot in the evolutionary design space for adhesive nanostructures.

12.3.2 Property (7) Nonsticky Default State

The discovery that maximal adhesion in isolated setae requires a small push perpendicular to the surface, followed by a small parallel drag (Autumn et al. 2000), explained the load dependence and directionality of adhesion observed at the whole-animal scale by Haase (1900) and Dellit (1934), and was consistent with the structure of individual setae and spatulae (Ruibal and Ernst 1965; Hiller 1968). In their resting state, setal stalks are recurved proximally. When the toes of the gecko are planted, the setae may become bent

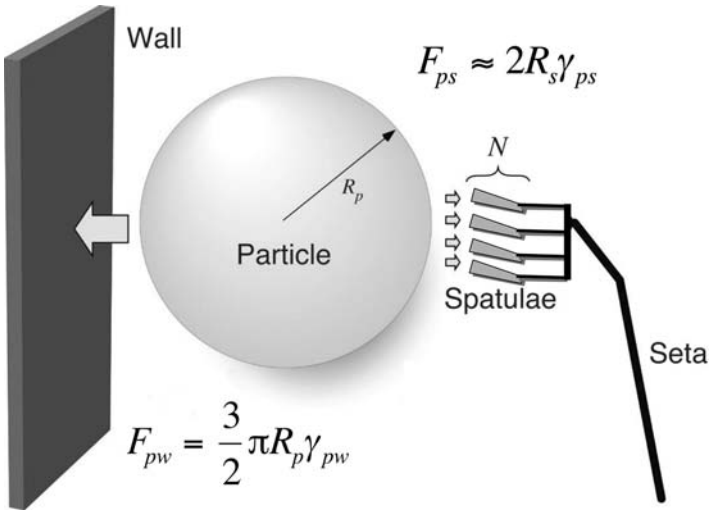

Fig. 12.3. Model of self-cleaning in gecko setae from Hansen and Autumn (2005). If we model spatulae as nanoscale strips of adhesive tape (Kendall 1975) that peel during detachment, the particle-spatula pulloff force is given by $F_{ps} \approx 2R_s\gamma_{ps}$, where γ_{ps} is the adhesion energy at the dirt particle-spatula interface, and $2R_s$ is the width of the spatula, and assuming negligible elastic energy storage. The pulloff force of the dirt particle from a planar wall, using the Johnson, Kendall, Roberts (JKR) model (Johnson et al. 1973) is $F_{pw} = \frac{3}{2}\pi R_p\gamma_{pw}$, where γ_{pw} is the adhesion energy of the particle to the wall. *N* represents the number of spatulae attached simultaneously to each dirt particle to achieve energetic equilibrium

out of this resting state, flattening the stalks between the toe and the substrate such that their tips point distally. This small preload and a micron-scale displacement of the toe or scansor proximally may serve to bring the spatulae (previously in a variety of orientations) uniformly flush with the substrate, maximizing their surface area of contact. Adhesion results and the setae are ready to bear the load of the animal's body weight.

To test the hypothesis that the default state of gecko setal arrays is to be nonsticky, Autumn and Hansen (2005) estimated the fraction of area able to make contact with a surface in setae in their unloaded state. Only less than 6.6% of the area at the tip of a seta is available for initial contact with a smooth surface, and 93.4% is air space. This suggests that, initially, during a gecko's foot placement, the contact fraction of the distal region of the setal array must be very low. Yet the dynamics of the foot must be sufficient to increase the contact fraction substantially to achieve the extraordinary values of adhesion and friction that have been measured in whole animals (Autumn et al. 2002b; Hansen and Autumn 2005; Irschick et al. 1996) and isolated setae (Autumn et al. 2000; Autumn et al. 2002b; Hansen and Autumn 2005). Thus gecko setae may be nonsticky by default because only a very small contact fraction is possible without mechanically deforming the setal array.

How much does the contact fraction increase during attachment? While there are no empirical measurements of the number of spatulae in contact as a function of adhesion (or friction) force, it is possible to estimate from measurements of single setae. Empirical measurements and theoretical estimates of spatular adhesion (Autumn et al. 2000, 2002b; Arzt et al. 2003; Huber et al. 2005a; Spolenak et al. 2004; Hansen and Autumn 2005) suggest that each spatula generates approximately 10–40 nN with approximately 0.02 μ^2 area, or approximately 500–2000 kPa. A single seta on a Si MEMs cantilever can generate approximately 917 kPa (Table 12.1). The value of 10 nN adhesion measured in single spatulae using an AFM (Huber et al. 2005a) implies that 4000 spatulae would need to be attached to equal the peak adhesion force (40 μN) measured in single setae (Autumn et al. 2002b). However, each seta contains not more than approximately 100–1000 spatulae (Ruibal and Ernst 1965; Schleich and Kästle 1986). Therefore a spatular force of 40 nN is more appropriate for a conservative estimate of setal contact fraction during attachment. In the case of a spatular adhesion force of 40 nN, the adhesive stress is 2000 kPa. Therefore a contact fraction of 46% is required to yield the setal stress. This suggests that unless the force of adhesion of a spatula has been greatly underestimated, the contact fraction must increase from 6% to 46%, or by approximately 7.5-fold, following preload and drag.

12.4 Modeling Adhesive Nanostructures

12.4.1 Effective Modulus of a Setal Array

The gecko adhesive is a microstructure in the form of an array of millions of high aspect ratio shafts. The effective elastic modulus, E_{eff}, (Persson 2003; Sitti and Fearing 2003) is much lower than the Young's modulus (E) of β-keratin. Thus arrays of setae should behave as a softer material than bulk β-keratin. E of beta-keratin in tension is approx. 2.5 GPa in bird feathers (Bonser and Purslow 1995) and 1.3–1.8 GPa in bird claws (Bonser 2000). Young's moduli of lizard beta keratins in general (Fraser and Parry 1996) and gecko beta keratins in particular (Alibardi 2003) remain unknown at present. The behavior of a setal array during compression and relaxation will depend on the mode(s) of deformation of individual setae. Bending is a likely mode of deformation (Simmermacher 1884) (Fig. 12.1D), and a simple approach is to model arrays of setae as cantilever beams (Persson 2003; Sitti and Fearing 2003; Glassmaker et al. 2004; Hui et al. 2004; Spolenak et al. 2005). One might question the applicability of models based on a simple geometry for the complex, branched structure of the seta. However, as with the JKR and Kendall models (Sects. 12.2.5.4 and 12.2.5.5) applied to spatulae, the simple cantilever model is surprisingly well supported by empirical measurements of setal arrays (Geisler et al. 2005).

The cantilever model of a single seta (Campolo et al. 2003; Sitti and Fearing 2003) is based on a cantilever beam under a lateral load, F at its tip. The resulting tip displacement due to bending is $\Delta = FL^3/3EI$, where L is the length, E is the elastic modulus of the material, and I is the area moment of inertia of the cantilever (Gere and Timoshenko 1984) (Fig. 12.4A). The lateral bending stiffness K_y is given by

$$K_y = \frac{3EI}{L^3} = \frac{3\pi R^4 E}{4L^3} \tag{12.1}$$

for a cylindrical cantilever of radius R, $I = \pi R^4/4$. For a cantilever at an angle ϕ to the substrate and under a normal load, F_n, the resolved force lateral to the cantilever is $F = F_n \cos\phi$ (Fig. 12.4B). This results in a lateral tip displacement of $\Delta = F_n \cos(\phi) L^3/3EI$, and a normal tip displacement of $\Delta_n = \Delta\cos\phi = F_n \cos^2(\phi) L^3/3EI$.

Next, to derive an effective elastic modulus (E_{eff}) for a model setal array, in the cantilever system above, we use Hooke's law, $\sigma = E_{eff}\ \varepsilon$, where σ and ε are the applied stress and resulting strain in the normal axis, respectively. The normal strain is $\varepsilon = \Delta_n/L_n$ (Fig. 12.4B), where $L_n = L\sin\phi$.

Now, for an array of cantilevers with density D (m^{-2}) in parallel at an angle ϕ and under a normal stress σ, the normal force acting on each cantilever tip is $F_n = \sigma/D$. The resulting normal displacement of the array is $\Delta_n = \sigma\cos^2(\phi) L^3/3EID$. Thus, $\varepsilon = \sigma\cos^2(\phi) L^2/3EID\sin\phi$, and the stress over the cantilever array is $\sigma = E_{eff}\ \sigma\cos^2(\phi) L^2 / 3EID\sin\phi$. Dividing by σ and solving for E_{eff} we reach a general equation for the effective stiffness of a cantilever array:

$$E_{eff} = 3EID\sin\phi / \cos^2(\phi)\ L^2 \tag{12.2}$$

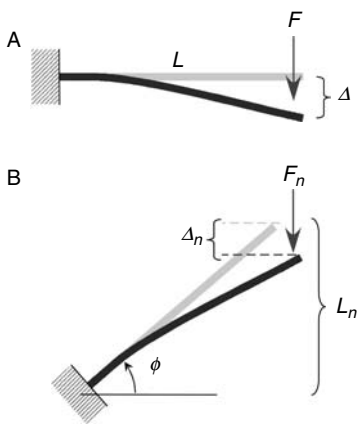

Fig. 12.4. Free body diagram of: (a) cantilever beam; (b) angled cantilever beam based on the model of Sitti and Fearing (2003). This model is similar to that of Persson (2003) who used a spring-based approach

For a cylindrical cantilever, we can substitute EI in Eq. (12.2) for $K_y L^3 / 3$ using Eq. (12.1), yielding

$$E_{eff} = \frac{K_y L D \sin\phi}{\cos^2\phi} \tag{12.3}$$

For a tokay seta-size cylindrical cantilever of R =2.1 μm, L =110 μm, E =1 GPa, the bending stiffness from Eq. (12.1) is K_y =0.0344 N/m. For E=2 GPa, K_y=0.0689 N/m.

I will now calculate the shaft angle ϕ (see Fig. 12.4B) required to yield an effective stiffness of 100 kPa (the upper limit of Dahlquist's criterion see Sect. 12.6) (Dahlquist 1969; Pocius 2002). A typical tokay setal array has approx 14,000 setae per mm^2 and $D = 1.44 \times 10^{10}$ m^{-2}. Using Eq. (12.3), a value of ϕ =50° is required for E =1 GPa, and ϕ =36.65° for E =2 GPa to yield E_{eff} =100 kPa.

We measured the forces resulting from deformation of isolated arrays of tokay gecko (*Gekko gecko*) setae to determine E_{eff} and test the validity of the cantilever model. We found that E_{eff} of tokay gecko setae falls near 100 kPa, close to the upper limit of Dahlquist's criterion for tack (Fig. 12.5) (Geisler et al. 2005). Additionally, we observed values of ϕ for tokay gecko setae near 43°, further supporting the validity of the cantilever model (Fig. 12.4; Geisler et al. 2005).

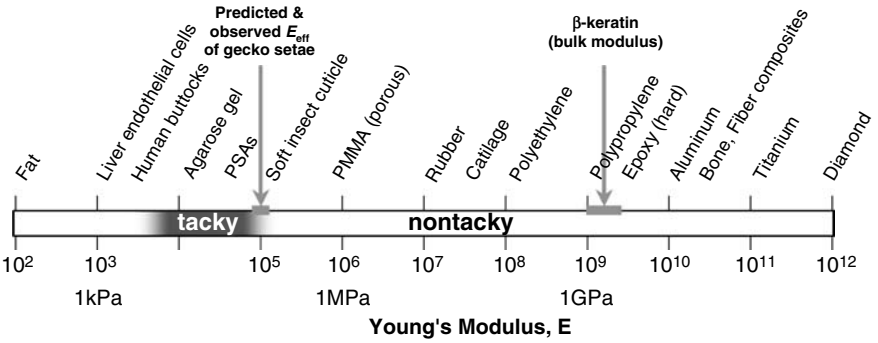

Fig. 12.5. Young's modulus (e) of materials including approximate values of bulk β-keratin and effective modulus (E_{eff}) of natural setal arrays (Geisler et al. 2005). A value of $E \approx$100 kPa (measured at 1 Hz) is the upper limit of the Dahlquist criterion for tack, which is based on empirical observations of pressure sensitive adhesives (PSAs; Dahlquist 1969; Pocius 2002). A cantilever beam model (Eq. 5.3; Sitti and Fearing 2003) predicts a value of E_{eff} near 100 kPa, as observed for natural setae and PSAs. It is notable that geckos have evolved E_{eff} close to the limit of tack. This value of E_{eff} may be tuned to allow strong and rapid adhesion, yet prevent spontaneous or inappropriate attachment

12.4.2 Rough Surface and Antimatting Conditions

The cantilever model predicts that a high density of setae should be selected for in increasing adhesive force of setal arrays. First, it follows from the JKR model (Autumn et al. 2002b; Arzt et al. 2003) that packing in more spatulae should increase adhesion in an array of setae. Second, the cantilever model suggests that thinner setal shafts should decrease E_{eff}, and promote a greater contact fraction on rough surfaces (Stork 1983; Scherge and Gorb 2001; Jagota and Bennison 2002; Campolo et al. 2003; Persson 2003; Persson and Gorb 2003; Sitti and Fearing 2003; Spolenak et al. 2005). The cantilever model also suggests that longer and softer setal shafts, and a lower shaft angle ϕ will result in better adhesion on rough surfaces because these parameters will reduce E_{eff}. On a randomly rough surface, some setal shafts should be bent in compression (concave), while others will be bent in tension (convex). The total force required to pull off a setal array from a rough surface should therefore be determined by the cumulative adhesive force of all the attached spatulae, minus the sum of the forces due to elastic deformation of compressed setal shafts.

If setae mat together (Stork 1983), it is likely that adhesive function will be compromised. Interestingly, the same parameters that promote strong adhesion on rough surfaces should also cause matting of adjacent setae (Persson 2003; Sitti and Fearing 2003; Glassmaker et al. 2004; Hui et al. 2004; Spolenak et al. 2005). The distance between setae and the stiffness of the shafts will determine the amount of force required to bring the tips together for matting to occur. It follows from the cantilever model that stiffer, shorter, and thicker stalks will allow a greater packing density without matting. As is the case for self-cleaning (Hansen and Autumn 2005), setae should be made of materials with lower surface energy to prevent self-adhesion and matting. Satisfying both antimatting and rough surface conditions may require a compromise of design parameters. Spolenak et al. (2005) devised "design maps" for setal adhesive structures, an elegant approach to visualizing the parametric tradeoffs needed to satisfy the rough surface and antimatting conditions while at the same time maintaining structural integrity of the material.

12.5 Scaling

Small and large organisms are dominated by different forces (McMahon and Bonner 1983). Inertial forces usually dwarf adhesive forces in organisms gecko-size and above. Geckos are unusual among macroscale organisms in having adhesive forces dominate their world. The astonishing adaptive radiation in geckos and their unique ecologies can be seen as an emergent property of integration across seven orders of magnitude in size (Pianka and Sweet 2005)–from the nanoscale spatula and the microscale seta to the mesoscale scansors and the macroscale body (Fig. 12.1).

While it is tempting to focus on the smallest level in the gecko adhesive system, integration of multiple levels in the compliance hierarchy is needed to achieve reliable and controllable adhesion and friction. Self-cleaning adhesive nanostructures cannot adhere if they never get near the surface. Compliant scansors and the compliant adipose or vascular tissue underlying the scansors may be important in spreading the load during foot placement (Russell 1986, 2002). The complex morphology and musculature of the toes, feet, and limbs play a critical role in bringing the compliant scansors to bear upon the substrate in the appropriate manner, and in detaching them without large forces (Russell 1975). Simulation studies of animal-like climbers suggest that tuning limb compliance correctly is much more important for climbing than for running. In particular, the ratios of linear and torsional compliances at the foot and ankle have an enormous effect on climbing stability and efficacy (Autumn et al. 2005a).

12.5.1 Scaling of Pad Area and Spatular Size

Shear force of the two front feet of pad-bearing lizards (geckos, anoles and skinks) is highly correlated with pad area, even when the effects of body size and phylogeny are accounted for (Irschick et al. 1996). However, there is significant variation in shear force among taxa of similar size and pad area, suggesting that other factors are important in determining the strength of the setal adhesive. The JKR model (Autumn et al. 2002b; Arzt et al. 2003) predicts that larger spatulae should result in lower forces, and this is supported by an inverse correlation between body mass and the size of the spatula or setal tip in lizards and arthropods (Arzt et al. 2003). It seems clear that geckos have superior adhesion and friction in comparison to other seta-bearing species, and one likely reason is small spatular size.

12.5.2 Scaling of Stress

Amontons' first law states that the relationship of shear force (friction) to load is a constant value, μ (the coefficient of friction). Amontons' second law predicts that μ is independent of the area of contact (Bhushan 2002; Ringlein and Robbins 2004). When pulled in shear (Autumn et al. 2000, 2002b), gecko setae seem to violate Amonton's laws, as do tacky polymers where the forces of adhesion can be much greater than the external load. Shear stress in setae increases greatly with a decrease in contact area A, suggesting that at larger scales, fewer spatulae are attached and/or the contact fraction within spatulae is reduced (Fig. 12.6; Table 12.1). The scaling of shear stress, τ, is exponential and scales as $\log \tau = 1.14 - 0.24 \log A$ ($R^2 = 0.99$). It is unknown whether stress is uniformly spread across the toe or foot (Russell 2002), or if there are high stress concentrations on the setal arrays of a few scansors. The force of

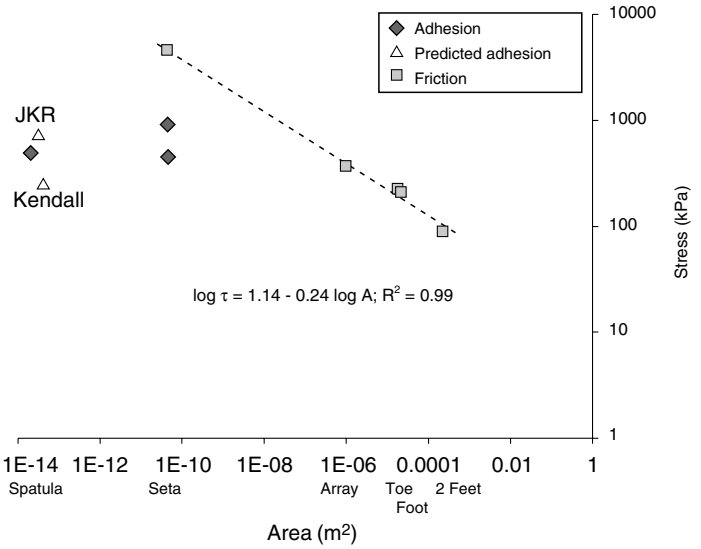

Fig. 12.6. Stress vs area in the gecko adhesive hierarchy. See Table 12.1 for numerical values and literature sources. JKR and Kendall model predictions for spatular adhesive stress (*triangles*) bound the measured value of Huber et al. (2005a). Text below the X-axis shows the level in the gecko adhesive hierarchy (Fig. 12.1)

only 2% of setae, and only 25% of setal arrays, are required to yield the maximum shear stresses measured at the whole-animal level. However, at the setal level, it appears that most spatulae must be strongly attached to account for theoretical and empirical values of adhesion, suggesting that the seta is highly effective at making contact with a smooth surface. If each spatula can generate 10–40 nN, it would take 1000–4000 spatulae to yield the 40 μN of adhesion measured in single setae. However, each seta bears only 100–1000 spatulae. Clearly further work is needed to resolve this discrepancy. The relationship between adhesion and friction also demands further investigation. Existing data suggest that friction at the seta level is about two to four times the adhesion.

12.6 Comparison of Conventional and Gecko Adhesives

Conventional adhesives are materials that are used to join two surfaces. Typically, adhesives are liquids that are chemically compatible with both surfaces and have sufficiently low viscosity that wetting of the surfaces occurs either spontaneously or with a small amount of pressure (Baier et al. 1968; Kinloch 1987; Pocius 2002). Surface treatments are often needed to raise the interfacial energies between one or both surfaces and the adhesive. Liquid

hard-set adhesives (e.g. epoxy or cyanoacrylate glues) flow easily during application, but cure to make a strong, permanent bond. Because they are stiff when cured, hard-set adhesives can resist plastic creep caused by sustained loading. However, hard-set adhesives are single-use: their bonds must be broken or dissolved for removal and once broken, hard-set adhesives do not rebond.

Conventional pressure sensitive adhesives (PSAs) are fabricated from soft, tacky, viscoelastic materials (Gay and Leibler 1999; Gay 2002; Pocius 2002). Tacky materials are those that exhibit spontaneous plastic deformation that increases true area of contact with the surface at the molecular scale. Theoretical considerations (Creton and Leibler 1996) agree with Dahlquist's (Dahlquist 1969; Pocius 2002) empirical observation that a Young's modulus (E) below 100 kPa (at 1 Hz) is needed to achieve a high contact fraction with the substrate. Additives known as tackifiers are commonly used to promote plastic deformation in PSAs during contact (Pocius 2002). PSAs such as masking tape or sticky notes are capable of repeated attachment and detachment cycles without residue because the dominant mechanism of adhesion is weak intermolecular forces. PSAs adhering with weak intermolecular forces can require much more energy to pull off of surfaces than do rigid adhesives relying on strong chemical bonds. As soft polymeric adhesives are pulled apart from a surface, polymer chains or bundles of polymer chains can be elongated into pillars in a process known as crazing. The total fracture energy can greatly exceed the sum of all the bond energies at the interface since work must be done on the craze as well as to break adhesive bonds at the interface. Thus the strong adhesion in polymeric adhesives results from long bonds rather than from strong bonds (Persson 2003). However, because they are soft polymeric materials, PSAs are prone to creep, degradation, self-adhesion, and fouling.

In contrast to the soft polymers of PSAs, the adhesive on the toes of geckos is made of hard protein (β-keratin) with E four to five orders of magnitude greater than the upper limit of Dahlquist's criterion. Therefore, one would not expect a β-keratin structure to function as a PSA by readily deforming to make intimate molecular contact with a variety of surface profiles. However, since the gecko adhesive is a microstructure in the form of an array of millions of high aspect ratio shafts (setae) the effective elastic modulus, E_{eff}, (Jagota and Bennison 2002; Persson 2003; Sitti and Fearing 2003; Glassmaker et al. 2004; Hui et al. 2004; Spolenak et al. 2005) is much lower than E of bulk β-keratin. The effective modulus of gecko setal arrays is close to 100 kPa (Geisler et al. 2005). Gecko setal arrays possess some of the properties of PSAs although the bulk material properties of β-keratin place it in the class of stiff, nonviscous materials (Fig. 12.5) (Dahlquist 1969; Creton and Leibler 1996; Gay and Leibler 1999; Gay 2002; Jagota and Bennison 2002; Pocius 2002; Persson 2003; Persson and Gorb 2003; Sitti and Fearing 2003).

There is emerging evidence that an array of gecko setae can act like a tacky, deformable material, while individual setae and spatulae retain the structural integrity of stiff protein fibers. This may enable the gecko adhesive to tolerate

heavy, repeated use without creep or degradation. Indeed, theoretical considerations suggest that the fibrillar structure of the gecko adhesive can be thought of as a permanent craze (Jagota and Bennison 2002; Persson 2003) that can raise the fracture energy relative to a solid layer of adhesive material. As with polymer crazes, setal structures under stress could store energy elastically in each seta of the array, and then as setae are pulled off, elastic energy could be dissipated internally without contributing to propagation of the crack between the adhesive and substrate (Hui et al. 2004; Jagota and Bennison 2002; Persson 2003). Unlike polymer crazes, setal structures may dissipate energy primarily elastically rather than plastically.

Gecko setae do not bond spontaneously on contact, as do PSAs. Gecko setae have a nonsticky default state (Autumn and Hansen 2005b), and require mechanical deformation to initiate adhesion and friction (Autumn et al. 2000; Autumn and Peattie 2002). Again in contrast to PSAs, gecko setae are anisotropic and possess a built-in release mechanism. Setae are sticky when forces are directed with the curvature of the shaft, and release when forces are directed away from the curvature of the shaft (Autumn et al. 2000; Autumn and Peattie 2002; Gao et al. 2005).

12.7 Gecko-inspired Synthetic Adhesive Nanostructures

Using a nanostructure to create an adhesive is a novel and bizarre concept. It is possible that, if it had not evolved, humans would never have invented it. With the inspiration of biology, the first generation of adhesive nanostructures is being developed (Fig. 12.1F). The growing list of benchmark properties–seven of which are presented in this chapter–can be used to evaluate the degree of geckolike function of synthetic prototypes. By these criteria, synthetic setae (Autumn et al. 2002b; Geim et al. 2003; Sitti and Fearing 2003; Peressadko and Gorb 2004; Northen and Turner 2005) are at a very early stage, and none has significantly geckolike properties. For example, consider the adhesion coefficient, $\mu' = F_{adhesion}/F_{preload}$, as a metric for geckolike adhesive function. By this criterion, the material of Geim et al. (2003) is not geckolike since it required a very large preload of 50 N to yield 3 N and 0.3 atm of adhesion, yielding a value of $\mu' = 0.06$. The synthetic setae of Northen and Turner (2005) perform significantly better with a $\mu' = 0.125$, but still well below the benchmark of real gecko setae where $\mu' = 8–16$. Effective design of geckolike adhesives will require deep understanding of the principles (Table 12.2) underlying the properties observed in the natural system. For example, synthetic setae that can attach without substantial preloads will likely require angled rather than vertical shafts (Sitti and Fearing 2003) to promote a bending rather than buckling mode of deformation.

Applications abound for a dry self-cleaning adhesive that does not rely on soft polymers or chemical bonds. Biomedical applications such as endoscopy

Table 12.2. Properties, principles, and parameters of the gecko adhesive system. This table lists known properties of the gecko adhesive, proposed principles (or models) that explain the properties, and model parameters for each property. JKR refers to the Johnson, Kendall, Roberts model of adhesion (Johnson et al. 1973)

Properties	Principles	Parameters
1. Anisotropic attachment (Autumn et al. 2000) 2. High μ′ (pulloff/preload) (Autumn et al. 2000)	Cantilever beam (Autumn et al. 2000; Sitti and Fearing 2003; Spolenak et al. 2004)	Shaft length, radius, den sity (Sitti and Fearing 2003) Shaft angle (Sitti and Fearing 2003)
3. Low detachment force (Autumn et al. 2000)	Low effective stiffness (Sitti and Fearing 2003; Persson 2003)	Shaft modulus (Sitti and Fearing 2003) Spatular shape (Persson and Gorb 2003; Spolenak et al. 2004)
	van der Waals (vdW) mechanism (Autumn et al. 2002a, b)	Spatular size (Arzt et al. 2003)
4. Material independence (Autumn et al. 2002a, b; Hiller 1968, 1969)	JKR-like contact mechanics (Autumn et al. 2002a, b; Arzt et al. 2002, 2003)	Spatular Shape (Gao and Yao 2004; Spolenak et al. 2004)
	Nanoarray (divided contact) (Autumn et al. 2002a, b; Gao and Yao 2004)	Spatular density (Arzt et al. 2003; Peattie et al. 2004)
5. Self-cleaning (Hansen and Autumn 2005)	Nanoarray (divided contact)	Spatular bulk modulus
6. Anti-self	Small contact area	Particle size, shape, surface energy
7. Nonsticky default state (Autumn and Hansen 2005)	Nontacky spatulae Hydrophobic, vdW spatulae	Spatular size, shape, surface energy

and tissue adhesives (Pain 2000; Menciassi and Dario 2003) are one example. However, any materials chosen for synthetic setae in biomedical applications would need to be nontoxic and nonirritating (Baier et al. 1968). Other applications include MEMS switching (Decuzzi and Srolovitz 2004), wafer alignment (Slocum and Weber 2003), micromanipulation (Pain 2000), and robotics (Autumn et al. 2005a). Since a nanostructure could be applied directly to a surface, it is conceivable that geckolike structures could replace screws, glues, and interlocking tabs in many assembly applications such as automobile dashboards or mobile phones.

Sports applications such as fumble-free football gloves or rock climbing aids (Irving 1955) could be revolutionary. Using gecko technology to climb is not a new idea. In a seventeenth century Indian legend, Shivaji and his Hindu warriors used adhesive lizards from the Deccan region as grappling devices

to scale a shear rock cliff and mount a surprise attack on a Maharashtrian clifftop stronghold (Ghandi 2002).

12.8 Future Directions in the Study of the Gecko Adhesive System

Adhesion in geckos remains a sticky problem that is generating at least as many new questions as answers. Much of the fertility of this area stems from an integration of biology, physics, and engineering. For example, the relationship between friction and adhesion is one of the most fundamental issues in surface science (Ringlein and Robbins 2004; Luan and Robbins 2005). One of the most striking properties (Table 12.2) of the gecko adhesive system is the coupling between adhesion and friction. Without a shear load, setae detach easily. Indeed, without shear loading of opposing toes or legs, a gecko could not hang from the ceiling. Integration of the macroscale system with the as yet undefined relationship between friction and adhesion at the nanoscale could yield important design principles for natural and synthetic setal structures.

Natural surfaces are rarely smooth, and an important next step will be to measure empirically the effect of surface roughness (Vanhooydonck et al. 2005) on friction and adhesion in gecko setae to test the predictions of the new generation of theoretical models for rough surface contacts with micro and nanostructures (Persson and Gorb 2003). Under real-world conditions where surfaces are fractal (Greenwood 1992; Persson and Gorb 2003), compliance is required at each level of the gecko adhesive hierarchy: spatula, seta, lamella, toe, and leg. Models including a spatular array at the tip of a seta have not yet been developed. Similarly, models of lamellar structure will be needed to explain function on roughness above the micron scale.

Biological diversity of setal and spatular structure is high and poorly documented. Basic morphological description will be required. Theory predicts that tip shape affects pulloff force less at smaller sizes (Gao and Yao 2004), so it is possible that part of spatular variation is due to phylogenetic effects, but material constraints such as tensile strength of keratin must be considered as well (Autumn et al. 2002b; Spolenak et al. 2005). The collective behavior of the setal array will be a productive research topic (Gao and Yao 2004). Diversity of the array parameters, density, dimension, and shape is great but not well documented. In particular, the shape of setal arrays on lamellae demands further investigation. Phylogenetic analysis (Harvey and Pagel 1991) of the variation in setal structure and function will be required to tease apart the combined effects of evolutionary history, material constraints, and adaptation (Autumn et al. 2002a).

The molecular structure of setae is not yet known. Setae are made primarily of β-keratin, but a histidine-rich protein or proteins may be present as

well (Alibardi 2003). One possible role of non-keratin proteins is as a glue that holds the keratin fibrils together in the seta (Fig. 12.1D) (Alibardi 2003). This suggests a possible role of genes coding for histidine-rich protein(s) in tuning the material properties of the setal shaft. The outer molecular groups responsible for adhesion at the spatular surface will also be an important topic for future research.

Clearly there is a great desire to engineer a material that functions like a gecko adhesive, yet progress has been limited. A biomimetic approach of attempting to copy gecko setae blindly is unlikely to succeed due to the complexity of the system (Fig. 12.1) and the fact that evolution generally produces satisfactory rather than optimal structures. Instead, development of biologically inspired adhesive nanostructures will require careful identification and choice of design principles (Table 12.2) to yield selected geckolike functional properties. As technology and the science of gecko adhesion advance, it may become possible to tune design parameters to modify functional properties in ways that have not evolved in nature.

It is remarkable that the study of a lizard is contributing to understanding the fundamental processes underlying adhesion and friction (Fakley 2001; Urbakh et al. 2004), and providing biological inspiration for the design of novel adhesives and climbing robots. Indeed, the broad relevance and applications of the study of gecko adhesion underscore the importance of basic, curiosity-based research.

Acknowledgments. I am grateful to many colleagues for their help with this chapter, including: Eduard Arzt, Sanford Autumn, Violeta Autumn, Emerson De Souza, Andrew Dittmore, Ron Fearing, Valeurie Friedman, Bob Full, Bill Geisler, Stas Gorb, Gerrit Huber, Jacob Israelachvili, Carmel Majidi, Anne Peattie, Holger Pfaff, Tony Russell, Andy Smith, and Simon Sponberg. Thanks to Stas Gorb and MPI Stuttgart for the Cryo-SEM image of a single seta. Thanks also to Carmel Majidi and Ron Fearing for Eqs. (12.1), (12.2) and (12.3). Supported by DARPA N66001-03-C-8045, NSF-NIRT 0304730, DCI/NGIA HM1582-05-2022 and Johnson & Johnson Dupuy-Mitek Corp.

References

Alibardi L (2003) Ultrastructural autoradiographic and immunocytochemical analysis of setae formation and keratinization in the digital pads of the gecko *Hemidactylus turcicus* (Gekkonidae, Reptilia). Tissue Cell 35:288–296

Altevogt R (1954) Probleme eines Fußes. Kosmos 50:428–430

Aristotle (350 B.C.E., 1918) *Historia animalium* translated by Thompson, D'A.W. Clarendon Press, Oxford

Arzt E, Enders S, Gorb S (2002) Towards a micromechanical understanding of biological surface devices. Z Metallkd 93:345–351

Arzt E, Gorb S, Spolenak R (2003) From micro to nano contacts in biological attachment devices. Proc Natl Acad Sci USA 100:10603–10606

Autumn K, Hansen W (2005) Ultrahydrophobicity indicates a nonadhesive default state in gecko setae. J Comp Physiol A Sensory Neural Behav Physiol (in press)

Autumn K, Peattie A (2002) Mechanisms of adhesion in geckos. Int Comp Bio 42:1081–1090

Autumn K, Liang YA, Hsieh ST, Zesch W, Chan W–P, Kenny WT, Fearing R, Full RJ (2000) Adhesive force of a single gecko foot-hair. Nature 405:681–685
Autumn K, Ryan MJ, Wake DB (2002a) Integrating historical and mechanistic biology enhances the study of adaptation. Quart Rev Biol 77:383–408
Autumn K, Sitti M, Peattie A, Hansen W, Sponberg S, Liang YA, Kenny T, Fearing R, Israelachvili J, Full RJ (2002b) Evidence for van der Waals adhesion in gecko setae. Proc Natl Acad Sci USA 99:12252–12256
Autumn K, Buehler M, Cutkosky M, Fearing R, Full RJ, Goldman D, Groff R, Provancher W, Rizzi AA, Saranli U et al (2005a) Robotics in scansorial environments. Proc SPIE 5804: 291–302
Autumn K, Hsieh ST, Dudek DM, Chen J, Chitaphan C, Full RJ (2006) Dynamics of geckos running vertically. J Exp Biol 209:260–272
Baier RE, Shafrin EG, Zisman WA (1968) Adhesion: mechanisms that assist or impede it. Science 162:1360–1368
Barthlott W, Neinhuis C (1997) Purity of the sacred lotus, or escape from contamination in biological surfaces. Planta (Heidelberg) 202:1–8
Bauer AM (1998) Morphology of the adhesive tail tips of carphodactyline geckos (Reptilia: Diplodactylidae). J Morphol 235:41–58
Bauer AM, Russell AP, Powell GL (1996) The evolution of locomotor morphology in *Rhoptropus* (Squamata: Gekkonidae): functional and phylogenetic considerations. Afr J Herpetol 45: 8–30
Baum C, Meyer W, Stelzer R, Fleischer L-G, Siebers D (2002) Average nanorough skin surface of the pilot whale (*Globicephala mela*, Delphinidae): considerations on the self-cleaning abilities based on nanoroughness. Marine Biol 140:653–657
Bellairs A (1970) The life of reptiles. Universe Books, New York
Bereiter-Hahn J, Matoltsy AG, Richards KS (1984) Biology of the integument 2: vertebrates. Springer, Berlin Heidelberg New York
Bhushan B (2002) Introduction to tribology. Wiley, New York
Biewener AA, Full RJ (1992) Force platform and kinematic analysis biomechanics: structures and systems a practical approach. IRL at Oxford Univ Press, New York, pp 45–73
Blackwall J (1845) On the means by which walk various animals on the vertical surface of polished bodies. Ann Nat Hist XV:115
Bonser RHC (2000) The Young's modulus of ostrich claw keratin. J Mat Sci Lett 19:1039–1040
Bonser RHC, Purslow PP (1995) The Young's modulus of feather keratin. J Exp Biol 198: 1029–1033
Brainerd EL (1994) Adhesion force of ants on smooth surfaces. Am Zool 34:128A
Braun M (1878) Zur Bedeutung der Cuticularborsten auf den Haftlappen der Geckotiden. Arb Zool Zoot Inst Würzburg 4:231–237
Braun M (1879) Über die Haftorgane an der Unterseite der Zehen bei Anolius. Arb Zool Zoot Inst Würzburg 5:31–36
Campolo D, Jones SD, Fearing RS (2003) Fabrication of gecko foot-hair like nano structures and adhesion to random rough surfaces. IEEE Nano 12–14 Aug 2003, San Francisco
Cartier O (1872a) Studien über den feineren Bau der Haut bei den Reptilien. I. Abt. Epidermis der Geckotiden. Arb Zool Inst Würzburg 1:83–96
Cartier O (1872b) Studien über den feineren Bau der Epidermis bei den Geckotiden. Verh Würzburger Phys Med Ges 1:239–258
Cartier O (1874) Studien über den feineren Bau der Epidermis bei den Reptilien. II. Abtheilung. Über die Wachsthumserscheinungen der Oberhaut von Schlangen und Eidechsen bei der Häutung. Arb Zool Zoot Inst Würzburg 1:239–258
Chen JJ, Peattie AM, Autumn K, Full RJ (2006) Differential leg function in sprawled-posture quadrupedal trotters. J Exp Biol 209:249–259
Chui BW, Kenny TW, Mamin HJ, Terris BD, Rugar D (1998) Independent detection of vertical and lateral forces with a sidewall-implanted dual-axis piezoresistive cantilever. Appl Phys Lett 72:1388–1390

Creton C, Leibler L (1996) How does tack depend on contact time and contact pressure? J Polymer Sci B Polymer Phys 34:545–554
Dahlquist CA (1969) Pressure-sensitive adhesives. In: Patrick RL (ed) Treatise on adhesion and adhesives, vol 2. Dekker, New York, pp 219–260
Decuzzi P, Srolovitz DJ (2004) Scaling laws for opening partially adhered contacts in MEMS. J Microelectromech Syst 13:377–385
Dellit W-D (1934) Zur Anatomie und Physiologie der Geckozehe. Jena Z Naturw 68:613–656
Dewitz H (1882) Wie ist es den Stubenfliegen und vielen anderen Insecten möglich, an senkrechten Glaswänden emporzulaufen? Sitz Ges Naturf Freunde, pp 5–7
Edwards JS, Tarkanian M (1970) The adhesive pads of heteroptera: a re-examination. Proc R Entomol Soc Lond 45:1–5
Emerson SB, Diehl D (1980) Toe pad morphology and mechanisms of sticking in frogs. Biol J Linnaean Soc 13:199–216
Fakley M (2001) Smart adhesives. Chem Ind 691–695
Fraser RDB, Parry DAD (1996) The molecular structure of reptilian keratin. Int J Biol Macromol 19:207–211
Gadow H (1901) The Cambridge natural history, vol 8. Amphibia and Reptiles. McMillan, London
Gao H, Yao H (2004) Shape insensitive optimal adhesion of nanoscale fibrillar structures. Proc Natl Acad Sci USA 101:7851–7856
Gao HJ, Wang X, Yao HM, Gorb S, Arzt E (2005) Mechanics of hierarchical adhesion structures of geckos. Mech Mater 37:275–285
Gay C (2002) Stickiness -some fundamentals of adhesion. Int Comp Bio 42:1123–1126
Gay C, Leibler L (1999) Theory of tackiness. Phys Rev Lett 82:936–939
Geim AK, Dubonos SV, Grigorieva IV, Novoselov KS, Zhukov AA (2003) Microfabricated adhesive mimicking gecko foot-hair. Nature Mat 2:461–463
Geisler B, Dittmore A, Gallery B, Stratton T, Fearing R, Autumn K (2005) Deformation of isolated gecko setal arrays: bending or buckling? 2. Kinetics. Society for Integrative and Comparative Biology, San Diego
Gennaro JGJ (1969) The gecko grip. Natural Hist 78:36–43
Gere JM, Timoshenko SP (1984) Mechanics of materials. Thomson Brooks/Cole, Independence, KY
Ghandi M (2002) The ughly buglies. Swagat. Media Transasia (India), Bangalore, India
Gillett JD, Wigglesworth VB (1932) The climbing organ of an insect, *Rhodnius prolixus* (Hemiptera, Reduviidae). Proc Rsoc Lond Ser B 111:364–376
Glassmaker NJ, Jagota A, Hui CY, Kim J (2004) Design of biomimetic fibrillar interfaces: 1. Making contact. J R Soc Lond Interface 1:1–11
Gorb EV, Gorb SN (2002) Attachment ability of the beetle *Chrysolina fastuosa* on various plant surfaces. Entomol Exp Appl 105:13–28
Green DM (1981) Adhesion and the toe-pads of treefrogs. Copeia 4:790–796
Greenwood JA (1992) Problems with rough surfaces. In: Singer IL, Pollock HM (eds) Fundamentals of friction: macroscopic and microscopic processes. Kluwer, Dordrecht, pp 57–76
Haase A (1900) Untersuchungen über den Bau und die Entwicklung der Haftlappen bei den Geckotiden. Arch Naturgesch 66:321–345
Han D, Zhou K, Bauer AM (2004) Phylogenetic relationships among gekkotan lizards inferred from Cmos nuclear DNA sequences and a new classification of the Gekkota. Biol J Linnaean Soc 83:353–368
Hanna G, Barnes WJP (1991) Adhesion and detatchment of the toe pads of tree frogs. J Exp Biol 155:103–125
Hansen W, Autumn K (2005) Evidence for self-cleaning in gecko setae. Proc Natl Acad Sci USA 102:385–389
Harvey PH, Pagel MD (1991) The comparative method in evolutionary biology. Oxford Univ Press, Oxford

Hecht MK (1952) Natural selection in the lizard genus *Aristelliger*. Evolution 6:112–124
Hepworth J (1854) On the structure of the foot of the fly. Quart J Microscop Sci 2:158–163
Hiller U (1968) Untersuchungen zum Feinbau und zur Funktion der Haftborsten von Reptilien. Z Morph Tiere 62:307–362
Hiller U (1969) Correlation between corona-discharge of polyethylene-films and the adhering power of *Tarentola m. mauritanica* (Rept.). Forma Functio 1:350–352
Hiller U (1971) Form und Funktion der Hautsinnesorgane bei Gekkoniden. Forma Functio 4:240–253
Hiller U (1975) Comparative studies on the functional morphology of two gekkonid lizards. J Bombay Nat Hist Soc 73:278–282
Holloway P (1969) The effects of superficial wax on leaf wettability. Ann Appl Biol 63:145–153
Hora SL (1923) The adhesive apparatus on the toes of certain geckos and tree frogs. J Proc Asiat Soc Beng 9:137–145
Huber G, Gorb S, Spolenak R, Arzt E (2005a) Resolving the nanoscale adjesion of individual gecko spatulae by atomic force microscopy. Biol Lett 1:2–4
Huber G, Mantz H, Spolenak R, Mecke K, Jacobs K, Gorb S, Arzt E (2005b) Evidence for capillarity contributions to gecko adhesion from single spatula nanomechanical measurements. Proc Nat Acad Sci USA 102:16293–16296
Hui CY, Glassmaker NJ, Tang T, Jagota A (2004) Design of biomimetic fibrillar interfaces. 2. Mechanics of enhanced adhesion. J R Soc Lond Interface 1:12–26
Irschick DJ, Austin CC, Petren K, Fisher R, Losos JB, Ellers O (1996) A comparative analysis of clinging ability among pad-bearing lizards. Biol J Linnaean Soc 59:21–35
Irving RLG (1955) A history of British mountaineering. Batsford, London
Israelachvili J (1992) Intermolecular and surface forces. Academic Press, New York
Jagota A, Bennison S (2002) Mechanics of adhesion through a fibrillar microstructure. Int Comp Bio 42:1140–1145
Jeffree C (1986) The cuticle, epicuticular waxes and trichomes of plants, with reference to their structure, functions and evolution. In: Juniper B, Southwood RS (eds) Insects and the plant surface. Arnold Publ, London, pp 23–64
Johnson KL (1985) Contact mechanics. Univ Cambridge Press, Cambridge
Johnson KL, Kendall K, Roberts AD (1973) Surface energy and the contact of elastic solids. Proc R Soc Lond Ser A 324:310–313
Kendall K (1975) Thin-film peeling -the elastic term. J Phys D Appl Phys 8:1449–1452
Kinloch AJ (1987) Adhesion and adhesives: science and technology. Chapman and Hall, New York
Lee YI, Kogan M, Larsen JRJ (1986) Attachment of the potato leafhopper to soybean plant surfaces as affected by morphology of the pretarsus. Entomol Exp Appl 42:101–107
Lees AD, Hardie J (1988) The organs of adhesion in the aphid *Megoura viciae*. J Exp Biol 136:209–228
Little P (1979) Particle capture by natural surfaces. Agricult Aviat 20:129–144
Luan B, Robbins MO (2005) The breakdown of continuum models for mechanical contacts. Nature 435:929–932
Maderson PFA (1964) Keratinized epidermal derivatives as an aid to climbing in gekkonid lizards. Nature 203:780–781
Mahendra BC (1941) Contributions to the bionomics, anatomy, reproduction and development of the Indian house gecko *Hemidactylus flaviviridis* Ruppell, part II. The problem of locomotion. Proc Indian Acad Sci Sec B 13:288–306
McMahon TA, Bonner JT (1983) On size and life. Scientific American Library, New York
Menciassi A, Dario P (2003) Bio-inspired solutions for locomotion in the gastrointestinal tract: background and perspectives. Philos Trans R Soc Lond Ser A Math Phys Eng Sci 361: 2287–2298
Northen MT, Turner KL (2005) A batch of fabricated dry adhesive. Nanotechnology 16: 1159–1166
Pain S (2000) Sticking power. New Scientist 168:62–67

Peattie AM, Fearing RS, Full RJ (2004) Using a simple beam model to predict morphological variation in adhesive gecko hairs. Society for Integrative and comparative Biology, New Orleans
Peressadko A, Gorb SN (2004) When less is more: experimental evidence for tenacity enhancement by division of contact area. J Adhesion 80:247–261
Persson BNJ (2003) On the mechanism of adhesion in biological systems. J Chem Phys 118:7614–7621
Persson BNJ, Gorb S (2003) The effect of surface roughness on the adhesion of elastic plates with application to biological systems. J Chem Phys 119:11437
Peterson JA, Williams EE (1981) A case study in retrograde evolution: the *onca* lineage in anoline lizards. II. Subdigital fine structure. Bull Museum Comp Zool 149:215–268
Pianka ER, Sweet SS (2005) Integrative biology of sticky feet in geckos. BioEssays 6:647–652
Pocius AV (2002) Adhesion and adhesives technology: an introduction, 2nd edn. Hanser, Munich
Ringlein J, Robbins MO (2004) Understanding and illustrating the atomic origins of friction. Am J Phys 72:884–891
Roll B (1995) Epidermal fine structure of the toe tips of *Sphaerodactylus cinereus*. J Zool 235:289–300
Rosenberg HI, Rose R (1999) Volar adhesive pads of the feathertail glider, *Acrobates pygmaeus* (Marsupialia; Acrobatidae). Can J Zool 77:233–248
Ruibal R, Ernst V (1965) The structure of the digital setae of lizards. J Morphol 117:271–294
Russell AP (1975) A contribution to the functional morphology of the foot of the tokay, *Gekko gecko* (Reptilia, Gekkonidae). J Zool Lond 176:437–476
Russell AP (1976) Some comments concerning the interrelationships amongst gekkonine geckos. In: Bellairs AA, Cox CB (eds) Morphology and biology of reptiles. Academic Press, London, pp 217–244
Russell AP (1979) Parallelism and integrated design in the foot structure of gekkonine and diplodactyline geckos. Copeia 1979:1–21
Russell AP (1981) Descriptive and functional anatomy of the digital vascular system of the tokay, *Gekko gecko*. J Morphol 169:293–323
Russell AP (1986) The morphological basis of weight-bearing in the scansors of the tokay gecko (Reptilia: Sauria). Can J Zool 64:948–955
Russell AP (2002) Integrative functional morphology of the gekkotan adhesive system (Reptilia: Gekkota). Integrative Comp Biol 42:1154–1163
Russell AP, Bauer AM (1988) Paraphalangeal of gekkonid lizards: a comparative survey. J Morphol 197:221–240
Russell AP, Bauer AM (1990a) *Oedura* and *Afroedura* (Reptilia: Gekkonidae) revisited: similarities of digital design, and constraints on the development of multiscansorial subdigital pads? Memoirs Queensland Museum 29:473–486
Russell AP, Bauer AM (1990b) Digit I in pad-bearing gekkonine geckos: alternate designs and the potential constraints of phalangeal number. Memoirs Queensland Museum 29:453–472
Russell AP, Rosenberg HI (1981) Self-grooming in *Diplodactylus spinigerus* (Reptilia: Gekkonidae) with a brief review of such behaviour in reptiles. Can J Zool 59:564–566
Scherge M, Gorb SN (2001) Biological micro- and nanotribology: nature's solutions. Springer, Berlin Heidelberg New York
Schleich HH, Kästle W (1986) Ultrastrukturen an Gecko-Zehen (Reptilia: Sauria: Gekkonidae). Amphibia-Reptilia 7:141–166
Schmidt HR (1904) Zur Anatomie und Physiologie der Geckopfote. Jena Z Naturw 39:551
Simmermacher G (1884) Haftapparate bei Wirbeltieren. Zool Garten 25:289–301
Sitti M, Fearing RS (2003) Synthetic gecko foot-hair micro/nano structures as dry adhesives. J Adhesion Sci Technol 17:1055–1073
Slocum AH, Weber AC (2003) Precision passive mechanical alignment of wafers. J Microelectromech Syst 12:826–834
Spolenak R, Gorb S, Gao HJ, Arzt E (2004) Effects of contact shape on the scaling of biological attachments. Proc R Soc Lond Ser A Math Phys Eng Sci 461:305–319

Spolenak R, Gorb S, Arzt E (2005) Adhesion design maps for bio-inspired attachment systems. Acta Biomaterialia 1, 5–13
Stork NE (1980) Experimental analysis of adhesion of *Chrysolina polita* (Chrysomelidae: Coleoptera) on a variety of surfaces. J Exp Biol 88:91–107
Stork NE (1983) A comparison of the adhesive setae on the feet of lizards and arthropods. J Nat Hist 17:829–835
Sun W, Neuzil P, Kustandi TS, Oh S, Samper VD (2005) The nature of the gecko lizard adhesive force. Biophys J 89:L14–L17
Urbakh M, Klafter J, Gourdon D, Israelachvili J (2004) The nonlinear nature of friction. Nature 430:525–528
Vanhooydonck B, Andronescu A, Herrel A, Irschick DJ (2005) Effects of substrate structure on speed and acceleration capacity in climbing geckos. Biol J Linnean Soc 85:385–393
Vinson J, Vinson J-M (1969) The saurian fauna of the Mascarene islands. Bull Maurit Inst 6: 203–320
Vitt LJ, Zani PA (1997) Ecology of the nocturnal lizard Thecadactylus rapicauda (Sauria: Gekkonidae) in the Amazon region. Herpetologica 53:165–179
Von Wittich (1854) Der Mechanismus der Haftzehen von *Hyla arborea*. Arch Anat Physiol Med 170–183
Wagler J (1830) Natürliches System der Amphibien. Cotta'sche Buchhandlung, Munich
Wainwright SA, Biggs WD, Currey JD, Gosline JM (1982) Mechanical design in organisms. Princeton Univ Press, Princeton
Weitlaner F (1902) Eine Untersuchung über den Haftfuß des Gecko. Verh Zool Bot Ges Wien 52:328–332
Williams EE, Peterson JA (1982) Convergent and alternative designs in the digital adhesive pads of scincid lizards. Science 215:1509–1511

13 Biomimetic Adhesive Polymers Based on Mussel Adhesive Proteins

Bruce P. Lee, Jeffrey L. Dalsin, and Phillip B. Messersmith

13.1 Introduction

Nature provides many outstanding examples of adhesive strategies from which chemists and material scientists can draw inspiration in their pursuit of new adhesive materials. As described in other chapters of this book, detailed studies of the adhesive mechanisms of geckos, mussels and other organisms during the past several decades have enhanced our understanding of the underlying physicochemical principles to the extent that direct translation of this knowledge into biomimetic strategies for synthesizing new practical adhesives is now possible. Although new biomimetic adhesives have the potential for impact in many areas of technology, one of the more compelling outlets for these materials is in healthcare delivery, which will be the focus of this chapter. Obvious parallels exist between the marine and human physiologic environment, and a strategy that works well in one context may be useful in the other.

Efforts to develop biomimetic adhesives are most effective when guided by detailed understanding of the key features and mechanisms of natural adhesives. A simple example of this is given by recent mimicry of gecko adhesive in photolithographically micropatterned polymers (Geim et al. 2003), an approach made possible by earlier studies elaborating the fine morphological detail and adhesive force of individual gecko foot setae (Autumn et al. 2000). In the case of secreted adhesives such as those employed by marine organisms, biomimetic efforts are only possible when there is basic understanding of the key macromolecular components and their compositions. In the case of barnacle adhesives only limited information is known about the adhesive mechanism and component proteins (Naldrett and Kaplan 1997; Kamino et al. 2000; Kamino 2001), providing little guidance to biomimetic efforts. Such is not the case with mussel adhesive proteins (MAPs), which have been extensively studied and the subject of numerous biomimetic efforts. We begin with a brief review of the unique chemical features of MAPs, a subject that is discussed in greater detail in a recent review (Waite et al. 2005) and in Chap. 7 of the present volume. Several

Department of Biomedical Engineering, Northwestern University, 2145 N Sheridan Road, Evanston, IL 60208, USA

Biological Adhesives
(ed. by A.M. Smith and J.A. Callow)

approaches to MAP biomimetics are being pursued in labs throughout the world, including extraction of native proteins, expression of genetically engineered MAPs, and chemical synthesis of MAP mimetic polymers. The emphasis of this review will be on synthetic polymer approaches that attempt to capture some of the remarkable adhesive properties of natural MAPs, as these strategies are currently the most promising. Finally, we describe the use of MAP mimetic polymers for fouling prevention, which is a rapidly emerging use for these polymers.

13.2 Mussel Adhesive Proteins and DOPA

The attachment apparatus of mussels is called the byssus, which is a bundle of threads extending from within the shell of the mussel, each of which terminates in an adhesive plaque attached to a substrate (Fig. 13.1) (Waite 1991, 1999). An entire byssal thread and adhesive plaque is formed by secretion of liquid protein from within glands of the mussel foot in a process that resembles polymer injection molding. Solidification of the liquid occurs rapidly to provide a stable attachment, and the process is sequentially repeated many times to deposit each byssal thread and plaque. The proteins of the byssal threads resemble collagen and elastin and will not be further discussed (Waite 1991). The adhesive plaque located at the distal end of each thread will be emphasized here, because this is where adhesion to the substrate is enforced. At least five *Mytilus edulis* foot proteins (Mefps) have been identified (Rzepecki et al. 1992; Waite 1999), and they all share a common distinguishing feature: the presence of 3,4-dihydroxyphenylalanine (DOPA), a residue formed by post-transitional hydroxylation of tyrosine. It is the 3,4-dihydroxyphenyl (catechol) side chain that gives DOPA its unique properties related to adhesion.

The DOPA content of Mefps range from a few percent to well above 20% (Waite et al. 2005). Mefp-3 and Mefp-5 are of special interest because of their high DOPA contents and presence closest to the plaque/substrate interface (Fig. 13.1). Mefp-3 and Mefp-5 have the highest DOPA contents of the foot proteins at 20 and 27 mol%, respectively, and also contain a large number of basic residues (arginine in Mefp-3 and lysine in Mefp-5) (Papov et al. 1995; Waite and Qin 2001). Mefp-3 and Mefp-5 are predominately found near the interface between the adhesive plaque and substratum (Warner and Waite 1999; Waite and Qin 2001), and may function as mediators of adhesion at the interface between the plaque and the foreign surface. Mefp-5 contains phosphoserine residues in a sequence reminiscent of acidic mineral-binding motifs that appear in statherin and osteopontin (Waite and Qin 2001). Little is known about the role of phosphoserine residues, although it is interesting to note that phosphoserines are known to bind to calcareous mineral surfaces, which are common substrates of mussels in the marine environment (Long et al. 1998; Meisel and Olieman 1998).

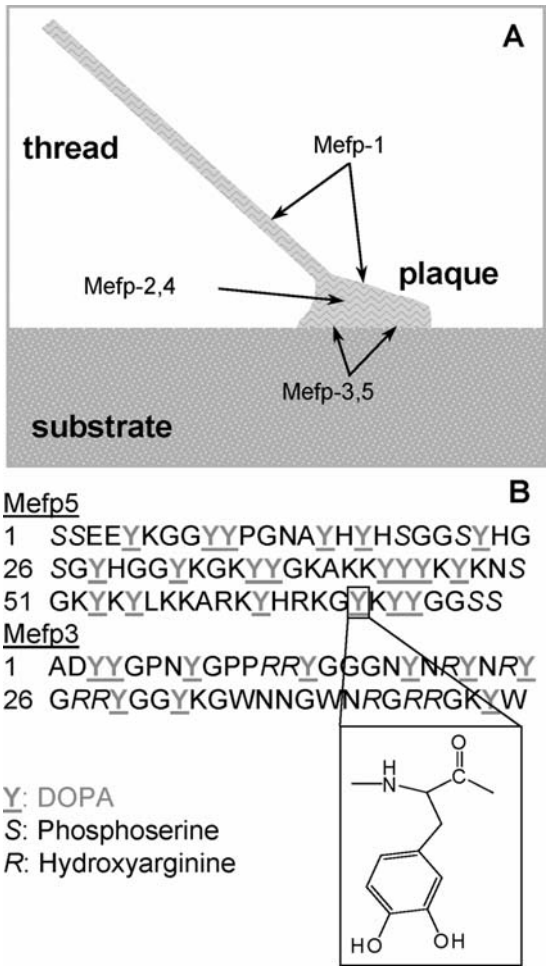

Fig. 13.1. (a) Schematic illustration of a byssal thread and adhesive plaque. (b) The sequences of the interfacial proteins Mefp-3 and Mefp-5 are shown along with the chemical structure of DOPA (B)

The DOPA residues found in these proteins are widely believed to fulfill two important roles: cohesion and adhesion. Cohesion, as we use the term here, refers to the bulk elastic properties of the adhesive, whereas adhesion refers very specifically to those physicochemical interactions occurring at the interface between adhesive pad and substrate. Both cohesive and adhesive properties of MAPs are important in achieving the final outcome of secure, water-resistant attachment to surfaces.

The role of DOPA is best understood as it relates to solidification of the secreted adhesive liquid, a process that derives from protein crosslinking

reactions giving rise to a highly crosslinked bulk protein matrix. There is general acceptance that the intermolecular crosslinking reactions are related to oxidation of DOPA to DOPA-quinone (Waite 1991; Yu et al. 1999), which can occur spontaneously at alkaline pH, which may be enzymatically catalyzed (Waite 1990; Kramer et al. 1991; Andersen et al. 1992) or which may form as a result of redox reactions involving transition metal ions such as Fe(III). Once formed, DOPA-quinone is capable of participating in a number of different reaction pathways leading to intermolecular cross-link formation (Rzepecki et al. 1995; Sugumaran 1998; Waite 1990, 1999). Several reaction pathways have been suggested (Waite 1990), including aryloxy coupling of DOPA phenyl rings, which can occur when diphenolic groups undergo one-electron oxidations (McDowell et al. 1999; Burzio and Waite 2000), and aryl-alkylamine addition based on Schiff base substitution and Michael-type addition (Waite 1990).

When it comes to interfacial adhesion, unfortunately the role of DOPA is far less understood. Until more information emerges regarding the molecular aspects of DOPA adhesion, we can only speculate as to some of the potential chemical interactions that may contribute to adhesion between DOPA-containing proteins and inorganic and organic surfaces. For example, DOPA residues may interact with organic surfaces through π electron interactions (Waite 1987, 1999). Such interactions may contribute to the cohesiveness of DOPA-containing materials and aid in the adsorption of MAPs to surfaces rich in aromatic compounds such as polystyrene (Baty et al. 1997). Catechol groups are also capable of being both hydrogen bond donor and acceptor, which may allow DOPA to compete well with water for H-bonding sites on hydrophilic and polar surfaces (Waite 1987, 1999). DOPA-containing compounds have been found to have mucoadhesive properties (Schnurrer and Lehr 1996; Deacon et al. 1998; Huang et al. 2002). It has been suggested that the H-bond ability of DOPA is one of the reasons that allows DOPA to interact with mucosal surfaces since this is one of the necessary properties of mucoadhesive polymers (Schnurrer and Lehr 1996). Similarly, H-bonding may be responsible for catechols' ability to adsorb exceptionally well to hydroxyapatite (Chirdon et al. 2003).

Mussels are known to accumulate metal ions in their byssal threads at a concentration significantly higher than that of the surrounding sea water (Coombs and Keller 1981; Szefer et al. 1997). Accumulation of these ions at such a high level is believed to be due to the presence of DOPA in the byssus (Swann et al. 1998). Catechols are capable of forming strong complexes with metal ions and these complexes are very stable, with log stability constants greater than 40 (at 20 °C, pH 10, log stability constant=47 and 45 for Al^{3+} and Fe^{3+}, respectively) (Waite 1987). Taylor et al. (1994, 1996) have shown that synthetic MAP mimetic peptides form bis- and tris-catecholate complexes with Fe^{3+} depending on the ratio of DOPA to ferric ion. Recent experiments from Wilker and coworkers suggest a possible role for DOPA-Fe^{3+} interactions during curing of MAPs (Sever et al. 2004). The affinity of catechols for metals

is not limited to soluble metal ions but is also extended to metal oxide surfaces (Kummert and Stumm 1980; Soriaga and Hubbard 1982; Hansen et al. 1995), and such complexes are likely to contribute to bonding between adhesive plaques and inorganic surfaces.

Finally, it is also conceivable that oxidized DOPA species may react with functional groups presented at organic surfaces. For example, amine, sulfhydryl, and other functionalities on surfaces may react as described above with DOPA-quinone to give rise to covalent bond formation between proteins of the adhesive plaque and a substrate surface.

13.3 Medical Adhesives: Requirements and Existing Materials

There is an ongoing need for new tissue adhesive materials for use in wound healing of both soft and hard tissues, as well as for adhesion of medical and dental implants to tissues. An ideal tissue adhesive should have the following properties (Sierra and Saltz 1996; Ikada 1997). In the liquid state the adhesive should have sufficient flow characteristics so that it can be easily applied to the tissue surface, and it should be able to displace water from the boundary layer to maximize interfacial interactions. The adhesive must be able to transform from the liquid state into the solid state under mild physiological conditions, and this physical change should be rapid so as to minimize surgery time. After curing, the bioadhesive needs to maintain strong adhesion to the appropriate tissue type (soft or hard) for a length of time that depends on the type of medical procedure, and must possess the bulk mechanical strength necessary to withstand mechanical forces present during the healing phase. Finally, the adhesive should be easily sterilized without affecting its properties, and have an adequate biological safety profile that includes low toxicity/immunogenicity.

Several synthetic and natural medical adhesives are currently used in a number of medical specialties. These include mainly fibrin, cyanoacrylate and gelatin-resorcinol-formaldehyde (GRF) glues, which will be briefly described here. Fibrin glue is an example of a biologically derived tissue adhesive that has been used for many years (Yang and Medawar 1940). Fibrin glue mimics the final stages of the blood coagulation cascade wherein fibrinogen is converted through the action of thrombin into fibrin, which self-assembles into a hydrogel that resembles a blood clot. Although fibrin glue rapidly cures, is highly adherent to tissues and is generally biocompatible, there is a major concern of blood-borne disease transmission from human-derived clot precursors, particularly hepatitis and HIV (Saltz et al. 1991). The cohesive strength of this material is very weak (Table 13.1), and as a result it is not generally used for wound closure (Weber and Chapman 1984). Fibrin glue is more widely used as a tissue sealant for hemostasis, an application for which it is much more suitable.

Table 13.1. Adhesive strengths of commercially available tissue adhesives

Tissue adhesive	Adhesive strength (Pa)	References
Fibrin glue	10^3–10^4	Siedentop et al. (1988); Albes et al. (1993); Chiversand Wolowacz (1997)
Cyanoacrylate	10^4–10^6	Khowassah and Shippy (1971); Albes et al. (1993); Chivers and Wolowacz (1997)
GRF	10^4–10^5	Albes et al. (1993); Chivers and Wolowacz (1997); Nomori and Horio (1997)

Cyanoacrylate adhesives have been shown to achieve quite high bond strengths and have been used in a wide range of in vivo applications including vascular repair (Brothers et al. 1989; Celik et al. 1991; Toriumi et al. 1991), retinal repair (Gilbert et al. 1989; Hartnett and Hirose 1998), and hemostasis (Goldin 1976; Kakio et al. 1993). The major concern with cyanoacrylates is that they release formaldehyde upon degradation (Refojo et al. 1971). Although the rate of formaldehyde release can be reduced through manipulation of the composition of the side chains, formaldehyde is histotoxic and can cause acute and chronic inflammation (Tseng et al. 1990; Toriumi et al. 1991).

Crosslinked gelatin has been in use as a tissue adhesive for many years (Tatooles and Braunwald 1966). The phenolic compound resorcinol was introduced into the mixture to improve the tissue bonding strength and formaldehyde was added as the cross-linking agent to create the tissue adhesive known as the gelatin-resorcinol-formaldehyde (GRF) glue (Cooper and Falb 1968). GRF glues exhibit higher bond strengths than fibrin glues, but are not as strong as cyanoacrylates (Table 13.1). Although GRF glues have been used clinically in Europe, the use of formaldehyde remains a major concern (Ikada 1997). Even if all the formaldehyde in the glue is consumed during the reaction to cross-link gelatin and resorcinol, formaldehyde can still be released during degradation of the glue. Less toxic aldehydes such as glutaraldehydes and glyoxal are being studied as replacements to formaldehyde (Ennker et al. 1994).

13.4 MAP-Mimetic Adhesive Polymers

It has long been a goal of many scientists to develop useful synthetic polymer adhesives that exhibit the wet adhesive capabilities of MAPs. The appeal of using mimics of MAPs as medical adhesives is especially understandable

when considering that mussel glues possess several key properties desired in a tissue adhesive: 1) the ability to solidify rapidly in an aqueous environment; 2) high adhesive and cohesive strength; and 3) versatile ability to adhere to both inorganic and organic surfaces. Several approaches have been taken toward the development of DOPA-containing polymers, which include extraction of natural MAPs, use of recombinant DNA technologies to express adhesive proteins, chemical synthesis of DOPA-containing peptides, and conjugation of DOPA to synthetic polymers. In this section we review progress in these various approaches, with particular emphasis on synthetic polymer mimics of MAPs and their possible clinical uses.

13.4.1 Extraction and Expression of MAPs

The purification and chemical analysis of MAPs was first reported by Waite and Andersen (Waite and Andersen 1978). Since then, numerous adhesive proteins from M. edulis as well as other species of mussels have been reported (Pardo et al. 1990; Papov et al. 1995; Waite and Qin 2001). The ultimate utility of isolation and purification of MAPs for commercial use remains debatable, however, as large numbers of mussels are needed for even a modest amount of purified protein (Burzio et al. 1997). A possible exception has been reported in the case of *Aulacomya ater*, where yield of purified adhesive protein can be 15–20 times more than other marine mussel species (Characklis 1990). In vitro cell culture and in vivo transplantation experiments showed that purified MAPs appeared to be non-toxic and well tolerated by biological systems (Olivieri et al. 1990; Pitman et al. 1989); however biological response to these proteins at the cell, tissue and systemic levels needs to be further investigated.

Although purified MAPs have been suggested for use in a variety of medical contexts, there exist only a handful of literature reports with sufficient experimental detail to allow adequate analysis and interpretation of the results (Grande and Pitman 1988; Green et al. 1987; Schnurrer and Lehr 1996; Ninan et al. 2003). Early studies focused on the use of MAPs for facilitating cell adhesion to substrate or tissue surfaces (Green et al. 1987; Grande and Pitman 1988). Mucoadhesive properties of MAPs have been explored in thin film (Schnurrer and Lehr 1996) and soluble form (Deacon et al. 1998). MAPs were highly mucoadhesive in both forms, suggesting possible future use of MAP-mimetic polymers for adhesion and drug delivery to the mucosal surfaces of the eye, gastrointestinal tract and reproductive tract.

More recently, purified MAPs have been investigated as potential tissue adhesives (Ninan et al. 2003). A highly concentrated paste of MAPs was applied to pig skin tissue surfaces and the bond strength determined mechanically. The results of this study suggest potential use as an adhesive, although the curing time of the MAP glue was too slow for possible clinical use and under most conditions the adhesive strength of MAP bonded tissue was

similar to or lower than fibrin glue. It is possible that chemical or enzymatic crosslinking reagents could improve the performance of the MAP glue.

Microbial production of marine adhesive proteins has been investigated using recombinant DNA technology. cDNA encoding of the adhesive proteins from different species of mussels has been carried out and microbial hosts such as *E. coli*, *S. cerevisiae*, and *B. subtilis* have been used to express the desired sequences (Maugh et al. 1988; Strausberg et al. 1989; Filpula et al. 1990; Hwang et al. 2004, 2005). Initially, the purified proteins lack the desired water-resistant adhesion and cohesive strength due to the absence of DOPA functionality as this is a post-translational modification (Strausberg et al. 1989). Monophenol catecholase such as tyrosinase was used to transform tyrosine residues into DOPA, and a conversion of up to 70% of tyrosine residues was reported (Marumo and Waite 1986; Yamamoto 1995). Successful adhesion to various substrates including polystyrene, glass, hydrogel, and collagen using recombinant adhesive proteins has been reported (Strausberg and Link 1990).

13.4.2 Chemical Synthesis of MAP Mimetic-Polymers

Chemical synthesis of peptide analogues of MAP has been extensively investigated by Yamamoto and colleagues (Yamamoto 1987; Yamamoto et al. 1995; Tatehata et al. 2000), who utilized solution methods to synthesize consensus repeat sequences of MAPS that were then chemically coupled to yield MAP-like polypeptides (**I**, Fig. 13.2). The adhesive strength to iron, alumina, glass, nylon, polyethylene, Teflon and pig skin was measured mechanically (Yamamoto 1987; Tatehata et al. 2000), or work of adhesion measured by wettability (contact angle) experiments (Yamamoto et al. 1995). Although these MAP mimetic polypeptides were generally found to be adhesive, the contribution of DOPA to adhesion was not entirely clear from these studies, as similar adhesive values were obtained for DOPA-free polypeptides (Yamamoto 1987; Yamamoto et al. 1995). In one notable case, however, in-vitro tissue adhesion to pig skin was clearly enhanced in polypeptides containing tyrosine, which was converted to DOPA and presumably further oxidized during curing of the adhesive (Tatehata et al. 2000). An in-vivo pig skin tissue adhesion study was also performed using these polypeptides, however no mechanical performance data was reported (Tatehata et al. 2001).

Deming and coworkers have synthesized MAP mimetic polypeptides (**II**, Fig. 13.2) by polymerization of *N*-carboxyanhydride monomers of lysine and DOPA and tested adhesion to steel, aluminum, glass and several synthetic polymer surfaces (Yu and Deming 1998; Yu et al. 1999). Copolypeptides containing 10 mol% DOPA were crosslinked via oxidation and adhered approximately ten times stronger to aluminum than a polylysine control polymer. Although suggestive of an adhesive role for DOPA, the results are difficult to interpret in view of the potential effects of DOPA crosslinking on

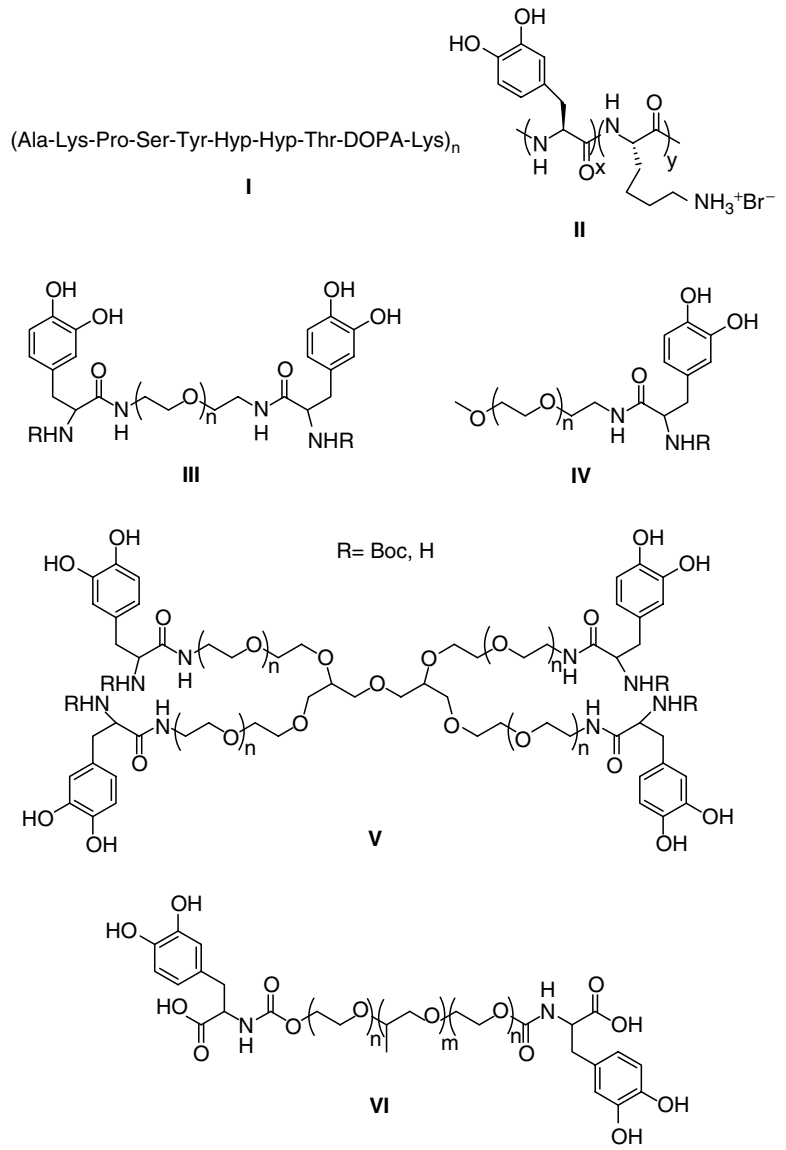

Fig. 13.2. Chemical structures of MAP mimetic polymers developed as gel-forming adhesives

cohesive strength of the polymer adhesive. A subsequent study of metal substrate adhesion by the same group using model peptide compounds and similar polypeptides further defined the role of non-oxidized DOPA as adhesive, and that of oxidized DOPA species as contributing primarily to cohesion (Yu et al. 1999).

In addition to purified MAPs and the expressed or chemically synthesized MAP mimetic polypeptides described above, functionalization of synthetic polymers with DOPA or DOPA-containing short peptides has emerged as a promising strategy for development of new biomimetic adhesives. Several examples of this approach can be found in the work of Lee et al. (2002), who chemically coupled single DOPA amino acid residues to poly(ethylene glycol) (PEG) polymers for synthesis of MAP mimetic hydrogels. The use of PEG as a platform for MAP mimetic polymers destined for clinical use is appealing due to its non-toxic and low-immunogenic nature (Harris 1992; Zalipsky and Harris 1997). Linear mono- and di-functionalized DOPA-PEGs were synthesized along with a four-arm branched PEG polymer with DOPA coupled to the end of each arm (**III**, **IV**, **V**, Fig. 13.2). Addition of oxidizing reagents (sodium periodate, horseradish peroxidase, and mushroom tyrosinase) to aqueous solutions of IV followed by molecular weight characterization revealed the formation of oligomers of methoxy-PEG-DOPA, presumably resulting from oxidative polymerization of DOPA endgroups.

Under similar conditions, III and V yielded rigid hydrogels within seconds to hours depending on polymer architecture, the type and concentration of oxidizing reagent, and the presence or absence of protecting group (R) on the N-terminus of DOPA. Based on spectroscopic observations, oxidation of the catechol side chain of DOPA resulted in the formation of highly reactive DOPA-quinone, which further reacted to form crosslinked products via one of several pathways, depending on the presence or absence of N-terminal protecting groups on the polymer. N-Boc protected III and V cross-linked via phenol coupling and quinone methide tanning pathways, whereas the same polymers containing a free amino group crosslinked via a pathway that resembled melanogenesis. Adhesive properties of the crosslinked gels were not reported, although an unpublished follow-up study utilizing polymer V and thermally triggered liposomal release of periodate (Burke and Messersmith) demonstrated that the tissue adhesive potential of PEG-DOPA hydrogels exceeds that of fibrin glue (Fig. 13.3).

The majority of MAP mimetic polymers described above rely on the use of oxidizing reagents to oxidize tyrosine and/or DOPA residues so as to take advantage of the ensuing crosslinking reactions for rapid solidification of the liquid or semi-solid polymer precursor. However, for in vivo medical applications there are potential concerns over the use of strong oxidizing reagents for curing of MAP mimetic polymers. As a result, new approaches to MAP mimetic polymer hydrogel formation that eliminate the need for DOPA oxidation are being developed (Huang et al. 2002; Lee et al. 2004).

The first oxidation-free approach to polymer gel formation took advantage of thermally triggered self-assembly of DOPA-containing block copolymers to induce a sol-gel transition between ambient and body temperature (Huang et al. 2002). Similarly to polymers III–V described above, this approach utilized endgroup functionalization of poly(ethylene oxide)-

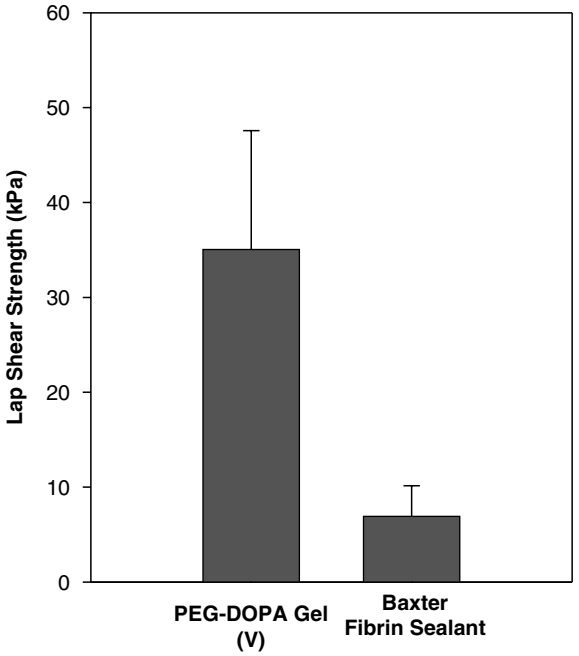

Fig. 13.3. Lap shear strength of adhesion to porcine skin for gel formed by polymer V and fibrin glue (Burke and Messersmith, unpublished data)

poly(propylene oxide)-poly(ethylene oxide) (PEO-PPO-PEO) block copolymers with DOPA residues (**VI**, Fig. 13.2). Aqueous solutions of PEO-PPO-PEO block copolymers exhibit interesting temperature-induced aggregation phenomena as a result of the hydrophobic nature of the PPO block (Alexandridis 1997). At low temperature and concentration, PEO-PPO-PEO block copolymers exist in solution as dissolved monomers, but self-assemble at higher concentrations and temperatures into block copolymer micelles that form under conditions defined by the critical micelle concentration (CMC, at constant temperature) and the critical micelle temperature (CMT, at constant concentration). Highly concentrated solutions of certain PEO-PPO-PEO block copolymers, such as Pluronic F127 ($PEO_{100}PPO_{65}PEO_{100}$) and F68 ($PEO_{78}PPO_{30}PEO_{78}$), exhibit sol-gel transitions when heated from ambient to body temperature. This physical behavior provides a basis for future use of these polymers for inducing gel formation in medical applications.

To create DOPA-modified block copolymers, hydroxyl endgroups of PEO-PPO-PEO block copolymers were activated by *N,N′*-disuccinimidyl carbonate and then reacted with DOPA or its methyl ester (Huang et al. 2002). DOPA-modified PEO-PPO-PEO block copolymers were freely soluble in cold water, and dye partitioning and differential scanning calorimetry analysis of these

solutions revealed that the copolymers aggregated into micelles at a characteristic temperature that was dependent on block copolymer composition and concentration in solution. Oscillatory rheometry demonstrated that above a block copolymer concentration of approximately 20 wt%, solutions of DOPA-modified PEO-PPO-PEO block copolymers exhibited sol-gel transitions upon heating. The gelation temperature could be tailored between ~23 and 46 °C by changing the composition, concentration and molecular weight of the block copolymer. Finally, rheological measurement of the bioadhesive interaction between polymer VI and bovine submaxillary mucin indicated that DOPA-modified Pluronic was significantly more bioadhesive than unmodified Pluronic. It was suggested that such polymers may be useful for drug delivery to mucosal tissue surfaces.

A second approach to oxidation-free crosslinking of MAP mimetic polymers into hydrogels relies on photopolymerization of a DOPA-containing monomer (Lee et al. 2004). The new monomers VII and VIII (Fig. 13.4) combine DOPA and a polymerizable methacrylate group with or without an oligomeric ethylene oxide linker, respectively. VII and VIII were copolymerized with poly(ethylene glycol) diacrylate (PEG-DA) using either ultraviolet (UV) or visible light, and the effect of DOPA-containing monomers on gelation time, gel conversion, and elastic modulus of the photocured hydrogels was investigated. While the presence of DOPA-containing monomers did not prevent polymerization, longer irradiation time was needed to achieve gelation when monomers VII and VIII were present in the precursor solution. Gel conversion, extent of DOPA incorporation, and elastic modulus also decreased with increasing DOPA concentration, suggesting a retarding effect on free radical polymerization. Despite this effect, DOPA was successfully incorporated into hydrogels with elastic moduli (ca. 50 kPa) suitable for many biomedical applications. The mechanical properties of the photopolymerized hydrogels are currently under evaluation. The incorporation of DOPA into hydrogels by photopolymerization may lead to new adhesive hydrogels for medical applications.

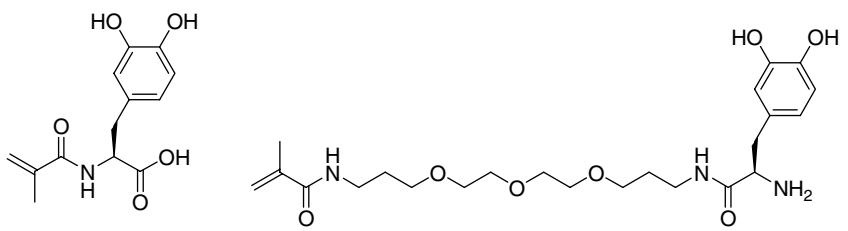

Fig. 13.4. Chemical structures of photopolymerizable DOPA-containing monomers

13.5 Antifouling MAP Mimetic Polymers

In this final section we elaborate on very recent developments regarding antifouling applications for MAP mimetic polymers. Control of initial nonspecific adsorption of proteins at biointerfaces is fundamental to studying the biological response to materials and is important in dictating clinical outcomes of implanted devices. In some applications it is important to limit nonspecific fouling of device surfaces, as this can affect performance and lead to adverse biological responses. Cell and bacterial colonization of surfaces is generally mediated by adsorbed proteins, thus surfaces which most effectively limit protein adsorption are less likely to support cell and bacterial adhesion.

A common method to reduce nonspecific cell and protein fouling is through the immobilization of antifouling polymers on biomaterials surfaces (Nath et al. 2004; Dalsin and Messersmith 2005). In the absence of active release of antifouling agents from the surface, experimental observations from many laboratories make an overwhelming case for the dependence of protein resistance on antifouling polymer surface density (Malmsten et al. 1998; Sofia et al. 1998; Kenausis et al. 2000; Pasche et al. 2003; Dalsin et al. 2005), with high polymer surface density providing better fouling resistance than low density coatings. Thus, the general goal in designing antifouling polymer strategies is to achieve a high density of stably immobilized antifouling polymer on the substrate of interest (Nath et al. 2004). This can be achieved through manipulation of such parameters as polymer design (chain length, anchoring chemistry, and antifouling polymer composition) and processing.

The idea of utilizing MAP-mimetic polymers for reducing or preventing fouling of surfaces is somewhat counterintuitive, since the presence of DOPA in these polymers should make them adhesive toward biological components. Indeed (Dossot et al. 2000), a commercial extract of mussel adhesive proteins (Cell-Tak™, Becton-Dickinson) is used to encourage cell adhesion on tissue culture labware (Arnoult et al. 1996). Yet, the pairing of an antifouling polymer with mimics of MAPs has revealed exciting new opportunities for control of protein, cell and bacterial fouling of surfaces by exploiting DOPA peptides as anchors for immobilization of polymers onto surfaces. Catechols are well known for their affinity to oxide and hydroxide surfaces (Connor et al. 1995; Chen et al. 2002; Chirdon et al. 2003), and several reports of catechols being used for anchoring small organic molecules and DNA onto oxide surfaces exist in the literature (Rice et al. 2000; Rajh et al. 2002; Xu et al. 2004).

The design and use of MAP mimetic polymers for this purpose is conceptually simple: one end of an antifouling polymer is conjugated to a DOPA residue or short peptide (Fig. 13.5), and the antifouling polymer is immobilized onto the substrate surface via the adhesive endgroup. A typical example

of this strategy consists of simple constructs of linear PEGs end-functionalized with one to three DOPA residues or an analogue of the consensus decapeptide repeat sequence of Mefp1 (IX and X, Fig. 13.5) (Dalsin et al. 2003). Polymers IX and X adsorbed to metal surfaces from solution, and the chemical composition of treated and untreated surfaces was assessed with X-ray photoelectron spectroscopy (XPS) and time-of-flight secondary ion mass spectrometry (TOF-SIMS). For Au surfaces treated with IX, the C1s XPS spectrum showed dramatic increases in the ether carbon component (286.0 eV) characteristic of PEG, while spectra from surfaces treated with mPEG-OH under identical conditions showed no difference from unmodified Au. Positive ion TOF-SIMS analysis indicated substantial increases in the ion fragments $C_2H_3O^+$ and $C_2H_5O^+$ typical of PEG after treatment with IX, indicating PEG deposition on the surface. Fouling resistance was assessed by 4-h culture with fibroblasts, which adhered and spread on unmodified Au but not on surfaces treated with IX.

A material of greater interest to the medical community is Ti, since its alloys are commonly employed in medical devices due to their excellent biocompatibility, corrosion resistance and high strength (Brunette et al. 2001). Ti surfaces have an adventitious layer of native oxide, and therefore the nature of the interaction between DOPA anchor and surface is expected to be quite different than on Au. XPS analysis of Ti modified with polymer IX provided evidence of a potential mechanism for DOPA-Ti binding. Quantitative analysis of raw XPS spectra suggested the occurrence of catechol-Ti charge-transfer complexes (Rodriguez et al. 1996) as evidenced by increasing depletion of surface hydroxyl groups on the substrates with longer DOPA peptides (Dalsin et al. 2005). Remarkably, an anchor composed of only one DOPA residue was sufficient to confer excellent short term antifouling

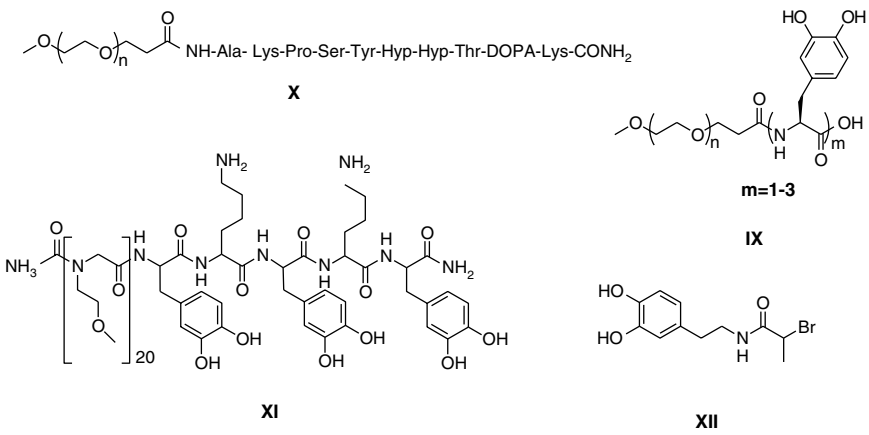

Fig. 13.5. Chemical structures of antifouling MAP mimetic polymers (IX–XI) and DOPA mimetic initiator (XII) for surface initiated polymerization

properties on Ti, reducing cell adhesion by as much as 98% compared to control. Control polymers having an identical structure but with tyrosine as anchor showed no reduction in cell attachment, which was attributed to differences in adhesive ability of the catechol functionality of DOPA and the phenol side chain of Tyr, providing a clear demonstration of the importance of posttranslational modification of Tyr in adhesion.

It is also clear from the cell attachment results on Au and Ti that DOPA does not bind equally well to all surfaces; a single DOPA residue was clearly sufficient for good anchorage of PEG onto Ti but insufficient on Au (Dalsin and Messersmith 2003; Dalsin et al. 2005), where only the decapeptide terminated PEG performed well in cell attachment assays. This result perhaps suggests that other amino acid residues play important adhesive roles on certain substrates. Given the observation many years ago that mussels attach to a great variety of substrates (Young and Crisp 1982; Crisp et al. 1985), additional experiments aimed at elucidating the strength of interactions between DOPA and a variety of substrates should be an important goal for the field.

The underlying basis for the good anti-fouling performance observed for surfaces modified with polymers IX and X is intrinsically related to low levels of nonspecific protein adsorption. The effect of anchoring group composition on adsorbed PEG density and protein resistance has been studied in great detail using PEGs end-coupled with 1–3 DOPA residues (Dalsin et al. 2005). It was found that the mass of PEG adsorbed onto Ti was strongly correlated to the number of DOPA residues in the anchoring peptide, with processing conditions playing an important role, as the highest polymer densities were achieved by adsorption of polymer under critical point conditions at elevated temperature and ionic strength. Serum protein adsorption experiments revealed a clear trend between polymer surface density and serum mass adsorbed, with levels of nonspecific protein adsorption approaching ~1 ng/cm^2 under optimal conditions.

In a recent paper, Statz et al. extended this general surface modification concept with the development of a new antifouling peptide mimetic polymer consisting of an *N*-methoxyethylglycine (peptoid) oligomer coupled to an Mefp-5 mimetic pentapeptide anchor consisting of alternating lysine and DOPA residues (XI, Fig. 13.5) (Statz et al. 2005). The hydrophilic methoxyethyl side chain of XI was selected for its ability to render the polymer water soluble and also for its resemblance to the repeat unit of PEG. Lysine residues were introduced into the peptide anchor in an effort to mimic the high Lys and DOPA content found in Mefp-5 (Waite and Qin 2001).

Protein adsorption to Ti surfaces modified with XI was very low, although the most notable outcome of this study was the long-term cell fouling resistance. The XI-modified Ti surfaces showed extremely low levels of cell attachment over a five-month in-vitro experiment, despite twice-weekly challenges with new cells. The long-term performance may be related to the design of the antifouling peptoid; unlike natural peptides that are easily degraded by

proteases found in the gut and bloodstream, enzymatic susceptibility is reduced in peptoids by the attachment of the peptoid side chain to the amide nitrogen, which leads to a protease-resistant backbone. Such polymers could potentially be used for long-lasting antifouling coatings in-vivo.

Finally, similar antifouling MAP mimetic polymer coatings can now be formed by so-called "graft-from" approaches, in which antifouling polymers are grown directly from surfaces adsorbed with a chemical species capable of initiating polymerization (Ma et al. 2004). These approaches have the theoretical advantage of achieving thicker and higher density layers of surface-bound polymer owing to a high density of initiation sites and growing chain ends. The basic requirement for this approach is a bifunctional molecule containing an initiating functional group coupled to a moiety capable of physical or chemical adsorption to the surface of interest. A biomimetic example of this approach is given by molecule XII (Fig. 13.5), which contains a catechol for adsorption to surfaces and a 2-bromoamide for initiation of radical polymerization (Fan et al., 2005). Adsorption of the initiator on Ti and subsequent atom transfer radical polymerization (ATRP) of oligo(ethylene glycol) methyl ether methacrylate (OEGMEMA) was used to produce a brush-type grafted polymer. Quantitative XPS confirmed the presence of the grafted poly(OEGMEMA) (POEGMEMA) layers according to the theoretical and observed carbon-to-oxygen ratios for the surface-tethered polymer. The absence of the Ti XPS signal of POEGMEMA grafted surfaces, in conjunction with spectroscopic ellipsometry, demonstrated dry POEGMEMA layer thickness of ~100 nm after 12 h of ATRP polymerization. This grafted polymer thickness is many times greater than can be achieved by monolayer adsorption of PEG-DOPA polymers described above. Biological response to the grafted POEGMEMA surfaces, assayed by 4-h fibroblast adhesion, showed decreases in cell adhesion greater than 90% for POEGMEMA thicknesses of ~50 nm or more, and was further demonstrated to be compatible with established photolithographic methods to pattern surfaces for spatial control of biointeractions. This type of bottom-up strategy coupled with simple patterning routines may be very useful in creating surfaces designed for diagnostic cell-based arrays or other devices where spatially controlled interactions are desired.

13.6 Conclusions

Mussel adhesive proteins have the remarkable ability to secure adhesion to both organic and inorganic surfaces in the presence of water. These basic properties are highly desired for applications in both medical and nonmedical settings. One conceivable approach to exploiting the adhesive properties of MAPs is to utilize full sequence MAPs themselves, either isolated and purified from mussel adhesive glands or generated in microbial expression systems.

These approaches have the theoretical advantage of utilizing the adhesive proteins in their native state without modification. However, these approaches do have their disadvantages. In the case of medical applications of MAPs, a strict regulatory environment of biological products will be a significant barrier to overcome. For MAPs purified from mussel tissue there also exists a significant limitation of scale, as production of commercial quantities of MAP adhesive will require enormous numbers of mussels. It may be possible in the future to generate large quantities of MAPs by genetic engineering approaches, although to our knowledge current expression systems are not capable of directly generating DOPA-containing MAPs.

Development of synthetic MAP mimetic polymers in academic labs has accelerated greatly in the last decade. Like the natural proteins that inspire them, DOPA has been incorporated into a variety of synthetic polymers to take advantage of its crosslinking chemistry as well as its ability to adhere to surfaces. Clinical uses for such biomimetic polymers in the future will not be restricted to surgical adhesives, as new MAP mimetic polymers are being developed for use as antifouling coatings for purposes of reducing protein, cell and bacterial fouling of medical device surfaces.

It is important to note that these synthetic efforts have benefited greatly from a rather advanced understanding of the unique composition and chemical behavior of natural MAPS. Most biomimetic studies have understandably focused on DOPA, since its unusually high concentration and unique chemical characteristics naturally suggest an important role in mussel adhesion. Unfortunately it is not always the case that one can easily identify a few key amino acids or design motifs around which to build a biomimetic strategy. For the adhesive strategies used by other species such as barnacles, the key functional features are currently either unknown or appear to be much more subtle. Thus, sophisticated synthetic mimics of animal, plant, bacterial, fungal and algal adhesives will emerge in the future as the biochemical and molecular keys to these other adhesive strategies become apparent.

Acknowledgments. The authors would like to acknowledge NIH (DE 14193 and DE 13030) and NASA (NCC-1-02037) for financial support of this work.

References

Albes JM, Krettek C, Hausen B, Rohde R, Haverich A, Borst HG (1993) Biophysical properties of the gelatin-resorcin-formaldehyde/glutaraldehyde adhesive. Ann Thorac Surg 56:910–915

Alexandridis P (1997) Poly(ethylene oxide)poly(propylene oxide) block copolymer surfactants. Curr Opin Colloid Interface Sci 2:478

Andersen SO, Jacobsen JP, Bojesen G, Roepstorff P (1992) Phenoloxidase catalyzed coupling of catechols. Identification of novel coupling products. Biochim Biophys Acta 1118:134–138

Arnoult C, Cardullo RA, Lemos JR, Florman HM (1996) Activation of mouse sperm T-type Ca^{2+} channels by adhesion to the egg zona pellucida. Proc Natl Acad Sci USA 93:13004–13009

Autumn K, Liang YA, Hsieh ST, Wzesch W, Chan WP, Kenny TW, Fearing R, Full RJ (2000) Adhesive force of a single gecko foot-hair. Nature 405:681–685

Baty AM, Leavitt PK, Siedlecki CA, Tyler BJ, Suci PA, Marchant RE, Geesey GG (1997) Adsorption of adhesive proteins from the marine mussel, Mytilus edulis, on polymer films in the hydrated state using angle dependent X-ray photoelectron spectroscopy and atomic force microscopy. Langmuir 13:5702–5710

Brothers MF, Kaufmann JC, Fox AJ, Deveikis JP (1989) n-Butyl 2-cyanoacrylate—substitute for IBCA in interventional neuroradiology: histopathologic and polymerization time studies. AJNR Am J Neuroradiol 10:777–786

Brunette DM, Tengvall P, Textor M, Thomsen P (2001) Titanium in medicine. Springer, Berlin Heidelberg New York

Burzio LA, Waite JH (2000) Cross-linking in adhesive quinoproteins: studies with model decapeptides. Biochemistry 39:11147–11153

Burzio LO, Burzio VA, Silva T, Burzio LA, Pardo J (1997) Environmental bioadhesion: themes and applications. Curr Opin Biotechnol 8:309–312

Celik H, Caner H, Tahta K, Ozcan OE, Erbengi A, Onol B (1991) Nonsuture closure of arterial defect by vein graft using isobutyl-2-cyanoacrylate as a tissue adhesive. J Neurosurg Sci 35:83–87

Characklis KC (1990) Biofilm processes. In: Characklis WG, Marshall KC (eds) Biofilms. Wiley, New York, pp 195–231

Chen LX, Liu T, Thurnauer MC, Csencsits R, Rajh T (2002) Fe_2O_3 nanoparticle structures investigated by X-ray absorption near-edge structure, surface modifications, and model calculations. J Phys Chem B 106:8539–8546

Chirdon WM, O'Brien WJ, Robertson RE (2003) Adsorption of catechol and comparative solutes on hydroxyapatite. J Biomed Mat Res 66B:532–538

Chivers RA, Wolowacz RG (1997) The strength of adhesive-bonded tissue joints. Int J Adh Adhesives 17:127–132

Connor PA, Dobson KD, Mcquillan AJ (1995) New Sol-Gel attenuated total-reflection infrared spectroscopic method for analysis of adsorption at metal-oxide surfaces in aqueous-solutions -chelation of Tio2, Zro2, and Al2o3 surfaces by Catechol, 8-Quinolinol, and Acetylacetone. Langmuir 11:4193–4195

Coombs TL, Keller PJ (1981) Mytilus byssal threads as an environmental marker for metals. Aquat Toxicol 1:291–300

Cooper CW, Falb RD (1968) Surgical adhesives. Ann NY Acad Sci 146:214–224

Crisp DJ, Walker G, Young GA, Yule AB (1985) Adhesion and substrate choice in Mussels and Barnacles. J Colloid Interface Sci 104:40–50

Dalsin JL, Messersmith PB (2003) Surface modification for protein resistance using a biomimetic approach. In: Thomas JL, Gower LA (eds) Materials inspired by biology, vol 774. Materials Research Society, Warrendale PA, USA, pp 75–80

Dalsin JL, Messersmith PB (2005) Bioinspired antifouling polymers. Materials Today 8:38–46

Dalsin JL, Hu B-H, Lee BP, Messersmith PB (2003) Mussel adhesive protein mimetic polymers for the preparation of nonfouling surfaces. J Am Chem Soc 125:4253–4258

Dalsin JL, Tosatti S, Vörös J, Textor M, Messersmith PB (2005) Protein resistance of titanium oxide surfaces modified by biologically inspired mPEG-DOPA. Langmuir 21:640–646

Deacon MP, Davis SS, Waite JH, Harding SE (1998) Structure and mucoadhesion of mussel glue protein in dilute solution. Biochemistry 37:14108–14112

Dossot M, Sylla M, Allonas X, Merlin A, Jacques P, Fouassier J-P (2000) Role of phenolic derivatives in photopolymerization of an acrylate coating. J Appl Poly Sci 78:2061–2074

Ennker J, Ennker IC, Schoon D, Schoon HA, Dorge S, Meissler J, Rimpler M, Helzer R (1994) The Impact of gelatin-resorcinol glue on aortic tissue: ahistomophologic evaluation. J Vasc Surg 20(1):34–43

Fan X, Lin L, Dalsin JL, Messersmith PB (2005) Biomimetic anchor for surface-initiated polymerization from metal substrates. J Am Chem Soc 127 (45):15843-15847

Filpula DR, Lee SM, Link RP, Strausberg SL, Strausberg RL (1990) Structural and functional repetition in a marine mussel adhesive protein. Biotechnol Prog 6:171–177

Geim AK, Dubonos SV, Grigorieva IV, Novoselov KS, Zhukov AA, Shapoval SY (2003) Microfabricated adhesive mimicking gecko foot-hair. Nature Materials 2:461–463
Gilbert CE, Grierson I, McLeod D (1989) Retinal patching: a new approach to the management of selected retinal breaks. Eye 3:19–26
Goldin AR (1976) Control of duodenal haemorrhage with cyanoacrylate. Br J Radiol 49:583–588
Grande DA, Pitman MI (1988) The use of adhesives in chondrocyte transplantation surgery. Preliminary studies. Bull Hosp Jt Dis Orthop Inst 48:140–148
Green K, Berdecia R, Cheeks L (1987) Mussel adhesive protein: permeability characteristics when used as a basement membrane. Curr Eye Res 6:835–837
Hansen DC, Dexter SC, Waite JH (1995) The inhibition of corrosion of S30403 stainless steel by a naturally occurring catecholic polymer. Corrosion Science 37:1423–1441
Harris JM (1992) Introduction to biotechnical and biomedical applications of poly(ethylene glycol). In: Harris JM (ed) Poly(ethylene glycol) chemistry: biotechnical and biomedical applications. Plenum Press, New York, pp 1–14
Hartnett ME, Hirose T (1998) Cyanoacrylate glue in the repair of retinal detachment associated with posterior retinal breaks in infants and children. Retina 18:125–129
Huang K, Lee B, Ingram D, Messersmith P (2002) Synthesis and characterization of self-assembling block copolymers containing adhesive moieties. Biomacromolecules 3:397–406
Hwang DS, Yoo HJ, Jun JH, Moon WK, Cha HJ (2004) Expression of functional recombinant mussel adhesive protein Mgfp-5 in Escherichia coli. Appl Environ Microbiol 70:3352–9
Hwang DS, Gim Y, Cha HJ (2005) Expression of functional recombinant mussel adhesive protein type 3A in Eschereschia coli. Biotechnology Progress 21:965–70
Ikada Y (1997) Tissue adhesives. In: Chu CC, von Fraunhofer JA, Greisler HP (eds) Wound closure biomaterials and devices. CRC Press, Boca Raton, Florida, pp 317–346
Kakio T, Ito T, Sue K, Sakaguchi K, Shiota T, Oka T, Kobashi H, Sakai N, Omoto M, Mikami M et al (1993) Hemostasis of gastric variceal hemorrhage by transileocoecal and transhepatic obliteration. Acta Med Okayama 47:39–43
Kamino K (2001) Novel barnacle underwater adhesive protein is a charged amino acid-rich protein constituted by a Cys-rich repetitive sequence. Biochem J 356:503–507
Kamino K, Inoue K, Maruyama T, Takamatsu N, Harayama S, Shizuri Y (2000) Barnacle cement proteins. Importance of disulfide bonds in their insolubility. J Biol Chem 273:27360–27365
Kenausis GL, Voros J, Elbert DL, Huang N, Hofer R, Ruiz-Taylor L, Textor M, Hubbell JA, Spencer ND (2000) Poly(L-lysine)-g-Poly(ethylene glycol) layers on metal oxide surfaces: attachment mechanism and effects of polymer architecture on resistance to protein adsorption. J Phys Chem B 104:3298–3309
Khowassah MA, Shippy RL (1971) In vitro investigation of the adhesive strength of cyanoacrylate bonds to human hard tooth structures. J Biomed Mat Res 5:159–68
Kramer KJ, Morgan TD, Hopkins TL, Christensen A, Schaefer J (1991) Insect cuticle tanning: enzymes and cross-link structure. Nat Occur Pest Bioreg 449:87–105
Kummert R, Stumm W (1980) The surface complexation of organic acids on hydrous g-alumina. J Colloid Interface Sc 75:373–385
Lee BP, Dalsin JL, Messersmith PB (2002) Synthesis and gelation of DOPA-modified poly(ethylene glycol) hydrogels. Biomacromolecules 3:1038–1047
Lee BP, Huang K, Nunalee N, Shull K, Messersmith PB (2004) Synthesis of 3,4-dihydroxyphenylalanine (DOPA) containing monomers and their copolymerization with PEG-diacrylate to form hydrogels. J Biomat Sci, Polym Ed 15:449–464
Long JR, Dindot JL, Zebroski HK, Suzanne, Clark RH, Campbell AA, Stayton PS, Drobny GP (1998) A peptide that inhibits hydroxyapatite growth is in an extended conformation on the crystal surface. Proc Natl Acad Sci USA 95:12083–12087
Ma H, Hyun J, Stiller P, Chilkoti A (2004) "Non-fouling" oligo(ethylene glycol)-functionalized polymer brushes synthesized by surface-initiated atom transfer radical polymerization. Adv Mater 16:338–341
Malmsten M, Emoto K, Van Alstine JM (1998) Effect of chain density on inhibition of protein adsorption by poly(ethylene glycol) based coatings. J Colloid Interface Sci 202:507–517

Marumo K, Waite JH (1986) Optimization of hydroxylation of tyrosine and tyrosine-containing peptides by mushroom tyrosinase. Biochim Biophys Acta 872:98–103
Maugh KJ, Anderson DM, Strausberg R, Strausberg SL, Mccandliss R, Wei T, Filpula D (1988) Recombinant bioadhesive proteins of marine animals and their use in adhesive compositions. USA patent no 87–US3048
McDowell LM, Burzio LA, Waite JH, Schaefer J (1999) Rotational echo double resonance detection of cross-links formed in mussel byssus under high-flow stress. J Biol Chem 274:20293–20295
Meisel H, Olieman C (1998) Estimation of calcium-binding constants of casein phosphopeptides by capillary zone electrophoresis. Anal Chim Acta 372:291–297
Naldrett MJ, Kaplan DL (1997) Characterization of barnacle (Balanus eburneus and B. crenatus) adhesive proteins. Mar Biol 127:629–635
Nath N, Hyun J, Ma H, Chilkoti A (2004) Surface engineering strategies for control of protein and cell interactions. Surface Sci 570:98–110
Ninan L, Monahan J, Stroshine RL, Wilker JJ, Shi R (2003) Adhesive strength of marine mussel extracts on porcine skin. Biomaterials 24:4091–4099
Nomori H, Horio H (1997) Gelatin-resorcinol-formaldehyde-glutaraldehyde glue-spread stapler prevents air leakage from the lung. Ann Thorac Surg 63:352–355
Olivieri MP, Loomis RE, Meyer AE, Baier RE (1990) Surface characterization of mussel adhesive protein films. J Adhes Sci Technol 4:197–204
Papov VV, Diamond TV, Biemann K, Waite JH (1995) Hydroxyarginine-containing polyphenolic proteins in the adhesive plaques of the marine mussel Mytilus edulis. J Biol Chem 270:20183–20192
Pardo J, Gutierrez E, Saez C, Brito M, Burzio LO (1990) Purification of adhesive proteins from mussels. Protein Expr Purif 1:147–150
Pasche S, De Paul SM, Voros J, Spencer ND, Textor M (2003) Poly(L-lysine)-graft-poly(ethylene glycol) assembled monolayers on niobium oxide surfaces: a quantitative study of the influence of polymer interfacial architecture on resistance to protein adsorption by ToF-SIMS and in situ OWLS. Langmuir 19:9216–9225
Pitman MI, Menche D, Song EK, Ben-Yishay A, Gilbert D, Grande DA (1989) The use of adhesives in chondrocyte transplantation surgery: in-vivo studies. Bull Hosp Jt Dis Orthop Inst 49:213–220
Rajh T, Chen LX, Lukas K, Liu T, Thurnauer MC, Tiede DM (2002) Surface restructuring of nanoparticles: an efficient route for ligand-metal oxide crosstalk. J Phys Chem B 106: 10543–10552
Refojo MF, Dohlman CH, Koliopoulos J (1971) Adhesives in ophthalmology: a review. Surv Ophthamol 15:217–236
Rice C, Ward M, Nazeeruddin M, Gratzel M (2000) Catechol as an efficient anchoring group for attachment of ruthenium-polypyridine photsensitizers to solar cells based on nanocrystalline films. New J Chem 24:651–652
Rodriguez R, Blesa MA, Regazzoni AE (1996) Surface complexation at the TiO2(anatase)/aqueous solution interface: chemisorption of catechol. J Colloid Interface Sci 177:122–131
Rzepecki LM, Hansen KM, Waite JH (1992) Characterization of a cystine-rich polyphenolic protein family from the blue mussel Mytilus edulis. Biol Bull 183:123–137
Rzepecki LM, Hansen KM, Waite JH (1995) Bioadhesives: dopa and phenolic proteins as component of organic composite materials. In: Principles of cell adhesion. CRC Press, Boca Raton, pp 107–142
Saltz R, Sierra D, Feldman D, Saltz MB, Dimick A, Vasconez LO (1991) Experimental and clinical applications of fibrin glue. Plast Reconstr Surg 88:1005–1015; discussion 1016–1017
Schnurrer J, Lehr C-M (1996) Mucoadhesive properties of the mussel adhesive protein. Int J Pharm 141:251–256
Sever MJ, Weisser JT, Monahan J, Srinivasan S, Wilker JJ (2004) Metal-mediated cross-linking in the generation of a marine-mussel adhesive. Angew Chem Int Ed 43:448–450

Siedentop KH, Harris DM, Sanchez B (1988) Autologous fibrin tissue adhesive: factors influencing bonding power. Laryngoscope 98:731–733
Sierra D, Saltz R (1996) Surgical adhesives and sealants: current technology and applications. Technomic Publ, Lancaster, PA
Sofia SJ, Premnath V, Merrill EW (1998) Poly(ethylene oxide) grafted to silicon surfaces: grafting density and protein adsorption. Macromolecules 31:5059–5070
Soriaga MP, Hubbard AT (1982) Determination of the orientation of aromatic molecules adsorbed on platinum electrodes. The effect of solute concentration. J Am Chem Soc 104:3937–3945
Statz AR, Meagher RJ, Barron AE, Messersmith PB (2005) New peptidomimetic polymers for antifouling surfaces. J Am Chem Soc 127:7972–7973
Strausberg RL, Link RP (1990) Protein-based medical adhesives. Trends Biotechnol 8:53–57
Strausberg RL, Anderson DM, Filpula D, Finkelman M, Link R, McCandliss R, Orndorff SA, Strausberg SL, Wei T (1989) Development of a microbial system for production of mussel adhesive protein. Adhesives Renewable Resources 385:453–464
Sugumaran M (1998) Unified mechanism for sclerotization of insect cuticles. Adv Insect Physiol 27:230–334
Swann CP, Adewole T, Waite JH (1998) Preferential manganese accumulation in dreissenid byssal threads. Comp Biochem Physiol B Biochem Mol Biol 119B:755–759
Szefer P, Ikuta K, Kushiyama S, Szefer K, Frelek K, Geldon J (1997) Distribution and association of trace metals in soft tissue and byssus of Mytilus edulis from the east coast of Kyushu Island, Japan. Arch Environ Contam Toxicol 32:184–190
Tatehata H, Mochizuki A, Kawashima T, Yamashita S, Yamamoto H (2000) Model polypeptide of mussel adhesive protein. I. Synthesis and adhesive studies of sequential polypeptides (X-Tyr-Lys)n and (Y-Lys)n. J Appl Polym Sci 76:929–937
Tatehata H, Mochizuki A, Ohkawa K, Yamada M, Yamamoto H (2001) Tissue adhesive using synthetic model adhesive proteins inspired by the marine mussel. J Adh Sci Tech 15: 1003–1013
Tatooles CJ, Braunwald NS (1966) The Use of crosslinked gelatin as a tissue adhesive to control the hemorrhage from liver and kidney. Surgery 50:17
Taylor SW, Luther GW III, Waite JH (1994) Polarographic and spectrophotometric investigation of Iron(III) complexation to 3,4-Dihydroxyphenylalanine-containing peptides and proteins from mytilus edulis. Inorg Chem 33:5819–5824
Taylor SW, Chase DB, Emptage MH, Nelson MJ, Waite JH (1996) Ferric ion complexes of a DOPA-containing adhesive protein from mytilus edulis. Inorg Chem 35:7572–7577
Toriumi DM, Raslan WF, Friedman M, Tardy ME Jr (1991) Variable histotoxicity of histoacryl when used in a subcutaneous site: an experimental study. Laryngoscope 101:339–343
Tseng YC, Tabata Y, Hyon SH, Ikada Y (1990) In vitro toxicity test of 2-cyanoacrylate polymers by cell culture method. J Biomed Mat Res 24:1355–1367
Waite JH (1987) Nature's underwater adhesive specialist. Int J Adh Adhesives 7:9–14
Waite JH (1990) The phylogeny and chemical diversity of quinone-tanned glues and varnishes. Comp Biochem Physiol B Comp Biochem 97:19–29
Waite JH (1991) Mussel beards: a coming of age. Chem Industry 2:607–611
Waite JH (1999) Reverse engineering of bioadhesion in marine mussels. Ann NY Acad Sci 875:301–309
Waite JH, Andersen SO (1978) 3,4-Dihydroxyphenylalanine in an insoluble shell protein of Mytilus edulis. Biochimt Biophys Acta 541:107–114
Waite JH, Qin X (2001) Polyphosphoprotein from the adhesive pads of Mytilus edulis. Biochemistry 40:2887–2893
Waite JH, Anderson NH, Jewhurst S, Sun C (2005) Mussel adhesion: finding the tricks worth mimicking. J Adhesion 81:1–21
Warner SC, Waite JH (1999) Expression of multiple forms of an adhesive plaque protein in an individual mussel, Mytilus edulis. Mar Biol 134:729–734

Weber SC, Chapman MW (1984) Adhesives in orthopaedic surgery. A review of the literature and in vitro bonding strengths of bone-bonding agents. Clin Orthop 191:249–261

Xu C, Xu K, Gu H, Zheng R, Liu H, Zhang X, Guo Z, Xu B (2004) Dopamine as a robust anchor to immobilize functional molecules on the iron oxide shell of magnetic nanoparticles. J Am Chem Soc 126:9938–9939

Yamamoto H (1987) Synthesis and adhesive studies of marine polypeptides. J Chem Soc Perkin Trans 1:613–618

Yamamoto H (1995) Marine adhesive proteins and some biotechnological applications. Biotechnol Genet Eng Rev 13:133–165

Yamamoto H, Ogawa T, Ohkawa K (1995) Wettability and adhesion of synthetic marine adhesive proteins and related model compounds. J Colloid Interface Sci 176:111–116

Yang JZ, Medawar PB (1940) Fibrin suture of peripheral nerves. Lancet 275:126–132

Young GA, Crisp DJ (1982) Marine animals and adhesion. In: Allen KW (ed) Adhesion-6. Applied Science Publishers, Barkling, UK, pp 279–313

Yu M, Deming TJ (1998) Synthetic polypeptide mimics of marine adhesives. Macromolecules 31:4739–4745

Yu M, Hwang J, Deming TJ (1999) Role of L-3,4-dihydroxyphenylalanine in mussel adhesive proteins. J Am Chem Soc 121:5825–5826

Zalipsky S, Harris JM (1997) Introduction to chemistry and biological applications of poly(ethylene glycol). In: Harris JM, Zalipsky S (eds) Poly(ethylene glycol): chemistry and biological applications, vol 680. American Chemical Society, Washington, DC, pp 1–13

Subject Index